

SsSci^{2nd}conference 2019

การประชุมสวนสุนันทาวิชาการด้านวิทยาศาสตร์และเทคโนโลยี
ระดับชาติและนานาชาติ ครั้งที่ 2
“วิทยาศาสตร์ เทคโนโลยี และนวัตกรรม เพื่อการพัฒนาที่ยั่งยืน”

The 2nd Suan Sunandha National and International Academic
Conference on Science and Technology (SsSci 2019)

“Science, Technology and Innovation
for Sustainable Development”

วันศุกร์ที่ 8 พฤศจิกายน 2562
8th November 2019

ณ โรงแรมเดอะรอยัลริเวอร์ กรุงเทพมหานคร
The Royal River Hotel, Bangkok, Thailand

ความเป็นมาของการประชุมสวนสุนันทาวิชาการด้านวิทยาศาสตร์และเทคโนโลยี ระดับชาติและนานาชาติ ครั้งที่ 2

“วิทยาศาสตร์ เทคโนโลยี และนวัตกรรม เพื่อการพัฒนาที่ยั่งยืน”

หลักการและเหตุผล

มหาวิทยาลัยราชภัฏเน้นการผลิตบัณฑิตที่มีคุณภาพเป็นเลิศโดยกระบวนการจัดการเรียนการสอนเพื่อการพัฒนาชุมชนและท้องถิ่นให้มีความเข้มแข็ง และยั่งยืน ตามยุทธศาสตร์ใหม่มหาวิทยาลัยราชภัฏเพื่อการพัฒนาท้องถิ่นตามพระบรมราโชบายของพระบาทสมเด็จพระเจ้าอยู่หัวรัชการที่ 10 และแผนยุทธศาสตร์ระยะ 20 ปี (พ.ศ. 2560 – 2579) โดยมีการขับเคลื่อนงานวิจัย สร้างความรู้และนวัตกรรมให้มีคุณภาพและได้มาตรฐานสากล ให้บริการทางวิชาการ ถ่ายทอดเทคโนโลยี น้อมนำแนวพระราชดำริ สร้างเครือข่ายและความร่วมมือกับภาคประชาชน ชุมชน ท้องถิ่น และผู้ประกอบการในการจัดการศึกษา ส่งเสริมเปลี่ยนแปลง และการพัฒนาก้าวหน้า อย่างต่อเนื่องและยั่งยืน ทัดเทียมกับนานาชาติอารยประเทศ ประกอบกับประเทศไทยมีนโยบายการพัฒนาเศรษฐกิจของประเทศที่ขับเคลื่อนด้วยนวัตกรรม (Thailand 4.0) โดยมีแนวคิดหลักคือ เปลี่ยนจากการขับเคลื่อนประเทศด้วยภาคอุตสาหกรรมไปสู่การขับเคลื่อนด้วยเทคโนโลยี การพัฒนาวิชาการ ความคิดสร้างสรรค์ นวัตกรรม วิทยาศาสตร์เทคโนโลยี การวิจัยและพัฒนาแล้วต่อยอดสู่เทคโนโลยีอุตสาหกรรมในหลายกลุ่มเป้าหมาย เช่น กลุ่มอาหาร เกษตร และเทคโนโลยีชีวภาพ กลุ่มสาธารณสุข สุขภาพ และเทคโนโลยีทางการแพทย์ กลุ่มดิจิทัล เทคโนโลยีอินเทอร์เน็ตที่เชื่อมต่อและบังคับอุปกรณ์ต่าง ๆ ปัญญาประดิษฐ์และเทคโนโลยีสมองกลฝังตัว รวมทั้งกลุ่มอุตสาหกรรมสร้างสรรค์ วัฒนธรรม และบริการที่มีมูลค่าสูง

คณะวิทยาศาสตร์และเทคโนโลยี มหาวิทยาลัยราชภัฏสวนสุนันทา ตระหนักถึงความสำคัญของการศึกษาวิจัยและพัฒนา เพื่อสร้างองค์ความรู้ใหม่ การพัฒนาการเรียนการสอน และการวิจัยประยุกต์ บนพื้นฐานการใช้ประโยชน์จากทรัพยากรของประเทศอย่างมีประสิทธิภาพ ได้ส่งเสริมและสนับสนุนการสร้างงานวิจัย และสร้างความร่วมมือทางวิชาการของนักศึกษา คณาจารย์ นักวิจัย และนักวิชาการจากสถาบันอุดมศึกษาในประเทศ และเครือข่ายมหาวิทยาลัยที่ทำข้อตกลงทางวิชาการ (MoU) ในต่างประเทศ รวมทั้งหน่วยงานเครือข่ายทั้งภาครัฐและเอกชน เพื่อให้ผลิตงานวิจัยที่มีคุณค่าต่อสังคม รวมทั้งส่งเสริมให้เกิดการเผยแพร่ผลงานวิจัยที่มีประโยชน์สู่สาธารณะ เพื่อก่อให้เกิดการนำผลงานวิจัยไปใช้ประโยชน์ด้านวิชาการ และการพัฒนา การต่อยอดสู่การใช้ประโยชน์เชิงพาณิชย์หรืออุตสาหกรรม นำไปสู่เป้าหมายเพื่อการพัฒนาได้อย่างยั่งยืน

จากความสำคัญดังกล่าว ทางคณะวิทยาศาสตร์และเทคโนโลยีจึงได้จัดทำโครงการประชุมสวนสุนันทาวิชาการด้านวิทยาศาสตร์และเทคโนโลยีระดับชาติและนานาชาติ ครั้งที่ 2 “วิทยาศาสตร์ เทคโนโลยี และนวัตกรรม เพื่อการพัฒนาอย่างยั่งยืน” ขึ้น เพื่อเป็นเวทีในการแลกเปลี่ยนประสบการณ์และความรู้ของนักศึกษา คณาจารย์ นักวิจัย และนักวิชาการจากสถาบันอุดมศึกษา รวมทั้งหน่วยงานที่สนใจทั้งภาครัฐและเอกชนทั้งในและต่างประเทศ ในสาขาวิชาต่าง ๆ จำนวน 8 กลุ่มสาระ ได้แก่

- 1) คอมพิวเตอร์ และเทคโนโลยีสารสนเทศ
- 2) คณิตศาสตร์ และสถิติ
- 3) ฟิสิกส์ และพลังงาน
- 4) เคมี และนิติวิทยาศาสตร์

- 5) ชีววิทยา เทคโนโลยีชีวภาพ และจุลชีววิทยา
- 6) วิทยาศาสตร์สิ่งแวดล้อม
- 7) วิทยาศาสตร์และเทคโนโลยีการอาหาร และคหกรรมศาสตร์
- 8) วิทยาศาสตร์การกีฬา และสุขภาพ

วัตถุประสงค์ของการประชุมสนันทาวิชาการ

1. เพื่อเป็นเวทีในการเผยแพร่ผลงานวิจัยและผลงานสร้างสรรค์ในระดับชาติและนานาชาติ
2. เพื่อส่งเสริมให้นักศึกษา คณาจารย์ นักวิจัย และนักวิชาการจากสถาบันอุดมศึกษา รวมทั้งหน่วยงานที่สนใจทั้งภาครัฐและเอกชน ตระหนักถึงความสำคัญของงานวิจัยและการเผยแพร่ผลงานวิจัยในการประชุมวิชาการระดับชาติและนานาชาติ
3. เพื่อตีพิมพ์เผยแพร่ผลงานวิจัยและผลงานสร้างสรรค์ในระดับชาติและนานาชาติ

ประโยชน์ที่คาดว่าจะได้รับการประชุมสนันทาวิชาการ

1. เป็นเวทีในการเผยแพร่ผลงานวิจัยและผลงานสร้างสรรค์ในระดับชาติและนานาชาติ
2. ส่งเสริมให้นักศึกษา คณาจารย์ นักวิจัย และนักวิชาการจากสถาบันอุดมศึกษา รวมทั้งหน่วยงานที่สนใจทั้งภาครัฐและเอกชน ตระหนักถึงความสำคัญของงานวิจัยและการเผยแพร่ผลงานวิจัย ในการประชุมวิชาการระดับชาติและนานาชาติ
3. การตีพิมพ์เผยแพร่ผลงานวิจัยและผลงานสร้างสรรค์ในระดับชาติและนานาชาติ



Conference Background

The 2nd Suan Sunandha National and International Academic Conference on Science and Technology (SsSci2019) “Science, Technology and Innovation for Sustainable Development”



The 2nd Suan Sunandha National and International Academic Conference on Science and Technology, entitled "Science, Technology and Innovation for Sustainable Development" is the prestigious event organizes by Faculty of Science and Technology, SSRU, to provide an excellent platform for the national and international academicians, researchers, industrial participants and students to share their findings and establish collaborations with each other's and experts. The conference will be held in Bangkok, Thailand on 8th November 2019.

The key intention of this conference is to provide opportunity for the national and international participants to share their ideas and experiences. In addition this conference will help the delegates and participants to establish research or business relations and future collaborations in their career path nationally and internationally. We hope the outcome will lead the major impact on updating the knowledge and research base scopes of conference's eight major topics.

This Conference is sponsored and organized by Faculty of Science and Technology, Suan Sunandha Rajabhat University. The conference would offer a large number of invited lectures and presentations from distinguished speakers. The best paper awards will be given for the papers judged to make the most significant contribution to the conference.

This conference provides respectable platform and decent opportunity for participants to exchange knowledge, share experiences and develop connections with faculty members, researchers from academia, industry, government and students. The conference includes eight major research areas:

1. Computer Science and Information Technology
2. Mathematics and Statistics
3. Physics and Energy
4. Chemistry and Forensic Science
5. Biology, Biotechnology, and Microbiology
6. Environmental Science and Technology
7. Food Science and Technology, and Home Economics
8. Sports and Health Science

เจ้าภาพร่วม และผู้สนับสนุน
Conference Co-hosts and Supporters

สำนักงานคณะกรรมการการอุดมศึกษา
Office of the Higher Education Commission



สำนักงานคณะกรรมการวิจัยแห่งชาติ
National Research Council of Thailand



Faculty of Science
University of Hradec Kralove (Czech Republic)



Okayama University (Japan)



Ho Chi Minh City Open University
(Vietnam)



Kazan Federal University
(Russian Federation)



Chia Nan University of Pharmacy and Science
(Taiwan)



มหาวิทยาลัยราชภัฏเชียงใหม่
Chiang Mai Rajabhat University



มหาวิทยาลัยราชภัฏนครศรีธรรมราช
Nakhon Si Thammarat Rajabhat University



มหาวิทยาลัยราชภัฏลำปาง
Lampang Rajabhat University



มหาวิทยาลัยราชภัฏมหาสารคาม
Rajabhat Mahasarakham University



มหาวิทยาลัยราชภัฏสกลนคร
Sakonkakhon Rajabhat University



มหาวิทยาลัยราชภัฏสุรินทร์
Surindra Rajabhat University



มหาวิทยาลัยราชภัฏพิบูลสงคราม
Pibulsongkram Rajabhat University



เจ้าภาพร่วม และผู้สนับสนุน
Conference Co-hosts and Supporters

มหาวิทยาลัยราชภัฏเทพสตรี
Thepsatri Rajabhat University



มหาวิทยาลัยราชภัฏนครราชสีมา
Nakhonratchasima Rajabhat University



มหาวิทยาลัยราชภัฏเพชรบุรี
Phetchaburi Rajabhat University



บริษัท อาไลติส เยน่า ฟารีอีสต์ (ประเทศไทย) จำกัด
Analytik Jena Far East (Thailand) Ltd.



บริษัท ฮิสโตเซนเตอร์ จำกัด
Histocenter Co.,Ltd (Thailand)
บริษัท สิทธิพรแอสโซซิเอต จำกัด
Sithiphorn Associates Co.,Ltd.



บริษัท วนาไซเอนซ์ จำกัด
Vana Science Co.,Ltd.



บริษัท ยูไนเต็ด แอนนาลิส แอนท์ เอนจิเนียริ่ง
คอนซัลแตนท์ จำกัด
United Analyst and Engineering Consultant Co., Ltd.



บริษัท เมอร์ค จำกัด
Merck Ltd.



บริษัท ซายน์ สเปค จำกัด
Scispec Co., Ltd.



บริษัท เพอร์กิน เอลเมอร์ จำกัด
PerkinElmer Co., Ltd.



คณะกรรมการผู้ทรงคุณวุฒิพิจารณาและกลั่นกรองบทความ Conference Committee

กลุ่มคอมพิวเตอร์และเทคโนโลยีสารสนเทศ

- | | |
|--|---|
| <ol style="list-style-type: none"> 1 รองศาสตราจารย์ ดร.พยุง มีสัจ
Assoc. Prof. Dr. Phayung Meesad 2 ผู้ช่วยศาสตราจารย์ ดร.มณเฑียร รัตนศิริวงศ์วุฒิ
Asst. Prof. Dr. Montean Rattanasirivongwut 3 รองศาสตราจารย์ ดร.พรฤดี เนติโสภาคกุล
Assoc. Prof. Dr. Ponrudee Netisopakul 4 ผู้ช่วยศาสตราจารย์ชฎิภักดิ์ เขมวิมุตติวงศ์
Asst. Prof. Dr. Chutipuk Kemwimoottiwong 5 ผู้ช่วยศาสตราจารย์ ดร.รมชัย ชื่นธวัช
Asst. Prof. Dr. Ronnachai Chuentawat 6 อาจารย์ ดร.นพดล ผู้มีจรรยา
Dr. Noppadon Phumeechaya 7 ผู้ช่วยศาสตราจารย์ ดร.พิจิตรา จอมศรี
Assist. Prof. Dr. Pijittra Jomsri | <p>มหาวิทยาลัยเทคโนโลยีพระจอมเกล้าพระนครเหนือ
King Mongkut's University of Technology North Bangkok</p> <p>มหาวิทยาลัยเทคโนโลยีพระจอมเกล้าพระนครเหนือ
King Mongkut's University of Technology North Bangkok</p> <p>สถาบันเทคโนโลยีพระจอมเกล้าเจ้าคุณทหารลาดกระบัง
King Mongkut's Institute of Technology Ladkrabang</p> <p>มหาวิทยาลัยราชภัฏเชียงใหม่
Chiang Mai Rajabhat University</p> <p>มหาวิทยาลัยราชภัฏนครราชสีมา
Nakhon Ratchasima Rajabhat University</p> <p>มหาวิทยาลัยราชภัฏนครปฐม
Nakhon Pathom Rajabhat University</p> <p>มหาวิทยาลัยราชภัฏสวนสุนันทา
Suan Sunandha Rajabhat University</p> |
|--|---|

กลุ่มคณิตศาสตร์ สถิติ

- | | |
|---|---|
| <ol style="list-style-type: none"> 1 รองศาสตราจารย์ ดร.ฉัฐไชย ลีนาวงศ์
Assoc. Prof. Dr. Chartchai Leenawong 2 ผู้ช่วยศาสตราจารย์ ดร.วิโรจน์ ดีกัจจะ
Asst. Prof. Dr. Wirot Tikjha 3 ผู้ช่วยศาสตราจารย์ ดร.บุรพา สิงหา
Asst. Prof. Dr. Boorapa Singha 4 ผู้ช่วยศาสตราจารย์ ดร.บงกช นิมตระกูล
Asst. Prof. Dr. Bongkoch Nimtrakul 5 ผู้ช่วยศาสตราจารย์ ดร.ณพฐ์ โสภีพันธ์
Asst. Prof. Dr. Nop Sopipan | <p>สถาบันเทคโนโลยีพระจอมเกล้าเจ้าคุณทหารลาดกระบัง
King Mongkut's Institute of Technology Ladkrabang</p> <p>มหาวิทยาลัยราชภัฏพิบูลสงคราม
Pibulsongkram Rajabhat University</p> <p>มหาวิทยาลัยราชภัฏเชียงใหม่
Chiang Mai Rajabhat University</p> <p>มหาวิทยาลัยราชภัฏเทพสตรี
Thepsatri Rajabhat University</p> <p>มหาวิทยาลัยราชภัฏนครราชสีมา
Nakhon Ratchasima Rajabhat University</p> |
|---|---|

กลุ่มฟิสิกส์ พลังงาน

- | | |
|--|--|
| <ol style="list-style-type: none"> 1 ผู้ช่วยศาสตราจารย์ ดร.นฤปดี ศรีสังข์
Asst. Prof. Dr. Naruebodee Srisang 2 ผู้ช่วยศาสตราจารย์ ดร.นววรรณ ทองมี
Asst. Prof. Dr. Navavan Thongmee 3 อาจารย์ ดร. ชเนษฎ์ วิชาศิลป์
Dr. Chanade Wichasilp 4 อาจารย์ ดร.ปกรณ์ ปรีชาบุรณะ
Dr. Pakorn Preechaburana 5 ผู้ช่วยศาสตราจารย์ ดร.กัณฑพัฒน์ กิตติอัครวาลย์
Asst. Prof. Dr. Kanthapat Kitti-atchawan 6 ผู้ช่วยศาสตราจารย์ ดร.เขมฤทัย งามะพัฒน์
Asst. Prof. Dr. Kheamrutai Thamaphat 7 รองศาสตราจารย์ ดร.ณรงค์ สังวารานที
Assoc. Prof. Dr. Narong Sangwanatee 8 รองศาสตราจารย์ ดร.อมรา อิทธิพงษ์
Assoc. Prof. Dr. Ammara Ittipongse | <p>สถาบันเทคโนโลยีพระจอมเกล้าเจ้าคุณทหารลาดกระบัง
King Mongkut's Institute of Technology Ladkrabang</p> <p>มหาวิทยาลัยราชภัฏพิบูลสงคราม
Pibulsongkram Rajabhat University</p> <p>มหาวิทยาลัยราชภัฏเชียงใหม่
Chiang Mai Rajabhat University</p> <p>มหาวิทยาลัยธรรมศาสตร์
Thammasat University</p> <p>มหาวิทยาลัยราชภัฏเทพสตรี
Thepsatri Rajabhat University</p> <p>มหาวิทยาลัยเทคโนโลยีพระจอมเกล้าธนบุรี
King Mongkut's University of Technology Thonburi</p> <p>มหาวิทยาลัยราชภัฏสวนสุนันทา
Suan Sunandha Rajabhat University</p> <p>มหาวิทยาลัยราชภัฏสวนสุนันทา
Suan Sunandha Rajabhat University</p> |
|--|--|



กลุ่มเคมี นิติวิทยาศาสตร์

- | | | |
|---|--|--|
| 1 | ศาสตราจารย์ พลตำรวจตรีหญิง ดร.พัชรา สินลอยมา
Prof. Pol .Maj. Gen. Patchara Sinloyma | โรงเรียนนายร้อยตำรวจ
Royal Police Cadet Academy |
| 2 | รองศาสตราจารย์ พันตำรวจเอก วรัชช วิชชวาณิชย์
Assoc. Prof. Pol. Col. Witchuvanit Witchuvanit | โรงเรียนนายร้อยตำรวจ
Royal Police Cadet Academy |
| 3 | ผู้ช่วยศาสตราจารย์ ดร.รพีพรรณ จันทร์มณี
Asst. Prof. Dr. Rapiphun Janmanee | มหาวิทยาลัยราชภัฏพิบูลสงคราม
Pibulsongkram Rajabhat University |
| 4 | ผู้ช่วยศาสตราจารย์.ดร.สายธาร ทองพร้อม
Asst. Prof. Dr. Saithan Thongphrom | มหาวิทยาลัยราชภัฏภูเก็ต
Phuket Rajabhat University |
| 5 | ผู้ช่วยศาสตราจารย์ ดร. สราวุฒิ สมนาม
Asst. Prof. Dr. Sarawut Somnam | มหาวิทยาลัยราชภัฏเชียงใหม่
Chiang Mai Rajabhat University |
| 6 | ผู้ช่วยศาสตราจารย์ ดร.วัลย์ลิกา สุขสำราญ
Asst. Prof. Dr. Wallika Suksomran | มหาวิทยาลัยราชภัฏเทพสตรี
Thepsatri Rajabhat University |
| 7 | ผู้ช่วยศาสตราจารย์ ดร.ธนากร เปลื้องกลาง
Asst. Prof. Dr. Thanakorn Pluangklang | มหาวิทยาลัยราชภัฏนครราชสีมา
Nakhon Ratchasima Rajabhat University |
| 8 | ผู้ช่วยศาสตราจารย์ ดร.วนิดา วอนสวัสดิ์
Asst. Prof. Dr. Wanida Wonsawat | มหาวิทยาลัยราชภัฏสวนสุนันทา
Suan Sunandha Rajabhat University |
| 9 | อาจารย์ ดร.พลอยทราย โอฮามา
Dr. Ploysai Ohama | มหาวิทยาลัยราชภัฏสวนสุนันทา
Suan Sunandha Rajabhat University |

กลุ่มชีววิทยา เทคโนโลยีชีวภาพ จุลชีววิทยา

- | | | |
|----|---|---|
| 1 | รองศาสตราจารย์ ดร.มรณี ต้อยเต็มวงศ์
Assoc. Prof. Dr. Kooranee Tuitemwong | มหาวิทยาลัยเกษตรศาสตร์
Kasetsart University |
| 2 | รองศาสตราจารย์ ดร.อัชฌันจิน จงจิตวิมล
Assoc. Prof. Dr. Touchkanin Jongjitvimol | มหาวิทยาลัยราชภัฏพิบูลสงคราม
Pibulsongkram Rajabhat University |
| 3 | ผู้ช่วยศาสตราจารย์ ดร.จิตศิริณ ก้อนคง
Asst. Prof. Dr. Chisiri Konkong | มหาวิทยาลัยราชภัฏพิบูลสงคราม
Pibulsongkram Rajabhat University |
| 4 | ผู้ช่วยศาสตราจารย์ ดร.กชนิภา อุดมทวี
Asst. Prof. Dr. Kotchanipha Udomthawee | มหาวิทยาลัยราชภัฏสุรินทร์
Surindra Rajabhat University |
| 5 | ผู้ช่วยศาสตราจารย์ ดร.ภฤชณ์ ปิ่นทอง
Asst. Prof. Dr. Krit Pinthong | มหาวิทยาลัยราชภัฏสุรินทร์
Surindra Rajabhat University |
| 6 | ผู้ช่วยศาสตราจารย์ ดร.กิตติศักดิ์ โชติกเดชาณรงค์
Asst. Prof. Dr. Kittisak Chotikadachanarong | มหาวิทยาลัยราชภัฏเชียงใหม่
Chiang Mai Rajabhat University |
| 7 | อาจารย์ ดร.ภคกุล สังข์สุริยะ
Dr.Pakkakul Sangsuriya | ศูนย์พันธุวิศวกรรมและเทคโนโลยีชีวภาพแห่งชาติ
National Center for Genetic Engineering and Biotechnology |
| 8 | ผู้ช่วยศาสตราจารย์ ดร.เทียมหทัย ชูพันธ์
Asst. Prof. Dr. Thiamhathai Choopan | มหาวิทยาลัยราชภัฏนครราชสีมา
Nakhon Ratchasima Rajabhat University |
| 9 | อาจารย์ ดร.ไตรวิทย์ รัตน์โรจน์พงศ์
Dr.Triwit Rattanarojpong | มหาวิทยาลัยเทคโนโลยีพระจอมเกล้าธนบุรี
King Mongkut's University of Technology Thonburi |
| 10 | ผู้ช่วยศาสตราจารย์ ดร. อมรพันธ์ อัจจิมาพร
Asst. Prof. Dr. Amornpan Ajjimaporn | มหาวิทยาลัยมหิดล
Mahidol University |
| 11 | ผู้ช่วยศาสตราจารย์ ดร.จันทนา กาญจน์กมล
Asst. Prof. Dr. Chantana Kankamol | มหาวิทยาลัยราชภัฏสวนสุนันทา
Suan Sunandha Rajabhat University |
| 12 | ผู้ช่วยศาสตราจารย์ ดร.ปิยะดา อาชายุทธการ
Asst. Prof. Dr. Piyada Achayuthakan | มหาวิทยาลัยราชภัฏสวนสุนันทา
Suan Sunandha Rajabhat University |
| 13 | อาจารย์ ดร.วัฒนา พันธุ์พีช
Dr.Wattana Panphut | มหาวิทยาลัยราชภัฏสวนสุนันทา
Suan Sunandha Rajabhat University |
| 14 | Dr. Mohammad Bagher Javadi Nobandegani | มหาวิทยาลัยราชภัฏสวนสุนันทา
Suan Sunandha Rajabhat University |
| 15 | Dr. Ha Thanh Dong | มหาวิทยาลัยราชภัฏสวนสุนันทา
Suan Sunandha Rajabhat University |



กลุ่มวิทยาศาสตร์สิ่งแวดล้อมและเทคโนโลยี

- | | | |
|----|--|---|
| 1 | รองศาสตราจารย์ ดร.สุเทพ ศิลพานันทกุล
Assoc. Prof. Dr. Suthep Silapanuntakul | มหาวิทยาลัยมหิดล
Mahidol University |
| 2 | รองศาสตราจารย์ ดร.เบญจภรณ์ ประภักดิ์
Assoc. Prof. Dr. Benjaphorn Prapagdee | มหาวิทยาลัยมหิดล
Mahidol University |
| 3 | ผู้ช่วยศาสตราจารย์ ดร.ชาญวิทย์ โฆษิตานนท์
Asst. Prof. Dr. Charnwit Kositanont | จุฬาลงกรณ์มหาวิทยาลัย
Chulalongkorn University |
| 4 | ผู้ช่วยศาสตราจารย์ ดร.เสาวนีย์ วิจิตรโกสุม
Asst. Prof. Dr. Saowanee Wijitkosum | จุฬาลงกรณ์มหาวิทยาลัย
Chulalongkorn University |
| 5 | ผู้ช่วยศาสตราจารย์ ดร.ธันวดี ศรีธาวิรัตน์
Asst. Prof. Dr. Thaunwadee Srithawirat | มหาวิทยาลัยราชภัฏพิบูลสงคราม
Pibulsongkram Rajabhat University |
| 6 | ผู้ช่วยศาสตราจารย์ ดร.เขมนิจจรรย์ สารีพันธ์
Asst. Prof. Dr. Khamanitjaree Saripan | มหาวิทยาลัยราชภัฏเทพสตรี
Thepsatri Rajabhat University |
| 7 | รองศาสตราจารย์ ดร.ไพบุลย์ แจ่มพงษ์
Assoc. Prof. Dr. Paiboon Jeamponk | มหาวิทยาลัยราชภัฏสวนสุนันทา
Suan Sunandha Rajabhat University |
| 8 | ผู้ช่วยศาสตราจารย์ ดร.อานัติ ต๊ะปินตา
Asst. Prof. Dr. Anat Thapinta | มหาวิทยาลัยราชภัฏสวนสุนันทา
Suan Sunandha Rajabhat University |
| 9 | รองศาสตราจารย์ ศิวพันธุ์ ชูอินทร์
Assoc. Prof. Sivapan Choo-In | มหาวิทยาลัยราชภัฏสวนสุนันทา
Suan Sunandha Rajabhat University |
| 10 | ผู้ช่วยศาสตราจารย์ ดร.ทัศนาวลัย อุฑารสกุล
Asst. Prof. Dr. Tatsanawalai Utarasakul | มหาวิทยาลัยราชภัฏสวนสุนันทา
Suan Sunandha Rajabhat University |

กลุ่มวิทยาศาสตร์และเทคโนโลยีการอาหาร คหกรรมศาสตร์

- | | | |
|---|---|---|
| 1 | รองศาสตราจารย์ ดร.ชื่นจิตต์ บุญเชิด
Assoc. Prof. Dr. Chuenchit Boonchird | มหาวิทยาลัยมหิดล
Mahidol University |
| 2 | รองศาสตราจารย์ ดร.ทัศนีย์ ลีมีสุวรรณ
Assoc. Prof. Dr. Tasanee Limsuwan | มหาวิทยาลัยเกษตรศาสตร์
Kasetsart University |
| 3 | รองศาสตราจารย์ ดร.คงศักดิ์ ศรีแก้ว
Assoc. Prof. Dr. Khongsak Srikaeo | มหาวิทยาลัยราชภัฏพิบูลสงคราม
Pibulsongkram Rajabhat University |
| 4 | ผู้ช่วยศาสตราจารย์ ดร.ธีรินทร์ ฉายศิริโชติ
Asst. Prof. Dr. Teerin Chysirichote | สถาบันเทคโนโลยีพระจอมเกล้าเจ้าคุณทหารลาดกระบัง
King Mongkut's Institute of Technology Ladkrabang |
| 5 | อาจารย์ ดร.ธนิดา ฉั่วเจริญ
Dr. Thanida Chuacharoen | มหาวิทยาลัยราชภัฏสวนสุนันทา
Suan Sunandha Rajabhat University |

กลุ่มวิทยาศาสตร์การกีฬา วิทยาศาสตร์สุขภาพ

- | | | |
|---|---|---|
| 1 | ผู้ช่วยศาสตราจารย์ ดร.วนิดา หลายวัฒนไพศาล
Asst. Prof. Dr. Wanida LAIWATTANAPAI SAN | จุฬาลงกรณ์มหาวิทยาลัย
Chulalongkorn University |
| 2 | ผู้ช่วยศาสตราจารย์ ดร.สมจินตนา ทวีทิพย์
Asst. Prof. Dr. Somjintana Toutip | มหาวิทยาลัยมหาสารคาม
Mahasarakham University |
| 3 | ผู้ช่วยศาสตราจารย์ ดร.ชยานิศ ลือวานิช
Asst. Prof. Dr. Chayanit Luevanich | มหาวิทยาลัยราชภัฏภูเก็ต
Phuket Rajabhat University |
| 4 | ผู้ช่วยศาสตราจารย์ ดร.อมรพันธ์ อัจจิมาพร
Asst. Prof. Dr. Amornpan Ajjimaporn | มหาวิทยาลัยมหิดล
Mahidol University |
| 5 | อาจารย์อัมพิกา นันท์บัญชา
Ampika Nanbancha | มหาวิทยาลัยมหิดล
Mahidol University |

Editorial Board

- | | | |
|---|--|--|
| 1 | ผู้ช่วยศาสตราจารย์ ดร.อานัติ ต๊ะปินตา
Asst. Prof. Dr. Anat Thapinta | มหาวิทยาลัยราชภัฏสวนสุนันทา
Suan Sunandha Rajabhat University |
| 2 | Prof. Dr. Hongjoo Kim | Kyungpook National University, Korea |
| 3 | Prof. Dr.-Ing. Mitra Djamal | Institut Teknologi Bandung, Indonesia |
| 4 | Assoc. Prof. Dr. Nguyen Hieu Trung | Can Tho University, Vietnam |



5	Prof. Dr. Subhash C. Pandey	Journal of Environmental Research and Development (JERAD), India
6	Prof. Emeritus Manit Rappon	Lakehead University, Canada
7	Assoc. Prof. Dr. Thanh Son Dao	Vietnam National University, Vietnam
8	Dr. Soo Rin Kim	Kyungpook National University, Korea
9	Dr. Vinh Truong Hoang	Ho Chi Minh City Open University, Vietnam
10	Dr. Wong Tze Jin	Universiti Putra Malaysia Bintulu Campus, Malaysia
11	Dr. Stephen Raymond Morley	Leicester Royal Infirmary, England

Editorial Managers

1	ผู้ช่วยศาสตราจารย์ ดร.อาณัติ ต๊ะปิ่นตา Asst. Prof. Dr. Anat Thapinta	มหาวิทยาลัยราชภัฏสวนสุนันทา Suan Sunandha Rajabhat University
2	ดร.วัฒนา พันธุ์พีช Dr. Wattana Panphut	มหาวิทยาลัยราชภัฏสวนสุนันทา Suan Sunandha Rajabhat University
3	ผศ.ดร.ทัศนาวลัย อุฑารสกุล Asst. Prof. Dr. Tatsanawalai Utarasakul	มหาวิทยาลัยราชภัฏสวนสุนันทา Suan Sunandha Rajabhat University
4	ผศ.ดร.พิจิตรา จอมศรี Asst. Prof. Dr. Pijitra Jomsri	มหาวิทยาลัยราชภัฏสวนสุนันทา Suan Sunandha Rajabhat University
5	ดร.นิช วงศ์ส่องจำ Dr. Nich Wongsongja	มหาวิทยาลัยราชภัฏสวนสุนันทา Suan Sunandha Rajabhat University
6	ดร.มนัสวี เดชกล้า Dr. Manussawee Dechkla	มหาวิทยาลัยราชภัฏสวนสุนันทา Suan Sunandha Rajabhat University
7	ดร.ธนิดา ฉั่วเจริญ Dr. Thanida Chuacharoen	มหาวิทยาลัยราชภัฏสวนสุนันทา Suan Sunandha Rajabhat University
8	ดร.สันสนีย์ แสนศิริพันธ์ Dr. Sansanee Sansiribhan	มหาวิทยาลัยราชภัฏสวนสุนันทา Suan Sunandha Rajabhat University
9	ดร.ชูเกียรติ ผุดพรมราช Dr. Chookait Pudprommarat	มหาวิทยาลัยราชภัฏสวนสุนันทา Suan Sunandha Rajabhat University
10	ดร.พลอยทราย โอฮามา Dr. Ploysai Ohama	มหาวิทยาลัยราชภัฏสวนสุนันทา Suan Sunandha Rajabhat University
11	ดร.สุริยัน สมพงษ์ Dr. Suriyan Sompong	มหาวิทยาลัยราชภัฏสวนสุนันทา Suan Sunandha Rajabhat University

กำหนดการการประชุมสวนสุนันทาวิชาการฯ



08.00 - 09.00 น.	ลงทะเบียน ณ บริเวณด้านหน้าห้องประชุมกรุงธนบอลล์รูม ชั้น 3
09.00 - 09.15 น.	กล่าวรายงานการประชุม โดย ผู้ช่วยศาสตราจารย์ ดร.อาณัติ ต๊ะปิ่นตา คณบดีคณะวิทยาศาสตร์และเทคโนโลยี
09.15 - 09.30 น.	กล่าวเปิดการประชุม โดย รองศาสตราจารย์ ดร.ฤเดช เกิดวิชัย อธิการบดีมหาวิทยาลัยราชภัฏสวนสุนันทา
09.30 - 10.00 น.	- พิธีมอบของที่ระลึกแก่เจ้าภาพร่วมและถ่ายภาพร่วมกัน - พิธีมอบรางวัลบทความวิจัยดีเด่น จำนวน 3 รางวัล โดย รองศาสตราจารย์ ดร.ฤเดช เกิดวิชัย อธิการบดีมหาวิทยาลัยราชภัฏสวนสุนันทา
10.00 - 10.30 น.	บรรยายพิเศษ เรื่อง “Recent Technology Breakthroughs in the Control of Iron Deficiency Anemia” โดย Prof.Dr.Michael Bruce Zimmermann Zurich Swiss Federal Institute of Technology (ETH), Switzerland
10.30 - 11.00 น.	บรรยายพิเศษ เรื่อง “Universities Facing Severe Challenges of Fewer Children Trend and International Competition” โดย Prof.Dr.Chih-Hsiang Liao Vice President of Chia Nan University of Pharmacy and Science, Taiwan
11.00 - 11.15 น.	รับประทานอาหารว่าง ณ ด้านหน้าห้องประชุมภาณุรังษีบอลล์รูม ชั้น 1
11.00 - 12.15 น.	นำเสนอผลงานวิจัยแบบภาคโปสเตอร์ ณ ด้านหน้าห้องประชุมภาณุรังษีบอลล์รูม ชั้น 1
11.15 - 12.15 น.	นำเสนอผลงานวิจัยแบบภาคบรรยาย ณ ห้องประชุม ชั้น 1, 2 และ 3
ห้องภาณุรังษี เอ	ชั้น 1 กลุ่มสาขาคอมพิวเตอร์และเทคโนโลยีสารสนเทศ (กลุ่มย่อยที่ 1)
ห้องภาณุรังษี ซี	ชั้น 1 กลุ่มสาขาคอมพิวเตอร์และเทคโนโลยีสารสนเทศ (กลุ่มย่อยที่ 2)
ห้องบงกชรัตน์ เอ	ชั้น 2 กลุ่มสาขาฟิสิกส์และพลังงาน
ห้องบงกชรัตน์ บี	ชั้น 2 กลุ่มสาขาวิทยาศาสตร์การกีฬาและวิทยาศาสตร์สุขภาพ
ห้องบงกชรัตน์ ซี	ชั้น 2 กลุ่มสาขาเคมีและนิติวิทยาศาสตร์
ห้องบุษบงกช เอ	ชั้น 2 กลุ่มสาขาวิทยาศาสตร์สิ่งแวดล้อมและเทคโนโลยี
ห้องบุษบงกช บี	ชั้น 2 กลุ่มสาขาชีววิทยา เทคโนโลยีชีวภาพ และจุลชีววิทยา
ห้องกรุงธนบอลล์รูม	ชั้น 3 กลุ่มสาขาวิทยาศาสตร์และเทคโนโลยีการอาหารและคหกรรมศาสตร์
12.15 - 13.15 น.	รับประทานอาหารกลางวัน ณ ห้องอาหารริมน้ำ ชั้น 1

- 13.15 – 15.30 น. นำเสนอผลงานวิจัยแบบภาคโปสเตอร์
ณ ด้านหน้าห้องประชุมภาณูรังษีบอลล์รูม ชั้น 1 (ต่อ)
พร้อมมอบวุฒิบัตรการนำเสนอผลงานวิจัยแบบภาคโปสเตอร์
- 13.15 – 14.45 น. นำเสนอผลงานวิจัยแบบภาคบรรยาย ณ ห้องประชุมชั้น 1, 2 และ 3 (ต่อ)
ห้องภาณูรังษี เอ ชั้น 1 กลุ่มสาขาคอมพิวเตอร์และเทคโนโลยีสารสนเทศ (กลุ่มย่อยที่ 1)
ห้องภาณูรังษี ซี ชั้น 1 กลุ่มสาขาคอมพิวเตอร์และเทคโนโลยีสารสนเทศ (กลุ่มย่อยที่ 2)
ห้องบงกชรัตน์ เอ ชั้น 2 กลุ่มสาขาฟิสิกส์และพลังงาน
ห้องบงกชรัตน์ บี ชั้น 2 กลุ่มสาขาวิทยาศาสตร์การกีฬาและวิทยาศาสตร์สุขภาพ
ห้องบงกชรัตน์ ซี ชั้น 2 กลุ่มสาขาคณิตศาสตร์และสถิติ
ห้องบุษบงกช เอ ชั้น 2 กลุ่มสาขาวิทยาศาสตร์สิ่งแวดล้อมและเทคโนโลยี
ห้องบุษบงกช บี ชั้น 2 กลุ่มสาขาชีววิทยา เทคโนโลยีชีวภาพ และจุลชีววิทยา
ห้องกรุงธนบอลล์รูม ชั้น 3 กลุ่มสาขาวิทยาศาสตร์และเทคโนโลยีการอาหารและคหกรรมศาสตร์
- 14.45 – 15.00 น. รับประทานอาหารว่าง ณ ด้านหน้าห้องประชุมกลุ่มย่อย ชั้น 1, 2 และ 3
- 15.00 – 17.00 น. นำเสนอผลงานวิจัยแบบภาคบรรยาย ณ ห้องประชุม 1, 2 และ 3 (ต่อ)
พร้อมมอบวุฒิบัตรการนำเสนอผลงานวิจัยแบบภาคบรรยาย ณ ห้องประชุมกลุ่มย่อย

Conference Schedule

08.00 - 09.00	Registration (Krungthon Ballroom, 3 rd floor front area)
09.00 - 09.15	Giving a briefing of the conference Asst. Prof. Dr. Anat Thapinta Dean of Faculty of Science and Technology
09.15 - 09.30	SsSci 2019 Opening ceremony Associate Professor Dr. Luedech Girdwichai President of Suan Sunandha Rajabhat University
09.30 - 10.00	Presenting a token of appreciation to the distinguished co-hosts and taking a group photo Presenting three awards for outstanding Associate Professor Dr. Luedech Girdwichai President of Suan Sunandha Rajabhat University
10.00 - 10.30	Keynote Speech “Recent Technology Breakthroughs in the Control of Iron Deficiency Anemia” Professor Dr. Michael Bruce Zimmermann Zurich Swiss Federal Institute of Technology (ETH), Switzerland
10.30 - 11.00	Keynote Speech “Universities Facing Severe Challenges of Fewer Children Trend and International Competition” Professor Dr. Chih-Hsiang Liao Vice President of Chia Nan University of Pharmacy and Science, Taiwan
11.00 - 11.15	Refreshment Breaks at Phanurandsi Ballroom, 1st floor front area
11.00 - 12.15	Poster presentation session (Phanurangsai Ballroom, 1st floor front area)
11.15 - 12.15	Oral presentation session (meeting room 1st, 2nd and 3rd floor)
Phanurangsai Room A, 1 st floor	Computer Science and Information Technology (Group 1)
Phanurangsai Room C, 1 st floor	Computer Science and Information Technology (Group 2)
Bongkotrat Room A, 2 nd floor	Physics and Energy
Bongkotrat Room B, 2 nd floor	Sports and Health Science
Bongkotrat Room C, 2 nd floor	Chemistry and Forensic Science
Busabongkot Room A, 2 nd floor	Environmental Science & Technology

Busabongkot Room B, 2nd floor Biology, Biotechnology and Microbiology
 Krungthon Ballroom, 3rd floor Food Science & Technology and Home Economics

12.15 – 13.15 Lunch at Rim Nam Terrace, 1st floor

13.15 – 15.30 **Poster presentation session (Phanurangsi Ballroom, 1st floor front area) (cont.)**
 Presenting poster presentation certificates at the presentation area

13.15 – 14.45 **Oral presentation session (Meeting room 1st, 2nd and 3rd floor) (cont.)**

Phanurangsi Room A, 1st floor Computer Science and Information Technology (Group 1)

Phanurangsi Room C, 1st floor Computer Science and Information Technology (Group 2)

Bongkotrat Room A, 2nd floor Physics and Energy

Bongkotrat Room B, 2nd floor Sports and Health Science

Bongkotrat Room C, 2nd floor Chemistry and Forensic Science

Busabongkot Room A, 2nd floor Environmental Science & Technology

Busabongkot Room B, 2nd floor Biology, Biotechnology and Microbiology

Krungthon Ballroom, 3rd floor Food Science & Technology and Home Economics

14.45 – 15.00 **Refreshment Breaks at front area of each meeting room (1st, 2nd and 3rd floor)**

15.00 – 17.00 **Oral presentation session (Meeting room 1st, 2nd and 3rd floor) (cont.)**

Presenting oral presentation certificates at the presentation rooms

Oral Presentation

Conference Sessions: Computer Science and Information Technology (Group 1)

Phanurangsi Room A, 1st floor (ห้องภาณูรังษี เอ ชั้น 1)

		Chairperson					Co-Chairperson
		Dr.Vinh Truong Hoang Vice-Dean, Faculty of Information Technology Ho Chi Minh City Open University ผู้ช่วยศาสตราจารย์ ดร.วรสิทธิ์ ชูชัยวัฒนา คณบดีวิทยาลัยครีเอทีฟดีไซน์แอนด์ เอ็นเตอร์ เทนเมนต์เทคโนโลยี มหาวิทยาลัยธุรกิจบัณฑิต					อาจารย์ ดร.กิตติคุณ มีทองจันทร์ หัวหน้าภาควิชาวิทยาศาสตร์ประยุกต์คณะวิทยาศาสตร์และเทคโนโลยี มหาวิทยาลัยราชภัฏสวนสุนันทา
No.	Time	Paper Code/ Registration Code	Name	Institute	Topic	International/ National	
1.	11.15-11.30	SSSCI2019_CS_4 SSSCI2019_O_121	Way Sokhom	Mahidol University	Development of Innovative Media for Communication Sangha in Phra Nakhon, Bangkok, Thailand	International	
2.	11.30.-11.45	SSSCI2019_CS_8 SSSCI2019_O_56	กรรณิการ์ กมลรัตน์ Kannikar Kamolrat	Sakon Nakhon Rajabhat University	Application Development for Pon-Yang- Kham Fattened Cattle in Sakon Nakhon Province on Android Operating System	National	
3.	11.45-12.00	SSSCI2019_CS_1 SSSCI2019_O_4	รุจีจันทร์ วิชิวานีเวศน์ Rujijan Vichivanives	มหาวิทยาลัยราชภัฏ สวนสุนันทา	การพัฒนาต้นแบบสมาร์ตฟาร์มการปลูกดอกมะลิ ด้วยอินเทอร์เน็ตของทุกสรรพสิ่ง	National	
4.	12.00-12.15	SSSCI2019_CS_6 SSSCI2019_O_44	จีระศักดิ์ นำประดิษฐ์ Jeerasak Numpradit	มหาวิทยาลัยเทคโนโลยี พระจอมเกล้าพระนครเหนือ	การบำบัดทางเลือกสำหรับโรคกลัวความสูงโดยใช้ ระบบความจริงเสมือน	National	
12.15-13.15		Buffet Lunch, Rim Nam Terrace, 1st floor					
5.	13.15-13.30	SSSCI2019_CS_9 SSSCI2019_O_71	ลูกหนู อู่ทอง Looknu Authong	Rajamangala University of Technology Suvarnabhumi	การนำเทคโนโลยีอินเทอร์เน็ตออฟติงค์มา ประยุกต์ใช้งาน	National	
6.	13.30-13.45	SSSCI2019_CS_10 SSSCI2019_O_80	ชัชชนันท์ น้าวน Chatchanun Namwon	มหาวิทยาลัยราชภัฏ พิบูลสงคราม	การวิเคราะห์พื้นที่ที่เหมาะสมในการตั้งโรงงาน อุตสาหกรรมชีวมวลอัดแห้งในจังหวัดพิษณุโลก	National	

No.	Time	Paper Code/ Registration Code	Name	Institute	Topic	International/ National
7.	13.45-14.00	SSSCI2019_CS_11 SSSCI2019_O_85	ศราวุธ พาจรทิต Sarawut Pajonetid	มหาวิทยาลัยราชภัฏ เชียงใหม่	โมบายแอปพลิเคชันสำหรับรู้จำสมุนไพรรบน ระบบปฏิบัติการแอนดรอยด์ โดยใช้ไลบรารีของเทน เซอร์โฟร	National
8.	14.00-14.15	SSSCI2019_CS_12 SSSCI2019_O_91	ประภาภรณ์ นพภาลัย Praphaporn Nopparai	มหาวิทยาลัยเทคโนโลยี พระจอมเกล้าพระนครเหนือ	การประยุกต์กระบวนการออกแบบประสบการณ์ ผู้ใช้ในการพัฒนาเว็บไซต์พาณิชย์อิเล็กทรอนิกส์ สำหรับผู้ประกอบการที่ไม่เชี่ยวชาญเทคโนโลยี	National
9.	14.15-14.30	SSSCI2019_CS_13 SSSCI2019_O_93	ธนาวุฒิ ฐูปูชา Thanawut Thoopucha	มหาวิทยาลัยราชภัฏ พิบูลสงคราม	การป้องกันและตรวจจับการรั่วไหลของน้ำภายใน บ้านผ่านระบบควบคุมการไหลของน้ำด้วยอุปกรณ์ เคลื่อนที่	National
10	14.30-14.45	SSSCI2019_CS_14 SSSCI2019_O_95	ศุภชัย พรหมประเสริฐ Supachai Promprasoet	มหาวิทยาลัยราชภัฏ พิบูลสงคราม	ระบบควบคุมการเปิดปิดคอมพิวเตอร์ทางไกลผ่าน อุปกรณ์เคลื่อนที่	National
14.45-15.00				Refreshment Break		
11.	15.00-15.15	SSSCI2019_CS_15 SSSCI2019_O_99	อุบลศิลป์ โพธิ์พรม Ubonsilp Phoprom	มหาวิทยาลัยราชภัฏ สกลนคร	การพัฒนาแอปพลิเคชันเพื่อสนับสนุนงานบริการ ด้วยมาตรฐานด้านเทคโนโลยีสารสนเทศ	National
12.	15.15-15.30	SSSCI2019_CS_16 SSSCI2019_O_83	พิสิษฐ์ แม้นวงศ์เดือนPisit Manwongdeon	มหาวิทยาลัยเทคโนโลยี พระจอมเกล้าพระนครเหนือ	การเพิ่มประสิทธิภาพการบริหารจัดการคลังสินค้า กรณีศึกษาบริษัทผู้ผลิตและจำหน่ายชิ้นส่วน อะไหล่เครื่องจักรกลการเกษตร	National
13.	15.30-15.45	SSSCI2019_CS_17 SSSCI2019_O_117	มนีรัตน์ ภารนนท์ Maneerat Paranan	มหาวิทยาลัยเทคโนโลยีราช มงคลตะวันออก วิทยาเขต จักรพงษ์ภูวนารถ	การพัฒนาเว็บปัญญาประดิษฐ์เพื่อการเทียบโอน หน่วยกิตส่งเสริมการเรียนรู้ตลอดชีวิต	National
14.	15.45-16.00	SSSCI2019_CS_18 SSSCI2019_O_120	อุบลศิลป์ โพธิ์พรม Ubonsilp Phoprom	มหาวิทยาลัยราชภัฏ สกลนคร	การพัฒนาระบบการบริการตอบคำถามอัตโนมัติ โดยเทคโนโลยี ไลน์ บอท (LINE BOT) ของ สถาบันวิจัยและพัฒนา มหาวิทยาลัยราชภัฏ สกลนคร	National
15.	16.00-16.15	SSSCI2019_CS_38 SSSCI2019_O_235	ปานจิต มุสิก	มหาวิทยาลัยราชภัฏ นครศรีธรรมราช	การพัฒนาระบบควบคุมอุณหภูมิและความชื้นใน โรงเรือนปลูกพืชจำลอง	National

SsSci^{2nd} conference 2019

Conference Sessions: Computer Science and Information Technology (Group 2)

Phanurangsi Room C, 1st floor (ห้องภาณูรังษี ซี ชั้น 1)

Chairperson		Co-Chairperson				
ผู้ช่วยศาสตราจารย์สมศักดิ์ ศรีสวการย์ คณบดีคณะวิทยาศาสตร์ มหาวิทยาลัยราชภัฏลำปาง		อาจารย์ ดร.นพดล ผู้มีจรรยา สาขาวิชาคอมพิวเตอร์ศึกษา คณะวิทยาศาสตร์และเทคโนโลยี มหาวิทยาลัยราชภัฏนครปฐม				
No.	Time	Paper Code/ Registration Code	Name	Institute	Topic	International/ National
1.	11.15-11.30	SSSCI2019_CS_24 SSSCI2019_O_152	พฤกษนันท์ คำลาพิศ Pruksanan Kamlapit	มหาวิทยาลัยพะเยา	การวิเคราะห์และพยากรณ์ช่องทางการจำหน่าย สินค้าในธุรกิจอีคอมเมิร์ซ	National
2.	11.30-11.45	SSSCI2019_CS_25 SSSCI2019_O_156	รัชดาพร คณางษ์ Ratchadaporn Kanawong,	มหาวิทยาลัยศิลปากร	Ginrai-Bot for Ordering and Recommending Healthy Food Online Application	National
3.	11.45-12.00	SSSCI2019_CS_26 SSSCI2019_O_158	สุทธิษา กันจู Suttisa Kunju	มหาวิทยาลัยพะเยา	การพัฒนาการส่งเสริมการขายเครื่องสำอางบน เฟสบุ๊ก กรณีศึกษาร้าน เอ็ม แอนด์ แพร์	National
4.	12.00-12.15	SSSCI2019_CS_28 SSSCI2019_O_162	Chaiyapan Charoensuk	มหาวิทยาลัย ราชภัฏพระนคร	แอปพลิเคชันช่วยแจ้งเตือน การรับประทานยา	National
12.15-13.15		Buffet Lunch, Rim Nam Terrace, 1 st floor				
5.	13.15-13.30	SSSCI2019_CS_29 SSSCI2019_O_163	สุมิตรา นวลมีศรี Sumitra Nuanmeesri	Suan Sunandha Rajabhat University	การพัฒนาเว็บไซต์และเว็บแอปพลิเคชันด้วยบุทส แตร์ป กรณีศึกษา นักศึกษาสาขาวิชาเทคโนโลยี สารสนเทศ คณะวิทยาศาสตร์และเทคโนโลยี มหาวิทยาลัยราชภัฏสวนสุนันทา	National
6.	13.30-13.45	SSSCI2019_CS_31 SSSCI2019_O_181	ทนาลักษณ์ ปราณีกุมาร Thanaluk Pranekunakol	Burapha University	การคัดกรองข้อมูลสำหรับระบบเซนเซอร์ไร้สาย ขนาดใหญ่โดย STackSTorm	National
7.	13.45-14.00	SSSCI2019_CS_32 SSSCI2019_O_202	กิตติพัฒน์ ปันพัก Kttipat Panfak	มหาวิทยาลัยเทคโนโลยีราชมงคลสุวรรณภูมิ	การออกแบบ FTP เพื่อใช้ในการรับส่งไฟล์ระหว่าง Client และ Server	National

No.	Time	Paper Code/ Registration Code	Name	Institute	Topic	International/ National
8.	14.00-14.15	SSSCI2019_CS_35 SSSCI2019_O_214	ปรีตาวรรณ เกษเมธีการุณ Preedawon Kadmateekarun	Suan Sunandha Rajabhat University	การพัฒนาแอปพลิเคชันระบบจัดการรดน้ำ อัตโนมัติ	National
9.	14.15-14.30	SSSCI2019_CS_36 SSSCI2019_O_221	กาญจนา ชัดิทะจักร์ Kanchana Kanthachak	มหาวิทยาลัยราชภัฏ เชียงใหม่	การส่งเสริมการอนุรักษ์ภูมิปัญญาท้องถิ่นด้านการ เพาะเลี้ยงครั้งโดยใช้เทคโนโลยีทางคอมพิวเตอร์	National
10	14.30-14.45	SSSCI2019_CS_21 SSSCI2019_O_130	จักรภัฏ เจนโรสง Jakapat Janethaisong	Rajamangala University of Technology Suvarnabhumi	การจัดการความปลอดภัยของดีเอ็นเอส	National
14.45-15.00 Refreshment Break						
11.	15.00-15.15	SSSCI2019_CS_39 SSSCI2019_O_250	ประชุม พันรอด	มหาวิทยาลัยราชภัฏเพชรบุรี	การพัฒนาระบบการจัดการห้องประชุมออนไลน์ คณะวิทยาศาสตร์และเทคโนโลยี มหาวิทยาลัยราช ภัฏเพชรบุรี	National
12.	15.15-15.30	SSSCI2019_CS_23 SSSCI2019_O_150	บพิตร ไชยนอก Bopit Chainok	มหาวิทยาลัยราชภัฏนครปฐม	ระบบตรวจวัดสภาพอากาศที่มีผลต่อคุณภาพน้ำใน บ่อเลี้ยงกุ้งขาว	National
13.	15.30-15.45	SSSCI2019_CS_20 SSSCI2019_O_123	วุฒิชัย นาคเพียทา Voottichai Nakpeata	Rajamangala University of Technology Suvarnabhumi	การนำโครงข่ายเฉพาะกิจมาประยุกต์ใช้งาน	National
14.	15.45-16.00	SSSCI2019_CS_19 SSSCI2019_O_122	พัทธนันท์ นาคยศ Pattanan Nakyos	Rajamangala University of Technology Suvarnabhumi	การนำโปรโตคอลมาใช้หาเส้นทางบนเครือข่ายไร้สาย	National
15.	16.00-16.15	SSSCI2019_CS_5 SSSCI2019_P_42	ชัชชฎา โพธิ์ลักษณะ Chatchuda Potiluck	Mahidol University	ระบบสารสนเทศควบคุมการประมวลผลการศึกษา กรณีศึกษาวิทยาลัยการจัดการ มหาวิทยาลัยมหิดล	National
16.	16.15-16.30	SSSCI2019_CS_7 SSSCI2019_P_45	อุไรวรรณ รักภกวางค์ Uraiwn Ruxpakawong	มหาวิทยาลัยราชภัฏ พิบูลสงคราม	การสร้างแบบทดสอบคำสั่งสืบค้นข้อมูล และตรวจ คำตอบ โดยอัตโนมัติ	National

SsSci^{2nd} conference 2019

Conference Sessions: Chemistry and Forensic Science

Bongkotrat Room C, 2nd floor (ห้องบงกชรัตน์ ซี ชั้น 2)

Chairperson	Co-Chairperson
ผู้ช่วยศาสตราจารย์ ดร.พูนศิริ ทิพย์เนตร คณบดีคณะวิทยาศาสตร์และเทคโนโลยี มหาวิทยาลัยราชภัฏเพชรบุรี	อาจารย์ ดร.พลอยทราย โอฮามา สาขาวิชาเคมี คณะวิทยาศาสตร์และเทคโนโลยี มหาวิทยาลัยราชภัฏสวนสุนันทา

No.	Time	Paper Code/ Registration Code	Name	Institute	Topic	International/ National
1.	11.15-11.30	SSSCI2019_CH_7 SSSCI2019_O_160	Pornpan Tana	Maha Sarakham Rajabhat University	The preparation of hybrid material of cobalt complex into mesoporous silica from the rice husk	International
2.	11.30-11.45	SSSCI2019_CH_11 SSSCI2019_O_182	Pasakorn Sangnikul	Maha Sarakham Rajabhat University	DFT investigation of toluene adsorption on silicon carbide nanosheet doping with transition metal for sensing application	International
3.	11.45-12.00	SSSCI2019_CH_19 SSSCI2019_O_604	Jitlada Chumee	Suan Sunandha Rajabhat University	The Effect of Viscosity-imparting Agent on Textural Properties of Toddy Palm Syrup	International
4.	12.00-12.15	SSSCI2019_CH_3 SSSCI2019_O_76	ดุสิตพร ศรีลักษณ์ Dusitporn Srilak	มหาวิทยาลัยเกษตรศาสตร์	อิทธิพลของสารตัวเติมต่อสมบัติเชิงกลของฟิล์มยางธรรมชาติโปรตีนตำผสมลิกนิน	National
12.15-13.15		Buffet Lunch, Rim Nam Terrace, 1 st floor				
5.	13.15-13.30	SSSCI2019_CH_6 SSSCI2019_O_140	ชุตินา ศิลาณีเวช Chutima Silamaneewet	มหาวิทยาลัยสงขลานครินทร์	ผลของการปรับสภาพขานอ้อยด้วยต่างที่มีต่อการเพิ่มผลผลิตน้ำตาลและองค์ประกอบทางเคมี	National
6.	13.30-13.45	SSSCI2019_CH_21 SSSCI2019_O_246	วัชรารณณ์ ประภาสะโนบล Vatcharaporn Prapasanol	มหาวิทยาลัยราชภัฏเพชรบุรี	การศึกษาสารพิษเคมี ปริมาณฟีนอลิกและฤทธิ์ต้านอนุมูลอิสระของจาวตาล	National

No.	Time	Paper Code/ Registration Code	Name	Institute	Topic	International/ National
7.	13.45-14.00	SSSCI2019_CH_22 SSSCI2019_O_243	ปัทมาพร ยอดสันติ Pattamaporn Yodsanti	มหาวิทยาลัยราชภัฏเพชรบุรี	การประเมินศักยภาพการเก็บกักคาร์บอนของต้น ตาลในจังหวัดเพชรบุรี	National
8.	14.00-14.15	SSSCI2019_CH_20 SSSCI2019_P_147	Wilasinee Sathitdetkunchorn	Rajabhat Nakhonratchasima University	การวิเคราะห์ตะกั่ว เหล็ก และแคดเมียม ในน้ำ บาดาล โดยเทคนิคอะตอมมิก แอบซอร์พ ชันสเปกโทรโฟโตเมทรี	National
9	14.15-14.30	SSSCI2019_CH_14 SSSCI2019_P_199	เอกชัย อั้งชะ Ekkachai Achcha	มหาวิทยาลัยราชภัฏนครสวรรค์	การเคลือบलयนิ้วมือแฝงด้วยรีดิวซ์แกรฟีน ออกไซด์บนกระจกเอฟทีโอโดยใช้การเคลือบ ไฟฟ้า	National
14.45-15.00		Refreshment Break				

SsSci^{2nd} conference 2019

Conference Sessions: Mathematics and Statistics
Bongkotrat Room C, 2nd floor (ห้องบงกชรัตน์ ซี ชั้น 2)

Chairperson		Co-Chairperson				
ผู้ช่วยศาสตราจารย์ ดร.ประยัตต์ แสงงาม ภาควิชาสถิติ คณะวิทยาศาสตร์ มหาวิทยาลัยศิลปากร		อาจารย์ ดร.ชูเกียรติ ผุดพรมราช หัวหน้าสาขาวิชาสถิติประยุกต์ คณะวิทยาศาสตร์และเทคโนโลยี มหาวิทยาลัยราชภัฏสวนสุนันทา				
No.	Time	Paper Code/ Registration Code	Name	Institute	Topic	International/ National
10.	14.30-14.45	SSSCI2019_MA_1 SSSCI2019_O_12	สิริพร หล้าปวงคำ Siriporn Lapouangkham	มหาวิทยาลัยเกษตรศาสตร์	เงื่อนไขบางประการของฟังก์ชันการบวก	National
14.45-15.00		Refreshment Break				
11.	15.00-15.15	SSSCI2019_MA_2 SSSCI2019_O_17	เจษฎา สุจริตธุระการ Jedsada Sutjaritthurakan	มหาวิทยาลัยราชภัฏภูเก็ต	ผลของการรณรงค์การสวมหน้ากากอนามัยที่มีผล ต่อตัวแบบเชิงคณิตศาสตร์การแพร่ระบาดของโรค หัด	National
12.	15.15-15.30	SSSCI2019_MA_3 SSSCI2019_O_77	ปณิธิ วิจิตรไกรวิน Paniti Vichitkraivin	มหาวิทยาลัยมหิดล	The Resistance Factors Affecting the Adoption of Healthcare Robots Technology in Thailand Government Hospital	National
13.	15.30-15.45	SSSCI2019_MA_5 SSSCI2019_O_86	สิทธิกร นาคขาว Siththikorn Nakkao	มหาวิทยาลัยเกษตรศาสตร์	เอกลักษณ์เชิงฟังก์ชันของอนุพันธ์	National
14.	15.45-16.00	SSSCI2019_MA_6 SSSCI2019_O_107	เยาวลักษณ์ ศรีเมือง Yaowaluk Srimuang	Faculty of Science, Ramkhamhang University	General Solution of the n -D Pompeiu Functional Equation	National
15.	16.00-16.15	SSSCI2019_MA_7 SSSCI2019_O_153	ธัญญาลักษณ์ เทพสุวรรณ Tunyaluk Thepsuwan	มหาวิทยาลัยเชียงใหม่	กิจกรรมการเรียนรู้เกี่ยวกับอัตราส่วนทองบน ร่างกายมนุษย์	National

No.	Time	Paper Code/ Registration Code	Name	Institute	Topic	International/ National
16.	16.15-16.30	SSSCI2019_MA_8 SSSCI2019_O_171	ศศิวิมล คณฑา Sasiwimon Raokhetkit Khontha	มหาวิทยาลัยธรรมศาสตร์	การศึกษาความเป็นไปได้ทางเศรษฐศาสตร์ในการ ลดขั้นตอนของการเคลือบแข็งในกระบวนการผลิต เลนส์	National
17.	16.30-16.45	SSSCI2019_MA_9 SSSCI2019_O_173	Rukchart Prasertpong รักชาติ ประเสริฐพงษ์	Nakhon Sawan Rajabhat University	ไอทีลภายในรัฟและควอซี-ไอทีลรัฟในปริภูมิการ ประมาณของกึ่งกลุ่มภายใต้ความสัมพันธ์พรีออ เคอร์และคอมแพทิเบิล	National
18.	16.45-17.00	SSSCI2019_MA_10 SSSCI2019_O_176	ธัญวรัตน์ ชัชรัตน์ Thanwarat Chatcharata	มหาวิทยาลัยราชภัฏ นครสวรรค์	ไป-ไอทีลรัฟและไป-ไอทีลเฉพาะรัฟในปริภูมิการ ประมาณของกึ่งกลุ่มภายใต้ความสัมพันธ์พรีออ เคอร์และคอมแพทิเบิล	National

SsSci^{2nd} conference 2019

Conference Sessions: Physics and Energy
Bongkotrat Room A, 2nd floor (ห้องบงกชรัตน์ เอ ชั้น 2)

Chairperson	Co-Chairperson
รองศาสตราจารย์ ดร.ปานจิต มุสิก คณบดีคณะวิทยาศาสตร์และเทคโนโลยี มหาวิทยาลัยราชภัฏนครศรีธรรมราช	รองศาสตราจารย์ ดร.ศิริชัย เทพา คณะพลังงาน สิ่งแวดล้อมและวัสดุ มหาวิทยาลัยเทคโนโลยีพระจอมเกล้าธนบุรี

No.	Time	Paper Code/ Registration Code	Name	Institute	Topic	International/ National
1.	11.15-11.30	SSSCI2019_PH_25 SSSCI2019_O_164	Nattapon Chantarapanich	Kasetsart Univeristy	Design and Analysis of Plastic Medical Tray for Implant Packaging	International
2.	11.30.-11.45	SSSCI2019_PH_27 SSSCI2019_O_192	Natthaphong Kamma	Khon Kaen University	A Polymeric Coating on Prelithiated Silicon-Based Nanoparticles for High Capacity Anodes used in Li-ion Batteries	International
3.	11.45-12.00	SSSCI2019_PH_1 SSSCI2019_O_6	Pinyapach Tiamduangtawan	มหาวิทยาลัยเกษตรศาสตร์	การพัฒนาวัสดุกักเก็บอนุภาคนิวตรอนที่สามารถซ่อมแซมตัวเองจากวัสดุเชิงประกอบ พอลิไวนิลแอลกอฮอล์ (PVA) และซาแมเรียมออกไซด์ (Sm ₂ O ₃)	National
4.	12.00-12.15	SSSCI2019_PH_2 SSSCI2019_O_7	กุลลิตา โกละนันท์ Kullita Kolanan	มหาวิทยาลัยเกษตรศาสตร์	การตรวจวิเคราะห์โลหะอะมัลกัมด้วยเทคนิคการเลี้ยวเบนของรังสีเอกซ์ และกล้องจุลทรรศน์อิเล็กตรอนแบบส่องกราด	National
12.15-13.15				Buffet Lunch, Rim Nam Terrace, 1st floor		
5.	13.15-13.30	SSSCI2019_PH_4 SSSCI2019_O_16	Wichan Lertlop	มหาวิทยาลัยราชภัฏ สวนสุนันทา	การกำหนดปัญหาให้นักศึกษาค้นคว้าเพื่อพัฒนาผลสัมฤทธิ์ทางการเรียนของนักศึกษาชั้นปีที่ 1 สาขาฟิสิกส์ประยุกต์ปีการศึกษา 2562	National

No.	Time	Paper Code/ Registration Code	Name	Institute	Topic	International/ National
6.	13.30-13.45	SSSCI2019_PH_7 SSSCI2019_O_37	อัศวิน ยอดรักษ์ Assawin Yodruk	มหาวิทยาลัยเทคโนโลยีพระ จอมเกล้าพระนครเหนือ	การพัฒนาเครื่องทดสอบความล้าแบบหมุนดัด Development of A Rotary-Bending Fatigue Tester	National
7.	13.45-14.00	SSSCI2019_PH_9 SSSCI2019_O_46	อภิฤดี ตัณฑเวชกิจ Apirudee Tentawechakit	มหาวิทยาลัยธรรมศาสตร์	การประเมินศักยภาพการอนุรักษ์พลังงาน กรณีศึกษา: โรงพยาบาลของรัฐขนาดใหญ่	National
8.	14.00-14.15	SSSCI2019_PH_10 SSSCI2019_O_47	พิศาล ปานสุข Pisan Pansook	มหาวิทยาลัยธรรมศาสตร์	การประเมินความคุ้มค่าทางเศรษฐศาสตร์ ของ การผลิตไฟฟ้าด้วยกังหันลมแบบ แนวตั้ง โดยใช้ ลมทั้งจากระบบกำจัดฝุ่นในโรงงานผลิตปูนกาว ซีเมนต์	National
9.	14.15-14.30	sssci2019_PH_23 sssci2019_O_157	รัชนิกร ปันล่า atchaneekorn Punla	Maejo University	การพัฒนาเซลล์แสงอาทิตย์เพอรอฟสไกต์โดยใช้ คอปเปอร์ออกไซด์เป็นวัสดุนำโฮลแบบชั้นคู่	National
10	14.30-14.45	SSSCI2019_PH_29 SSSCI2019_O_136	Pich Khoem รวิภัทร ลากเจริญสุข Ravipat Lapcharoensuk	สถาบันเทคโนโลยีพระจอม เกล้าเจ้าคุณทหารลาดกระบัง	การวิเคราะห์ความแม่นยำของเครื่องเนียร์ อินฟราเรดสเปกโตรมิเตอร์สำหรับการตรวจสอบ คุณภาพน้ำเค็ม	National
14.45-15.00				Refreshment Break		
11.	15.00-15.15	SSSCI2019_PH_30 SSSCI2019_O_155	มครินทร์ กาญจนสุด Makkaryn Kanchanasoot	มหาวิทยาลัยเกษตรศาสตร์	การออกแบบและประยุกต์ใช้เซลล์ไฟฟ้าชีวภาพ จากพืช เพื่ออุปกรณ์ไฟฟ้าแรงดันต่ำ	National
12.	15.15-15.30	SSSCI2019_PH_31 SSSCI2019_O_224	อรอนงค์ เสนาะจิต Ornanong Sanorchit	มหาวิทยาลัยราชภัฏ เทพสตรี	การหาสัมประสิทธิ์การลดทอนรังสีแกมมาของ แผ่นเส้นใยชานอ้อยกับ BaSO ₄ โดยมีน้ำยารักษา เป็นตัวประสาน	National
13.	15.30-15.45	SSSCI2019_PH_32 SSSCI2019_O_237	Petcharat Jaiboon	Sakon Nakhon Rajabhat University	Effect of drying temperature on quality of RD6 variety brown parboiled glutinous rice	National
14.	15.45-16.00	SSSCI2019_PH_33 SSSCI2019_O_249	ชนษัญญา วิชาศิลป์	มหาวิทยาลัยราชภัฏ เชียงใหม่	การเปรียบเทียบศักยภาพเซลล์ไฟฟ้าเคมีที่ใช้น้ำ หมักชีวภาพจากผลไม้	National
15.	16.00-16.15	SSSCI2019_PH_5 SSSCI2019_O_21	บัณฑิต จิตต์สุภาพ Bantom Chitsupap	มหาวิทยาลัยบูรพา	การควบคุมเครื่องปรับอากาศแบบท่อนำสารทำ ความเย็นร่วมเพื่อการประหยัดพลังงานไฟฟ้า	National

SsSci^{2nd} conference 2019

Conference Sessions: Biology, Biotechnology and Microbiology

Busabongkot Room B, 2nd floor (ห้องบุษบงกช บี ชั้น 2)

		Chairperson					Co-Chairperson
		ผู้ช่วยศาสตราจารย์ ดร.ปวย อุ๋นใจ ภาควิชาชีววิทยา คณะวิทยาศาสตร์ มหาวิทยาลัยมหิดล					อาจารย์ ดร.มณฑาทิพ สุธาธรรม หัวหน้าสาขาวิชาชีววิทยา คณะวิทยาศาสตร์และเทคโนโลยีมหาวิทยาลัยราชภัฏสวนสุนันทา
No.	Time	Paper Code/ Registration Code	Name	Institute	Topic	International/ National	
1.	11.15-11.30	SSSCI2019_BT_1 SSSCI2019_O_19	ฤทัยรัตน์ สิริวัฒนรัชต์ Ruthairat Siriwattanarat	มหาวิทยาลัยราชภัฏ สวนสุนันทา	ความหลากหลายของชนิดพันธุ์ปลาน้ำจืดใน คลองแสนแสบพื้นที่กรุงเทพมหานคร	National	
2.	11.30.-11.45	SSSCI2019_BT_2 SSSCI2019_O_28	Pornsiri Bumrungham พรศิริ บำรุงธรรม	มหาวิทยาลัยธรรมศาสตร์	การโคลน การแสดงออก และการศึกษาลักษณะ ของรีคอมบิแนนท์แมนนาเนส	National	
3.	11.45-12.00	SSSCI2019_BT_9 SSSCI2019_O_89	รพีพรรณ กองตุม Rapeepan Kongtoom	มหาวิทยาลัยราชภัฏ หมู่บ้านจอมบึง	การศึกษาสมบัติบางประการของพันธุ์พริก พื้นเมือง(พริกกะเหรียง) ที่ปลูกในพื้นที่ภาค ตะวันตกของประเทศไทย	National	
4.	12.00-12.15	SSSCI2019_BT_11 SSSCI2019_O_103	Krit Phinetsathian ฤกษ์ณิ พิเนตรเสถียร	มหาวิทยาลัยราชภัฏ สกลนคร	ความหลากหลายทางชีวภาพของพืชให้สีย้อม จังหวัดสกลนคร	National	
12.15-13.15		Buffet Lunch, Rim Nam Terrace, 1 st floor					
5.	13.15-13.30	SSSCI2019_BT_12 SSSCI2019_O_108	Araya Pranprawit อารยา ปรานประวีตร	Suratthani Rajabhat University	ความสามารถในการต้านโรคเบาหวานผ่านการ ยับยั้งการทำงานของเอนไซม์จากผักพื้นบ้าน ท้องถิ่นในเขตพื้นที่ หมู่ 9 ตำบลขุนทะเล อำเภอ เมือง จังหวัดสุราษฎร์ธานี	National	
6.	13.30-13.45	SSSCI2019_BT_20 SSSCI2019_O_141	Asro Hajiabdullah อัซรอ หะยีอับดุลเลาะ	มหาวิทยาลัยสงขลานครินทร์	การผลิตกรดซึนิกจากกากน้ำตาลด้วยเชื้อ Actinobacillus succinogenes	National	

No.	Time	Paper Code/ Registration Code	Name	Institute	Topic	International/ National
7.	13.45-14.00	SSSCI2019_BT_21 SSSCI2019_O_144	รัชนีกร สวามิ Ruchnekorn Swami	มหาวิทยาลัยบูรพา	การยับยั้งเชื้อแบคทีเรียของไฟโคไซยานินจากสาหร่าย <i>Arthrospira platensis</i> และสาหร่าย <i>Synechocystis</i> sp. PCC6803	National
8.	14.00-14.15	SSSCI2019_BT_28 SSSCI2019_O_220	กัลทิมา พิชัย Kaltima Pichai	มหาวิทยาลัยราชภัฏเชียงใหม่	การเก็บรักษาเชื้อยีสต์จากน้ำหมักเปลือกสับปะรด โดยวิธีการทำแห้งแบบเยือกแข็ง	National
9.	14.15-14.30	SSSCI2019_BT_29 SSSCI2019_O_222	กัญญ์วรา วงศ์แพทย์ Kanwara Wongpaet	มหาวิทยาลัยราชภัฏเชียงใหม่	พฤติกรรมของนกเป็ดแดง (<i>Dendrocygna javanica</i>) บริเวณอ่างเก็บน้ำ ภายในมหาวิทยาลัย	National
10	14.30-14.45	SSSCI2019_BT_31 SSSCI2019_O_225	Peangjai Jianwitchayakul เพียงใจ เจียรวิชญกุล	มหาวิทยาลัยราชภัฏเทพสตรี	ความหลากหลายทางชีวภาพของไส้เดือนดินในจังหวัดลพบุรีที่มีศักยภาพในการผลิตปุ๋ยหมักมูลไส้เดือนจากผักตบชวา	National
14.45-15.00		Refreshment Break				
11.	15.00-15.15	SSSCI2019_BT_33 SSSCI2019_O_229	รุ่งนภา ทากัน Rungnapa Tagun	มหาวิทยาลัยราชภัฏเชียงใหม่	ผลกระทบของมลพิษในระบบนิเวศนาข้าวต่อสิ่งมีชีวิตในอำเภอมะแตง จังหวัดเชียงใหม่	National
12.	15.15-15.30	SSSCI2019_EN_15 SSSCI2019_O_106	กิตติมา เกตุสอาด Kittima Ketsa-ad	มหาวิทยาลัยมหิดล	การคัดแยกแบคทีเรียต้านทานแคดเมียมที่สร้างสารลดแรงตึงผิวชีวภาพและสภาวะที่เหมาะสมในการสร้างสารลดแรงตึงผิวชีวภาพ	National
13.	15.30-15.45	SSSCI2019_BT_38 SSSCI2019_O_245	ไกรฤกษ์ ทวีเชื้อ Kraierk Taweechue	มหาวิทยาลัยราชภัฏเพชรบุรี	การศึกษาเพื่อทราบลำดับนิวคลีโอไทด์และความผันแปรของยีนมัยโอสแตตินในแพะ (<i>Capra hircus</i>) ที่เลี้ยงในจังหวัดเพชรบุรี	National
14.	15.45-16.00	SSSCI2019_BT_39 SSSCI2019_O_247	พรอริยา ฉิรินัง Pornariya Chirinang	มหาวิทยาลัยราชภัฏเพชรบุรี	คุณสมบัติเป็นโพรไบโอติกของ <i>Lactobacillus plantarum</i> 3C2-10 ที่ผลิตสารลดแรงตึงผิวชีวภาพจากเปลือกส้ม	National
15.	16.00-16.15	SSSCI2019_BT_32 SSSCI2019_P_228	วัชรี หาญเมืองใจ Watcharee Hanmoungjai	มหาวิทยาลัยราชภัฏเชียงใหม่	ผลการเจริญของเส้นใยเห็ดจิ้งจกบนอาหารเลี้ยงเชื้อสูตรดัดแปลงชนิดต่าง ๆ	National

SsSci^{2nd} conference 2019

Conference Sessions: Environmental Science & Technology

Busabongkot Room A, 2nd floor (ห้องบุษบกช เอ ชั้น 2)

Chairperson	Co-Chairperson
ผู้ช่วยศาสตราจารย์สุรศักดิ์ นุ่มมีศรี คณบดีคณะวิทยาศาสตร์และเทคโนโลยี มหาวิทยาลัยราชภัฏเชียงใหม่	ผู้ช่วยศาสตราจารย์ ดร.ทัศนาวลัย อุฑารสกุล สาขาวิชาวิทยาศาสตร์สิ่งแวดล้อม คณะวิทยาศาสตร์และเทคโนโลยีมหาวิทยาลัยราชภัฏสวนสุนันทา

No.	Time	Paper Code/ Registration Code	Name	Institute	Topic	International/ National
1.	11.15-11.30	SSSCI2019_EN_1 SSSCI2019_O_22	พรทิพย์ วิมลทรง Pornthip Wimonsong	มหาวิทยาลัยราชภัฏ สุราษฎร์ธานี	การวิเคราะห์แผนเผชิญเหตุทุกภัยระดับจังหวัด ของประเทศไทย	National
2.	11.30.-11.45	SSSCI2019_EN_2 SSSCI2019_O_34	ชำนาญพงษ์ เฉลิมเผ่า Chamnanpong Chalernpow	มหาวิทยาลัยมหิดล	การผลิตก๊าซไฮเทนชีวภาพจากของเสียทาง การเกษตรและอุตสาหกรรม	National
3.	11.45-12.00	SSSCI2019_EN_3 SSSCI2019_O_43	ภัทรลภา ฐานวิเศษ Phatlapha Thanwiset	Sakon Nakhon Rajabhat University	แนวทางการจัดการขยะภายในมหาวิทยาลัย ราชภัฏสกลนคร	National
4.	12.00-12.15	SSSCI2019_EN_4 SSSCI2019_O_48	สุวิมล คุปติวุฒิ Suwimon Kooptiwoot	Suan Sunandha Rajabhat University	Mining waste separation behavior related factor	National
12.15-13.15				Buffet Lunch, Rim Nam Terrace, 1st floor		
5.	13.15-13.30	SSSCI2019_EN_5 SSSCI2019_O_50	ทศพร นิละไพจิตร Todsaporn Neelapaijit	มหาวิทยาลัยเทคโนโลยี พระจอมเกล้าธนบุรี	การประเมินคาร์บอนฟุตพริ้นท์จากกิจกรรมของ ตลาดชุมชน	National
6.	13.30-13.45	SSSCI2019_EN_6 SSSCI2019_O_53	สุวิมล คุปติวุฒิ Suwimon Kooptiwoot	Suan Sunandha Rajabhat University	Development of a garbage bin selection expert system for waste separation	National
7.	13.45-14.00	SSSCI2019_EN_13 SSSCI2019_O_105	วิเวียน จุลมนต์ Vivian Chullamon	Thammasat University	การวิเคราะห์ความเหมาะสมของพื้นที่ด้วย GIS เพื่อเลือกที่ตั้งโรงงานแปรรูปมูลฝอยเป็น พลังงานในจังหวัดปทุมธานี	National
8.	14.00-14.15	SSSCI2019_EN_18 SSSCI2019_O_116	Aphiranan Phongjetpuk	Mahidol University	การประเมินปริมาณการใช้น้ำ และผลกระทบต่อ ด้านความขาดแคลนน้ำในการผลิตกระแสไฟฟ้า	National

No.	Time	Paper Code/ Registration Code	Name	Institute	Topic	International/ National
9.	14.15-14.30	SSSCI2019_EN_22 SSSCI2019_O_145	ไพบุลย์ แจ่มพงษ์ Paiboon Jeamponk	มหาวิทยาลัยราชภัฏ สวนสุนันทา	ผลกระทบจากปัญหาภาวะหมอกควันต่อปัญหา สุขภาพอนามัยของประชาชนที่มาเข้ารับบริการ ที่โรงพยาบาลเชียงใหม่ เชียงราย	National
10	14.30-14.45	SSSCI2019_EN_23 SSSCI2019_O_148	วัลย์พร ฟ่อนพันธ์ Walaiporn Phonphan	มหาวิทยาลัยราชภัฏ สวนสุนันทา	การติดตามการเปลี่ยนแปลงพื้นที่ป่าชายเลน จังหวัดสมุทรสงครามด้วยเทคโนโลยีการสำรวจ ระยะไกล	National
14.45-15.00 Refreshment Break						
11.	15.00-15.15	SSSCI2019_EN_26 SSSCI2019_O_166	นิช วงศ์สงจำ Nich Wongsongja	มหาวิทยาลัยราชภัฏสวนสุนันทา	การศึกษาการมีส่วนร่วมของชุมชนด้านสังคม และสิ่งแวดล้อมบริเวณรอบโรงไฟฟ้าพลังน้ำ เขื่อนศรีนครินทร์ จังหวัดกาญจนบุรี Promotion of Community Participation for Saline Soil Remediation by	National
12.	15.15-15.30	SSSCI2019_EN_29 SSSCI2019_O_184	วรารณ โกศลวิตร Waraporn Kosanlavit	มหาวิทยาลัยราชภัฏ นครราชสีมา	Alternative Technology of Bio-Organic Fertilizers and Nano Material at Krabueang Yai, Phimai District, Nakhon Ratchasima Province	National
13.	15.30-15.45	SSSCI2019_EN_30 SSSCI2019_O_186	นฤพร เวชกุลชัย Naruporn Wetchayagulchai	มหาวิทยาลัยธรรมศาสตร์	การเลือกเทคโนโลยีที่เหมาะสมสำหรับ การแปรขยะมูลฝอยเป็นพลังงาน กรณีศึกษา จังหวัดปทุมธานี	National
14.	15.45-16.00	SSSCI2019_EN_33 SSSCI2019_O_203	นิตินาถ เจริญโกคราช Nitinarth Charoenpokarj	Suan Sunandha Rajabhat University	ความหลากหลายชนิด ความชุกชุมและความคล้ายคลึง ของนก ในถิ่นที่อยู่อาศัยของนก บริเวณชายฝั่ง ทะเล เพื่อการอนุรักษ์และการท่องเที่ยวเชิงนิเวศ อำเภอเมือง จังหวัดสมุทรสงคราม	National
15.	16.00-16.15	SSSCI2019_EN_35 SSSCI2019_O_243	ปัทมาพร ยอดสันติ	มหาวิทยาลัยราชภัฏเพชรบุรี	การประเมินศักยภาพการเก็บกักคาร์บอนของต้น ตาลในจังหวัดเพชรบุรี	National
16.	16.15-16.30	SSSCI2019_EN_17 SSSCI2019_O_115	วนิดา ชูอักษร Wanida Chooaksorn	มหาวิทยาลัยธรรมศาสตร์ ศูนย์รังสิต	การศึกษาคุณภาพน้ำจากต้นน้ำดื่มหยอดเหรียญ บริเวณรอบ มหาวิทยาลัยธรรมศาสตร์ ศูนย์ รังสิต	National

SsSci^{2nd} conference 2019

Conference Sessions: Food Science & Technology and Home Economics

Krungthon Ballroom, 3rd floor (ห้องกรุงธนบอลรูม ชั้น 3)

Chairperson		Co-Chairperson	
รองศาสตราจารย์ ดร.รัชชณิน จงจิตวิมล คณบดีคณะวิทยาศาสตร์และเทคโนโลยี มหาวิทยาลัยราชภัฏพิบูลสงคราม		อาจารย์ ดร.ธนิดา ฉั่วเจริญ หัวหน้าสาขาวิชาวิทยาศาสตร์และเทคโนโลยีการอาหาร คณะวิทยาศาสตร์และเทคโนโลยี มหาวิทยาลัยราชภัฏสวนสุนันทา	

No.	Time	Paper Code/ Registration Code	Name	Institute	Topic	International/ National
1.	11.15-11.30	SSSCI2019_FT_19 SSSCI2019_O_114	Supatchalee Sirichokworrakit	Suan Sunandha Rajabhat University	The effect of extraction methods on phenolic, anthocyanin, and antioxidant activities of Riceberry bran	International
2.	11.30-11.45	SSSCI2019_FT_1 SSSCI2019_O_8	ฐานวีร์ ลอยแก้ว Thanawee Loikaeo	มหาวิทยาลัยรังสิต	ศึกษาศสมบัติทางกายภาพ เคมี และ โภชนาการของแป้งแค้นตะวัน เพื่อนำมาแทนที่แป้งสาลีบางส่วนในผลิตภัณฑ์ขนมอบ	National
3.	11.45-12.00	SSSCI2019_FT_3 SSSCI2019_O_29	กัญญาพัชร เพชรภรณ์ Kanyapat Petcharaporn	มหาวิทยาลัยราชภัฏ สวนสุนันทา	นวัตกรรมการผลิตกระเทียมเจียวไร้มันพร้อมรับประทาน ด้วยเทคโนโลยีการทอดด้วยหม้อไร้มัน (Air Fryer)	National
4.	12.00-12.15	SSSCI2019_FT_5 SSSCI2019_O_38	จุฑามาศ มุลวงศ์ Jutamas Moolwong	มหาวิทยาลัยราชภัฏ สวนสุนันทา	การศึกษสภาวะที่เหมาะสมการผลิตน้ำพริกลงเรือดำรับวังสวนสุนันทา กึ่งสำเร็จรูปด้วยเครื่องทำแห้งแบบลูกกลิ้ง	National
12.15-13.15 Buffet Lunch, Rim Nam Terrace, 1st floor						
5.	13.15-13.30	SSSCI2019_FT_18 SSSCI2019_O_104	ชูลิทธิ์ หงษ์กุลทรัพย์ Choosit Hongkulsap	มหาวิทยาลัย ราชภัฏสวนสุนันทา	ผลของการทำแห้งแบบแช่เยือกแข็งต่อความคงตัวของสารสกัดจาก ดอกกระเจียว	National
6.	13.30-13.45	SSSCI2019_FT_20 SSSCI2019_O_146	ณัฐพล ประเทิงจิตต์ Nattapol Prathengjit	มหาวิทยาลัย ราชภัฏสวนสุนันทา	การพัฒนาคุกกี้โดยใช้แป้งมันเทศสีม่วงและแป้งข้าวทนต์แทนแป้งสาลี	National

No.	Time	Paper Code/ Registration Code	Name	Institute	Topic	International/ National
7.	13.45-14.00	SSSCI2019_FT_21 SSSCI2019_O_172	วรกร วิวัชรากรกุล Worakorn Wiwatcharakornkul	จุฬาลงกรณ์มหาวิทยาลัย	ลายพิมพ์เอชพีทีแอลซี ฤทธิ์ต้านอนุมูลอิสระ และปริมาณสารประกอบฟีนอลิกทั้งหมด ของ ดอกไม้ 5 ชนิดในพิกัดเกษตร	National
8.	14.00-14.15	SSSCI2019_FT_22 SSSCI2019_O_174	ธีรยุทธ์ พูนจันทร์นา Teerayut Poonjunna	มหาวิทยาลัย ราชภัฏนครศรีธรรมราช	การพัฒนาผลิตภัณฑ์เนยประ Development of Pra Butter Products	National
9.	14.15-14.30	SSSCI2019_FT_18 SSSCI2019_O_104	วารภรณ์ สงศรีอินท Waraporn Songsriin	มหาวิทยาลัย ราชภัฏนครศรีธรรมราช	การใช้ผงลูกประทดแทนผงอัลมอนดีในมาภา รอง	National
10	14.30-14.45	SSSCI2019_FT_14 SSSCI2019_O_88	ครองศักดิ์ ภัคธนกนก Kongsakda Phakthanakanok	มหาวิทยาลัย ราชภัฏหมู่บ้านจอมบึง	ผลของการอบแห้งต่อลักษณะบางประการของ เอนไซม์โปรตีเอสจากเหง้าสับประรด	National
14.45-15.00				Refreshment Break		
11.	15.00-15.15	SSSCI2019_FT_26 SSSCI2019_O_191	วันดี แก้วสุวรรณ Wandee Kaewsuwan	Nakhon Sri Thammarat Rajabhat Univerisity	กรรมวิธีการผสมต่อลักษณะเนื้อสัมผัสของ กลัวยอบชุบแป้งทอด	National
12.	15.15-15.30	SSSCI2019_FT_27 SSSCI2019_O_207	อรุณชัย ตั้งเจริญบำรุงสุข Arunchai Tangcharoenbumrungasuk	มหาวิทยาลัยราชภัฏสุรินทร์	การศึกษาเพื่อความเป็นไปได้ในการใช้ อินพราเรตสเปกโทรสโกปีและคีโมเมทริกส์เป็น สิ่งบ่งชี้ทางภูมิศาสตร์ในการระบุแหล่งต้นทาง ของข้าวหอมมะลิ	National
13.	15.30-15.45	SSSCI2019_FT_30 SSSCI2019_O_242	สุนธรา สุนธร์ธารา	มหาวิทยาลัยราชภัฏเพชรบุรี	การใช้มอลทิทอลทดแทนน้ำตาลทรายในขนมตาล	National
14.	15.45-16.00	SSSCI2019_FT_32 SSSCI2019_O_248	ธนิดา ชาญชัย	มหาวิทยาลัยราชภัฏเพชรบุรี	อาหารท้องถิ่นเมืองเพชร	National
15.	16.00-16.15	SSSCI2019_FT_12 SSSCI2019_P_73	นันทยาภรณ์ เมืองแดง Nanyaporn Mueangdang	มหาวิทยาลัยราชภัฏ พิบูลสงคราม	การทดแทนแป้งมันสำปะหลังด้วยผงลูกจันใน ลอดช่องสิงคโปร์	National
16.	16.15-16.30	SSSCI2019_FT_31 SSSCI2019_O_244	สุนธรา สุนธร์ธารา	มหาวิทยาลัยราชภัฏเพชรบุรี	การพัฒนาวาฟเฟิลเพื่อสุขภาพจากข้าวโพดงอก	National
17.	16.30-16.45	SSSCI2019_FT_28 SSSCI2019_P_227	ขนิษฐา อินทร์ประสิทธิ์ Khanittha Inprasit	กรมวิทยาศาสตร์บริการ	การศึกษาสมบัติสารยึดเกาะผสมระหว่างปลาย ข้าวบดกับไฮโดรคอลลอยด์ในการปรับปรุงเนื้อ สัมผัสของขนมปลายข้าวแผ่นอบกรอบ	National

SsSci^{2nd} conference 2019

Conference Sessions: Sports and Health Science
Bongkotrat Room B, 2nd floor (ห้องบงกชรัตน์ ปี ชั้น 2)

Chairperson	Co-Chairperson
<p>ดร.ภคกุล สังข์สุริยะ นักวิจัยห้องปฏิบัติการอนุพันธุศาสตร์และเทคโนโลยีชีวภาพสัตว์น้ำ ศูนย์พันธุวิศวกรรมและเทคโนโลยีชีวภาพแห่งชาติ (BIOTEC) สำนักงานพัฒนาวิทยาศาสตร์และเทคโนโลยีแห่งชาติ (สวทช.)</p>	<p>อาจารย์ ดร.คมกฤษ รัตตะมณี หัวหน้าสาขาวิชาวิทยาศาสตร์การกีฬาและสุขภาพ คณะวิทยาศาสตร์และเทคโนโลยี มหาวิทยาลัยราชภัฏสวนสุนันทา</p>

No.	Time	Paper Code/ Registration Code	Name	Institute	Topic	International/ National
1.	11.15-11.30	SSSCI2019_SP_15 SSSCI2019_P_128	Churairat Srimanee	Mahidol University	Biomonitoring of metals exposure in Aranyik handicraft workers	International
2.	11.30.-11.45	SSSCI2019_SP_1 SSSCI2019_O_11	Jatuporn Ounprasertsuk	มหาวิทยาลัย ราชภัฏสวนสุนันทา	บุคลิกภาพ 5 มิติ และการจัดการความขัดแย้ง ของนักศึกษา มหาวิทยาลัยราชภัฏแห่งหนึ่งใน ประเทศไทย	National
3.	11.45-12.00	SSSCI2019_SP_2 SSSCI2019_O_15	Luckwirun Chotisiri	มหาวิทยาลัย ราชภัฏสวนสุนันทา	The Development of Line Application for Home Visit among NCD Patients	National
4.	12.00-12.15	SSSCI2019_SP_5 SSSCI2019_O_23	Wachiaporn Chotipanut	มหาวิทยาลัย ราชภัฏสวนสุนันทา	ผลของโปรแกรมความสุขต่อพฤติกรรม ส่งเสริมสุขภาพจิตผู้สูงอายุในตำบลบางนางลี่ อำเภออัมพวา จังหวัดสมุทรสงคราม	National
12.15-13.15 Buffet Lunch, Rim Nam Terrace, 1st floor						
5.	13.15-13.30	SSSCI2019_SP_9 SSSCI2019_O_33	ภูวสิทธิ์ ภูลวรรณ Mr.Phoowasit Phoolawan	มหาวิทยาลัย ราชภัฏสกลนคร	พฤติกรรมป้องกันโรคเบาหวานของ ประชาชนกลุ่มเสี่ยงในตำบลจันทอน อำเภอเมือง จังหวัดสกลนคร	National

No.	Time	Paper Code/ Registration Code	Name	Institute	Topic	International/ National
6.	13.30-13.45	SSSCI2019_SP_29 SSSCI2019_O_219	ดาวิณี ชินวงค์ Dawinee Chinnawong	มหาวิทยาลัย ราชภัฏสุรินทร์	การศึกษาผลของตำรับยาพอกเข้าในผู้ป่วยข้อ เข้าเสื่อม ณ โรงพยาบาลสังขะและโรงพยาบาล ส่งเสริมสุขภาพตำบลม อำเภอสังขะ จังหวัด สุรินทร์	National
7.	13.45-14.00	SSSCI2019_SP_30 SSSCI2019_O_233	เอกสิทธิ์ ไชยปิ่น	มหาวิทยาลัย ราชภัฏนครราชสีมา	การพัฒนารูปแบบกิจกรรมส่งเสริมสุขภาพโดย กระบวนการมีส่วนร่วมของผู้สูงอายุ เทศบาล ตำบลหนองบัว อำเภอไชยปราการ จังหวัด เชียงใหม่	National
8.	14.00-14.15	SSSCI2019_SP_31 SSSCI2019_O_232	Preetiwat Wonnabussapawich	มหาวิทยาลัย ราชภัฏนครราชสีมา	ผลของโปรแกรมการยืดเหยียดกล้ามเนื้อที่ ส่งผลต่อสมรรถภาพทางกายของนักกีฬาระดับ มัธยมศึกษาจังหวัดนครราชสีมา	National
9.	14.15-14.30	SSSCI2019_SP_32 SSSCI2019_O_238	จิตติมา ลำยอง	วิทยาลัยการสาธารณสุข สิรินธร	ประสิทธิผลของรูปแบบการจัดการเรียนการ สอนโดยใช้ปัญหาเป็นหลักเรื่องการดูแลรักษา ผู้ป่วยระบบหัวใจและหลอดเลือดต่อผลสัมฤทธิ์ การเรียนรู้ ทักษะการแก้ปัญหา การทำงานเป็น ทีม และความคิดเห็นของนักศึกษา หลักสูตร ประกาศนียบัตรวิชาชีพชั้นสูง สาขาปฏิบัติการ ฉุกเฉินการแพทย์ วิทยาลัยการสาธารณสุข สิรินธร จังหวัดตรัง	National
10	14.30-14.45	SSSCI2019_SP_33 SSSCI2019_O_241	อัสมาต์ ใจเที่ยง	มหาวิทยาลัยราชภัฏ นครศรีธรรมราช	คุณภาพชีวิตและภาวะโภชนาการของเกษตรกร ชาวสวนยางพาราที่ตำบลนาเคียน อำเภอเมือง จังหวัดนครศรีธรรมราช	National
14.45-15.00				Refreshment Break		
11.	15.00-15.15	SSSCI2019_SP_8 SSSCI2019_O_32	ทิพย์วารินทร์ เบ็ญจนิรัตน์ Tipvarin Benjanirut	มหาวิทยาลัยราชภัฏ สวนสุนันทา	ความต้องการและการเข้าถึงบริการด้านสุขภาพ ของผู้สูงอายุในชนบทจังหวัดสมุทรสงคราม	National

Poster Presentation

SsSci ^{2nd} conference
2019

Phanurangsi Ballroom, 1st floor front area: หน้าห้องประชุมภาณุรังษี ชั้น 1

Conference Schedule: กำหนดการนำเสนอผลงาน

- 11.00-16.00 Poster presentation for participation
- 13.00-15.00 Poster presentation for evaluation committee (นำเสนอผลงานและการตรวจให้คะแนนโดยกรรมการผู้ทรงคุณวุฒิ)
- 15.00-16.00 Poster presentation awards ceremony (พิธีมอบรางวัลนำเสนอผลงานวิชาการประเภทโปสเตอร์)

No.	Paper Code/ Registration Code	Topic	Theme	Name	Institute
1.	SSSCI2019_CS_22 SSSCI2019_P_142	การจำแนกนักศึกษาตามคุณลักษณะและคณะที่เรียน โดยใช้เทคนิคการจำแนกข้อมูลด้วยวิธีต้นไม้การตัดสินใจ กรณีศึกษานักศึกษามหาวิทยาลัยหอการค้าไทย	Computer Science and Information Technology	สิริธร เจริญรัตน์ Sirithorn Jalearnrat	มหาวิทยาลัยหอการค้าไทย
2.	SSSCI2019_CS_27 SSSCI2019_P_159	โมเดลการทำนายพฤติกรรมความเสี่ยงการเกิดภาวะความเครียดทางการเมือง	Computer Science and Information Technology	สมจินต์ จันทระเจษฎากร Somjin Junatarajessadkorn	มหาวิทยาลัยราชภัฏนครปฐม
3.	SSSCI2019_CS_30 SSSCI2019_P_165	การประยุกต์วิธีการเอจิลส์สำหรับกิจกรรมในการเรียนการสอน	Computer Science and Information Technology	สกวรัตน์ จงพัฒนานกร Sakauwrat Jongpattanakorn	มหาวิทยาลัยเกษตรศาสตร์
4.	SSSCI2019_CS_33 SSSCI2019_P_211	การเปรียบเทียบประสิทธิภาพการทำนายสีหมึกพิมพ์ยูวีเฟล็กโซกราฟีบนฉลากพอลิโพรพิลีนโดยใช้โครงข่ายประสาทเทียมและซอฟต์แวร์การทำนายสี	Computer Science and Information Technology	ณัฐวิทย์ โสหา Natthawut Soha	จุฬาลงกรณ์มหาวิทยาลัย
5.	SSSCI2019_MA_4 SSSCI2019_P_78	ทัศนคติและพฤติกรรมของนิสิตระดับปริญญาตรีมหาวิทยาลัยบูรพา ที่มีต่อการใช้บริการรถตู้โดยสารเส้นทางกรุงเทพฯ (รังสิต) – บางแสน	Mathematics and Statistics	ปรียารัตน์ นาคสุวรรณ Preyarat Naksuwan	มหาวิทยาลัยบูรพา

No.	Paper Code/ Registration Code	Topic	Theme	Name	Institute
6.	SSSCI2019_MA_11 SSSCI2019_P_189	Stratified Unified Ranked Set Sampling for Asymmetric Distributions	Mathematics and Statistics	Chainarong Pianpailoon	Sakon Nakhon Rajabhat University
7.	SSSCI2019_MA_12 SSSCI2019_P_193	ความสัมพันธ์ระหว่างลำดับจากคอปและลำดับพี โบนซ์ซีตต์แปลง	Mathematics and Statistics	ณัฐฉิณีย์ คงนวล Nattinee Khongnual	มหาวิทยาลัยราชภัฏ นครศรีธรรมราช
8.	SSSCI2019_MA_13 SSSCI2019_P_205	ผลกระทบของปริมาณน้ำฝนที่มีผลต่อตัวแบบ สำหรับโรคมือ เท้า ปาก	Mathematics and Statistics	กิตติภัทร พลเดช Kittipat Pondach	มหาวิทยาลัยราชภัฏ นครศรีธรรมราช
9.	SSSCI2019_PH_8 SSSCI2019_P_40	การเตรียมไม้เทียมจากพลาสติก และเส้นใย มะพร้าว	Physics and Energy	สิงหนเดช แต่งจวง Singhadej Tanguank	มหาวิทยาลัยราชภัฏอุตรดิตถ์
10.	SSSCI2019_PH_11 SSSCI2019_P_64	Energy Absorption and Exposure Buildup Factors for Coconut fiber gypsum board	Physics and Energy	Kittisak Sriwongsa	มหาวิทยาลัยศิลปากร
11.	SSSCI2019_PH_12 SSSCI2019_P_65	Evaluation of radiation shielding properties for samarium bismuth borate glasses	Physics and Energy	Kittisak Sriwongsa	มหาวิทยาลัยศิลปากร
12.	SSSCI2019_PH_13 SSSCI2019_P_66	Evaluated shielding radiation and exposure build up factor for La ₂ O ₃ based glasses	Physics and Energy	Kittisak Sriwongsa	มหาวิทยาลัยศิลปากร
13.	SSSCI2019_PH_14 SSSCI2019_P_94	Energy Conservation of Split Type Air Conditioner in Mechanical Engineering Department Building of RMUTL Tak	Physics and Energy	Yuttana Sriudom	Rajamangala University of Technology Lanna Tak
14.	SSSCI2019_PH_15 SSSCI2019_P_110	การประยุกต์วิธีการหาค่าสภาพต้านทานไฟฟ้าของ ชั้นดินเพื่อค้นหาแหล่งน้ำบาดาล และการแก้ภัย แล้ง	Physics and Energy	ธนะวัฒน์ รังสูงเนิน Thanawat RangSungnoen	NakhonRatchasima Rajabhat University
15.	SSSCI2019_PH_16 SSSCI2019_P_111	Development of quantum mechanics learning by integrated teaching using normal scattering effects on charge transport in a metal/superconductor junction	Physics and Energy	ภาณุพัฒน์ ชัยวร Panupat Chaiworn	มหาวิทยาลัยราชภัฏเชียงใหม่
16.	SSSCI2019_PH_19 SSSCI2019_P_131	ประสิทธิภาพของเครื่องย่อยชีวมวลและเครื่องอัด แห้งเชื้อเพลิงจากเศษเหลือทิ้งทางการเกษตร	Physics and Energy	พงษ์ศักดิ์ จิตตบุตร Pongsuk Jittabut	มหาวิทยาลัยราชภัฏ นครราชสีมา

No.	Paper Code/ Registration Code	Topic	Theme	Name	Institute
17.	SSSCI2019_PH_20 SSSCI2019_P_143	อิทธิพลของการปรับสภาพทางความร้อนต่อ โครงสร้างจุลภาคและสมบัติของผิวพ่นเคลือบ ความร้อนของโลหะผสมนิกเกิล-โครเมียม-โม ลิบดีนัม-อะลูมิเนียม	Physics and Energy	อรัชพร ศรีจันทร์ Aradchaporn Srichen	Chiang Mai University
18.	SSSCI2019_PH_21 SSSCI2019_P_151	การเผาถ่าน วิธีดั้งเดิมของชุมชนในบริเวณอ่างเก็บ น้ำห้วยเสนง	Physics and Energy	ลำพูน เหลาราช Lumpoon Laorach	มหาวิทยาลัยราชภัฏ สุรินทร์
19.	SSSCI2019_PH_22 SSSCI2019_P_154	การเตรียม เฟสโครงสร้างและสมบัติทางไดอิเล็ก ตริกของวัสดุเซรามิก Na _{1/3} Ca _{1/3} Yb _{1/3} Cu ₃ Ti ₄ O ₁₂	Physics and Energy	จุฑาทพล จำปาแถม Jutapol Jumpatam	มหาวิทยาลัยราชภัฏ สุรินทร์
20.	SSSCI2019_PH_24 SSSCI2019_P_161	โครงสร้างโพลีไดโนสคริสตัลของดั่งขาโต Carvedon serratus Olivier เพศผู้	Physics and Energy	ฐิติพร เจาะจง Thitiporn Jorjong	มหาวิทยาลัยราชภัฏ พิบูลสงคราม
21.	SSSCI2019_PH_26 SSSCI2019_P_167	Conductive Composite Paper from Cellulose Fiber by in situ polymerization of pyrrole	Physics and Energy	Siripassorn Sukkhawuttigit	มหาวิทยาลัยธรรมศาสตร์ ศูนย์ รังสิต
22.	SSSCI2019_PH_28 SSSCI2019_P_195	การเตรียมและศึกษาคุณสมบัติเฉพาะของถ่านกัม มันต์จากกล้วยน้ำว้า โดยวิธีการกระตุ้นด้วย โพแทสเซียมคาร์บอเนต	Physics and Energy	ภาคิน อินทร์ชิตจ้อย พรทิพย์ ภูมิying	มหาวิทยาลัยราชภัฏ นครสวรรค์
23.	SSSCI2019_CH_1 SSSCI2019_P_54	การใช้ตัวดูดซับแบบผสมสำหรับการเก็บตัวอย่าง สารก่อเพลิงชนิดเหลวตกค้าง	Chemistry and Forensic science	นิสาลักษณ์ ทาเครือ Nisalak Thakheru	มหาวิทยาลัยเชียงใหม่
24.	SSSCI2019_CH_2 SSSCI2019_P_75	การสังเคราะห์ถ่านกัมมันต์จากเปลือกผสมจุลสับปะรด ด้วยการกระตุ้น โดยใช้โพแทสเซียม ไฮดรอกไซด์ และ โซเดียมไฮดรอกไซด์	Chemistry and Forensic science	พูนฉวี สมบัติศิริ Punchavee Sombatsiri	มหาวิทยาลัยราชภัฏ ลำปาง
25.	SSSCI2019_CH_4 SSSCI2019_P_109	Synthesis and Evaluation of Molecularly Imprinted Polymer as a Selective Material for Vanillin	Chemistry and Forensic science	วีรณัฐ คฤหานนท์ Wiranut Karuehanon	มหาวิทยาลัยราชภัฏลำปาง
26.	SSSCI2019_CH_5 SSSCI2019_P_129	การปรับปรุงคุณภาพของผ้าไหมด้วยสนิมเหล็ก	Chemistry and Forensic science	วีรญา สิงคินภา Weeraya singkanipa	มหาวิทยาลัยราชภัฏสุรินทร์

No.	Paper Code/ Registration Code	Topic	Theme	Name	Institute
27.	SSSCI2019_CH_8 SSSCI2019_P_168	Participation of Evidence Collection in Forensic Science by the Foundation Officer	Chemistry and Forensic science	Somchart Ketpan	มหาวิทยาลัยราชภัฏสวนสุนันทา
28.	SSSCI2019_CH_9 SSSCI2019_P_170	Effects of PEG-based triazolyl substituents on copper-catalyzed aerobic alcohol oxidation	Chemistry and Forensic science	ชมทิตา บ่อทรัพย์ Chomtisa Borsap	มหาวิทยาลัยมหิดล
29.	SSSCI2019_CH_10 SSSCI2019_P_178	Formulation of Calcium Tablets by Direct Compression Tableting	Chemistry and Forensic science	Auttapol Hogjalern	Chulalongkorn University
30.	SSSCI2019_CH_13 SSSCI2019_P_198	Rapid Analysis of Alpha-Mangostin Content in Mangosteen Pericarps by Near-Infrared Spectroscopy	Chemistry and Forensic science	ศุมาพร เกษมสำราญ Sumaporn Kasemsumran	มหาวิทยาลัยเกษตรศาสตร์
31.	SSSCI2019_CH_15 SSSCI2019_P_208	การศึกษาองค์ประกอบเคมี และประสิทธิภาพของสารสกัดสมุนไพรพื้นบ้านต่อการยับยั้งเชื้อราสาเหตุโรคไหม้ข้าว	Chemistry and Forensic science	วัชรภรณ์ ทาหาร Watcharaporn Thahan	มหาวิทยาลัยราชภัฏเชียงราย
32.	SSSCI2019_CH_16 SSSCI2019_P_209	การเตรียมและการวิเคราะห์ลักษณะของอิมัลชันเชิงซ้อนที่เตรียมได้จากน้ำมันถั่วดาวอินคาด้วยเทคนิคสองขั้นตอน	Chemistry and Forensic science	ภัทรฤทัย ปิญชานไรวินท์ Pattararuethai Piyachanraiwin	จุฬาลงกรณ์มหาวิทยาลัย
33.	SSSCI2019_CH_17 SSSCI2019_P_210	Selection of alternative commercial amine solutions for acid gases removal	Chemistry and Forensic science	Aomkwan Lueadkrungsri	จุฬาลงกรณ์มหาวิทยาลัย
34.	SSSCI2019_CH_18 SSSCI2019_P_216	การตรวจวัดปริมาณโปรตีนบนผลิตภัณฑ์จากยางธรรมชาติ ด้วยเทคนิคพื้นผิวขยายสัญญาณรามาน	Chemistry and Forensic science	Apichat Phengdaam	Prince of Songkla University
35.	SSSCI2019_BT_3 SSSCI2019_P_63	ประสิทธิภาพของสารสกัดหยาบของฝอยทองต่อการควบคุมไรโซปลาในเห็ดหูหนู	Biology, Biotechnology and Microbiology	Suphak Kondara สุภัค คนดารา	Pibulsongkram Rajabhat University
36.	SSSCI2019_BT_4 SSSCI2019_P_67	การศึกษาเชื้อราที่ก่อโรคเน่าในมันสำปะหลังในเขตอำเภอวังทอง จังหวัดพิษณุโลก	Biology, Biotechnology and Microbiology	อารีญา ประเสริฐกรรณ์ Arriya Prasertgun	Pibulsongkram Rajabhat University

No.	Paper Code/ Registration Code	Topic	Theme	Name	Institute
37.	SSSCI2019_BT_6 SSSCI2019_P_79	การเปรียบเทียบวัสดุฝังชนิดต่าง ๆ เพื่อทำพรอนไม้มันแข็งแบบสามมิติ ที่เก็บรักษาด้วยพอลิเอสเตอร์เรซิน	Biology, Biotechnology and Microbiology	พรอนันต์ บุญก่อน Pornanan Boongorn	มหาวิทยาลัยราชภัฏลำปาง
38.	SSSCI2019_BT_7 SSSCI2019_P_82	ผลของการต้มและการนึ่งต่อศักยภาพในการต้านอนุมูลอิสระและปริมาณสารประกอบฟีนอลิกของผักโขม	Biology, Biotechnology and Microbiology	ชนิกานุจน์ จันทร์มาทอง Chanikan Junmatong	มหาวิทยาลัยราชภัฏ พิบูลสงคราม
39.	SSSCI2019_BT_10 SSSCI2019_P_101	ผลของสารสกัดจากใบและผลตีปัสติการยับยั้งเชื้อ <i>Penicillium digitatum</i> และ <i>Colletotrichum gloeosporioides</i> สาเหตุโรครีซ	Biology, Biotechnology and Microbiology	อังคณา เชื้อเจ็ดตน Angkana Chuajedton	มหาวิทยาลัยราชภัฏลำปาง
40.	SSSCI2019_BT_13 SSSCI2019_P_124	Using ultrafiltration technique for concentrate influenza virus from the supernatant.	Biology, Biotechnology and Microbiology	ทรศนีย์ บุญยทรศนีย์ Darsaniya Punyadarsaniya	Mahanakorn University of technilogy
41.	SSSCI2019_BT_14 SSSCI2019_P_125	Screening and identification of the phytase producing bacteria isolated from natural environments and swine manure	Biology, Biotechnology and Microbiology	สงกรานต์ เชื้อครุฑ Songkran Chuakrut	Naresuan University
42.	SSSCI2019_BT_18 SSSCI2019_P_133	ผลของสารสกัดมะขามเทศต่อการยับยั้งแบคทีเรียก่อโรค	Biology, Biotechnology and Microbiology	หฤทัย ไทยสุชาติ Haruthai Thaisuchat	มหาวิทยาลัยราชภัฏลำปาง
43.	SSSCI2019_BT_19 SSSCI2019_P_134	การศึกษาขนาดและรูปแบบของโปรตีนไวเทลลินในแม่พันธุ์กึ่งกุลาคาที่ได้รับอาหารผสมฮอร์โมน 17 β -estradiol	Biology, Biotechnology and Microbiology	ศรีภาพรพรณ ธาระนารถ Sripapan Tharanart	มหาวิทยาลัยบูรพา วิทยาเขต จันทบุรี
44.	SSSCI2019_BT_22 SSSCI2019_P_183	ผลของสารออกฤทธิ์ทางชีวภาพจากสารสกัดใบมะรุมนในการป้องกันความเป็นพิษของเอทานอลในยีสต์ <i>Saccharomyces cerevisiae</i>	Biology, Biotechnology and Microbiology	วิสุตา ชุมสวัสดิ์ Wisuta Chumsawat	Mahidol University
45.	SSSCI2019_BT_24 SSSCI2019_P_201	แบคทีเรียจากลำไส้ขมดที่มีศักยภาพย่อยกลูคาสำหรับผลิตกาแฟหมักระดับอุตสาหกรรม	Biology, Biotechnology and Microbiology	ธีรวัฒน์ งามนอก Teerawat Ngamnok	มหาวิทยาลัยเชียงใหม่
46.	SSSCI2019_BT_26 SSSCI2019_P_215	ประสิทธิภาพของเจลแอดมัลติวจากสารสกัดกระเทียมและข่าลิงต่อการยับยั้งสี	Biology, Biotechnology and Microbiology	สุวิชญา บัวชาติ Suwichaya Buachard	มหาวิทยาลัยราชภัฏ กำแพงเพชร

No.	Paper Code/ Registration Code	Topic	Theme	Name	Institute
47.	SSSCI2019_BT_27 SSSCI2019_P_217	การสกัดคอลลาเจนชนิดที่ 2 จากเศษของครีบบล้าหมักซึ่งเป็นของเสียในอุตสาหกรรมอาหารทะเล	Biology, Biotechnology and Microbiology	Siripong Somsiriwon	Chulalongkorn University
48.	SSSCI2019_BT_30 SSSCI2019_P_223	ผลของสารสกัดหยาบจากกล้วยไม้ต่อการยับยั้งการเจริญเติบโตของจุลินทรีย์บางชนิด	Biology, Biotechnology and Microbiology	วิมลรัตน์ พงษ์ไตรทิพย์ Wimonrat Phottraithip	มหาวิทยาลัยราชภัฏเชียงใหม่
49.	SSSCI2019_BT_35 SSSCI2019_P_234	การศึกษาเบื้องต้นถึงความหลากหลายชนิดและสังคมพืชในป่าผลัดใบภายหลังการสัมปทานทำไม้ บริเวณป่าชุมชนบ้านทุ่งฮ้าง อำเภอแจ้ห่ม จังหวัดลำปาง	Biology, Biotechnology and Microbiology	ชัตนารี มีสุขโข	มหาวิทยาลัยราชภัฏลำปาง
50.	SSSCI2019_EN_11 SSSCI2019_P_100	การศึกษาคุณภาพน้ำที่เปลี่ยนแปลงไปในกระบวนการแช่ฟอกเปลือกปอกระเจา	Environmental science and technology	ประภา โชะสลาม Prapa Sohsalam	มหาวิทยาลัยเกษตรศาสตร์
51.	SSSCI2019_EN_12 SSSCI2019_P_102	การลดฝุ่นขนาด 2.5 ไมครอนด้วยการติดตั้งแผงบังแดดพร้อมพืชใบแคบและใบกว้าง	Environmental science and technology	เอกรัตน์ ปานแร่ Akarat Panrare	จุฬาลงกรณ์มหาวิทยาลัย
52.	SSSCI2019_EN_14 SSSCI2019_P_81	ความหลากหลายทางชีวภาพของสิ่งมีชีวิตในน้ำและคุณภาพน้ำผิวดิน ภายในมหาวิทยาลัยราชภัฏพิบูลสงคราม (ส่วนทะเลแก้ว)	Environmental science and technology	ศิริรัตน์ จิตบรรเทา Silorat Jitbanthao	มหาวิทยาลัยราชภัฏพิบูลสงคราม
53.	SSSCI2019_EN_31 SSSCI2019_P_187	ความสัมพันธ์ระหว่างคุณภาพน้ำและไดอะตอมในชุมชนแบบยึดเกาะ เพื่อหาแนวโน้มในการประยุกต์ใช้ในการประเมินคุณภาพน้ำ	Environmental science and technology	เอกชัย ญาณะ Ekkachai Yana	มหาวิทยาลัยราชภัฏลำปาง
54.	SSSCI2019_FT_2 SSSCI2019_P_25	ผลของฟอสเฟต น้ำและโซ่ขาวต่อคุณภาพของผลิตภัณฑ์หมูสับ	Food Science and Home Economics	มาลี ชัมศรีสกุล Malee Simsriskul	มหาวิทยาลัยเทคโนโลยีพระจอมเกล้าพระนครเหนือ
55.	SSSCI2019_FT_4 SSSCI2019_P_31	ผลของโซเดียมแลคเตทที่มีต่อคุณภาพเนื้อปลาบดแช่เยือกแข็งที่ผลิตจากปลาอีสก (<i>Probarbus jullieni</i>)	Food Science and Home Economics	ปัทมา ภาสุถาน Pattama Phasuthan	มหาวิทยาลัยเทคโนโลยีพระจอมเกล้าพระนครเหนือ
56.	SSSCI2019_FT_6 SSSCI2019_P_41	ออกแบบและพัฒนาเครื่องคัดแยกข้าวเปลือกออกจากข้าวกล้องแบบตะแกรงโยก สำหรับโรงสีข้าวชุมชน	Food Science and Home Economics	สุกัญญา ทองโยธี Sukanya Thongyothee	มหาวิทยาลัยราชภัฏวชิรวิทยาดอนแก้ว

No.	Paper Code/ Registration Code	Topic	Theme	Name	Institute
57.	SSSCI2019_FT_7 SSSCI2019_P_49	การสกัดและความคงตัวของแอนโทไซยานินจากข้าวหอมมะลิสีน้ำตาล	Food Science and Home Economics	Wipada Siri-anusornsak วิภาดา ศิริอนุสรณ์ศักดิ์,	Kasetsart University
58.	SSSCI2019_FT_8 SSSCI2019_P_61	การใช้หมอลดทอหดแทนน้ำตาลซูโครสในเมอแรงค์	Food Science and Home Economics	ภรณ์ ลิ้มปิสุต Pouranee Limpisut	มหาวิทยาลัยเทคโนโลยีพระจอมเกล้าพระนครเหนือ
59.	SSSCI2019_FT_9 SSSCI2019_P_62	การพัฒนาผลิตภัณฑ์ข้าวพองปราศจากน้ำมันจากข้าวกล้องหับทิมซุมแพ	Food Science and Home Economics	กมลทิพย์ มั่นภักดี Kamontip Manpakdee	มหาวิทยาลัยเทคโนโลยีพระจอมเกล้าพระนครเหนือ
60.	SSSCI2019_FT_11 SSSCI2019_P_72	Development of high anthocyanin crispy rice bar	Food Science and Home Economics	Nuttawut Lainumngan	Institute of Food Research and Product Development
61.	SSSCI2019_FT_16 SSSCI2019_P_96	การศึกษาสำหรับอาหารไทยทรงดำตามประเพณี กรณีศึกษา : ตำบลบ่อทอง อำเภอบางระกำ จังหวัดพิษณุโลก	Food Science and Home Economics	วรรณิสา สุดวังยาง Wannisa Sutwangyang,	มหาวิทยาลัยราชภัฏพิบูลสงคราม
62.	SSSCI2019_FT_17 SSSCI2019_P_97	การศึกษาตำรับอาหารพื้นบ้านชาวไทย-ยวน กรณีศึกษา : หมู่บ้านสมอแข ตำบลสมอแข อำเภอเมือง จังหวัดพิษณุโลก	Food Science and Home Economics	บัติตา ทับทิมเพชรราชกุล Bantita Tubtimpeachranggul	มหาลัยราชภัฏพิบูลสงคราม
63.	SSSCI2019_FT_24 SSSCI2019_P_185	การพัฒนาผลิตภัณฑ์ขนมปังปราศจากกลูเตน	Food Science and Home Economics	ปวีณ์สุดา ชีปนวัฒนา Paweesuda Keepanawattana	Kasetsart University
64.	SSSCI2019_SP_11 SSSCI2019_P_39	Effects of walking meditation and massage on neuropathic symptoms in persons with type-2 diabetic peripheral neuropathy	Sports and Health Science	พิชญา สุขไพบูลย์ Ms.Pichaya Sukphaibool	มหาวิทยาลัยศรีนครินทรวิโรฒ
65.	SSSCI2019_SP_12 SSSCI2019_P_60	A Research of Model of Professional Basketball Management for Professional Basketball Players	Sports and Health Science	Jatuporn Banroengsanoh	Kasetsart University
66.	SSSCI2019_SP_13 SSSCI2019_P_113	ความรู้ ทักษะ การปฏิบัติตนในการดูแลสุขภาพช่องปาก และสภาวะทันตสุขภาพของนักเรียนมัธยมศึกษาตอนต้น อำเภวารินชำราบ จังหวัดอุบลราชธานี	Sports and Health Science	Banhan Aemprakhon	วิทยาลัยการสาธารณสุขสิรินธร

No.	Paper Code/ Registration Code	Topic	Theme	Name	Institute
67.	SSSCI2019_SP_14 SSSCI2019_P_118	การจัดการกองทุนหลักประกันสุขภาพระดับ ท้องถิ่นหรือพื้นที่ กรณีศึกษาองค์การบริหารส่วน ตำบลบัวงาม อำเภอเดชอุดม จังหวัดอุบลราชธานี	Sports and Health Science	Sarawut Saiboon	วิทยาลัยการสาธารณสุข สิรินธร จังหวัดอุบลราชธานี
68.	SSSCI2019_SP_16 SSSCI2019_P_135	Factors Related to achievement of Athlete at Institute of Physical Education participating in the University Games of Thailand.	Sports and Health Science	Thitipong Sukdee	มหาวิทยาลัยการกีฬาแห่งชาติ
69.	SSSCI2019_SP_19 SSSCI2019_P_138	ความชุกของฮีโมโกลบินอีในกลุ่มชาติพันธุ์ลาวเทิง ในสาธารณรัฐประชาธิปไตยประชาชนลาว	Sports and Health Science	Amkha Sanephonasa	Chulalongkorn University
70.	SSSCI2019_SP_20 SSSCI2019_P_139	ปัจจัยที่มีผลต่อพฤติกรรมการซื้อยาของประชาชน ในตำบลเชียงดา อำเภอสร้างคอม จังหวัดอุดรธานี	Sports and Health Science	สรญา แสนมาโนช Soraya Saenmanot	มหาวิทยาลัยราชภัฏอุดรธานี
71.	SSSCI2019_SP_22 SSSCI2019_P_177	The Development of Promoting Model for Quality of Life of Elderly with a Retro Dance	Sports and Health Science	Atthaphol Rodkaew	มหาวิทยาลัยราชภัฏพิบูล สงคราม
72.	SSSCI2019_SP_23 SSSCI2019_P_179	การพัฒนาโปรแกรมการเสริมสร้างการรับรู้ ความสามารถของตนเองในการป้องกันการ ตั้งครรภ์ก่อนวัยอันควร	Sports and Health Science	ชลดา กิ่งมาลา Chonlada Kingmala	วิทยาลัยพยาบาลบรมราชชนนี สุรินทร์
73.	SSSCI2019_SP_24 SSSCI2019_P_180	การศึกษาความเครียดและการเผชิญความเครียด ในญาติผู้ดูแลผู้สูงอายุที่เจ็บป่วยด้วยโรคเรื้อรังใน ชุมชน	Sports and Health Science	ภาวิณี แผงสุข Pavinee Pangsuk	วิทยาลัยพยาบาลบรมราชชนนี สุรินทร์
74.	SSSCI2019_SP_25 SSSCI2019_P_188	ความรู้และทัศนคติต่อวิชาชีพสาธารณสุข ของ นักศึกษาสาขาวิชาสาธารณสุขศาสตร์ คณะ วิทยาศาสตร์และเทคโนโลยี มหาวิทยาลัยราชภัฏ สุรินทร์	Sports and Health Science	นราวุธ สิ้นสุพรรณ Narawut Sinsupun	มหาวิทยาลัยราชภัฏสุรินทร์
75.	SSSCI2019_SP_26 SSSCI2019_P_231	พฤติกรรมการดื่มเครื่องดื่มแอลกอฮอล์ และ พฤติกรรมการสูบบุหรี่ของนักศึกษาชั้นปี 1 มหาวิทยาลัยราชภัฏสุรินทร์	Sports and Health Science	นภา วงษ์ศรี Napha Wongsri	มหาวิทยาลัยราชภัฏสุรินทร์

No.	Paper Code/ Registration Code	Topic	Theme	Name	Institute
76.	SSSCI2019_SP_27 SSSCI2019_P_204	Enhancement of visual perception in primary education: A case study of Mae Tha school, Lampang province	Sports and Health Science	Chatsuda Mata	มหาวิทยาลัยราชภัฏลำปาง
77.	SSSCI2019_SP_28 SSSCI2019_P_218	พฤติกรรมอนามัยที่เป็นปัจจัยเสี่ยงต่อการติดเชื้อพยาธิกับภาวะโภชนาการของประชาชนโดยรอบอ่างเก็บน้ำสำคัญในจังหวัดสุรินทร์	Sports and Health Science	จีระเดช อินทเจริญสถานต์ Jeeradach Intajarurnsan	มหาวิทยาลัยราชภัฏสุรินทร์
78.	SSSCI2019_CS_2 SSSCI2019_O_5	การพัฒนาซอฟต์แวร์อ่านบทคัดย่อรูปเล่มโครงการวิทยากรคอมพิวเตอร์	Computer Science and Information Technology	นิตานาด เตชะเพชรไพบุลย์ Nisanart Tachpetpaiboon	มหาวิทยาลัยราชภัฏสวนสุนันทา
79.	SSSCI2019_CS_3 SSSCI2019_O_9	การพยากรณ์ปริมาณฝุ่น PM2.5 โดยใช้วิธีวิเคราะห์อนุกรมเวลาด้วยเทคนิคเหมืองข้อมูลกรณีศึกษา: กรุงเทพฯ เขตบางรัก	Computer Science and Information Technology	ทศภูมิ รันระนา Tusaphum Runrana	มหาวิทยาลัยสยาม
80.	SSSCI2019_PH_3 SSSCI2019_O_13	กัมมันตภาพรังสีในทรายชายหาด	Physics and Energy	อมรา อธิพิงษ์ Ammara Ittipongse	Suan Sunandha Rajabhat
81.	SSSCI2019_BT_16 SSSCI2019_O_90	การใช้แอกติโนมัยซีทต้านทานแคดเมียมกับพืชร่วมกันในการส่งเสริมการบำบัดแคดเมียมในดินปนเปื้อน	Biology, Biotechnology and Microbiology	ภัสรารณณ์ ฐูปเพ็ง Patsaraporn Thooppeng	Mahidol University
82.	SSSCI2019_BT_17 SSSCI2019_O_98	ความสามารถของแอกติโนมัยซีทต้านทานแคดเมียมในการกำจัดแคดเมียมออกจากน้ำและการละลายแคดเมียมในดิน	Biology, Biotechnology and Microbiology	โชตินันท์ จันประดิษฐ์ Chotinan Junpradit	Mahidol University
83.	SSSCI2019_BT_25 SSSCI2019_O_206	ฤทธิ์ต้านอนุมูลอิสระ ด้านเชื้อแบคทีเรีย และด้านการเกิดไบโอฟิล์มของสารสกัดสารสกัด จ้อยฉั่วต่อเชื้อในช่องปาก	Biology, Biotechnology and Microbiology	วรพรรณณี เผ่าทองสุข Worapannee Powtongsook	มหาวิทยาลัยหัวเฉียวเฉลิมพระเกียรติ
84.	SSSCI2019_BT_34 SSSCI2019_O_738	ผลของ Non-albicans <i>Candida</i> species ร่วมกับ <i>Streptococcus mutans</i> ต่อความสามารถในการก่อโรคฟันผุ	Biology, Biotechnology and Microbiology	วิรัชพัชร แสนเสนาะ Wirunphat Sansanoa	จุฬาลงกรณ์มหาวิทยาลัย
85.	SSSCI2019_FT_29 SSSCI2019_O_785	การพัฒนาคุณภาพน้ำมันปาล์มสำหรับการทอดอาหารโดยใช้สารสกัดจากสมุนไพร	Food Science and Home Economics	ปฎิญา จิยพิงศ์	กรมวิทยาศาสตร์บริการ

No.	Paper Code/ Registration Code	Topic	Theme	Name	Institute
86.	SSSCI2019_SP_17 SSSCI2019_O_55	ประสิทธิผลของการสอนด้วยชุดสื่อวีดิทัศน์เรื่อง การเช็ดตัวลดไข้ โดยประยุกต์ทฤษฎีแรงจูงใจใน การป้องกันโรคของผู้ดูแลเด็กป่วยแผนกศัลยกรรม เด็ก โรงพยาบาลจุฬาลงกรณ์ สภากาชาดไทย	Sports and Health Science	ฐมาพร เชี่ยวชาญ Tamaporn Chaiwcharn	มหาวิทยาลัย ศรีนคริน ทรวิโรฒ

นานาชาติ

International

ชื่อเรื่อง	หน้า
DEVELOPMENT OF INNOVATIVE MEDIA FOR COMMUNICATION SANGHA IN PHRA NAKHON, BANGKOK, THAILAND Ven. Way Sokhom	1
Application Development for Pon-Yang-Kham Fattened Cattle in Sakon Nakhon Province on Android Operating System Kannikar Kamolrat and Naravit Rakkaen	18
Energy Conservation of Split Type Air Conditioner in Mechanical Engineering Department Building of RMUTL Tak Yuttana Sriudom, Anurat Tewata, Yutthana Munklang, Zinnia Rattipat, Yupparat Jankaew and Yopparat Impitak	27
Design and Analysis of Plastic Medical Tray for Implant Packaging Nattapon Chantarapanich, Tamnuwat Valeeprakhon, Sujin Wanchat and Melvin Stainley Veerasakul	38
Conductive Composite Paper from Cellulose Fiber by in Situ Polymerization of Pyrrole S. Sukkhawuttigit, S. Ummartyotin and Y. Infahsaeng	44
A Polymeric Coating on Prelithiated Silicon-Based Nanoparticles for High Capacity Anodes used in Li-ion Batteries Natthaphong Kamma, Yutthanakon Kanaphan, Sunisa Buakeaw, Songyoot Kaewmala, Jeffrey Nash, Sutham Srilomsak and Nonglak Meethong	56
Effect of drying temperature on quality of RD6 variety brown parboiled glutinous rice Petcharat Jaiboon and Somchart Soponronnarit	64
The preparation of hybrid material of cobalt complex into mesoporous silica from the rice husk Pornpan Tana, Netchanok Jansawang and Patcharaporn Pimchan	71
Effect of PEG-based triazolyl substituents of copper-catalyzed aerobic alcohol oxidation Chomtisa Borsap, Vasut Nakarajouyphon and Preeyanuch Sangtrirutnugul	81
DFT investigation of toluene adsorption on silicon carbide nanosheet doping with transition metal for storage and sensor application Pasakorn Sangnikul, Chanukorn Tabtimsai, Wandee Rakrai and Banchob Wannoo	88
Rapid Analysis of Alpha-Mangostin Content in Anti-Acne Gel by Near-Infrared Spectroscopy	97

ชื่อเรื่อง	หน้า
Sumaporn Kasemsumran, Udomlak Sukatta, Krairuek Ngowsuwan, Sirimada Monkolwit, Nattaporn Sinunta and Prapassorn Rugthaworn Screening and identification of the phytase producing bacteria isolated from natural environments and swine manure	103
Songkran Chuakrut, Apiwat Limsawad, Lakkhana Pom Khet and Aunchalee Thanwisai Development of high anthocyanin crispy rice bar	112
Nuttawut Lainumngen, Janpen Saengprakai, Siriporn Tanjor, Wasan Phanpho and Aran Phodsoongnoen The effect of extraction methods on phenolic, anthocyanin, and antioxidant activities of Riceberry bran	123
Supatchalee Sirichokworrakit, Hathairat Rimkeeree, Withida Chantrapornchai, Udomluk Sukatta and Prapassorn Rukyhaworn A Research of Model of Professional Basketball Management for Professional Basketball Players	133
Jatuporn Banroengsanoh Biomonitoring of metals exposure in Aranyik handicraft workers	137
Churairat Srimanee, Suwalee Worakhunpiset, Yanin Limpanont and Kraichat Tantrakanapa The Effect of Viscosity-imparting Agent on Textural Properties of Toddy Palm Syrup	147
Jitlada Chumee, Saowanee Kumpun, Ploysai Ohama and Daungporn Pupaka	

DEVELOPMENT OF INNOVATIVE MEDIA FOR COMMUNICATION SANGHA IN PHRA NAKHON, BANGKOK, THAILAND

¹

Ven. Way Sokhom¹

Faculty of Social Sciences and Humanities Mahidol University, in Nakhonpathom Bangkok, Thailand

E-mail;waysokhom@gmail.com

Abstract

This research used mixed methods such as qualitative method and quantitative method. Objective of the study were to: 1) to study the states and problems of innovative media development for communication, case study Sangha in Phranakhon, Bangkok, Thailand. 2) To develop the approaches for increasing efficiency development of innovative media for communication, case study Sangha in Phranakhon, Bangkok, Thailand. The same group of this study was Sangha in Phra Nakhon district such as abbot of 14 temples and general 130 monks (all of the monks) who are belong to temples for questionnaire interview and total of 140 monks. The research has found out of two methodologies such as: Qualitative Methodology, research has been conducted to use interviewing Semi-Structure and research has been designed data that from Quantitative Methodology to create questionnaire for interview. There are 7 issues having to these: Population, Research developing, Research design, Examining quality of research instrument which is used in the research, Data collection, Data analysis and Statistics for data analysis and scope of content to study theories and research relation for development of innovative media for communication Sangha in Phra Nakhon district. In six concepts such as: System, Strategies, Resources, Budget, Efficiency and Information of Management. The research instrument was Questionnaire and Semi-Structure. Statistics of the study were frequency, percentage, mean, and S.D. and Graph plot.

The research outcome showed the sample group of respondent monks in Phra Nakhon district, Bangkok, Thailand and 130 monks appeared that the first factor, System of the Administrative monk need to focus on organization to competition, so that, it should improve process of innovative media development for communication and buy new equipment related to innovative media for communication. The secondly factor, about the Strategies of the administrative monks should improve process strategy gain advantage to the temple because head monk of organization has used a new strategy plan for develop of temple. The thirdly factor, about Resource of the administrative monks has been created by the network innovation effectively, such as human-ware, hardware, software, and supported people, so that Abbot need a good quality of resource. The fourthly factor, about Budget of the administrative monks could have budget for manage and saving money to support the project of temple in the future. The fifthly factor, about Efficiency of the administrative monks could implement, enforcement of technologies, products, and services, it still need knowledge, joint venture, training staff, team work and good efficiency. And the lastly factor, about Information & Management of the administrative monks could have suitability of advertising of information for using two of communication that by sending information one face to face and message one temple to another temple get information rapidly. The another objectiveness found that 10 Abbots in Phra Nakhon district for communication innovation development about how to inform internet using carefully which may conflict to monk discipline, efficiency temple net-work for all member in temple and people around the temples service by rapidly and convenience, group line creating for uploading message and saving of work, maintain the equipment to repair for saving budget; otherwise, the Sangha of organization should develop how to use telephone, mobile, internet, email and line, electronic, VDO conference, package program data

base, Facebook, YouTube, computer and notebook that no have the conflict to monk discipline also.

Keywords: DEVELOPMENT; INNOVATIVE; MEDIA; COMMUNICATION; SANGHA

INTRODUCTION

1.1 Background and significance of the study

South East Asia that got potential of Buddhist more than 2561 and have result in life, so religion and culture can service life that it was very important for belief and reaction for do good in the religion. The power of Buddhist is very important for power of government, administration, management and Sangha of Thailand. Primitive world that was leader manage for old modern that have only leader and vice assistant of leader when they fight with enemy, but in theses world will be development and improvement more faster followed by globalization after study of public administration and it has process of administration such as: policy, authority, morality, society, planning, organizing, staffing, directing, coordinating, reporting and budgeting. All of processes above leader should follow all steps for administration.

In present, everything in the world is changing such as: administration, management, technology, knowledge base economy and digital economy. Including, Sangha of Buddhist monk live in society and meet globalization that Sangha has problem related the development of innovative media for communication. Therefore, researcher has interested in studying development of innovative media for communication of Sangha administration and offer benefit to study administration of Sangha development.

The most important that found the four problems of Sangha in Thailand such as: Firstly, structure of centralization authority and less efficiency. Secondly, closely relationship with power of government. Thirdly, live far a way of society and estranged of social that was not pick up and finally, lack of monitoring and improving of discipline. (Phra Phisarn Wattanakun (Titapunyo), 2558 B.E.), pp. 246-247.

Beside to this case, Phra Dhamakhoschan (P.A. Payutto Phra Yun Dhamaketo) said that the sangha organization administration should be getting done through other people by five principles, one of those is directing that mean how to use communication for planning operation and the monk administration should have human relation and leadership. (Phra Dhamakhosachan, P.A. Payutto, 1999 C.E, p.18)

RESEARCH OBJECTIVE

2.1 Objective of the study

1.2.1 To study the states and problems of innovative media development for communication. Case study Sangha in Phranakhon, Bangkok, Thailand.

1.2.2 To develop the approaches for increasing efficiency development of innovative media for communication. Case study Sangha in Phranakhon, Bangkok, Thailand.

2.2 Terms of definition

Development of Innovation Media for Communication means about improvement the of method and instrument using for communicating between Sangha organization and temples under juristic of Phra Nakhon district that could have been effectiveness in two-ways of communication.

Sangha administration means management of Sangha in Phra Nakhon, Bangkok, Thailand in 14 temples of 140 monks including of all kind of management both state and private sectors whiles the word Administration and Management are used to replace each other but mostly, Administration is used for state organization and non-profit organization meanwhile, Management is used for private business in the most.

2.3 Expected outcome

All of relative data by development of innovative media for communication Case Study in Phranakhon, Bangkok, Thailand and researcher use in society and effect in to policy of high class top monk of academic.

1.6.1 To get understanding of data in old communication and new innovation of Sangha and be an approach to solve of Sangha and public organization.

1.6.2 To give this data and suggest to top head of monk (Phra Mahatherasamakhom) for correct and understanding to develop head monk of Phra Nakhon district in Bangkok, Thailand.

1.6.3 To give this data to government update new policy and give to general public for citizen understanding and development of innovative media for communication Sangha administration.

2.4 Conceptual of Study

Study Valuables

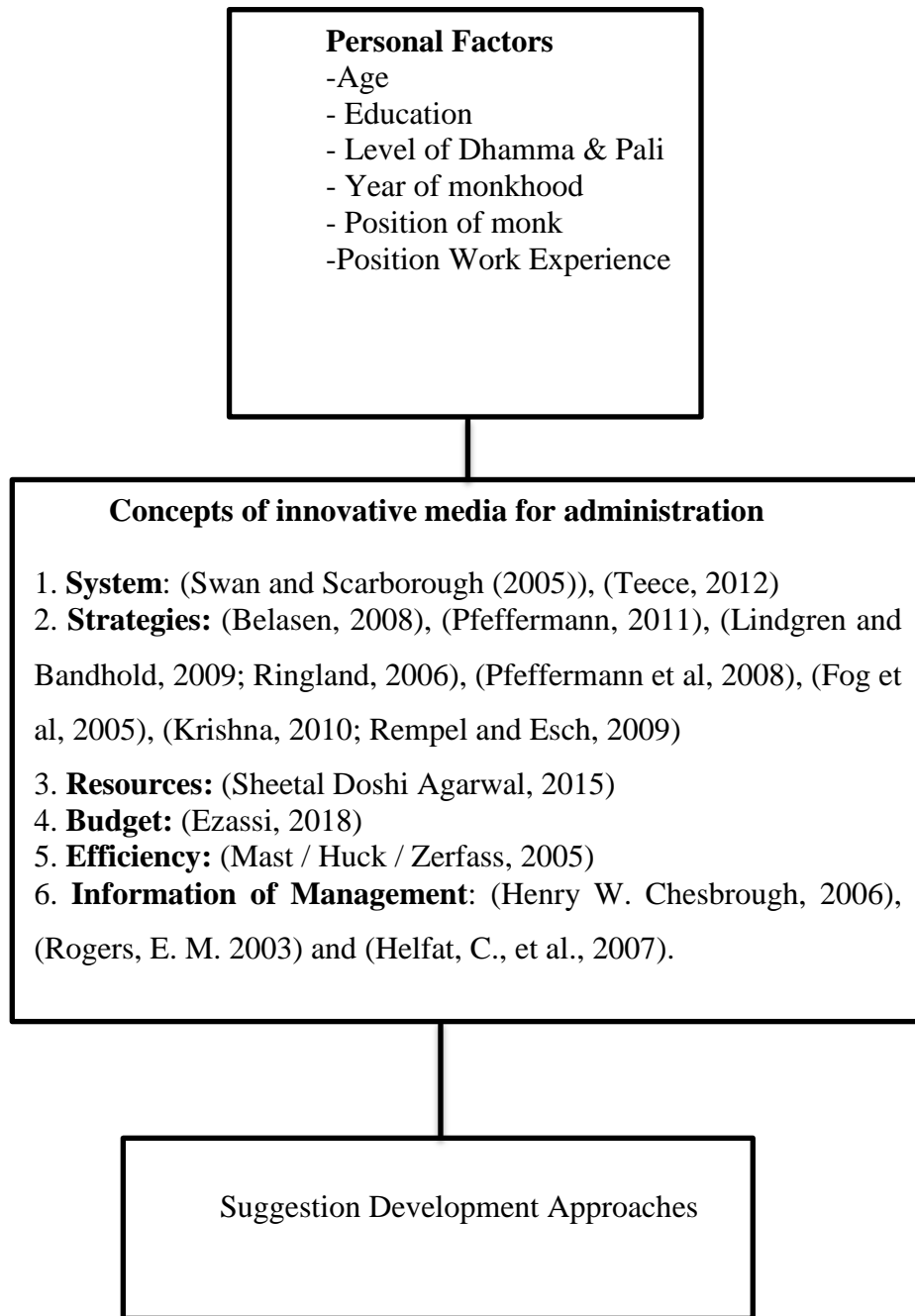


Figure 1-1 Conceptual of Study

RESEARCH METHODOLOGY

This research is about Development of Innovative Media for Communication Case Study: Sangha in Phranakhon, Bangkok, Thailand by mixed methodology. The researcher has found out of two methodologies such as: Qualitative Methodology, researcher has been conducted to use interviewing Semi-Structure and researcher has been designed data that from Quantitative Methodology to create questionnaire for interview. There are 7 issues having to these:

3.1 Population

3.1.1 Population for Qualitative Methodology

To study development of innovative media for communication of Sangha in Phranakhon district have 14 temples such as 1. Wat Phra Chetuphon Vimolmangklaram Rajwaramahaviharn, 2. Wat Mahadhat Yuwarachrangsarit, 3. Wat Suthat Thepwararam, 4. Wat Chanasongkram, 5. Wat Sam Phraya, 6. Wat Sangveswit sayaram, 7. Wat Thepthidaram Worawihan, 8. Wat Ratchburana Ratchaworawihan, 9. Wat Intharawihan Phraramlung, 10. Wat Rachanatdaram, 11. Wat Wat Mahan Pharam Worawihan, 12. Wat Parinayok Worawihan, 13. Wat Eeam Waranut and 14. Wat Mai Armataros. Therefore, interview such as head monk of Phra Nakhorn district 1 monks, Secretary of Phra Nakhorn district 1 monks, Head monk of communes 2 monks and secretary monk of communes 2 that total are 6 monks and general of monk in Phranakhon. In Phranakhon district have 14 temples that researcher selected for qualitative data to interview all of temples in Phranakhon area. Hence, researcher will conduct interview with semi-structure questionnaires.

3.1.2 Population for Quantitative Methodology

Abbot of 14 temples around Phra Nakhon district and general 140 monks (all of the monks) who are belongs to temples for questionnaire interview and the progress of questionnaire had lost 10 questionnaires that monks didn't respond to researcher.

3.2. Research Developing

1. Research instrument is used in collecting data in order to use in this research was interviewing semi-structure which researcher created by study from documents, theories and reviewing related literatures then bring those information to be semi-structure interviewing in six concepts.

2. The questionnaire which is used in this research including of 3 parts as follow:

Part 1, the first was a questionnaire about personal factors of respondents. (Check list) classified as age, education, level of Dhamma & Pali, year of monkhood, position monk and position work experience.

Part 2, Question about objective of development of innovative media for communication the following criteria such as: System, Strategies, Resources, Budget, Efficiency and Information of Management, which applied from Likert's 5 rating scales model and weighted the level as follows;

Level 1 means the states or problems had been the least.

Level 2 means the states or problems had been the less.

Level 3 means the state or problems had been moderate.

Level 4 means the state or problems had been much.

Level 5 means the state or problems had been the most.

Part 3 opened ended of how to develop the approaches for increasing efficiency of Sangha.

3.3 Research Design

Instrument making in this research, the researcher has operated instrument making to use in this research about ADDIE Model such as 1.Analysis 2.Design 3.Development 4.Implementation and 5.Evaluation as follow:

3.3.1 Analysis concept and theory

Analysis document about questionnaire (semi-structured interview by one on one/face to face) and book, literature, theory and related for research conceptual study to six guidelines such as System, Strategies, Resources, Budget, Efficiency and Information of Management for selecting the items making.

3.3.2 Design

Selected concept and theory are design a semi-structure interview, to design questionnaires and to generate questions for respondents. Thus, researcher has to design all of questions based on conceptual framework between quantitative questions and qualitative semi-structure questionnaires.

3.3.3 Development

The researcher has been proved semi-structure interview and questionnaires by using Indexed of Items of objective congress. Indexes of Item of Objective Congruence (IOC) to develop semi- structured interview and questionnaires for research tool validity value above 0.67 and proved reliability of questions researcher has been used Cronbach's Alpha value was 0.954.

3.3.4 Implementation

Qualitative interview 6 monks such as head monk of Phra Nakhon district 1 monks, Secretary of Phra Nakhon district 1 monks, Head monk of communes 2 monks and secretary monk of communes 2 that total are 6 monks.

Quantitative questionnaires abbot of 14 temples around Phra Nakhon district and 134 general monks who belong to the temples for questionnaire interview Sangha in Phranakhon district and Phranakhon district have 14 temples such as 1. Wat Phra Chetuphon Vimolmangklararm Rajwaramahaviharn, 2. Wat Mahadhat Yuwarachrangsarit, 3. Wat Suthat Thepwararam, 4. Wat Chanasongkram, 5. Wat Sam Phraya, 6. Wat Sangveswit sayaram, 7. Wat Thepthidaram Worawihan, 8. Wat Ratchburana Ratchaworawihan, 9. Wat Intharawihan Phraramlung, 10. Wat Rachanatdaram, 11. Wat Wat Mahan Pharam Worawihan, 12. Wat Parinayok Worawihan, 13. Wat Eeam Waranut and 14. Wat Mai Armataros and in 134 general monks who belong to temples.

3.3.5 Evaluation

Qualitative evaluation technique, research has been evaluated data to categories on six guidelines by using triangulation technique quantitative evaluation techniques, researcher used computer analysis package program and researcher evaluated arithmetic mean \bar{x} according to the scores as follow;

1.00 to 1.49 inform to state or problem is the least level

1.50 to 2.49 informs to state or problem is the less level.

2.50 to 3.49 inform to state or problem is moderate level.

3.50 to 4.49 inform to state or problem is much level.

4.50 to 5.00 inform to state or problem is the most level.

3.4 Data analysis

3.4.1 Researcher has been merged data between quantitative data and qualitative data to present approaches for increasing efficiency development innovative media for communication.

RESEARCH RESULTS

Outcome of data analysis of the topic “Development of Innovative Media for Communication Sangha in Phra Nakhon, Bangkok, Thailand”, researcher has spent one month for collecting questionnaires and semi-structure interview from monks at Phra Nakhon district, in Bangkok, Thailand some 130 monks for questionnaires and some 10 monks for semi-structure interview that total all 140 monks which has started since of this process duration of study on April 1st, 2019 – May 1st, 2019 after that researcher has taken the datas to analyses.

4.1 Quantitative Data is all data as table of Statistics and Histogram:

Data processing, researcher has used computer program, SPSS statistic that used in data analysis. Statistic that used is called Descriptive Data. Researcher submitted the analysis in 3 parts such as:

Part 1 the first was a questionnaire about personal factors of respondents of monks that is studies about frequency and percentage, mean, standard deviation.

Part 2 question about objective of development of innovative media for communication the following criteria such as: System, Strategies, Resources, Budget, Efficiency and Information of Management, which applied from Likert’s 5 rating scales model and weighted the level that is studied about percentage, mean, standard deviation and descriptive data of questions.

Part 3 Part opened end of how to develop the approaches for increasing efficiency of Sangh in Phra Nakhon district, Bangkok, Thailand.

Part 1 personal factors of respondents of monks

The respondents of data analysis had conducted in 130 respondents

Table 4-1 number of respondents in age

N	Valid	130
	Missing	0

Table 4-2 frequency and percentage of respondents in age factor

	Frequency	Percent	Valid Percent	Cumulative Percent
Valid 1.00 (20 - 30 years)	33	25.4	25.4	25.4
2.00 (31 - 40 years)	42	32.3	32.3	57.7
3.00 (41- 50 years)	33	25.4	25.4	83.1
4.00 (51- 60 years)	17	13.1	13.1	96.2
5.00 (Over 60 years)	5	3.8	3.8	100.0
Total	130	100.0	100.0	

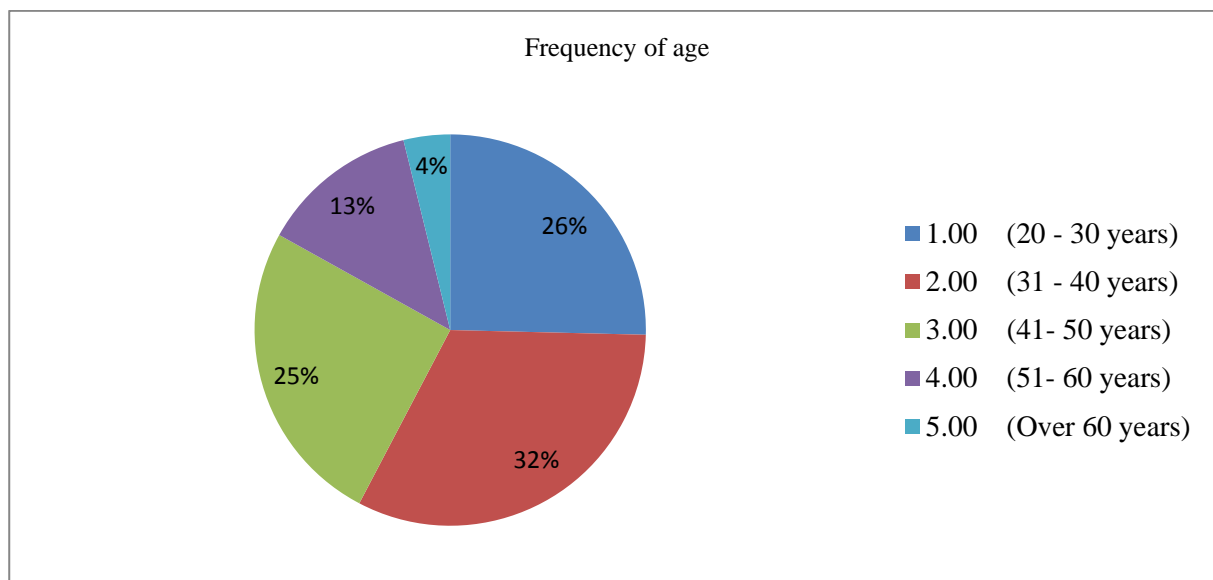


Figure 4 - 2 Frequency of age

In this research has analyzed in age factor that presented respondents age between 20 – 30 years have 33 respondents and 25.4 percentage, respondents age between 31 – 40 years have 42 respondents and 32.3 percentage, respondents age between 41 – 50 years have 33 respondents and 25.4 percentage, respondents age between 51 – 60 years have 17 respondents and 13.1 percentage and respondents age between over 60 years have 5 respondents and 3.8 percentage.

Part 2 objective of development of innovative media for communication

Question A1 is the hierarchical monk mechanisms of control could support innovation media for communication.

Table 4-3 descriptive data of question A1

	N	Minimum	Maximum	Mean	Std. Deviation
A1	130	1.00	5.00	3.0308	.98782
Valid N (listwise)	130				

For the first question presented respondent is 130 persons, answered minimum of attitude is 1 level that means least attitude system and maximum of attitude of system is 5 levels, mean is 3.03 and standard deviation is 0.99 that is the hierarchical monk mechanisms of control could support innovation media for communication is moderate in attitude of system.

Question A2 is the organization of the Buddhist monastery temples is flexible and open to use of innovative media development for communication.

Table 4-4 descriptive data of question A2

	N	Minimum	Maximum	Mean	Std. Deviation
A2	130	1.00	5.00	3.0615	.86941
Valid N (listwise)	130				

For the second question presented respondent is 130 persons, answered minimum of attitude is 1 level that means least attitude system and maximum of attitude of system is 5 levels, mean is 3.06 and standard deviation is 0.87 that is the organization of the Buddhist monastery temple is flexible and open to use of innovative media development for communication is moderate in attitude of system.

Question A3 is the organization of Buddhist temples use input method media mix wireless, satellites, Cable and as an innovative media development for communication.

Table 4-5 descriptive data of question A3

	N	Minimum	Maximum	Mean	Std. Deviation
A3	130	1.00	5.00	3.0846	.88951
Valid N (listwise)	130				

For the third question presented respondents are 130 persons, answered minimum of attitude is 1 level that means least attitude system and maximum of attitude of system is 5 levels, mean is 3.08 and standard deviation is 0.89 that is the organization of Buddhist temples use input method media mix wireless, satellites, Cable and as an innovative media development for communication is moderate in attitude of system.

Question A4 is the organization of Buddhist temple has process for innovation media development for communication.

Table 4-6 descriptive data of question A4

	N	Minimum	Maximum	Mean	Std. Deviation
A4	130	1.00	5.00	2.8692	.91828
Valid N (listwise)	130				

For the four question presented respondents are 130 persons, answered minimum of attitude is 1 level that means least attitude system and maximum of attitude of system is 5 levels, mean is 2.87 and standard deviation is 0.92 that is the organization of Buddhist temple has process for innovation media development for communication is little in attitude of system.

Question A5 is the organization of Buddhist temple need to create new outcome system innovative media development for communication from other organizations.

Table 4-7 descriptive data of question A5

	N	Minimum	Maximum	Mean	Std. Deviation
A5	130	1.00	5.00	2.8692	.91828
Valid N (listwise)	130				

For the four question presented respondents are 130 persons, answered minimum of attitude is 1 level that means least attitude system and maximum of attitude of system is 5 levels, mean is 2.87 and standard deviation is 0.92 that is the organization of Buddhist temple need to create new outcome system innovative media development for communication from other organizations is little in attitude of system.

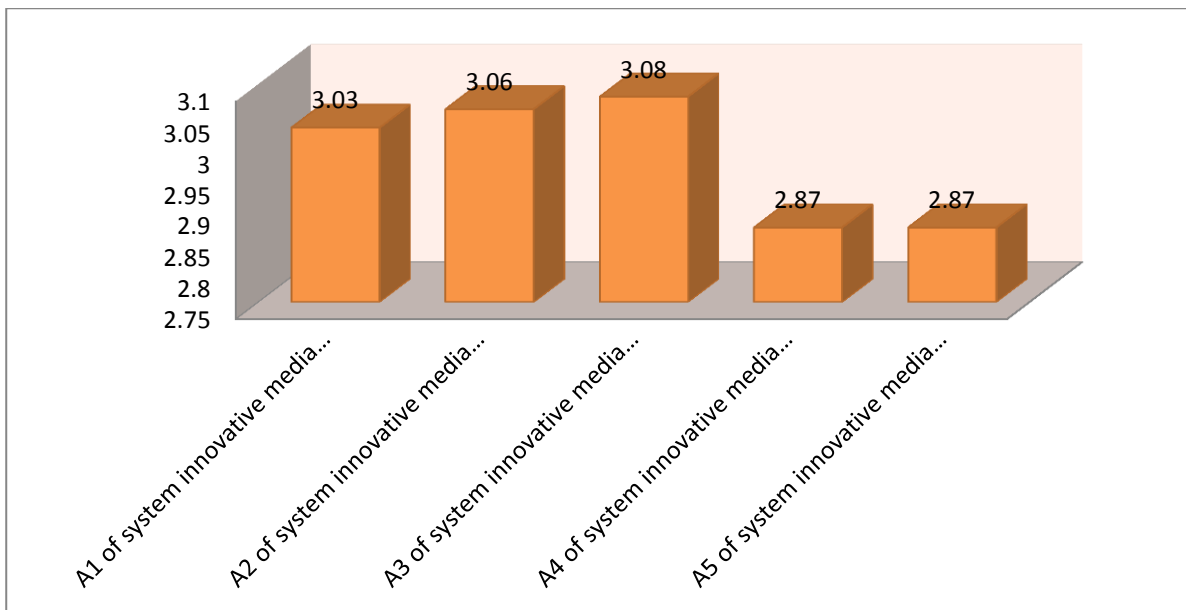


Figure 4-3 Comparison of details in system innovative media development for communication

The data are presented system innovative media development for communication found 3 factors should develop to success as follows: the hierarchical monk mechanisms of control could support innovation media for communication (A1: average is 3.03), the organization of the Buddhist monastery temple is flexible and open to use of innovative media development for communication (A2: average is 3.06) and the organization of Buddhist temples use input method media mix wireless, satellites, Cable and as an innovative media development for communication (A3: average is 3.08) however, to improve the system innovative media development for communication should improve to success as follows: the organization of Buddhist temple has process for innovation media development for communication (A4: average is 2.87) and the organization of Buddhist temple need to create new outcome system innovative media development for communication from other organizations (A5: average is 2.87).

Part 3, opened ended of how to develop the approaches for increasing efficiency of Sangha in Phra Nakhon district, Bangkok, Thailand such as:

About the system suggestion; the Sangha organization of Phra Nakhon district should have technological course in major of Dhamma learning in Pali step 1 to Pali step 9, and also has modern innovation learning course in education of Sangha system.

About the strategy suggestion; Sangha organization of Phra Nakhon district should develop communication media and create the innovation media for monks, study the state of problem in each location for study discovering, analyzing, researching, evaluating, advising and teaching all of monk to perceive Sangha strategy of development innovative media communication.

About resource suggestion; the Sangha organization of Phra Nakhon district should have people-ware, learning resources, modern innovation service, specific communication service organization ,

Personnel, enhancement and knowledge, object material, university or institute of communication and internship training course for Sangha resource of development innovative media communication.

About budget suggestion; the Sangha organization of Phra Nakhon district should have the budgeting for net-working internet and Wi-Fi.

About efficiency suggestion; the Sangha organization of Phra Nakhon district should have been efficiency budgeting, controlled-laws protecting error happening, and got readiness and focusing on practical more than theoretical performance.

About information & management suggestion; the Sangha organization of Phra Nakhon district should have personnel training course in modern equipment.

4.2 Qualitative results of Development of Innovative Media for Communication Sangha in Phra Nakhon, Bangkok, Thailand from semi-structures of 10 monks such as:

The recommendation of 10 Abbots in Phra Nakhon district for communication innovation development about how to inform internet using carefully which may conflict to monk discipline, efficiency temple net-work for all member in temple and people around the temples service by rapidly and convenience, group line creating for uploading message and saving of work, maintain the equipment to repair for saving budget; otherwise, the Sangha of organization should develop how to use telephone, mobile, internet, email and line, electronic, VDO conference, package program data base, Facebook, YouTube, computer and notebook that no have the conflict to monk discipline also.

4.3 Improvement factors for Development of Innovative Media for Communication Sangha in Phra Nakhon, Bangkok, Thailand

The administrative monks should improve administration as follow:

1. To focus on process for innovative media development for communication (A4).
2. To focus on outcome system innovative media development for communication from other organization (A5).
3. To focus on strategies management of the organization Buddhist temple has innovative media development for communication decision making process of the stakeholders (B1).
4. To focus on there is a clear of strategies innovative media development for communication of the organization Buddhist temple (B2).

5. To focus on strategies to gain advantage other organization (B3).
6. To focus on strategies of the organization Buddhist temple related companies of innovative media development for communication (B4).
7. To focus on there is human-ware of volunteer for support system innovative media development for communication (C1).
8. To focus on there is hardware for using innovative media development for communication (C2).
9. To focus on there is software management for innovative media development for communication (C3).
10. To focus on the community support in innovation media development for communication (C5).
11. To focus on the budgeting for innovative media development for communication is enough for hardware (D1).
12. To focus on the budgeting for innovative media development for communication is enough for software (D2).
13. To focus on the budget supported the strategy of innovative development for communication (D3).
14. To focus on there is budgeting of provident fund for innovative media development for communication (D4).
15. To focus there is knowledge joint venture of innovative media development for communication (E1).
16. To focus on there is training staff for innovative media development for with team work in the organization of Buddhist temple (E2).
17. To focus on checking and balancing the data through the innovative media development for communication with team work in the organization of Buddhist temple (E3).
18. To focus on the relationship between head organization temple of Sangha in using innovative media for communication (E4).
19. To focus on the environment of general monks can select innovative media development for communication (F1).
20. To focus on the information of context applies for Buddhist of organization (F2).
21. To focus on the information technology is updated by information of technology innovative media development for communication (F3).

4.4 Improvement framework

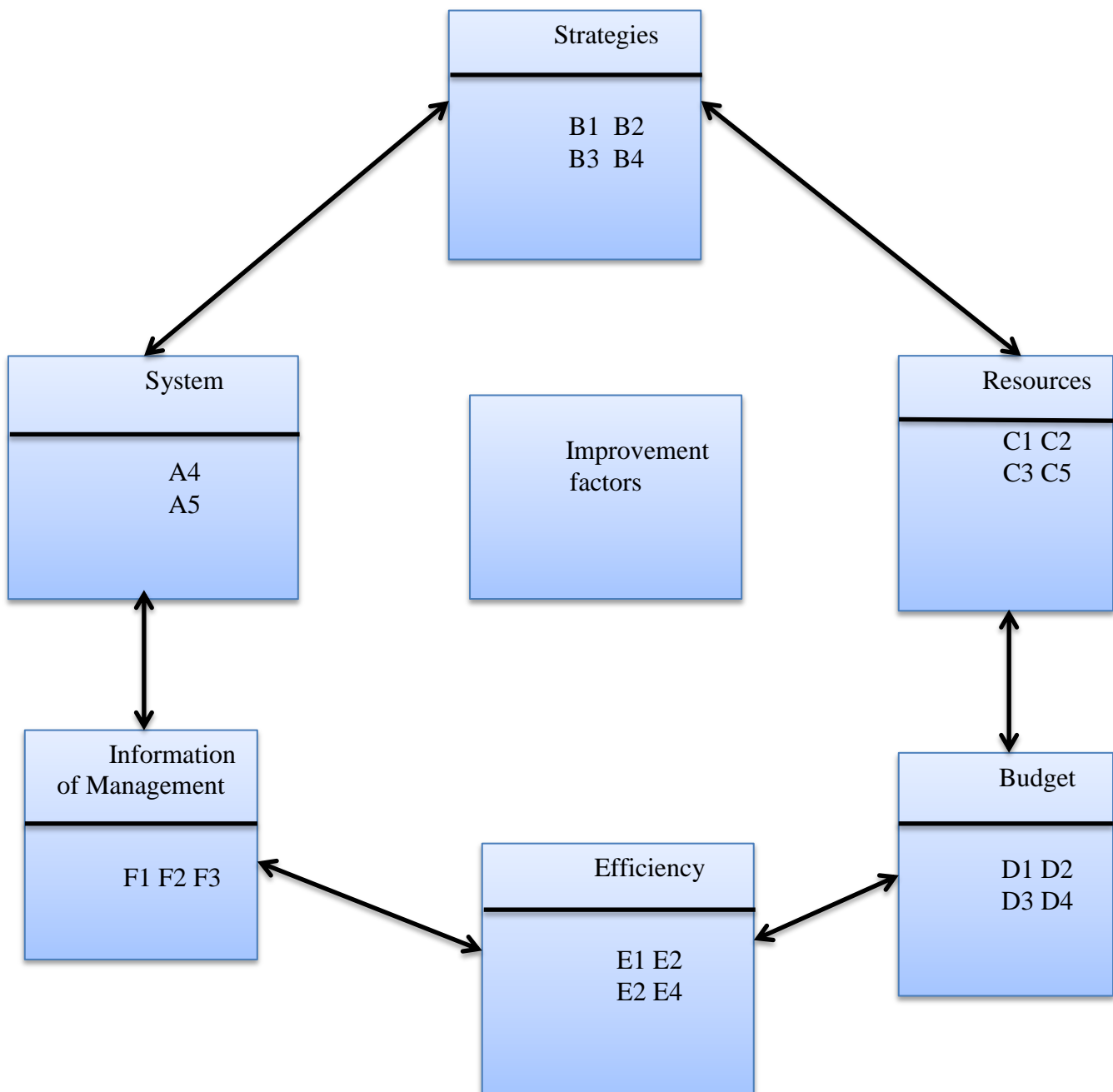


Figure 4-4 Improvement frameworks

References

- Belasen, A. (2008). **The Theory and Practice of Corporate Communication: A Competing Values Perspective**. Sage Publications, Thousand Oaks, CA.
- EZASSI Technology to innovate faster. (2018). **Innovation Budget: Innovation Budget Planning: 8 Things to consider**. Retrieved from <https://ezassi.com/innovation-budget-planning-8-things-consider/>
- Fog K., Budtz. C. and Yakaboylu. B. (2005). **Storytelling Branding in Practice**. Springer. Business and Management. Retrieved from <https://www.springer.com>
- Helfat, C., Finkelstein, S., Mitchell, W., Peteraf, M., Singh, H. Teece, D. and Winter, S. (2007). **Dynamic Capabilities: Understanding Strategic Change in Organization**. Malden, MA: Blackwell.
- Henry W. Chesbrough. (2006). **Open Innovation: The New Imperative for Creating and Profiting from Technology**. Boston, Massachusetts: HARVARD BUSINESS SCHOOL PRESS.
- Krishna V. (2010). **Auction Theory**. San Diego: Academic Press.
- Mast, C., Huck, S., and Zerfass, A. (2005). **Innovation communication**. Outline of the concept and empirical findings from Germany. *Innovation Journalism*, 2(7), 1-14.
- Pfeffermann, N., Hulsmann, M., and Scholz-Reiter, B. (2008). **Framing Innovations to Grasp Stakeholders' Attention: A Dynamic Capability-Based Conception of Innovation Communication**. Research Report 2007/08 International Graduate School Dynamics in Logistics, Vol. 01, 2008, pp.40-44.
- Pfeffermann, N. (2011). **The Scent of Innovation-Towards an Integrate Management Concept for Visual and Scent Communication of Innovation**. In M. Hulsmann & N. Pfeffermann (Eds.), *Strategies and Communications for Innovation* (Chapter 12). Berlin, Germany: Springer.
- Phra Phisarn Wattanakun (Titapunyo). (2558 B.E., January – April). **Communication for Sangha's Administration to Society**. Education Review Magazine of Mahchulalongkornrajavidyalay University.
- Phra Dhamakhosachan, (P.A. Payutto, 1999 C.E, p.18) **Buddhist way in administration Edit fourth**. Bangkok: Mahchulalongkornrajavidyalay University. Print-Hall.

- Rempel, J. E. & Esch, F.-R. (2009). **Olfaktorische Reize in der Kommunikation**. In M. Bruhn, F.-R. Esch, & T. Langer (Eds.), *Handbuch Kommunikation: Grundlagen, innovative Ansätze, prak-tische Umsetzungen* (pp. 285-315). Wiesbaden: Gabler Verlag.
- Ringland D. (2006). **Scenario Planning Managing for the Future**. (2nd ed.) Chichester. Wiley.
- Rogers, E. M. (2003). **Diffusion of innovation**. (5th ed.) New York: Free Press.
- Sheetal Doshi Agarwal. (2015). **The Process of Networked Civi Innovation: Examining the Role of Values, Resources, and Power in Community-Based Technology Projects**. Washington, Published by Pro Quest LLCC (2015).
- Swan, J. and Scarborough, H. (2005). 'The politics of networked innovation', *Human Relations*, 58:913-943.
- Teece, D. J. (2012). "Next-Generation Competition: New Concepts for Understanding, How Innovation Shapes Competition and Policy in the Digital Economy". *Journal of Law, Economics, and Policy*, Vol.9/1, George Mason University School of Law, Fairfax Drive Arlington, VA, pp.97-118.

Application Development for Pon-Yang-Kham Fattened Cattle in Sakon Nakhon Province on Android Operating System

Kannikar Kamolrat^{1,a}, Naravit Rakkaen^{1,b}

¹ Computer Department, Science and Technology Faculty, Sakon Nakhon Rajabhat University, Thailand
E-mail; ^akannikar@snru.ac.th, ^bnaravit.ra57@snru.ac.th

Abstract

Pon-Yang-Kham Fattened Cattle, Thai-French beef cattle, is a high-quality beef that has been popular with both Thai and foreigners. Also, it is the top economic animal of Sakon Nakhon Province. Therefore, this research was done to provide another public relations channel for Pon-Yang-Kham Fattened Cattle Sakon Nakhon Province to make it more well-known through mobile phones, which is a very popular communication device. The purposes of the research were to develop an application for Pon-Yang-Kham Fattened Cattle in Sakon Nakhon Province on Android operating system, to assess the efficiency of the application, and to assess user satisfaction towards the application. The research started by gathering information about Pon-Yang-Kham Fattened Cattle then analyzed and designed the application, which consisted of web application and mobile application. After that, the application was implemented and tested. It was then assessed the efficiency by experts. Lastly, its user satisfaction was assessed by a sample group using an assessment form.

The developed application had six main menus, including Pon-Yang-Kham history, breeds, fattening methods, types of beef, livestock farmer groups, and recommend restaurants. The efficiency assessment result by five experts was at a high level, with an average score of 4.26. The satisfaction assessment result by 100 users was at a high level, with an average score of 4.15. In summary, the developed application had acceptable efficiency and could be used as a tool for publicizing Pon-Yang-Kham Fattened Cattle information. Suggestions for further development, the application should have a channel for contacting experts, and for sharing knowledge or notifying about news and promotions.

Keywords: Pon-Yang-Kham Fattened Cattle; Application; Android Operating System;

1. Introduction

Ko Khun Pon Yang Kham or Pon-Yang-Kham Fattened Cattle is derived from crossbred Thai-French beef cattle. The cattle have emerged from artificial insemination between 3 breeds, including Charolais originated in France, which is the main breed, Simmental originated in Switzerland, and Limusin originated in France (Pon Yang Kham Livestock Cooperatives, 2015). When the crossbred cattle are about 2 years old, they will undergo the "cattle fattening" process by deworming, vaccination, and castration before putting in the stables. Pon Yang Kham Livestock Cooperatives use a technique that lets the cattle listen to music to make them eat a lot of food and believe that the beef will be tender. The cattle are fed mainly with natural foods, which divided into a coarse meal that is grass or straw and supplemented with exceptional food made of grains. This makes the beef have a sweeter aroma and more flavor. The stables are well looked after: clean the floor, collect manure, shower and brush the cattle, make them eat more food. This method helps shorten the period of cattle fattening from about 1 year to 8-9 months. When the fattening process is finished, the cattle are dissected in standard slaughterhouses. The meat is incubated for 7 days before grading the marbling, then cut into pieces and defined the name according to the French 17 parts using the standards of France (Pon Yang Kham Livestock Cooperatives, 2016). Pon-Yang-Kham Fattened Cattle the top economic animal of Sakon Nakhon province but still lacking variety and up-to-date public relations channels. The use of mobile technology for product promotion in marketing is prevalent. Because currently, mobile phones are widespread communication devices for communication and accessing information. The operating system using on most mobile phones is Android because it is a prevalent open-source operating system from Google Inc. Due to a large number of devices using Android, the devices come at many different prices and can work on devices with different screen sizes and

resolutions. These allow consumers to choose as needed. As for programmers, developing a program for Android is not difficult, because there are development information and the Android SDK (software development kit) provided for developers to learn. When developers want to publish or distribute the developed programs, they can distribute the applications through the Android Market. But if talking about the structure of the development language, the Android SDK uses the structure of Java Language in programming. Because the program developed must be working under Dalvik Virtual Machine, just like Java programs that run under Java Virtual Machine (Virtual Machine is comparable to the environment in which the program is running). In addition, there are a large number of open-source Android software, so interested developers can easily study the original software. Furthermore, the popularity of Android has increased dramatically (Canalys, 2018). A mobile application, most commonly referred to as an app, is a type of application software designed to run on a mobile device, such as a smartphone or tablet computer. Mobile applications frequently serve to provide users with similar services to those accessed on PCs. Apps are generally small, individual software units with limited function (Black|Line IT, 2019). For example, there are apps for agriculture (Ministry of Agriculture and Cooperatives, 2018), transportation (Office of Transport and Traffic Policy and Planning, 2016), health (Thai Health Promotion Foundation, 2015), and Tourism (Unardi F., Kusuma D., & Zhang A., 2019). As mentioned above, the Pon-Yang-Kham Fattened Cattle in Sakon Nakhon Province on Android operating system were developed.

2. Objectives

1. To develop an application for Pon-Yang-Kham Fattened Cattle in Sakon Nakhon Province on Android operating system.
2. To assess the efficiency of the application for Pon-Yang-Kham Fattened Cattle in Sakon Nakhon Province on Android operating system.
3. To assess user satisfaction towards the application for Pon-Yang-Kham Fattened Cattle in Sakon Nakhon Province on Android operating system.

3. Methodology

The research methodology used in the application development is as the following.

3.1. Research framework

Based on the current information of Pon Yang Kham in Sakon Nakhon Province, the researcher had the idea to develop a tool to help provide information and publicize for tourists or those interested in Pon Yang Kham Fattened Cattle. Figure 1 shows the conceptual framework of this research.

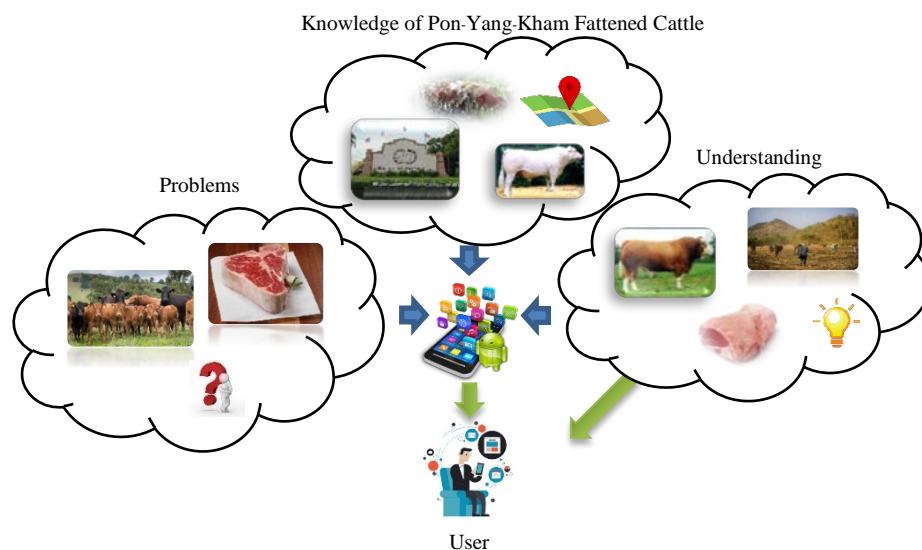


Figure 1. Conceptual framework of the research

From Figure 1, details are described here.

Problems: The channels for publicizing Pon Yang Kham Fattened Cattle in Sakon Nakhon are limited.

Knowledge of Pon-Yang-Kham Fattened Cattle: Information about Pon Yang Kham Fattened Cattle in Sakon Nakhon Province that the application has collected.

Understanding: People who study this application have a better understanding of Pon Yang Kham Fattened Cattle in Sakon Nakhon province.

User: The user of the application means general users or those who are interested in information about Pon Yang Kham Fattened Cattle in Sakon Nakhon province.

3.2. Studying and information gathering

For this step, the researcher studied and gathered various information as listed.

1. Study and collection of information about Pon Yang Kham Fattened Cattle by asking experts and reading documents in Pon Yang Kham Livestock Cooperatives.

2. Study application development on Android using Java language, study the PHP language used to write a web application with MySQL, study the extraction of data from a web application to display on the application in the form of JSON.

3. Study the information about creating the efficiency assessment form and the user satisfaction assessment form.

3.3. System analysis and design

After studying and collecting relevant information about Pon Yang Kham Fattened Cattle, the information is used to analyze and design the system using the use case diagram and sequence diagram, as shown.

3.3.1. Use case diagram

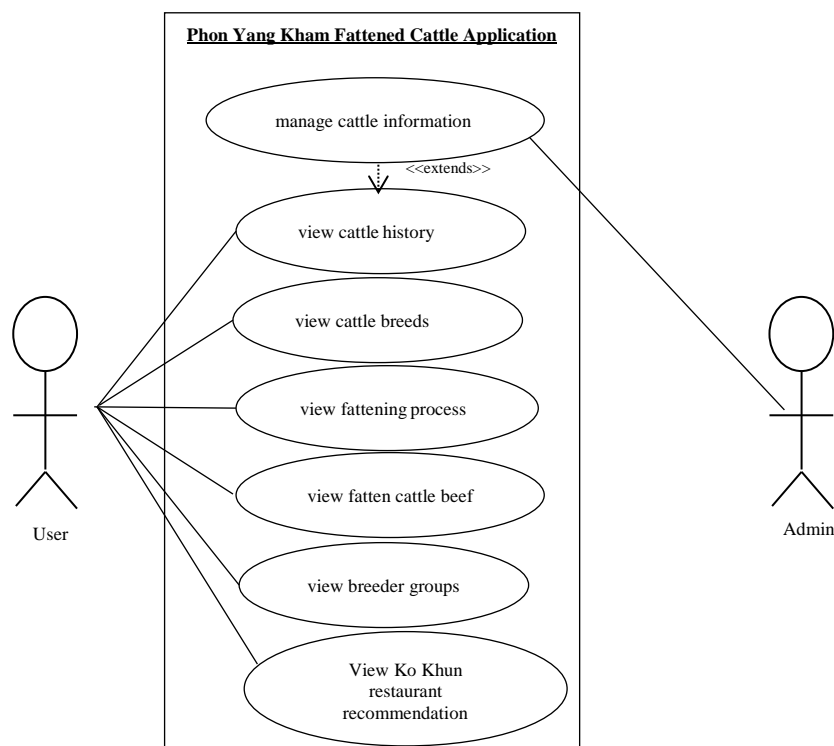


Figure 2. Use case diagram

3.3.2. Sequence Diagram

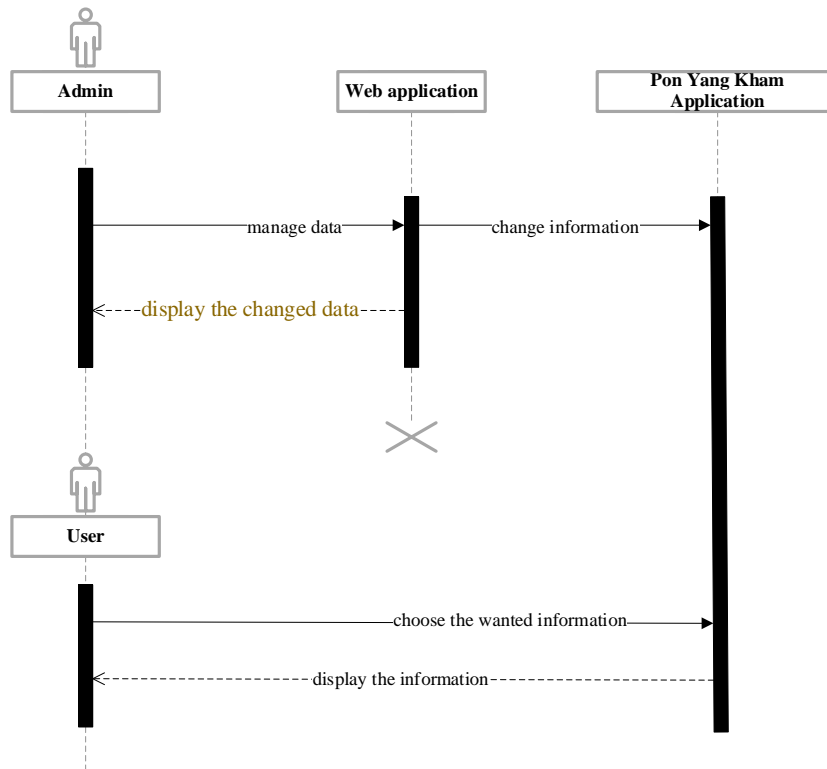


Figure 3. Sequence diagram

3.4. System Development and testing

The application development is divided into 2 parts: The Android application on the smartphone and web applications for data management.

The Android application is developed with Android SDK, JDK (Java Development Kit) SE 8u121, and Java for use on smartphones running Android 6.0 or higher.

The web application is developed with PHP language for website coding, MySQL and JSON data extraction format for extracting data from the web application to display on the mobile application.

For system testing, the developers initially tested the functionality of the application using white-box testing. Then, the application's efficiency was evaluated by experts. And the satisfaction from the sample groups is collected after experimenting with the application.

3.5. Research instruments

The research instruments consisted of:

1. The developed Pon Yang Kham Fattened Cattle in Sakon Nakhon province application on Android.
2. The application efficiency assessment form for experts
3. The user satisfaction assessment form for the application users

3.6. Assessment of efficiency and satisfaction towards the application

Once the developed application testing was finished. The application was brought to 5 consisted of 1 mobile technology expert, 1 graphic expert, 1 system expert, and 2 Pon Yang Kham Fatten Cattle experts; who evaluate its effectiveness. After that, the satisfaction was assessed the sample group of 100 users. The application efficiency and user satisfaction were at a high level and can actually be used.

4. Results and discussions

The details of the results of the Pon Yang Kham Fattened Cattle in Sakon Nakhon province on Android application development operating system are following:

4.1. Information management page for administrators

The information management page is a web application screen for managing Pon Yang Kham Fatten Cattle data. In which the administrators can add, delete, or edit the data as in Figure 4.



Figure 4. The application screen for information management by administrators

4.2. The first screen of the application

The first screen of the application on a smartphone has a start button, as in Figure 5.



Figure 5. The first screen of the application

4.3. The main menu screen of the application

The main menu screen consists of 6 main menus, namely Pon Yang Kham Fattened Cattle history, Pon Yang Kham Fattened Cattle breeds, Pon Yang Kham Fattening method, Pon Yang Kham Fattened Cattle beef, Pon Yang Kham Fattened Cattle livestock farmer groups, and recommend Pon Yang Kham Fattened Cattle Restaurants; the sample menus are shown in Figure 6.



Figure 6. Example of an application's main menu screen

4.4. The information display screens

There are 2 types of screens the information display screen which are

4.4.1 Information display screen 1 level

For the 1 level information display screen, when the user selects a menu to view data, the application will display the details of that data only the first level, as shown in Figure 7.



Figure 7. Example of a 1-level information display

4.4.2 Information display screen 2 levels

For the 2 level information display screen, when the user selects to view information, the application will show the details of all 2 levels of data. Such as, when selecting the Pon Yang Kham Fattened Cattle Breed menu, at level 1 the application will show names of all breeds for users to choose. But when choosing a breed of Pon Yang Kham Fatten Cattle, it will show details of that breed in level 2, as in Figure 8.



Figure 8. Example of a 2-level information display

4.5. Location screen of Pon Yang Kham Fattened Cattle restaurants

The screen showing the location of Pon Yang Kham Fattened Cattle Sakon Nakhon Province restaurants is shown as an example in Figure 9.

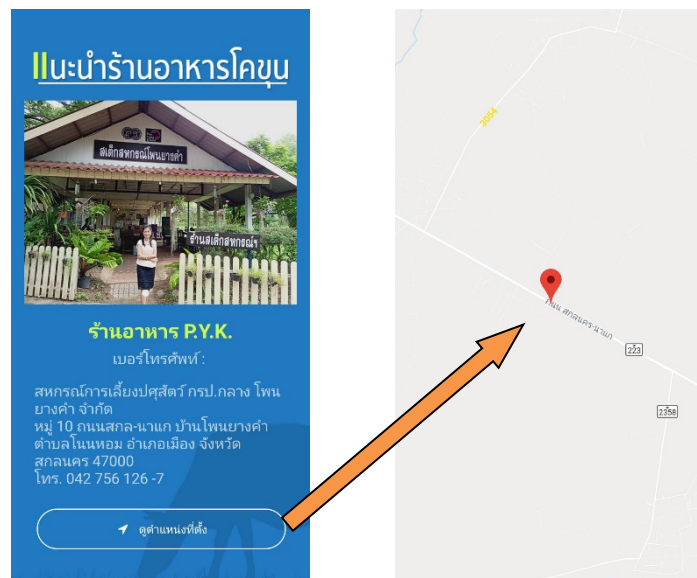


Figure 9. Example of location screen

4.6. Efficiency assessment results and satisfaction assessment results

The details of the application efficiency results by 5 experts are in the following table.

Table 1. Result of application efficiency assessment by experts

Topics	average	S.D.
The application functionality		
1. Application can add, delete, and edit information correctly.	4.80	0.45
2. The application is easy to use.	4.20	0.45
3. The application is reliable.	4.20	0.45
Average per topic	4.40	0.51
The application meets the requirement		
1. The application offers useful information.	4.20	0.45
2. The application offers information that meets the needs of users.	4.20	0.45
3. The application classifies data clearly and appropriately.	4.27	0.46
Average per topic	4.27	0.46
The application processing		
1. The Correctness of data inputted into the application.	4.40	0.55
2. Accuracy of results obtained from application processing.	4.40	0.55
3. Speed of processing of application.	4.00	0.71
Average per topic	4.27	0.59
The form and image of the application		
1. Appropriateness of the font size in the application	4.20	0.45
2. Appropriateness of font styles and colors in the application	4.00	4.00
3. Appropriateness of images in the application	4.20	0.45
4. Appropriateness of menu button placement in the application	4.20	0.45
Average per topic	4.15	0.37
Overall average	4.26	0.48
	*(0.05)	

Note * Standard error

From Table 1, a summary of the assessment result by experts ranks topics by the average score from max to min. The application functionality has an average of 4.40. The application meets the requirement, and the application processing both have an average of 4.27. While the form and image of the application has an average of 4.15. The overall average score is 4.26, with a standard error of 0.05, indicating that the experts' opinions do not differ much that the application's efficiency is high.

For user satisfaction evaluation result by the sample group of 100 people is at a high level with the overall average of 4.15. The respondents were 46 males and 54 females. In conclusion, the developed Pon Yang Kham Fattened Cattle application has acceptable efficiency, can be used as a tool to publicize the information of Pon Yang Kham Fattened Cattle Sakon Nakhon Province to become more known.

5. Conclusions and suggestions

In summary, the developed Pon Yang Kham Fattened Cattle application consists of 6 main menus: Pon Yang Kham Fattened Cattle history, Pon Yang Kham Fattened Cattle breeds, Pon Yang Kham Fattening method, Pon Yang Kham Fattened Cattle beef, Pon Yang Kham Fattened Cattle livestock

farmer groups, and recommend Pon Yang Kham Fattened Cattle Restaurants. The assessment result by 5 experts is at a high level with an overall average score of 4.26. And the user satisfaction towards the application by the sample group of 100 people is at a high level with the overall average of 4.15. It can be concluded that the efficiency of the developed application is accepted. The application can be used as a tool to promote Pon Yang Kham Fattened Cattle Sakon Nakhon Province's information. The results are consistent with the research by Nakphon A., & Kamolrat K. (2017) and Thongsiri T., & Kamolrat K. (2017) on publicizing the products of Sakon Nakhon Province. The suggestions for further development are additional channels should be added for contacting experts, and knowledge sharing or notification for news and various promotions. Currently, the app can be run on Android only, therefore it should be further developed for other mobile platforms.

References

- Black|Line IT. (2019). *What is a Mobile App?*. Retrieved from <https://blacklineit.com/2017/04/12/whats-difference-mobile-app-mobile-responsive-website>
- Canalys. (2018). *Android Operating System*. Retrieved from <https://www.canalys.com/newsroom>
- Ministry of Agriculture and Cooperatives. (2018). *Mobile Application*. Retrieved from https://www.moac.go.th/service_all-mobile_app
- Nakphon A., & Kamolrat K. (2017). *Application Development for Thai Blueberry in Sakon Nakhon Province on Android Operating System*. The 9th National Conference on Information Technology (NCIT2017), Thailand 2017.
- Office of Transport and Traffic Policy and Planning. (2016). *Applications under the Ministry of Transport*. Retrieved from <http://www.otp.go.th/index.php/post/view?id=1774>
- Pon Yang Kham Livestock Cooperatives. (2015). *History of Pon Yang Kham Livestock Cooperatives*. Retrieved from <http://www.coopthai.com/pykcoop/History.html>
- Pon Yang Kham Livestock Cooperatives. (2016). *Guide to Raising Cattle Fattening for Farmers*. Sakon Nakhon. Thai Health Promotion Foundation. (2015). *DoctorMe Application*. Retrieved from <https://www.doctorme.in.th>
- Thai Health Promotion Foundation. (2015). *DoctorMe Application*. Retrieved from <https://www.doctorme.in.th>
- Thongsiri T., & Kamolrat K. (2017). *Application Development for Church in Sakon Nakhon Province on Android Operating System*. The 9th National Conference on Information Technology (NCIT2017), Thailand 2017.
- Unardi F., Kusuma D., & Zhang A. (2019). *Traveloka*. Retrieved from <https://www.traveloka.com/en>

Energy Conservation of Split Type Air Conditioner in Mechanical Engineering Department Building of RMUTL Tak

Yuttana Sriudom^{1, a}, Anurat Tewata^{1, b}, Yutthana Munklang¹, Zinnia Rattipat², Yupparat Jankaew²,
Yopparat Impitak²

¹Faculty of Engineering, Rajamangala University of Technology Lanna Tak

²Faculty of business, Rajamangala University of Technology Lanna Tak

E-mail; ^aYuttana.sriudom@gmail.com, ^b A.Tewata@gmail.com

Abstract

This research aimed to conserve energy of split type air conditioners in mechanical engineering department building of Rajamangala University of Technology Lanna Tak. There are eight air conditioners with the capacities of 25,345.6 BTU/hr for each air conditioner. From the past operation, the air conditioners were missed of maintenance for the both of evaporator and condenser units. So, their cooling efficiencies were lower than standard range. In this research, the air conditioners were maintenance and then, were compared for their energy efficiency ratios (EER) with the values before maintenance. The result from comparison was found that after maintenance the average EER of them were increased from 6.7 to 10.6 BTU/hr/W. The EER was increased about 3.9 BTU/hr/W or 58.2% of the EER before maintenance. The air conditioner maintenance could reduce electricity energy consumption about 10,044.8 kWh/yr accounted for 32,517.1 baht/yr. From this result, it indicated that usually cleaning and maintenance air conditioners made them have lower electricity energy consumption than the ones not usually cleaning and maintenance. Moreover, usually cleaning and maintenance made them operate with full efficiency.

Keywords: Energy Conservation, Split Air Condition, Energy Efficiency Ratio, Maintenance;

1. Introduction

Thailand is in the tropical zone near the equator. So it has warm and humid climate most of the year. The average temperature of the country is between 19 to 38°C. The hottest period is in the middle of April when air conditioners play an important part of energy consumption. Its ratio is about 60% of all energy consumption. To conserve energy consumption of the air conditioners without reducing users' comfort while the cost is saved, it is necessary to know about operating manners of each type of air conditioners as well as how to choose the appropriate size and type of air conditioner for the room. Including the right way for installation, using and maintenance of air conditioners should be known, too. From these reasons, many researchers have tried to find out the way to increase their efficiencies and reduce their energy consumptions. For the example, ChenWei-HanMo et.al. investigated the effect of an energy saving device (ESD) on the performance of a split-type air conditioner (SAC). The ESD was fabricated using a moisture-transferring and quick-drying textile (MTQDT), a condensate pipeline, and a distributor. The MTQDT was coated on the shell surface of the compressor to absorb the condensate expelled by a condensate pipeline and distributor to enable evaporative cooling of the compressor. The SAC was tested under various outdoor air conditions (29, 32, and 37°C; 55% relative humidity) and under a fixed indoor air condition (26°C; 50% relative humidity), and the performance of the SAC before and after ESD installation was compared. Results demonstrated that the MTQDT effectively improved compressor cooling and the efficiency of the SAC. Compared with the SAC without an ESD under the optimal condition, the shell temperature of the compressor, high-side pressure, and power consumption of the proposed SAC were 15.1°C, 2.7%, and 9.2% lower, respectively. Moreover, the dehumidification capacity and energy efficiency ratio of the proposed SAC were 25.4% and 7.3% higher, respectively. S. Theerakulpisut and S. Priprem dealt with an experiment to improve the energy efficiency of small split-type air conditioners by cooling the condenser air using water condensate resulting from dehumidification of air in the evaporator. The condensate was sprayed into the condenser air stream of an experimental air conditioning unit via a nozzle and small water pump driven by the condenser fan shaft. Energy consumption of the air conditioner was compared between two cases, namely running the air conditioner with and without condenser air cooling. It was found in this study that cooling the condenser air could reduce the power

consumption by about 4%. It was also discovered that reducing the temperature of the condenser air by 1° C would reduce the energy consumption of the unit by 2.1%. Adel A. Eidana et.al presented an experimental study to enhance the performance of a small air condition (A/C) system by mean of direct evaporative cooling method. A setup of cooling system is designed to simulate extremely hot weather that the dry bulb temperature (DBT) reaches the vicinity of 55 °C which represents the highest possible weather temperature that was recorded during summer. The proposed design utilizing an evaporative cooling cycle which the air flows over wet pads before it goes through the condenser. Four different parameters are considered to be studied, namely coefficient of performance (COP), energy saving, cooling capacity and the compressor auto-shut down in very high weather temperature. The results showed significant enhancement to the entire A/C system performance which the refrigeration capacity is increased in the range of 5% to 7.5% and there is 0.12A to 0.16A electrical current reduction for each temperature degree reduction. Moreover, and the compressor continued working even with a voltage drop of 16% (185 V instead of 220 V) which can help overcoming a serious problem that middle east countries (such Iraq) suffer during summer.

The energy conservation promotion Act, A.D. 2007, came into force since November 24, 2007. Factories and business buildings were set as target group where energy conservation must be planned and systematically operated. The state would arrange for technical and technological support of energy conservation including to its financial support. There are about 8,552 controlled buildings in Thailand. The buildings in Rajamangala University of Technology Lanna Tak (RMUTL Tak) have quite high energy consumptions. Especially, the high electric energy cost about 800,000 - 900,000 baht per year. Hence, the mechanical engineering department building was selected as study case to survey and analyze its electric energy consumption in order to find out the way for energy

conservation. Then the analytical result from this study case could be used as guidance for energy conservation of the other buildings in RMUTL Tak.

2. Objective

To improve the efficiency of split type air conditioners in mechanical engineering department building of RMUTL Tak.

3. Methodologies

3.1 Theories

1. A Split type air conditioner consists of two units; namely outdoor unit or condensing unit and the indoor unit or fan coil unit for controlling temperature and humidity of the air passing through it. The main equipment diagram of the air conditioning system is shown in figure 1.

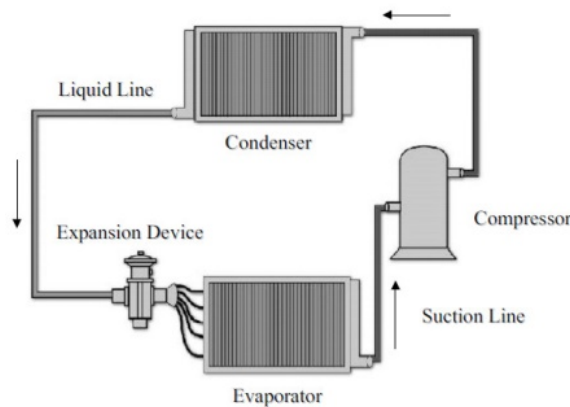


Figure 1. Vapor - compression refrigeration system

The principles of the vapor - compression refrigeration system is evaporation and condensation in different pressure conditions as follows:

1.1 The compressor compresses refrigerant vapor to high pressure and high temperature condition.

1.2 The condenser acts to reject heat from the high pressure refrigerant causing condensation of the refrigerant.

1.3 The expansion valve or capillary tube acts to reduce the pressure of the refrigerant so that it can be evaporated at low temperature.

1.4 The evaporator serves to absorb heat from the air conditioning area for refrigerant evaporation. Then, the refrigerant vapor is transported to the compressor and compressed to the high pressure again.

2. Efficiency or performance of refrigeration of the split type air conditioners is generally estimated in 3 types as follows:

2.1 The coefficient of performance (COP) is the ratio between the cooling capacity (Watt) and the power (Watt) used for cooling air in the air conditioning system. The COP is calculated as shown in equation (1)

$$\text{COP} = (Q/W) = (m^o(\Delta h_{\text{out}})/m^o(\Delta h_{\text{in}})) \quad (1)$$

Where

Q is the cooling capacity of the air conditioning system (W).

W is the power rating of the air conditioner (W).

mo is the refrigerant flow rate (kg/s).

Δh_{out} is the enthalpy difference between the evaporator outlet and inlet (kJ/kg).

Δh_{in} is the enthalpy difference between the compressor outlet and inlet (kJ/kg).

2.2 Energy efficiency ratio (EER) is the ratio between the cooling capacity (Btu/hr) and the power (Watt) used for cooling air in the air conditioning system. The EER is presented in the unit of BTU/hr/W as shown in equation (2)

$$EER = Q/W \quad (2)$$

Where

Q is the cooling capacity of the air conditioning system (Btu/hr).

W is the power rating of the air conditioner (W).

2.3 Electrical power per ton refrigeration (CHP) is the ratio between the power used for the air conditioner for cooling (kW) and the cooling capacity (Ton of refrigeration; TR) as shown in equation (3)

$$CHP = kW/TON \quad (3)$$

Where

CHP is the electrical power per ton of refrigeration (kW/TR).

kW is the electrical power rating at full load (kW).

TON is the total cooling capacity at full load (TR).

TON can be calculated from equation (4).

$$TON/TR = 5.707 \times 10^{-3} \times CMM \times (hr - hs) \quad (4)$$

Where

CMM is the volumetric flow rate of cool air circulating through the air conditioner m^3/min .

hr is the enthalpy of return air (kJ/kg dry air).

hs is the enthalpy of supply air (kJ/kg dry air).

From the definitions of the three values above, it can be seen that the definition of EER, COP and CHP are reciprocal. The lowest value of CHP, the highest value of EER and COP indicated the highest performance of the air conditioner. Their mathematical relationships are shown in figure (5) and (6):

$$CHP = 12/EER \quad (5)$$

$$COP = EER/3.412 \quad (6)$$

Note: When the motor and heat exchanger efficiencies are 100%.

3. Psychrometric chart as shown in Figure 2 consists of

3.1 Dry bulb temperature (DB) as shown on the horizontal axis of the chart can be measured by a thermometer.

3.2 Wet bulb temperature (WB) is the saturated air temperature displayed on the diagonal of the chart. The wet bulb temperature can be measured by a thermometer covered in water-soaked cloth.

3.3 Dew point temperature (DP) is the temperature which the ambient air must be cooled to reach 100% relative humidity assuming there is no further evaporation into the air; it is the point where condensation (dew) and clouds would form. It can be read by dragging the horizontal line from the state to the 100% relative humidity curve on the left of the chart.

3.4 Relative humidity (%RH) is the ratio of the fraction of water vapor in the air to the fraction of saturated moist air at the same temperature and pressure.

3.5 Humidity Ratio (HR) is a unit for measuring the mass of water vapor per 1 unit mass of dry air.

3.6 Enthalpy (h) is the total amount of heat energy of the moist air and therefore includes the amount of heat of the dry air and the water vapor in the air.

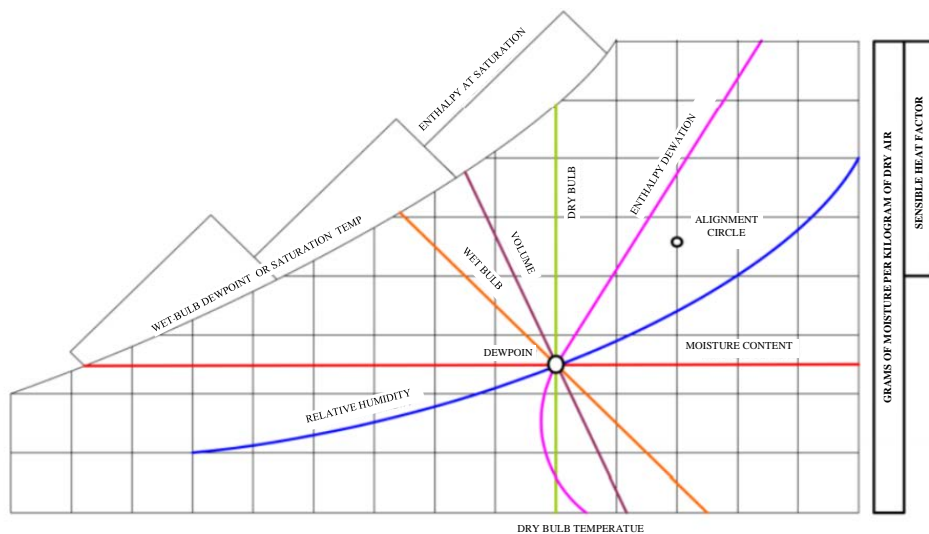


Figure 2. Psychrometric chart.

4. Ministry of energy's notification on identification of minimum coefficient of performance, cooling efficiency and electrical energy per ton of refrigeration of air conditioning system in the

building A.D.2009 designated air conditioning performance for small-sized air-conditioners as shown in Table 1.

Table 1. Identification of minimum coefficient of performance and cooling efficiency for small-sized air-conditioners.

Size of air conditioners (Watt)	COP (Watt/Watt)	EER (Btu/hr/Watt)
Less than 12,000	22.3	11

5. Measuring tools and equipment

5.1 Hot wire type anemometer (Brand: TES-1340 TES) as shown in figure 3



Figure 3. Hot wire type anemometer.

5.2 Thermometer and hygrometer (Brand: AZ 7755) as shown in figure 4.



Figure 4. Thermometer and hygrometer.

5.3 Power meter (Brand: Lutron DW-6093SD) as shown in figure 5.



Figure 5. Power meter.

6. Measurement procedure

6.1 Measured and recorded some variables before cleaning and maintenance the air conditioners which consists of

1. Measured for the width and the length of the return air inlet with a measuring tape to calculate the cross-sectional area.

2. Measured the temperature ($^{\circ}\text{C}$) and relative humidity (%RH) of the return air using a thermometer and hygrometer.

3. Measured the temperature ($^{\circ}\text{C}$) and relative humidity (%RH) of the supply air using a thermometer and hygrometer.



Figure 6. Measuring of temperature and relative humidity of return and supply air.

4. Measured the air velocities of the return air using an anemometer and should measure at least 3 points to calculate the average air velocity. In this regard, the reason for choosing the return side rather than the supply side were:

- The return side had a larger cross-sectional area, resulting in laminar flow and the measured velocity was more stable than the supply side.

- The return air had a certain direction which was perpendicular to the cross-sectional area in contrast to the supply air direction which depended on the air flow blade adjustment.



Figure 7. Air velocities measurement.

5. Measured the total electric power of the air conditioner using power meter.



Figure 8. Electric power measurement and recording.

6. Determined the working time percentage of the compressor by counting the working and non-working time of compressor.

7. Cleaned the air conditioner parts, consisting of air filter panel, drain tray, front grille, middle cover and air flow blades.



Figure 9. Air filter of air conditioner which lack of cleaning and maintenance.



Figure 10. Air filter cleaning.

6.2 Measured and recorded the variables after cleaning and maintenance the air conditioners by following the same steps as in heading 6.1 (1 - 6).

4. Result

After measuring and recording the data from 8 split type air conditioners (each size of 25,345.6 Btu / hr) in mechanical engineering department building, their performances were determined and

compared between before and after maintenance. The results of some air conditioners were shown as examples in Table 2 and Table 3.

Table 2 Examples of comparison of data recording and performance analysis between before and after maintenance.

	units	Air conditioner					
		No.1		No.2		No.3	
		Before	After	Before	After	Before	After
Rating from nameplate							
Cooling capacity	Btu/hr	25,345.6	25,345.6	25,345.6	25,345.6	25,345.6	25,345.6
Electrical power rating	kW	7.381	7.381	7.381	7.381	7.381	7.381
EER	-	11.04	11.04	11.04	11.04	11.04	11.04
Duration	years	6	6	6	6	6	6
Supply air conditions							
Temperature	°C	14.7	12.9	14.4	13.1	15.1	13.7
Relative humidity	%	87.94	83.53	89.33	87.767	86.16	79.55
Enthalpy	kJ/kg	37.95	32.48	37.56	31.38	38.49	33.53
Return air conditions							
Temperature	°C	28.1	24.6	29.1	24.5	28.7	25.1
Relative humidity	%	36.89	44.75	32.91	45.31	35.9	48.3
Enthalpy	kJ/kg	50.54	46.6	50.32	46.7	51.33	49.68
Volumetric air flow	CMM	21.62	25.43	19.05	19.92	18.22	19.92
Outdoor air temperature	°C	33.3	33.3	33.3	33.3	33.3	33.3
Electrical power consumption	kW	2.745	2.648	2.635	2.156	2.403	2.056
Cooling capacity	Btu/hr.	18,641	24,591	16,647	20,900	16,021	22,032
CHP	-	1.77	1.29	1.73	1.18	1.80	1.12
EER	-	6.79	9.29	6.92	10.17	6.66	10.72

Note: Table shows the result examples of 3 air conditioners (from all 8 air conditioners)

From Table 1, air conditioner maintenance resulted in decreasing of electrical power consumption. The air conditioner maintenance could reduce dust accumulation and blockage in the evaporator section. Then the air could ventilate through the evaporator easily and could exchange heat efficiently. So the power consumption in air conditioner decreased. As shown in Table 1 before maintenance, electrical power consumption of air conditioner No.1, 2 and 3 were 2.745, 2.635 and 2.403 kW when

after maintenance they were 2.648, 2.156 and 2.056 kW, respectively. Decreasing of electrical power consumption resulted in higher efficiency of air conditioner (EER).

Table 3 Examples of economic analysis comparison between before and after maintenance.

	Units	Air conditioner					
		No.1		No.2		No.3	
		Before	After	Before	After	Before	After
Cooling capacity	Btu/hr	18,641	24,591	16,647	20,900	16,021	22,032
Electrical power consumption	kW	2.745	2.248	2.605	2.156	2.618	2.081
kW/TR	-	1.77	1.29	1.73	1.18	1.80	1.12
Working hours	hr/yr	2,920	2,920	2,920	2,920	2,920	2,920
Electrical energy consumption	kWh/yr	8015.4	6564.16	7606.6	6295.52	7644.56	6076.52
Electricity charge per kWh	฿/kWh	2.9	2.9	2.9	2.9	2.9	2.9
Electricity charge per year	฿/yr	23,244.7	19,036.1	22,059.1	18,257.0	22,169.2	17,621.9
Electrical energy saved	kWh/yr	1,451.24		1,311.08		1,568.04	
Electricity charge saved per year	฿/yr	4,208.60		3,802.13		4,547.32	

Note: Table shows the results of 3 air conditioners (from all 8 air conditioners)

The results from cleaning and maintenance of the 8 split type air conditioners in mechanical engineering department building were as follows:

Electrical energy saved = 10,044.8 kWh/yr
 Electricity charge saved per year = 32,517.1 ฿/yr
 Ton of oil equivalent saved = 10,044.8 x (85.21/109)
 = 0.000856 ktoe/yr

The air conditioner maintenance in mechanical engineering department building could decrease the electrical energy consumption for 10,044.8 kWh/yr and save electricity charge for 32,517.1 baht/yr or equal to ton of oil equivalent of 0.000856 toe/yr.

5. Conclusion

From the results of cleaning and maintenance 8 split type air conditioners (Each size of 25,345.6 Btu/hr) in mechanical engineering department building to compare their efficiencies between before and after maintenance, it was found that before maintenance, the average energy efficiency ratio was 6.7 Btu/W and after maintenance, it was 10.6 Btu/W. It was increased about 3.9 Btu/W or 58.2%. The electrical energy consumption could be saved 10,044.8 kWh/yr accounted in electricity charge of 32,517.1 ฿/yr. Moreover, this energy consumption can converted into ton of oil equivalent about 0.000856 ktoe/yr. These results indicated that usually cleaning and maintenance air conditioners made them have lower electricity energy consumption than the ones not usually cleaning and maintenance and resulted in the high efficiency of air conditioners system.

Acknowledgement

This work would not have been possible without the financial support of the National Research Council of Thailand (NRCT). We would like to thank the mechanical engineering department of faculty of engineering, Rajamangala University of Technology Lanna Tak for supporting of equipment and facilities in this research.

References

- Adel A. Eidana, Kareem J. Alwana, Assaad AlSahlanib and Mohamed Alfahham. (2017). Enhancement of the Performance Characteristics for Air-Conditioning System by Using Direct Evaporative Cooling in Hot Climates, *Energy Procedia*, Vol. 142, Pages 3998-4003. <https://doi.org/10.1016/j.egypro.2017.12.311>
- Chen, Wei Han, Mo, Huai En, Teng, and Tun Ping. (2018). Performance improvement of a split air conditioner by using an energy saving device, *Energy and Buildings*, Vol. 174, Pages 380-387. <https://doi.org/10.1016/j.enbuild.2018.06.055>.

- Ebrahim Hajidavalloo. (2007). Application of evaporative cooling on condenser of window - air conditioner. *Applied Engineering*. Vol. 27, Pages. 1937 -1943.
- McQuiston, F.C., Parker, J.D., and Spitler, J.D., (2005). *Heating, Ventilating, and Air Conditioning Analysis and Design*. John Wiley&Sons, Inc., New York.
- S. Theerakulpisut and S. Pripem. (2001). Improving energy efficiency of split-type air conditioners by cooling the cooling air, *Engineering and Applied Science Research (EASR)*, Vol. 28, No.2-3, 127-136.
- Stockers, W. F. & Jones, J. W. (1982). *Refrigeration & Air conditioning*. Singapore: McGraw-Hill international Editions.

Design and Analysis of Plastic Medical Tray for Implant Packaging

Nattapon Chantarapanich^{1,2,a}, Tamnuwat Valeeprakhon^{2,3,b}, Sujin Wanchat^{1,2,c}, Melvin Stainley Veerasakul^{1,d}

¹Department of Mechanical Engineering, Faculty of Engineering at Sriracha,
Kasetsart University, Chonburi, Thailand

²Digital Industrial Design and Manufacturing Research Group, Faculty of Engineering at Sriracha,
Kasetsart University, Chonburi, Thailand

³Department of Computer Engineering, Faculty of Engineering at Sriracha,
Kasetsart University, Chonburi, Thailand

E-mail; ^anattapon@eng.src.ku.ac.th, ^btamnuwat@eng.src.ku.ac.th, ^csujin@eng.src.ku.ac.th, ^dmelvin.ve@ku.th

Abstract

Plastic medical tray is commonly used for medical device packaging such as implant or surgical instruments. The tray can be underwent gamma ray exposure to sterilize the medical devices inside. The tray keeps medical devices free from micro-living organisms and protects them from contaminated external environments. The plastic sheet is usually used for producing the tray which turns into final tray shape using thermoforming. During tray design process, factors such as dimension of medical devices, ergonomics, and strength, have to be taken into consideration. Computer Aided Design/ Three-dimensional Printing (CAD/3DP) technologies is applied for validation the tray geometry whereas finite element methods is applied for strength analysis. Three-dimensional (3D) models of the tray, which is referenced from dimension of medical device, are 3D printed to tested ergonomics for operating room (OR) nurses handling. After that, 3D models are evaluated the strength to ensure the safety during delivery. From the analysis, geometry of tray is appropriate for handling with sufficient strength. Bottom corner of tray is critical point since it presents high stress magnitude. The load of 54.6 kg-f deforms the tray less than 0.5-mm confirms the high stack storage.

Keywords: Plastic Medical Tray; Medical Device; Packaging Design; Packaging Analysis

1. Introduction

Medical devices, especially a long-term implanted in body, requires sterile condition before serving to the surgery. Package for protecting medical device away from contamination is considered as a compulsory requirements supplement to implant design process. Desired characteristics of medical device packaging includes sterilization compatibility, ease of forming, heat resistance during sealing, strength, and economic-scale (Bix, 2009).

Generally, various sterilization methods are used to deactivate micro-living organisms which are autoclaves, steam, ethylene oxide gas, and gamma-ray radiation. For short duration use invasive medical device or non-invasive medical device, the first four sterilization methods are used. However, the long term invasive implant or instrument in contact to blood such as surgical glove, orthopaedic implant, and prosthesis, gamma-ray radiation is usually selected as a sterilization method. The gamma ray method present the advantages in a high Sterility Assurance Level (SAL) and is simple to control. Compared to the other aforementioned techniques, they presents complications in penetration in narrow cavity, and long period of time for the process.

Gamma ray method uses Cobalt-60 (⁶⁰Co) or Cesium-137 (¹³⁷Ce) to generate the radiation. A-dose of 25 kGy is considered as a reference for sterilization (Silindir et al., 2009). In order to design the implant package which is good when undergoes the gamma ray sterilization, rigid plastic type is usually selected to make a package.

Shape of package should depends on the shape of implant. The optimal gap between package and implant is required. The large gap may introduce the movement (momentum) of implant which could lead to damage of package during transportation. The lower gap may be difficult to get the implant

out of the package. In addition, the shape should be able to handle by operating room (OR) staff during opening and transferring from unsterilized zone to sterilize zone.

The packages are kept in-stack to minimize the storage space in hospital. Strength of package is important to withstand the weight above it. Analysis of the strength can define the maximum storage package in vertical direction. The deformation of package could lead to tear of plastic and eliminate sterile condition.

In this paper, it presents a case study of packaging design for humerus endoprosthesis for a medical device company. The endoprosthesis is intended to replace the tumor bone region, composing of four parts which are head, neck, body, and stem. The body and stem are available in three sizes in order to make it selectable for various resection bone length. The requirements from the company is to design the single package which fit to all parts for economic matters.

2. Materials and Methods

The design process was begun with collecting the requirement from the company including product specification. The product is an endoprosthesis made of cobalt chromium and titanium. It intends to replace tumor bone region and is used inside the body for a long period. It composes of four parts which all of them needs to fit in single size packaging. In addition, the endoprosthesis requires undergoing gamma sterilization.

In order to design the packaging, the 3D CAD models of endoprosthesis was reversely created using CAD software (VISI, Vero Software, UK). External shape of endoprosthesis is considered as important. The unnecessary detail of 3D model was neglected that not related to packaging design.

The package was designed based on 3D CAD models of endoprosthesis in such a way that (1) it has a shape which can be hold by single hand, (2) it can be fit all components of endoprosthesis, and (3) it is feasible to manufacture with thermoforming process.

After finishing the design, the test for fitting was first evaluated in CAD Software. The 3D model of endoprosthesis components was virtually filled one by one to see any obstruction during filling process.

The models of packaging and endoprosthesis was then three dimensionally printed using fused deposition modeling (FDM) machine. The printed model were used to evaluate functions and containing. Adjustment and modification of the packaging model was once again revised, if its functions is not met the requirements.

When the 3D model was dimensionally and functionally reviewed and revised, the 3D CAD model of packaging was evaluated the strength using Finite Element (FE) method (ABAQUS, Dassault Systèmes, USA). In order to generate the FE model for analysis, four node tetrahedral elements type were created based on topology of 3D CAD mode of packaging. The evaluation was performed under various compression circumstances. Displacement was simulated on the upper surface of package i.e. 0.5-mm, 1.0-mm, 2.0-mm, and 4.0-mm. Material assigned in the FE analysis was assumed to be linear elastic, which elastic modulus and poisson's ratio has to be included. The Equivalent Von Mises (EQV) stress of each case was compared to yield strength of materials.

3. Results and Discussion

Decision for endoprosthesis was designed as medical tray. Its dimension was 150 mm length x 125 mm width x 47 mm height. Size of the tray width was less than size of hand, this allows OR personal to carry on with single hand. The tray has a taper angle of degree to allow ejection from the mold during the thermoforming process. All components of endoprosthesis could be fit into the tray as shown in Figure 1. The edge of tray were offset from the main portion by 8-mm, this is to stick the sterile barrier film covering on.

The 3D models of tray and prosthesis were printed using FDM machine to test the containing function. Since the components of endoprosthesis are smaller than tray cavity, the components were covered with sterile pouch before putting into the tray. This also reduces the movement of the

components inside the tray as it pouch pushes the cavity walls in all sides to balance position of the components in place. In addition, the pouch also make it is easy for OR personal to remove the pouch from the tray in sterile condition using scissor with low risk of touching contaminated area.



Figure 1. Tray and example of component filling test.

The choice for materials made of tray was Polyethylene Terephthalate (PET) family. PET are suitable for making tray and good for radiation sterilization method (Bix, 2009). Thus, the material of properties of PET was tested according to ASTM D638-14 (ASTM, 2014) for gathering input for FE analysis. PET filaments was printed to produce the specimen type I of ASTM D638-14. The specimens were used for tensile testing using Universal Testing Machine (Instron Model No. 9582, USA) at Geo-Informatics and Space Technology Development Agency (Public Organization). Three specimens were tested at speed of 5 mm/min. The test was terminated when the specimen broke apart. From the test, average elastic modulus is $1,850 \pm 28.5$ MPa, and the average tensile strength is 39.8 ± 3.9 MPa. For poisson's ratio, it was not possible to get the data from tensile test. During the FE analysis, it was then assumed to be 0.30.

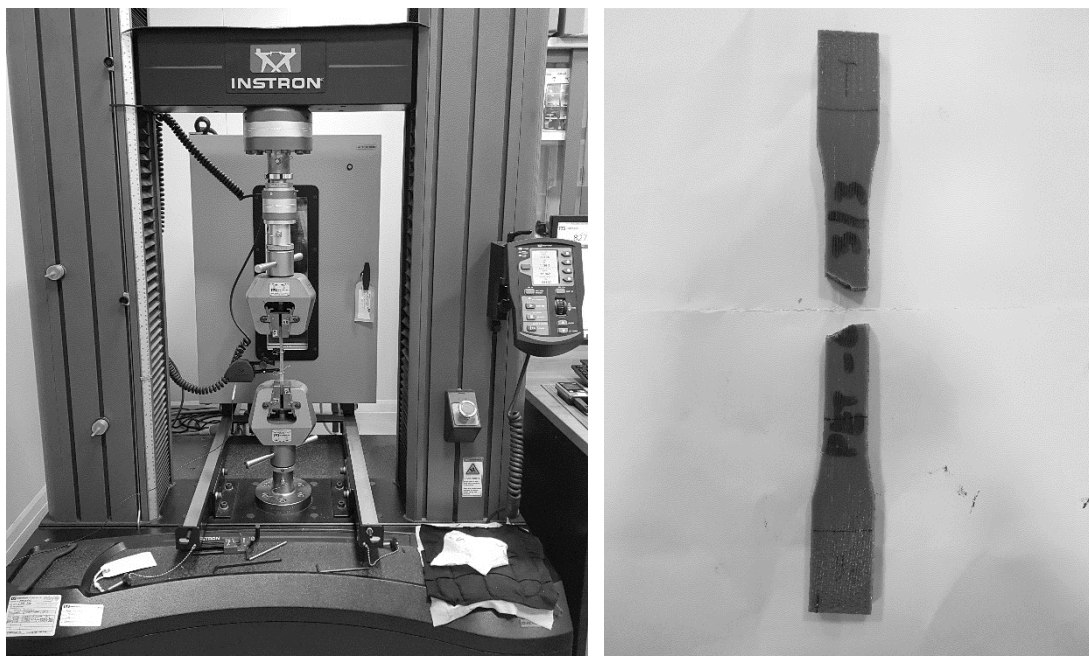


Figure 2. Test for Mechanical properties of material.

For the FE test, thickness of PET sheet was 0.7 mm. The results shows that the high EQV stress portion of tray was at the four bottom corners and the upper edge, as shown in Figure 3. Higher compression leads to higher stress and required more compression loads At 2 mm and 4 mm compression, the EQV stress at upper edge is critical level. High compression loads can cause breakage or tear at upper edge. The stress level at 1-mm compression was still at risk, since the high stress area is large. The safe use for tray was to allow maximum compression at 0.5 mm, which corresponds to 536.4 N (54.6 kg). This is sufficient to withstand the stack storage.

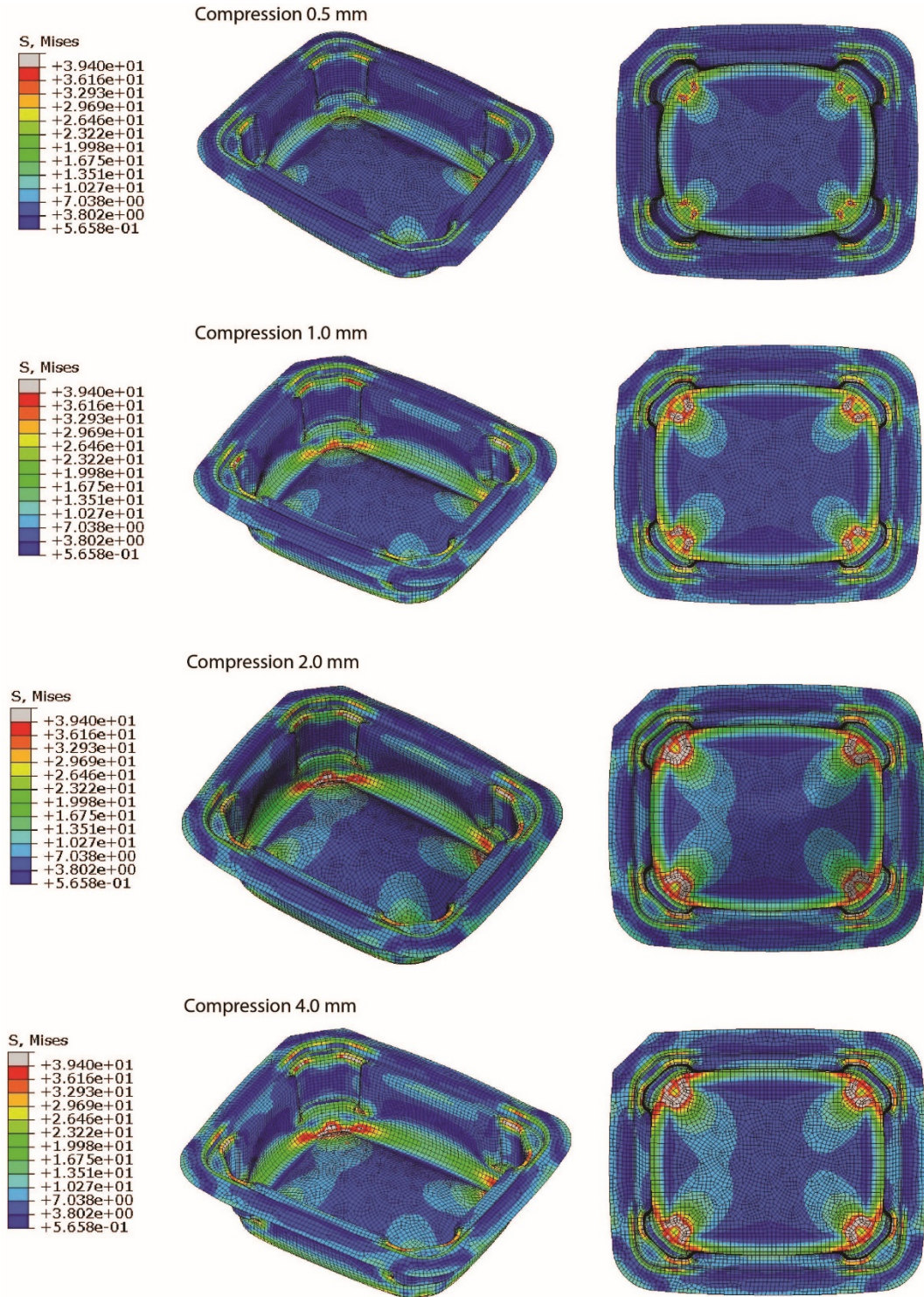


Figure 3. FE compression test result.

As a result, the 3D model of medical packaging tray was used for production. Figure 4 shows the finished shape of PET tray used for endoprosthesis.

There is still less work published which presents the whole design process specifically for medical device package. Other works related to medical device package focused on cost analysis (Reymondon, 2006), packaging analysis using imaging (Hindelang et al, 2015), and packaging materials (Wasikiewicz et al, 2008). Therefore, this current work is considered to be an explained in detail paper which describing method in medical packaging design, from design input consideration to final production.



Figure 4. Tray.

Scope of this work focuses on design process and its rationale in design which do not include the test of packaging i.e. bioburden, sterility test, and aging acceleration. These tests are required to determine the gamma dose used for sterilization prosthesis, amount of microorganism exhibited on the prosthesis, and shelf life. This should be done by the manufacturer to conform ISO13485:2016 standard.

4. Conclusions

This study presents the case study of packaging design for endoprosthesis. The characteristic required for design input includes: (1) the package can undergo sterilization with gamma radiation, (2) the package can be hold by single hand, (3) the package is fitted for dimension of endoprosthesis components, and (4) the package has sufficient strength. The output for the design has dimension of 150 x 125 x 47 mm. The materials made of package was PET. The package presents the sufficient strength by withstanding 54.6 kg compression load.

5. Conflict of Interest

None.

6. References

- ASTM (2014), D638-14, Standard Test Method for Tensile Properties of Plastics.
- Bix L., & Fuente J. (2009). Medical Device Packaging. In Yam K.L. (Eds.), *The Wiley Encyclopedia of Packaging Technology* (pp.713-727). Hoboken, NJ: John Wiley & Sons.
- Hindelang F., Zurbach R., Roggo Y. (2015). Micro Computer Tomography for medical device and pharmaceutical packaging analysis. *Journal of Pharmaceutical and Biomedical Analysis* 108, 38-48.
- Reymondon F., Pellet B., & Marcon E. (2006). Methodology for designing medical devices packages based on sterilisation costs. *IFAC Proceedings Volumes (IFAC-Papers Online)*, 12(PART 1).
- Silindir M., & Özer A.Y. (2009). Sterilization Methods and the Comparison of E-Beam Sterilization with Gamma Radiation Sterilization. *FABAD Journal of Pharmaceutical Sciences*, 34, 43-53.
- Wasikiewicz J.M., Roohpour N., Paul D., Grahn M., Ateh D., Rehman I., & Vadgama, P. (2008). Polymeric barrier membranes for device packaging, diffusive control and biocompatibility. *Applied Surface Science*, 255, 340-343.

Conductive Composite Paper from Cellulose Fiber by in Situ Polymerization of Pyrrole

S. Sukkhawuttigit^{1, a}, S. Ummartyotin^{2, b} Y. Infahsaeng^{1, c}

¹Division of Physics, Faculty of Science and Technology, Thammasat University, Klong Nueng, Klong Luang, Pathum-Thani, Thailand

²Division of Materials and Textile Technology, Faculty of Science and Technology, Thammasat University, Klong Nueng, Klong Luang, Pathum-Thani, Thailand

E-mail; ^ass.siripassorn@gmail.com , ^bsarute.ummartyotin@gmail.com, ^cyingyot.infahsaeng@gmail.com

Abstract

Currently, conducting polymers such as Polypyrrole (PPy), have been extensively interested due to their interesting features of conductivity, low-cost fabrication, and stability under ambient conditions and at high temperature. Herein, polypyrrole was polymerized on the surface of cellulose fibers (CFs) by using a sequence of fiber impregnation in FeCl₃ solutions and re-dispersion in a pyrrole solution via in situ chemical polymerization of monomer-pyrrole. The structure, morphology, and thermal properties were investigated. The results revealed the uniformity of PPy on the surface of CFs. Moreover, conductivity of $184 \times 10^{-4} \text{ S} \cdot \text{cm}^{-1}$ was obtained from a composite sheet of CFs:PPy with the PPy of 0.20 ml. Also, the decreasing of dielectric and impedance in CFs:PPy composite sheet can be observed as the increasing of CFs:PPy ratio. Chemical polymerization has been very successful in the production of composite materials of conductivity polymers with CFs.

Keywords: Cellulose; Polypyrrole; Conductive composite materials; In-situ Synthesized.;

1. Introduction

Typically, the electronic devices were made of silicon, conductive glass or hard plastic, which is an importance part for high performance device, but such materials still have limitations in terms of brittleness, cost of materials and complex production processes. Moreover, some plastic, especially micro-plastic, is not environmental-friendly. Consequently, non-reused materials can lead to an environmental problem. To overcome this issue, bio-based materials have been developed under the concept of “green” and sustainable development, which can naturally decompose and pollution reduction. Therefore, the renewable natural materials are the important topic in the 21st century. (Mohanty, Misra, & Drzal, 2002)

The development of alternative bio-based materials which has similar properties such as electrical, thermal, flexibility and mechanical properties, is crucial. Nowadays, the cellulose has been widely studied and developed due to its renewability, availability, non-toxicity, low-cost, biodegradability, thermal and chemical stability (Wang, Lu, & Zhang, 2016). One of the interesting developments of cellulose is conductive paper, which is very important for electronic device application such as TFT, OLED, organic photovoltaic device, stored battery, and sensor (Fu et al., 2016), (Ummartyotin & Manuspiya, 2015b), (Ummartyotin & Manuspiya, 2015a). Recently, the conductive paper was successfully fabricated with a sheet resistance of 25 kΩ (Zhong et al., 2013).

To develop the conductive paper, conductive polymers are interesting material due to its unique properties that allow it to be used in a variety of electrical application. Typically, chemical polymerization has been successful in the production of composite materials of conductive polymers with the matrix. Recently, the conductive nanocrystal cellulose:polypyrrole composite hydrogel were in situ synthesized. By doping with sodium p-toluenesulfonate (TsONa), the hydrogel showed a high electrical conductivity of $8.8 \times 10^{-3} \text{ S/cm}$ (Y. Li, Zhang, Ni, & Xiao, 2018). Moreover, the effect of polypyrrole and ionic liquid (IL) nanocoatings on the electrical properties of cellulose film has been

investigated. The conductivity of such nanocomposite film was 1.2×10^{-4} and 4.3×10^{-5} S/cm on the surface and along the thickness direction, respectively (Mahadeva & Kim, 2011). Combination of bio-based materials such as cellulose with conductive polymer has been extensively developed as a multi-function electronic device (Du, Zhang, Liu, & Deng, 2017). Recently, many researchers have extensively attended to develop such composite material. The organic or inorganic composite materials were a material that can be obtained from the combination of various materials to get new properties. To prepare the conductive composites of bacterial cellulose (BC) and polypyrrole, Muller and co-worker prepared through in situ oxidative chemical polymerization of pyrrole by using FeCl_3 as oxidant agent (Müller, Rambo, Recouvreux, Porto, & Barra, 2011). Makara and co-worker prepared nanopapers from cellulose nanofibers (CNF) and polypyrrole with high mechanical performance and with the electrical conductivity of 5.2×10^{-2} S/cm (Lay, Méndez, Delgado-Aguilar, Bun, & Vilaseca, 2016). Pyrrole and cellulose are therefore an interesting material that shows the connection between cellulose fibers and conductive polymers. There were flexibility and capacitance properties that make it more useful in using technology.

In this work, the cellulose fiber obtained from the remaining pulp is mixed with polypyrrole (PPy) via in situ polymerization using ferric chloride as oxidant agent. An amount of PPy is varied, then the morphology, mechanical, and electrical properties are investigated.

2. Objectives

1. Preparation of composited material of cellulose and polypyrrole via in situ polymerization.
2. Study the morphology, mechanical, and electrical conductivity properties of cellulose composite materials.

3. Methodology (Materials and Methods)

3.1. Materials

A wastepaper pulp was provided from SCG packaging public company limited, Thailand, and was stored in a desiccator in order to prevent the moisture adsorbent. Pyrrole was supplied by Sigma Aldrich and used as received for the chemical synthesis of polypyrrole. The rest of materials, FeCl_3 and HCl, were also supplied by Sigma Aldrich and used without further purification.

3.2. Methods

3.2.1. Cellulose suspension

The piece of paper pulp with an area of ca. $10 \times 10 \text{ cm}^2$, was ripped to be a thin sheet. Then the pulp was mixed with deionized water DI of 500 ml for overnight under magnetic stirrer. The obtained suspension was concentrated and subsequently washed with distilled water by repeated centrifuged cycles at 500 rpm. As a result, suspension of cellulose fiber (CFs) was obtained and stored at 4°C prior use.

3.2.2. Preparation of Cellulose fibers (CFs) and CFs:PPy paper

CFs suspension of 45 ml) 0.4 g dry weight (was dispersed in 30 ml of HCl and stirred by for 5 minutes. After that, the CFs suspension was filtered for 24 hr through a paper filter with 0.1 μm pore size and washed subsequently with DI water. The wet sheet was then dried between two membranes under an applied pressure of 0.141 psi.

For the preparation of CFs:PPy paper, the various volume of pyrrole solution (0.05, 0.10, 0.15, 0.20 ml) was dissolved in 30 ml of 0.5M HCl and, then, mixed with the CFs dispersion and stirred for 5 minutes. A defiant amount of FeCl_3 was dissolved in 30 ml aqueous of 0.5M HCl solution and added to the CFs:pyrrole dispersion to initiate oxidative polymerization. The oxidant (FeCl_3) to pyrrole was fixed at 6 % w/w ratio. The final mixture was stirred at room temperature for 30 minutes. At the end, the mixture was filtered using paper filter and washed subsequently 30 ml of 0.5M HCl and DI water

to remove any small gas bubbles and to allow a better organization of CFs:PPy structures without undesired side effects, such as crystal structure damage (Ali et al., 2014).

3.2.3. Characterizations

3.2.3.1. Fourier Transform Infrared Spectroscopy (FTIR)

FTIR absorption spectra (PerkinElmer, spectrum 100) of cellulose and CFs/PPy composites were recorded in the range of 4000 cm^{-1} to 650 cm^{-1} using Attenuated Reflection Infrared Spectroscopy (ATR) mode.

3.2.3.2. X-Ray Diffractometer (XRD)

X-ray diffraction patterns of CFs, CFs:PPy composites were carried out by Bruker, D8 ADVANCE using Co radiation at 40 kV voltage. The XRD patterns were recorded in a diffraction angle (2θ) range from 5° to 50° .

3.2.3.3. Thermogravimetric Analysis (TGA)

The TGA characteristics of the CFs:PPy composite were investigated by TGA (METTLER TOLEDO, TGA/DSC3+1600). Each sample was heated at a heating rate of $10^\circ\text{C}/\text{min}$ under nitrogen atmosphere from room temperature to 700°C .

3.2.3.4. Field Emission Scanning Electron Microscope (FE-SEM)

The morphological properties of the CFs and CFs:PPy composite were analyzed using FE-SEM (Hitachi, S-4800) at an acceleration voltage of 5 kV. The fiber diameter was measured and counted at 1000x magnification. Prior to the investigation, the samples were stored in desiccators to reduced humidity. Each sample was placed on carbon tape and sputtered with gold particles before being analyzed.

3.2.3.5. Mechanical properties

The sample was cuter into the rectangle shape with the width of 20 mm and length of 30 mm. The thickness of sample was ca 0.07-0.09 mm. The testing speed was 5 mm/min. The tensile tests were conducted using as Instron Universal material testing machine (Instron 55R4502, S/NH 3342) equipped with a 100N load cell.

3.2.3.6. Conductivity

The conductivity properties of CFs:PPy substrate was characterized by Four Point Probe System (Jandel RM3000) using the cylindrical four-point probe head (Jandel Engineering Limited).

3.2.3.7. Dielectric and Impedance

Impedance were measured using an impedance probe (1260 Impedance Gain-Phase Analyzer 12600012_Gmacd/CB Solartron) at room temperature and at various frequencies ranging from 10 Hz to 10 MHz.

4. Results and discussion

4.1. FTIR analysis

The FTIR spectra of CFs and CFs:PPy composites are shown in Fig. 1. The spectrum of the prepared CFs show the peaks at 3335.69 cm^{-1} which is the characteristic for stretching vibration of the hydroxyl group (O-H group) in polysaccharides (Rosa et al., 2010). The peak located at 1633 cm^{-1} correspond to stretching vibrations of C-C bonds (Poletto, Pistor, Zeni, & Zattera, 2011). The absorption bands at 1377.85 , 1250.26 , 1161.10 , 1052.43 , and 897.03 cm^{-1} belong to stretching and bending vibrations of $-\text{CH}_2$, $-\text{CH}$, $-\text{OH}$ and C-O bonds in cellulose, respectively (Fackler et al., 2011; Xu, Yu, Tesso, Dowell, & Wang, 2013). From FTIR spectra of CFs:PPy composites at different PPy concentration, it was observed that the peak 3277 cm^{-1} was shifted from 3335.69 cm^{-1} , this may be due to chemical bonding between N-H in the polypyrrole ring and the $-\text{OH}$ of cellulose (Müller et al., 2011). The fundamental vibrations of pyrrole ring observed at 1541.08 cm^{-1} and 1458 cm^{-1} , which, can be assigned to the C=C and C-C ring stretching modes, respectively (Chougule et al., 2012; Hansora, Shimpi, & Mishra, 2015). The peak around 1046 cm^{-1} can be assigned to N-H in - plane deformation (Ho, Jun, & Kim, 2013), while the peak at 781 cm^{-1} is due to C-N out-of-plane deformation in PPy (Chougule et al., 2012). The absorption peak at about 1125 - 1159 cm^{-1} and 883.68 cm^{-1} may be relate to linkage between polypyrrole and cellulose chain in 1161.10 cm^{-1} and 867.03 cm^{-1} .

4.2. Crystallography structures

The crystallography structures of CFs and CFs:PPy composites were characterized using XRD measurements as shown in figure 2. The X-ray pattern clearly exhibits the broaden peaks at 2θ of 16° and 22° for both CFs and CFs:PPy composite. The clearly peaks can be assigned to the crystalline structure of cellulose (Ford, Mendon, Thames, & Rawlins, 2010). Also, the broaden characteristic of various CFs:PPy composites were exhibited in the region of 15° - 25° which is the amorphous phase of polypyrrole (Luo et al., 2010).

4.3. Thermogravimetric analysis

The degradation temperatures of CFs and CFs:PPy papers were studied by thermogravimetric analysis as shown in figure 3. As seen in the figure, CFs and CFs:PPy showed main weight loss in three stages. For CFs, it demonstrates that the thermal stability of the prepared CFs in much higher than that of composites in the temperature lower than 250°C . As composite is hygroscopic, nearly 8% weight loss is occurred at 100°C . The second stage of weight loss started at 250°C and continued up to 500°C with rapidly 80% of weight loss. The last stages of temperature at $>500^\circ\text{C}$ almost 100% of weight loss can be observed for all conditions. For CFs:PPy composites, the first stage range between room temperature and 250°C showed about a 13% of weight loss. The second stage of weight loss started at 250°C and continued up to 500°C during which there was nearly an 80% of gradually weight loss. The last states of temperature up to 500°C during which there was a 100% of weight loss. From the above analysis, it clearly shows that the thermal stability of CFs was greatly affected by incorporating PPy. The incorporated PPy lowered the starting thermal degradation of CFs.

4.4. FE-SEM analysis

The morphology of CFs, CFs:PPy composites was studied using Field Emission Scanning Electron Microscope as shown in figure 4. The figure 4 (a) shown that the CFs surface is rather straight

and smooth without the formation of cross-link between fiber. It is important to note that CFs appears to be a uniform fibrous network. For CFs:PPy composites as shown in figure 4 (b-e), the formation of PPy on the CFs in the form of clusters and cross-link between fiber network can be observed (ElNahrawy, Haroun, Hamadneh, & Al-Dujaili, 2017), which involving the formation of H-bonds between the cellulose and the polypyrrole chain. These interactions were a result of both intermolecular and intramolecular forces, causing the composites sheet to be less cellulose fiber density.

4.5. Mechanical properties

The tensile strength, Young's modulus, and elongation at break of neat CFs and CFs:PPy composite were presented in table 1. Not surprisingly, tensile strength and young's modulus were decreased as the increasing of PPy additive. This effect may be caused by the inter-percolation of PPy between CFs network. However, the elongation at break of composite is not dramatically reduced, when increasing the amount of additive. After the polymerization process of pyrrole, PPy network may be grouped to be clusters which can be observed from the SEM image. Therefore, PPy network was poorly dispersed into cellulose fibers matrix by present preparation.

4.6. Conductivity properties

The electrical conductivities of CFs:PPy composites with different amount of PPy were measured using a four - point probe technique. Table 2 shows the sheet resistance, resistivity, and electrical conductivities of CFs:PPy composites. The experimental setup and parameters calculation is described in literature (J. Li, Wang, & Ba, 2012). The CFs has basically no conductivity, while the resistance and resistivity of CFs: PPy composites decrease as the increasing of PPy additive. Consequently, the electrical conductivities of CFs:PPy composites are increased up to 1.84×10^{-2} S/cm at 0.20 ml PPy. Compare to the conductivity of typically semiconductor ($10^{-7} - 10^5$ S/cm), the conductivity of CFs:PPy is in a range of promising application of electronic device.

4.7. Dielectric properties

Fig. 5. shows dielectric properties of CFs and CFs:PPy composite materials. Typically, the dielectric properties of polymer composites can be affected by the polymer type or dopant type. The variation of dielectric constant (permittivity, ϵ') and loss tangent as a function of frequency for the prepared samples with different composition of PPy are presented. The dielectric constants were very high at low frequency and were slightly decreased when the frequency increased. Note that the dielectric constant of CFs is more rapidly decreased when compare to that of CFs:PPy composites. The reducing of dielectric constants can be expressed by the relaxation behavior. With high region of frequency, the charge has insufficient time of re-orientation under applied external field and it was therefore presented as a lower of dielectric properties. In additional, the loss tangent of CFs and CFs:PPy composite is not significantly difference. All conditions exhibit the slightly increasing of loss tangent at high frequency.

4.8. Impedance properties

Fig. 6. shows the complex impedance spectra with the variation of the imaginary part of the complex impedance (Z'') versus its real part (Z'). The frequency range was from 10 Hz to 10 MHz and the applied AC signal was 0.5 V. The impedance spectra are characterized as semicircle, which is most probably result of the facilitated transport of the doping anions in the bulk of the composites.

The transport of the doping anions can be enhanced by increased amount of PPy (Nakata & Kise, 1993; Porjazoska Kujundjiski, Chamovska, & Grchev, 2014). Noted that the best fit of experimental data to model was obtained using a constant phase element (CPE) rather than an ideal capacitor. The equivalent circuit model is shown in Fig 6. Noted that the best fit of experimental data to model was obtained using a constant phase element (CPE) rather than an ideal capacitor. The capacitance of 3.168×10^{-11} F can be obtained from the composites at 0.20 ml PPy. The equivalent circuit model is shown in Fig 6.

5. Conclusions

A cellulose paper was demonstrated with the aid of in-situ synthesized conductive cellulose (CFs):polypyrrole (PPy) network. Chemical polymerization has been very successful in the production of composite materials of conductivity polymers with CFs. Increasing polypyrrole content in the composite affected the features of cellulose. The morphology of CFs exhibited a very straight and smooth surface. When PPy was composited with CFs, the PPy clusters were formed on the CFs. Increasing of the PPy amount causes the reduction of mechanical properties due to interpercolation of PPy in cellulose. Also, the decreasing of dielectric and impedance in CFs:PPy composites sheet can be observed as the increasing of CFs:PPy ratio. Moreover, conductivity of 184×10^{-4} S/cm was obtained from a composites sheet of CFs:PPy(0.20).

6. Tables

Table 1. Mechanical properties of CFs and CFs:PPy composites.

Composite	Tensile strength (MPa)	Young's modulus (MPa)	Elongation at break (%)
CFs	2.038 ± 0.761	248.940 ± 85.926	1.404 ± 0.440
CFs:PPy0.05	0.798 ± 0.520	109.652 ± 73.871	1.180 ± 0.234
CFs:PPy0.10	0.554 ± 0.341	109.858 ± 68.977	0.698 ± 0.119
CFs:PPy0.15	0.213 ± 0.285	39.715 ± 53.154	0.868 ± 0.331
CFs:PPy0.20	0.026 ± 0.020	2.962 ± 3.546	1.524 ± 0.389

Table 2. Conductivity of the CFs and CFs:PPy composites.

Sample	Resistance (Ω) $\times 10^3$	Resistivity (Ωm) $\times 10^3$	Conductivity ($\text{S}\cdot\text{cm}^{-1}$) $\times 10^4$
CFs	-	-	-
CFs:PPy(0.05)	10.7 ± 0.742	67.4 ± 4.66	1.49 ± 0.106
CFs:PPy(0.10)	1.19 ± 0.0944	7.51 ± 0.593	13.3 ± 1.05
CFs:PPy(0.15)	0.735 ± 0.0792	4.62 ± 0.498	21.9 ± 2.44
CFs:PPy(0.20)	0.0938 ± 0.0241	0.589 ± 0.151	184 ± 58.9

7. Figures

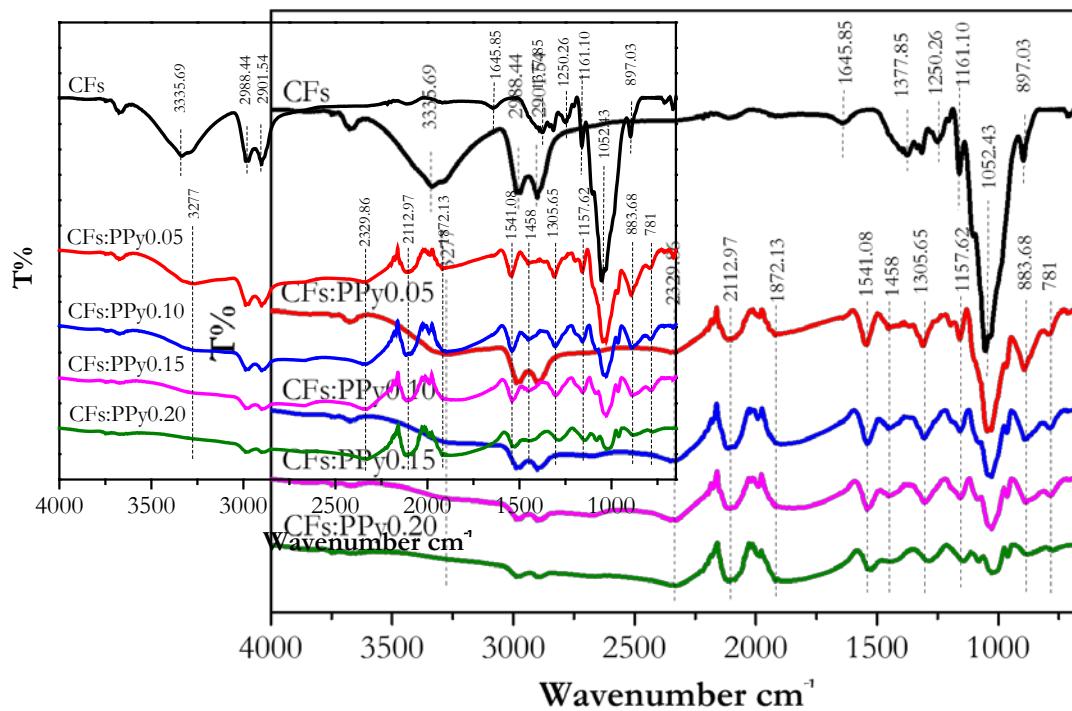


Figure 1. FTIR spectra of CFs and CFs:PPy composites.

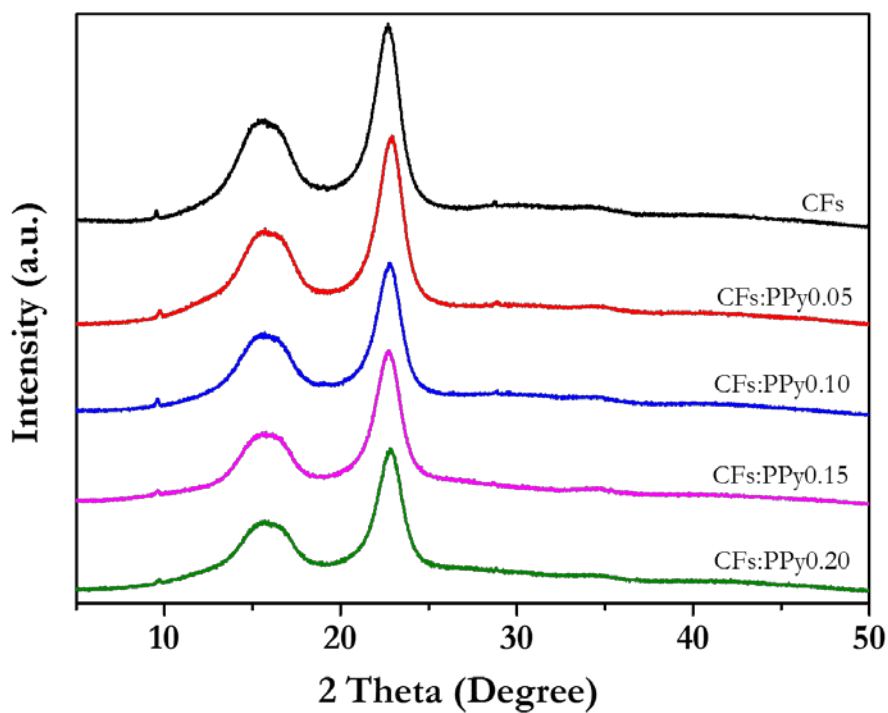


Figure 2. XRD patterns of CFs and CFs:PPy composites.

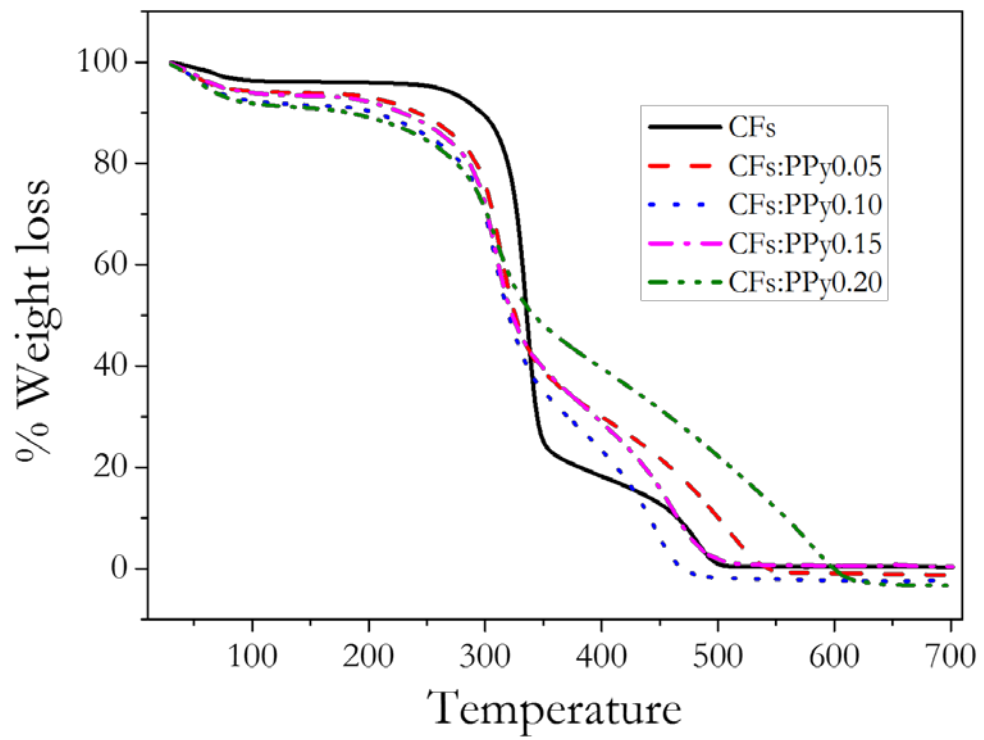


Figure 3. TGA of CFs and CFs:PPy composites.

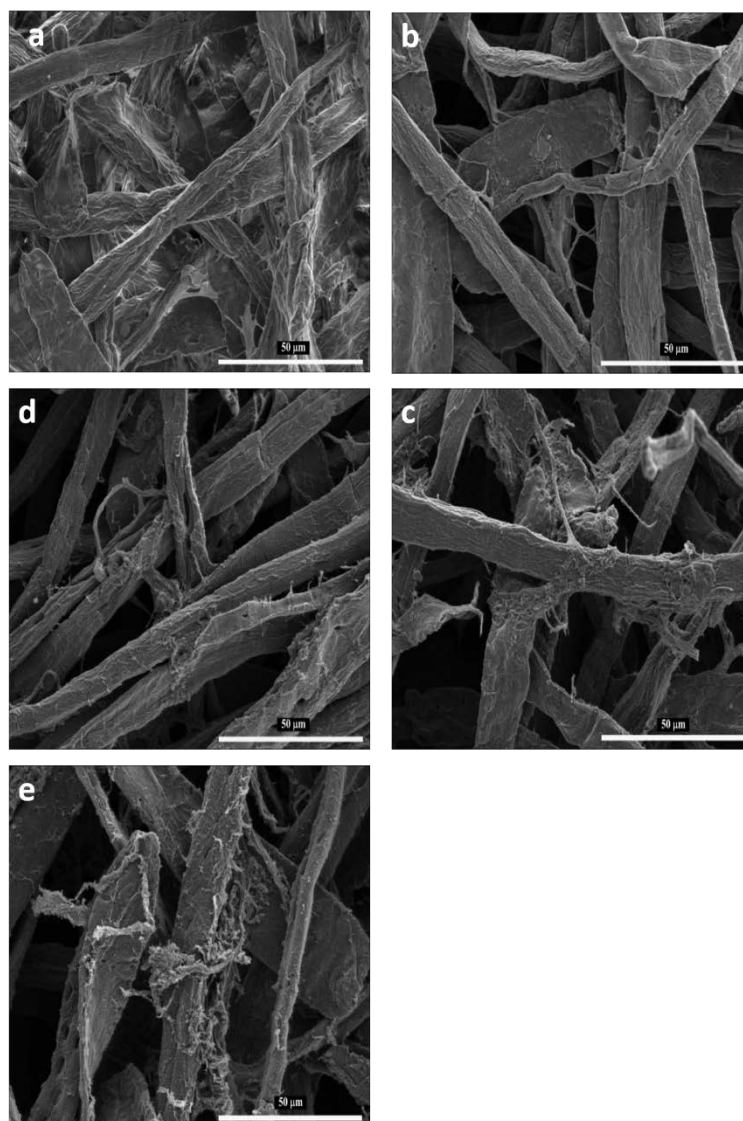


Figure 4. FE-SEM of composite materials with different pyrrole preparation condition) a (CFs
b (CFs:PPy0.05)c (CFs:PPy0.10)d (CFs:PPy0.15)e (CFs:PPy0.20).

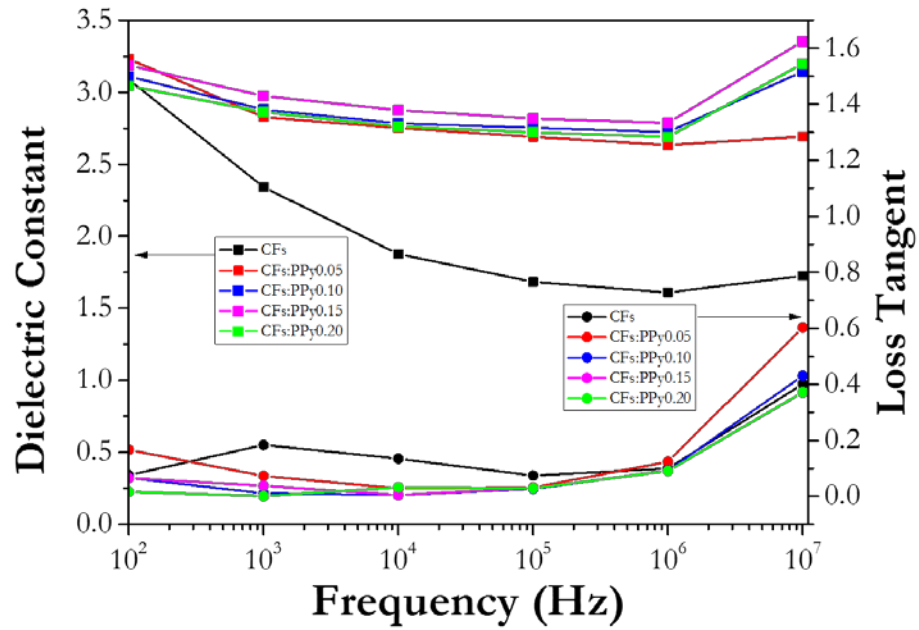


Figure 5. Variation of dielectric constant and loss tangent of CFs and CFs:PPy composites with frequency.

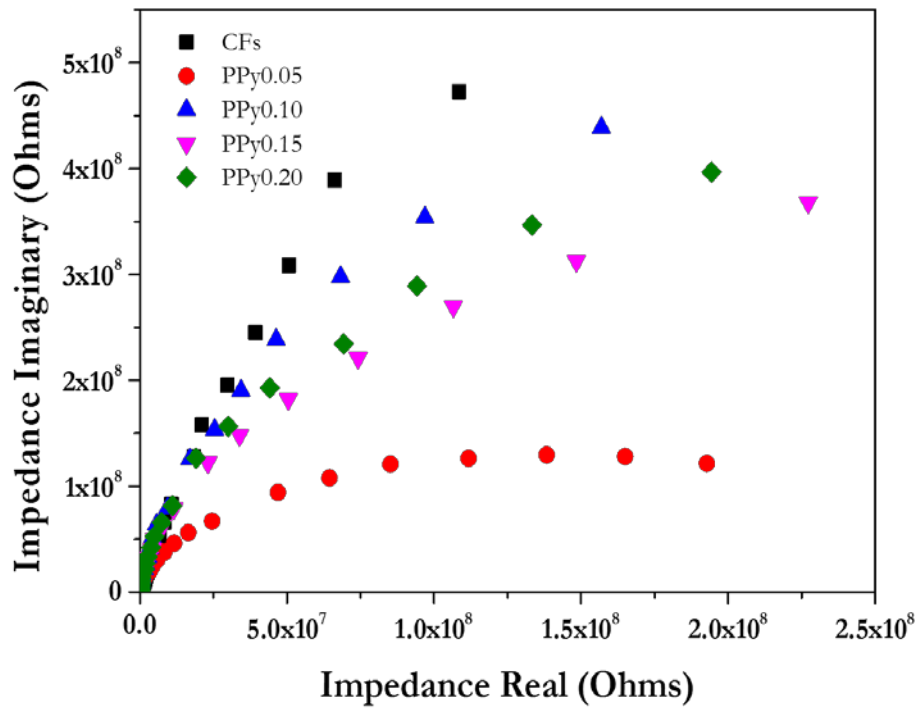


Figure 6. Impedance spectra of CFs and CFs:PPy composites.

Acknowledgements

The authors would like to thank for the financial support provided by Thammasat University under the National Research Council of Thailand (NRCT)

References

- Ali, F., Reinert, L., Lévêque, J.-M., Duclaux, L., Muller, F., Saeed, S., & Shah, S. S. (2014). Effect of sonication conditions: solvent, time, temperature and reactor type on the preparation of micron sized vermiculite particles. *Ultrasonics sonochemistry*, *21*(3), 1002-1009.
- Chougule, M., Dalavi, D., Mali, S., Patil, P., Moholkar, A., Agawane, G., . . . Patil, V. (2012). Novel method for fabrication of room temperature polypyrrole–ZnO nanocomposite NO₂ sensor. *Measurement*, *45*(8), 1989-1996.
- Du, X., Zhang, Z., Liu, W., & Deng, Y. (2017). Nanocellulose-based conductive materials and their emerging applications in energy devices-A review. *Nano Energy*, *35*, 299-320.
- ElNahrawy, A. M., Haroun, A. A., Hamadneh, I., & Al-Dujaili, A. H. (2017). Conducting cellulose/TiO₂ composites by in situ polymerization of pyrrole. *Carbohydrate polymers*, *168*, 182-190.
- Fackler, K., Stevanic, J. S., Ters, T., Hinterstoisser, B., Schwanninger, M., & Salmén, L. (2011). FT-IR imaging microscopy to localise and characterise simultaneous and selective white-rot decay within spruce wood cells. *Holzforschung*, *65*(3), 411-420.
- Ford, E. N. J., Mendon, S. K., Thames, S. F., & Rawlins, J. W. (2010). X-ray diffraction of cotton treated with neutralized vegetable oil-based macromolecular crosslinkers. *Journal of Engineered Fibers and Fabrics*, *5*(1), 155892501000500102.
- Fu, J., Zhang, J., Song, X., Zarrin, H., Tian, X., Qiao, J., . . . Chen, Z. (2016). A flexible solid-state electrolyte for wide-scale integration of rechargeable zinc–air batteries. *Energy & Environmental Science*, *9*(2), 663-670.
- Hansora, D., Shimpi, N., & Mishra, S. (2015). Graphite to graphene via graphene oxide: an overview on synthesis, properties, and applications. *Jom*, *67*(12), 2855-2868.
- Ho, T. A., Jun, T.-S., & Kim, Y. S. (2013). Material and NH₃-sensing properties of polypyrrole-coated tungsten oxide nanofibers. *Sensors and Actuators B: Chemical*, *185*, 523-529.
- Lay, M., Méndez, J. A., Delgado-Aguilar, M., Bun, K. N., & Vilaseca, F. (2016). Strong and electrically conductive nanopaper from cellulose nanofibers and polypyrrole. *Carbohydrate polymers*, *152*, 361-369.
- Li, J., Wang, Y., & Ba, D. (2012). Characterization of semiconductor surface conductivity by using microscopic four-point probe technique. *Physics Procedia*, *32*, 347-355.
- Li, Y., Zhang, H., Ni, S., & Xiao, H. (2018). In situ synthesis of conductive nanocrystal cellulose/polypyrrole composite hydrogel based on semi-interpenetrating network. *Materials Letters*, *232*, 175-178.
- Luo, Y.-L., Fan, L.-H., Xu, F., Chen, Y.-S., Zhang, C.-H., & Wei, Q.-B. (2010). Synthesis and characterization of Fe₃O₄/PPy/P (MAA-co-AAm) trilayered composite microspheres with electric, magnetic and pH response characteristics. *Materials Chemistry and Physics*, *120*(2-3), 590-597.
- Mahadeva, S. K., & Kim, J. (2011). Enhanced electrical properties of regenerated cellulose by polypyrrole and ionic liquid nanocoating. *Proceedings of the Institution of Mechanical Engineers, Part N: Journal of Nanoengineering and Nanosystems*, *225*(1), 33-39.
- Mohanty, A. K., Misra, M., & Drzal, L. (2002). Sustainable bio-composites from renewable resources: opportunities and challenges in the green materials world. *Journal of Polymers and the Environment*, *10*(1-2), 19-26.
- Müller, D., Rambo, C., Recouvreux, D., Porto, L., & Barra, G. (2011). Chemical in situ polymerization of polypyrrole on bacterial cellulose nanofibers. *Synthetic Metals*, *161*(1-2), 106-111.

- Nakata, M., & Kise, H. (1993). Preparation of Polypyrrole-Poly(vinyl chloride) Composite Films by Interphase Oxidative Polymerization. *Polymer Journal*, 25(1), 91-94. doi:10.1295/polymj.25.91
- Poletto, M., Pistor, V., Zeni, M., & Zattera, A. J. (2011). Crystalline properties and decomposition kinetics of cellulose fibers in wood pulp obtained by two pulping processes. *Polymer Degradation and Stability*, 96(4), 679-685.
- Porjazoska Kujundjiski, A., Chamovska, D., & Grchev, T. (2014). Capacitive properties of polypyrrole/activated carbon composite. *Hemijska industrija*, 68, 63-63. doi:10.2298/HEMIND140305063P
- Rosa, M., Medeiros, E., Malmonge, J., Gregorski, K., Wood, D., Mattoso, L., . . . Imam, S. (2010). Cellulose nanowhiskers from coconut husk fibers: Effect of preparation conditions on their thermal and morphological behavior. *Carbohydrate polymers*, 81(1), 83-92.
- Ummartyotin, S., & Manuspiya, H. (2015a). A critical review on cellulose: from fundamental to an approach on sensor technology. *Renewable and Sustainable Energy Reviews*, 41, 402-412.
- Ummartyotin, S., & Manuspiya, H. (2015b). An overview of feasibilities and challenge of conductive cellulose for rechargeable lithium based battery. *Renewable and Sustainable Energy Reviews*, 50, 204-213.
- Wang, S., Lu, A., & Zhang, L. (2016). Recent advances in regenerated cellulose materials. *Progress in Polymer Science*, 53, 169-206.
- Xu, F., Yu, J., Tesso, T., Dowell, F., & Wang, D. (2013). Qualitative and quantitative analysis of lignocellulosic biomass using infrared techniques: a mini-review. *Applied Energy*, 104, 801-809.
- Zhong, Q., Zhong, J., Hu, B., Hu, Q., Zhou, J., & Wang, Z. L. (2013). A paper-based nanogenerator as a power source and active sensor. *Energy & Environmental Science*, 6(6), 1779-1784.

A Polymeric Coating on Prelithiated Silicon-Based Nanoparticles for High Capacity Anodes used in Li-ion Batteries

Natthaphong Kamma¹, Yutthanakon Kanaphan¹, Sunisa Buakeaw¹, Songyoot Kaewmala²
Jeffrey Nash³, Sutham Srilomsak^{1,2} and Nonglak Meethong^{1,2,a}

¹Materials Science and Nanotechnology Program, Department of Physics, Faculty of Science, Khon Kaen University, Khon Kaen 40002, Thailand

²Institute of Nanomaterials Research and Innovation for Energy (IN-RIE), Research Network of NANOTEC-KKU (RNN), Khon Kaen University, Khon Kaen 40002, Thailand

³Graduate School, Udon Thani Rajabhat University, Udon Thani 41000, Thailand
Corresponding Author's Email: ^anonmee@kku.ac.th

Abstract

High performance lithium ion batteries are in demand for use in consumer electronics as well as in hybrid and electric vehicles. Silicon is a promising candidate anode material due to its high theoretical specific capacity of 4,200 mAh g⁻¹ and low discharge potential. However, a high irreversible capacity loss due to a solid electrolyte interphase formation on the surface of Si anodes during the 1st cycle limits its practical applications. Prelithiation is considered an attractive method that can be used to compensate for the active lithium losses during the 1st cycle. Prelithiated Si based nanoparticles are considered more practical than their micron-sized counterparts due to their better electrochemical and mechanical properties. However, one of the primary difficulties that these NPs usually exhibit is surface oxidation to Li₂O when the material comes into contact with moisture and oxygen during electrode fabrication, leading to poor electrochemical stability. In this work the surface stability of prelithiated Si-based nanoparticles was modified via a polymeric nano-coating method. The results demonstrate that coating with 1-fluorooctane is an effective strategy to mitigate irreversible capacity loss and provide electrochemical stability for high performance next generation lithium ion batteries.

Keywords: Lithium ion batteries; Silicon; Prelithiation

Introduction

Lithium ion batteries (LIBs) are playing an essential role in the development of electric vehicles (EVs) and grid energy storage technologies owing to their high energy density, low self-discharge, and long cycle life (Kennedy, Patterson, & Camilleri, 2000; Tarascon & Armand, 2001). Silicon (Si) represents an attractive candidate anode material to replace commercial graphite as a way of improving the energy density of LIBs. This is due to its high theoretical specific capacity of 4,200 mAh g⁻¹ (through the formation of a Li_{4.4}Si alloy). This is ten times higher than that of commercial graphite anodes with a relatively low electrochemical potential (370 mV) (Kasavajjula, Wang, & Appleby, 2007; Yin, Wan, & Guo, 2012). However, practical applications that achieve a satisfactory high capacity and stable cycling performance have not been realized since a large volume change (>400%), (Hui Wu & Cui, 2012) causes mechanical stress within the electrode leading to its rapid structural failure and poor electrical contact with the active material (Beaulieu, Eberman, Turner, Krause, & Dahn, 2001; Domi, Usui, Iwanari, & Sakaguchi, 2017).

Therefore, novel nanostructural designs of silicon-based electrode materials have been utilized to mitigate the volume expansion of the silicon structure and improve its cycling performance (N. Liu, Li, Pasta, & Cui, 2014; N. Liu et al., 2014; Son et al., 2015; Hui Wu & Cui, 2012). This can be facilitated by effective diffusion of active lithium and electrons (Y. Wang, Li, He, Hosono, & Zhou, 2010). However, a drawback to this approach is that the high surface area of these nanostructured materials significantly increases solid electrolyte interphase (SEI) formation during the first cycle

(Aurbach, 1994). SEI formation on silicon anodes during the first cycle causes highly irreversible capacity losses of 50-80% and can result in low Coulombic efficiency (CE) (DiLeo et al., 2013; Hu et al., 2013; H. Wu et al., 2013; X. Wu, Wang, Chen, & Huang, 2003) depending on the structure of the silicon and the composition of the anode composite. The irreversible loss of active lithium anode material during the first cycle can be mitigated by prelithiation, which has been previously achieved. Experimentally, the commercial prelithiation reagent used is stabilized lithium metal powder (SLMP). It can be drop-cast onto an electrode material serving as an anode, such as graphite, SiO₂, Si or CNT-based electrodes (Forney, Ganter, Staub, Ridgley, & Landi, 2013; Z. Wang et al., 2014). However, SLMP is hard to synthesize and is inhomogeneously distributed within the electrodes. Another approach is to use mechanical stirring of the Si anode material with Li metal at high temperatures to form Li_xSi NPs (Yom, Seong, Cho, & Yoon, 2018; J. Zhao et al., 2014; Jie Zhao et al., 2018). The resulting material suffers from surface oxidation that forms a Li₂O passivation layer when in contact with moisture and oxygen converting Li_xSi to Li_xSi–Li₂O NPs with a rather low potential and high capacity. These Li_xSi NP anode materials with fine structures typically show improved electrochemical performance and worsened stability on exposure to air with high relative humidity (RH) (J. Zhao et al., 2015). Therefore, surface coating may be an appropriate alternative to improve stability and yield higher capacities. For example, Li_xSi NPs mixed with poly(styrene-butadiene-styrene) (SBS) polymer and graphene can be used as an anode (J. Zhao et al., 2017). Also, Li_xSi NPs can be protected by an artificial solid electrolyte interphase (Y. Liu et al., 2017; Jie Zhao et al., 2017; J. Zhao et al., 2015). These coatings are effective to some extent and it is still necessary use them in a dry room.

This work proposes a polymeric-coating on the surface of prelithiated Si-based NPs (Li_xSi NPs). They are made using a prelithiation method to fabricate electrode materials that compensate for first-cycle capacity losses and reduce the unwanted reactions encountered by Li_xSi NPs exposed to air or other reactive environments. These materials are prepared using a thermal prelithiation forming a polymer shell around the NPs in a reaction of Li_xSi NPs with 1-fluorooctane, thereby producing a continuous and dense coating over the Li_xSi NPs. The 1-fluorooctane was selected because of its excellent chemical behavior in nonpolar solvents such as cyclohexane. It is highly reactive with Li_xSi NPs (J. Zhao et al., 2014). The LiF and other lithium compounds with long hydrophobic carbon chains effectively protect the reactivity of Li_xSi NPs when exposed to an ambient environment though the formation of a dense outer coating (J. Zhao et al., 2015). It is of great importance to develop relatively stable coated-Li_xSi NPs, which can be easily handled during the process of battery assembly.

Experimental

Materials preparation

40 and 80 μ L aliquots of 1-fluorooctane (CH₃(CH₂)₇F, Sigma Aldrich) were each mixed in 20 ml of anhydrous cyclohexane and then stirred at 60 °C for 2 h. Next, Li_xSi NPs (200 mg) were synthesized via a modified hydride destabilization method (Vajo, Mertens, Ahn, Bowman, & Fultz, 2004). These Li_xSi NPs were dispersed in anhydrous cyclohexane (Sigma Aldrich) with vigorous stirring for 1 h to obtain a suspension with 5 mg ml⁻¹ of Li_xSi NPs. The 40 μ L 1-fluorooctane solution and the Li_xSi NP suspension were homogeneously mixed at room temperature inside a glovebox under an Ar atmosphere for 1 h with vigorous stirring. After mixing, the coated-Li_xSi NPs were washed with cyclohexane and centrifuged to remove unreacted 1-fluorooctane and then dried under a vacuum. This process was repeated using the 80 μ L 1-fluorooctane mixture. The samples made up with 40 and 80 μ L aliquots of 1-fluorooctane are referred to as the coated-40 and coated-80 samples, respectively.

Structural and Morphological characterization

X-ray diffraction (XRD) (PANalytical, Empyrean) was performed to examine the crystal structure of the experimental samples using Cu-K α radiation with a step size of 0.01° and over a 2 θ range of 10°-80°. Transmission electron microscopy (FEI, TECNAI G2 20) was used to investigate the microstructural properties of the Li_xSi-coated NP materials.

Electrochemical testing

Swagelok type cells were assembled in an Ar-filled glove box to evaluate the electrochemical properties of these materials. The Li_xSi or coated-Li_xSi NP materials were mixed with carbon black

(Super P, Alfa Aesar) and polyvinylidene fluoride (PVDF-Kynar 2801, Arkema) (65:20:15 by weight) in a 1,3 dioxolane (DOL, Sigma Aldrich) solvent, which was then mechanically stirred to form a slurry. The resulting slurry was coated on copper foil using a doctor blade and then dried under a vacuum at 80 °C overnight. The Swagelok type cells consisted of discs of the prepared anode and a Li metal foil (Alfa Aesar), used as counter and reference electrodes, respectively. A 1.0M LiPF₆ solution in a 1:1 w/w ratio of ethylene carbonate (EC) and dimethyl carbonate (DMC), 1 vol% of vinylene carbonate and 2 vol% of fluoroethylene carbonate was used as an electrolyte with a Celgard 2400 (MTI) separator. Galvanostatic charge/discharge tests were done between 0.01-1.2 V at a C/20 rate (1C = 4.2 A g⁻¹) using a multi-channel tester (BST8 MA, MTI).

Results and discussion

The Li_xSi NPs were synthesized via a modified hydride destabilization method using commercial Si, which exhibits surface oxidation that forms a Li_2O passivation layer when in contact with moisture and oxygen during the synthesis of Li_xSi NPs. This leads to poor electrochemical stability. Therefore, modifying the surface of Li_xSi NPs was done via a polymeric nano-coating with the reduction of 1-fluorooctane in cyclohexane, as depicted in Figure 1a, to prevent further oxidation. The morphology of the Li_xSi NPs with a size range of 10 to 20 nm and of the coated-40 and coated-80 samples are respectively shown in Figure 1b-d. Generally, the surfaces of Li_xSi NPs consisted of lithium fluoride (LiF) and other lithium compounds such as lithium alkyl carbonates with long hydrophobic carbon chains. This is similar to the reaction mechanism employing butyllithium (Wilke, 2003; J. Zhao et al., 2015). Li_xSi NPs transfer a single electron to a C–F bond in 1-fluorooctane forming a C radical and F^- , and a second electron transfer converts the C radical into a carbanion (reaction 1). Additionally, O_2 and CO_2 in the glovebox may react with alkyl lithium to form a complex mixture of lithium compounds (reaction 2).

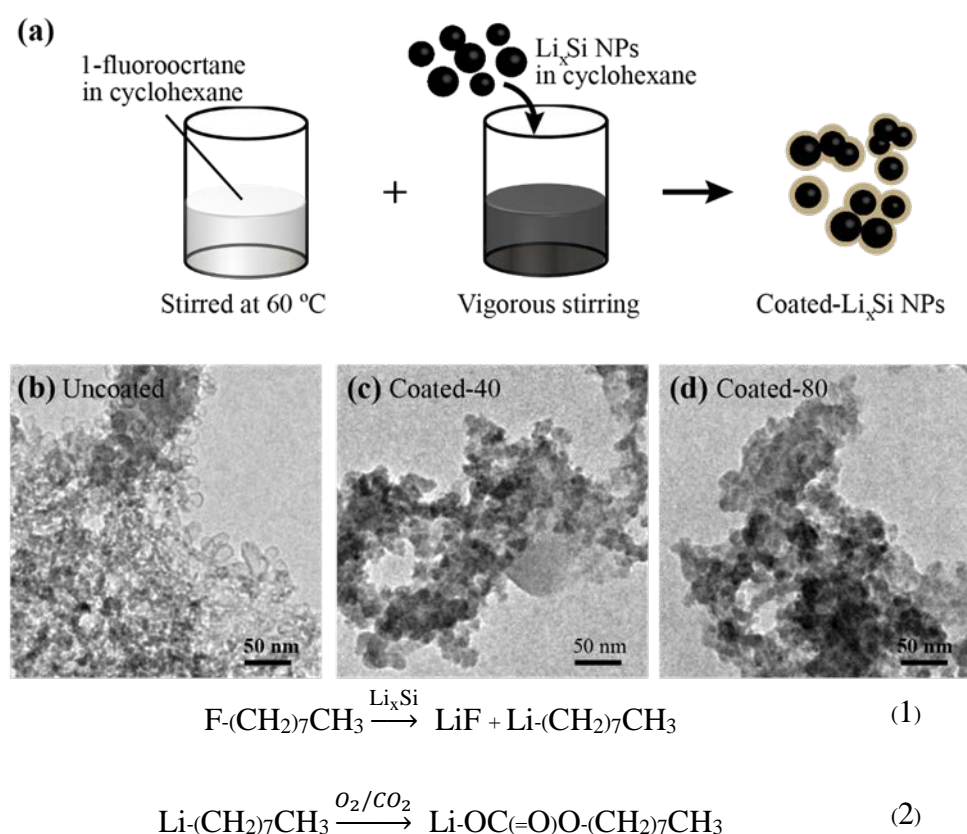


Figure 1. (a) Schematic diagram of the coated Li_xSi NPs passivation layer formed by chemical reactions via 1-fluorooctane. (b-d) TEM images of the Li_xSi NPs, coated-40 and coated-80 samples, respectively.

The XRD patterns of all the uncoated and coated samples are shown in Figure 2. The coated and uncoated samples at 0 h of exposure to ambient air exhibited quite similar XRD patterns, showing diffraction peaks of the $\text{Li}_{22}\text{Si}_5$ (PDF No. 01-073-2049), $\text{Li}_{12}\text{Si}_7$ (PDF No. 00-040-0942), Li_2O (PDF No. 01-073-0593), and LiOH phases (space group $P4/mmm$ with PDF No. 01-076-0911, and $P4/mmm$ with PDF No. 00-001-1021) as given in Figure 2a. The $\text{Li}_{22}\text{Si}_5$ and $\text{Li}_{12}\text{Si}_7$ phases are formed as a result of the pre-lithiation process, while the Li_2O and LiOH phases are formed due to reactions with O_2 and water vapor in the ambient environment. The coated and uncoated samples at 6 h of exposure to ambient air with $20\pm 2\%$ RH showed different amounts of Li_2O and LiOH phases compared to those with 0 h of exposure. After exposure to ambient air for 6 h, the XRD pattern of the uncoated sample showed significantly higher peak intensities of the Li_2O and LiOH phases. However, the XRD patterns of the coated samples showed similar peak intensities of these phases. The coated-80 sample showed slightly lower amounts of Li_2O and LiOH phases than that of the coated-40 sample due to a thicker surface coating. This indicates that our method using polymeric coating can effectively protect pre-lithiated Li_xSi NPs and prevent further surface oxidation for at least 6 h. This polymeric coating method is effective because both LiF and lithium alkyl carbonate with long hydrophobic carbon chains can serve to form an effective passivation layer on the surfaces of Li_xSi NPs, retarding reactions of metallic lithium with O_2 and water vapor in an ambient environment (Stubblefield & Bach, 1972; Jie Zhao et al., 2017).

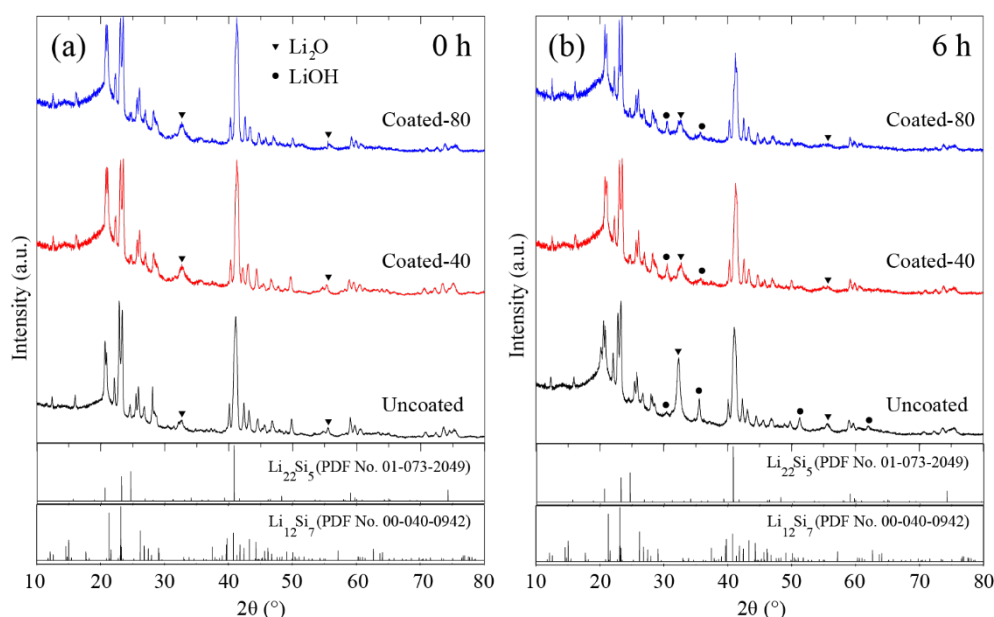


Figure 2. XRD patterns of the uncoated, coated-40 and coated-80 samples after (a) 0 h and (b) 6 h of exposure to ambient air with $20\pm 2\%$ RH.

A study of the electrochemical properties of the initial Li_xSi NPs and coated- Li_xSi NP materials (coated-40 and coated-80 sample) at $20\pm 2\%$ RH after 0 h, 6 h, and 24 h exposure to ambient air was carried out using Swagelok-type cells. All samples were fabricated using Li metal as counter electrodes. The electrolyte solution consisted of 1.0 M LiPF_6 in a 1:1 w/w ratio of ethylene carbonate (EC) and dimethyl carbonate (DMC), 1 vol% of vinylene carbonate and 2 vol% of fluoroethylene carbonate with a Celgard 2400 disc as a separator. All the specific capacities and current densities are reported based on the weight of active material in the anodes. The electrochemical behaviour of the initial Li_xSi NPs and coated- Li_xSi NP anodes was evaluated using galvanostatic charge/discharge measurements during their first cycle (Figure

3a-c). The samples after 0 h of exposure showed first charge capacities of about 1,395, 1,371 and 1,091 mAh g^{-1} for the uncoated, coated-40 and coated-80 samples, respectively. After exposure to an ambient environment with $20\pm 2\%$ RH for 6 h, the uncoated sample showed negligible capacity, while the coated-40 sample retained 839 mAh g^{-1} and the coated-80 sample retained 1025 mAh g^{-1} . This indicates that the coated-40 sample showed a capacity decay of 39% while the coated-80 sample lost less than 6% of its capacity. After 24 h of exposure to the ambient environment, the coated-40 sample exhibited a capacity of 405 mAh g^{-1} , which is a capacity decay of 70% of its initial capacity. The coated-80 sample still delivered a stored capacity of 677 mAh g^{-1} , which is a capacity decay of 38% of its initial capacity. This indicates that even though the coated-80 sample was protected from further surface oxidation for about 6 h, the coating thickness needs to be optimized to prevent reactions of metallic lithium with O_2 and water vapor in an ambient environment for longer exposure times. This topic will be our focus in future experiments. Figure 3d summarizes the results of effect of air exposure.

Figure 3e shows the cycling performance of the electrodes prepared from the coated-40 and coated-80 samples after 6 h of exposure to ambient air. It is noteworthy that the cycling stability of the 6 h air exposed coated-40 sample was quite similar to that of the coated-80 sample. However, the absolute discharge capacity after 6 h at $20\pm 2\%$ RH of the coated-80 sample was higher than that of the coated-40 sample. The discharge capacities after 10 cycles were $\sim 860 \text{ mAh g}^{-1}$ and $\sim 630 \text{ mAh g}^{-1}$ for the coated-80 and coated-40 samples, respectively. This shows that the discharge capacity of the coated samples was a function of the concentration of the 1-fluorooctane used in forming the coating. A thicker coating is more effective in preventing reactions with O_2 and moisture resulting in superior electrochemical performance.

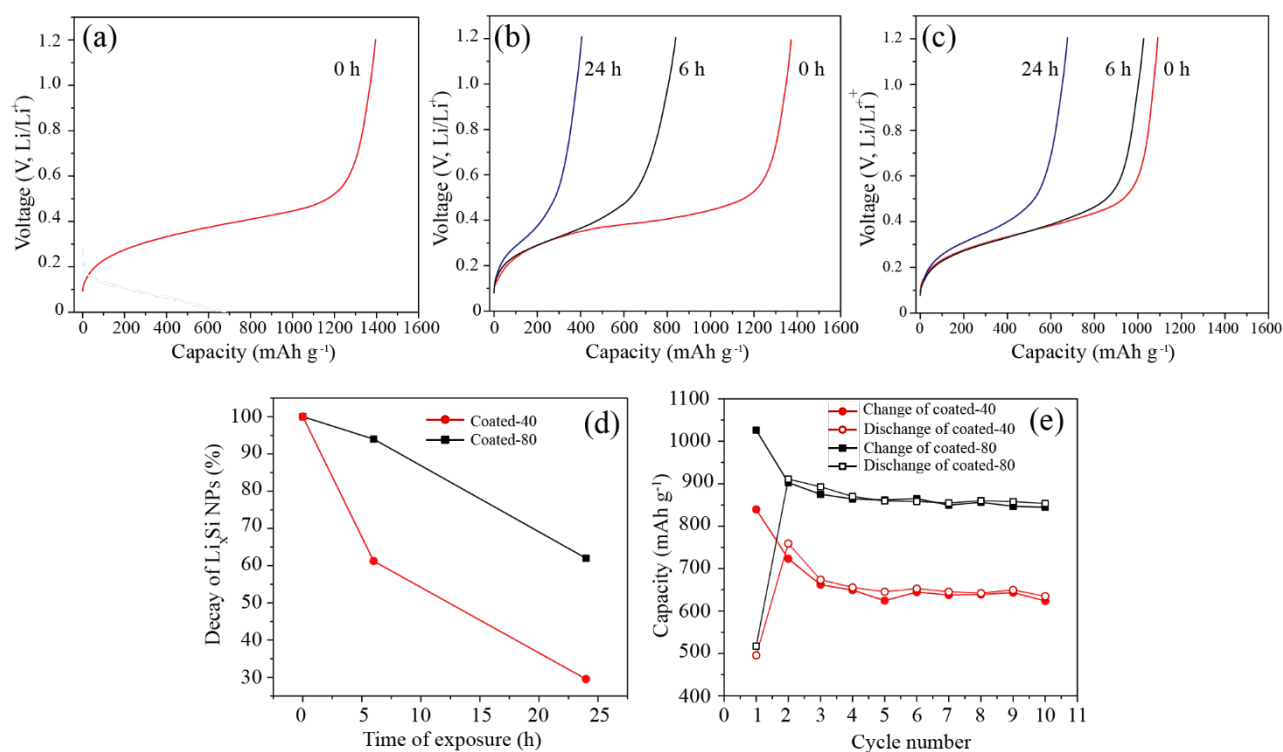


Figure 3. Voltage profiles during first charging cycle of (a) uncoated (b) coated-40 (c) coated-80 samples under ambient conditions for various durations ($20\pm 2\%$ RH). (d) the change in capacity of the coated anodes as a function of exposure time, (e) the cycling stability of the electrodes prepared from the 6 h air exposed coated-40 and coated-80 samples at a C/20 rate ($1\text{C} = 4.2 \text{ A g}^{-1}$).

Conclusions

We successfully developed a polymeric coating method for pre-lithiated Li_xSi NPs, with a size range of 10-20 nm, using a chemical reaction involving 1-fluorooctane. LiF and lithium alkyl carbonate compounds with long hydrophobic carbon chains can serve as an effective passivation layer on the surfaces of Li_xSi NPs. This polymeric coating layer can retard reactions of metallic lithium with O_2 and water vapor inhibited negative reactions under ambient conditions, improved electrochemical performance, and improved the ease of electrode fabrication. The coated-40 and coated-80 samples showed similar capacity decays in an ambient environment at $20\pm 2\%$ RH after 6 h, but the coated-80 sample had higher capacities after 10 cycles. This indicates that polymer coating methods are potentially useful in industrial battery fabrication. Thus, application of polymeric coatings on the surfaces of lithium containing anode materials is a promising approach that may facilitate prelithiation methods for high performance next-generation lithium ion batteries.

References

- Aurbach, D. (1994). The correlation between the surface chemistry and the performance of Li-carbon intercalation anodes for rechargeable 'Rocking-Chair' type batteries. *Journal of The Electrochemical Society*, 141(3), 603.
- Beaulieu, L., Eberman, K., Turner, R., Krause, L., & Dahn, J. (2001). Colossal reversible volume changes in lithium alloys. *Electrochemical and Solid-State Letters*, 4(9), A137-A140.
- DiLeo, R. A., Ganter, M. J., Thone, M. N., Forney, M. W., Staub, J. W., Rogers, R. E., et al. (2013). Balanced approach to safety of high capacity silicon-germanium-carbon nanotube free-standing lithium ion battery anodes. *Nano Energy*, 2(2), 268-275.
- Domi, Y., Usui, H., Iwanari, D., & Sakaguchi, H. (2017). Effect of mechanical pre-lithiation on electrochemical performance of silicon negative electrode for lithium-ion batteries. *Journal of The Electrochemical Society*, 164(7), A1651-A1654.
- Forney, M. W., Ganter, M. J., Staub, J. W., Ridgley, R. D., & Landi, B. J. (2013). Prelithiation of silicon-carbon nanotube anodes for lithium ion batteries by stabilized lithium metal powder (SLMP). *Nano letters*, 13(9), 4158-4163.
- Hu, L., Liu, N., Eskilsson, M., Zheng, G., McDonough, J., Wågberg, L., et al. (2013). Silicon-conductive nanopaper for Li-ion batteries. *Nano Energy*, 2(1), 138-145.
- Kasavajjula, U., Wang, C., & Appleby, A. J. (2007). Nano- and bulk-silicon-based insertion anodes for lithium-ion secondary cells. *Journal of Power Sources*, 163(2), 1003-1039.
- Kennedy, B., Patterson, D., & Camilleri, S. (2000). Use of lithium-ion batteries in electric vehicles. *Journal of Power Sources*, 90(2), 156-162.
- Liu, N., Li, W., Pasta, M., & Cui, Y. (2014). Nanomaterials for electrochemical energy storage. *Frontiers of Physics*, 9(3), 323-350.
- Liu, N., Lu, Z., Zhao, J., McDowell, M. T., Lee, H. W., Zhao, W., et al. (2014). A pomegranate-inspired nanoscale design for large-volume-change lithium battery anodes. *Nature Nanotechnology*, 9(3), 187-192.
- Liu, Y., Lin, D., Yuen, P. Y., Liu, K., Xie, J., Dauskardt, R. H., et al. (2017). An artificial solid electrolyte interphase with high Li-ion conductivity, mechanical strength, and flexibility for stable lithium metal anodes. *Advanced Materials*, 29(10).
- Son, I. H., Hwan Park, J., Kwon, S., Park, S., Rummeli, M. H., Bachmatiuk, A., et al. (2015). Silicon carbide-free graphene growth on silicon for lithium-ion battery with high volumetric energy density. *Nature Communications*, 6, 7393.

- Stubblefield, C. B., & Bach, R. O. (1972). Solubility of lithium fluoride in water. *Journal of Chemical and Engineering Data*, 17(4), 491-492.
- Tarascon, J. M., & Armand, M. (2001). Issues and challenges facing rechargeable lithium batteries. *Nature*, 414, 359-367.
- Vajo, J. J., Mertens, F., Ahn, C. C., Bowman, R. C., & Fultz, B. (2004). Altering hydrogen storage properties by hydride destabilization through alloy formation: LiH and MgH₂ destabilized with Si. *The Journal of Physical Chemistry B*, 108(37), 13977-13983.
- Wang, Y., Li, H., He, P., Hosono, E., & Zhou, H. (2010). Nano active materials for lithium-ion batteries. *Nanoscale*, 2(8), 1294-1305.
- Wang, Z., Fu, Y., Zhang, Z., Yuan, S., Amine, K., Battaglia, V., et al. (2014). Application of stabilized lithium metal powder (SLMP®) in graphite anode – A high efficient prelithiation method for lithium-ion batteries. *Journal of Power Sources*, 260, 57-61.
- Wilke, G. (2003). Fifty years of Ziegler catalysts: consequences and development of an invention. *Angewandte Chemie International Edition*, 42(41), 5000-5008.
- Wu, H., & Cui, Y. (2012). Designing nanostructured Si anodes for high energy lithium ion batteries. *Nano Today*, 7(5), 414-429.
- Wu, H., Yu, G., Pan, L., Liu, N., McDowell, M. T., Bao, Z., et al. (2013). Stable Li-ion battery anodes by in-situ polymerization of conducting hydrogel to conformally coat silicon nanoparticles. *Nature Communications*, 4, 1943.
- Wu, X., Wang, Z., Chen, L., & Huang, X. (2003). Ag-enhanced SEI formation on Si particles for lithium batteries. *Electrochemistry Communications*, 5(11), 935-939.
- Yin, Y., Wan, L., & Guo, Y. (2012). Silicon-based nanomaterials for lithium-ion batteries. *Chinese science bulletin*, 57(32), 4104-4110.
- Yom, J. H., Seong, I. W., Cho, S. M., & Yoon, W. Y. (2018). Optimization of heat treatment conditions for fabricating pre-lithiated silicon monoxide as an anode material for lithium-ion batteries. *Journal of The Electrochemical Society*, 165(3), A603-A608.
- Zhao, J., Liao, L., Shi, F., Lei, T., Chen, G., Pei, A., et al. (2017). Surface fluorination of reactive battery anode materials for enhanced stability. *Journal of the American Chemical Society*, 139(33), 11550-11558.
- Zhao, J., Lu, Z., Liu, N., Lee, H. W., McDowell, M. T., & Cui, Y. (2014). Dry-air-stable lithium silicide-lithium oxide core-shell nanoparticles as high-capacity prelithiation reagents. *Nature Communications*, 5, 5088.
- Zhao, J., Lu, Z., Wang, H., Liu, W., Lee, H. W., Yan, K., et al. (2015). Artificial solid electrolyte interphase-protected Li_xSi nanoparticles: an efficient and stable prelithiation reagent for lithium-ion batteries. *Journal of the American Chemical Society*, 137(26), 8372-8375.
- Zhao, J., Sun, J., Pei, A., Zhou, G., Yan, K., Liu, Y., et al. (2018). A general prelithiation approach for group IV elements and corresponding oxides. *Energy Storage Materials*, 10, 275-281.
- Zhao, J., Zhou, G., Yan, K., Xie, J., Li, Y., Liao, L., et al. (2017). Air-stable and freestanding lithium alloy/graphene foil as an alternative to lithium metal anodes. *Nature Nanotechnology*, 12(10), 993-999.

Effect of drying temperature on quality of RD6 variety brown parboiled glutinous rice

Petcharat Jaiboon^{1,a}, Somchart Soponronnarit^{2,b}

¹Program of Physics, Faculty of Science and Technology, Sakon Nakhon Rajabhat University, Sakon Nakhon, Thailand

²School of Energy, Environment and Material, King Mongkut's University of Technology Thonburi, Bangkok, Thailand

E-mail: ^apetcharat@snru.ac.th, ^bisomarit@kmutt.ac.th

Abstract

The aim of this research was to investigate an effect of drying temperature on quality of RD6 variety brown parboiled glutinous rice. RD6-paddy was soaked at temperature of 70 ± 5 °C in an insulated tank for 3 h; the ratio between paddy and hot water was 1.0:1.3, then drain and temper for 30 min. The initial moisture content of paddy was 50-52% (d.b.). 250 g of moist parboiled paddy was dried by fluidized bed dryer using superheated steam as a media at temperature of 110 °C, 130 °C and 150 °C. The velocity of superheated steam was 2.3 m/s until the moisture content of paddy down to 21-23% (d.b.) after that, the parboiled paddy was shade-dried until the moisture content to 14-16% (d.b.) and kept at 5 °C in a refrigerator for quality tests i.e., head brown parboiled rice yield, color, microstructure and thermal property. It was found that, head brown parboiled rice yield was increased when dried at high temperature whereas its color in terms of L^* , a^* and b^* were decreased. When drying at over temperature of 130 °C revealed fully degree of gelatinization and the starch granules was fused themselves in brown parboiled glutinous rice. The results lead to conclude that, higher head brown parboiled rice yield dependent on drying at high temperature.

Keywords: Color; Fluidized bed drying; Head brown rice yield; Parboiled glutinous rice

1. Introduction

Rice Department 6; RD6 is one famous cultivar of glutinous rice. It is product and consume in the north and northeastern part of Thailand. It is used as a raw material for producing a wide variety of product such as sweet rice cake and rice pudding and also consumed in the form of steamed rice. Parboiling process is a hydrothermal treatment of paddy that improves the milling, nutritional, and organoleptic attributes of rice. The process involves soaking or steeping, steaming, and drying. Soaking rice at room temperature is conventional and widely practiced but takes a long time to reach a moisture content of around 30g/100 g wb. Warm- or hot-water soaking is a common method to shorten soaking time and the soaking temperature below the starch gelatinization is recommended to minimize kernel splitting and subsequent leaching of solids and phytochemicals (Subba Rao & Bhattachaya, 1966). Drying with superheated steam in a fluidized bed dryer can included the step of steaming and drying which can save drying time and prevent the yellowing of rice grains that easily occurs at high temperature (Soponronnarit, et al., 2006). Teachapairoj, et al. (2003) reported that soaked rice with high temperature of water and drying with a superheated steam fluidized bed dryer could be improved high head rice yield. Despite many researchers having reported the advantages of parboiling process and superheated steam fluidized bed drying but the information of brown parboiled glutinous rice dried with superheated steam in a fluidized bed dryer is very limited. Therefore, the aim of this study was to investigate the effect of various drying temperatures with superheated steam fluidization

technique on the quality of brown parboiled glutinous rice, i.e., head brown parboiled rice yield, color, thermal property and microstructure were determined.

2. Objective

To investigate effect of drying temperature on quality of RD6 variety brown parboiled glutinous rice.

3. Methodology

3.1. Materials

The RD6 paddy (*Oryza sativa L.*) was procured from the Rice Research Institute, Sakon Nakhon province, Thailand. The initial moisture content of provided paddy was 12-13% (d.b.). The paddy was soaked in hot water at a temperature of 70 ± 5 °C in an insulated tank. The ratio between paddy and hot water was 1.0:1.3 and soaking time for 3 h. Then it was drained and tempered for 30 min to created uniform gradient of moisture content. The moisture content of soaked paddy was about 50-52% (d.b.). It was determined according to Soponronnarit & Prachayawarakorn (1994).

3.2. Equipment

A drying system was developed by the Faculty of Engineering, Maharakham University, Thailand. The system consists of a boiler, a pressure regulator, a steam conveying pipeline, a drying chamber, a backward curve fan, an auxiliary heater, a fresh-air supply valve, a steam-flow valve, and control system as shown in Figure 1. This system can be run in the hot air mode or the superheated steam mode by control a fresh-air supply valve and a steam-flow valve.

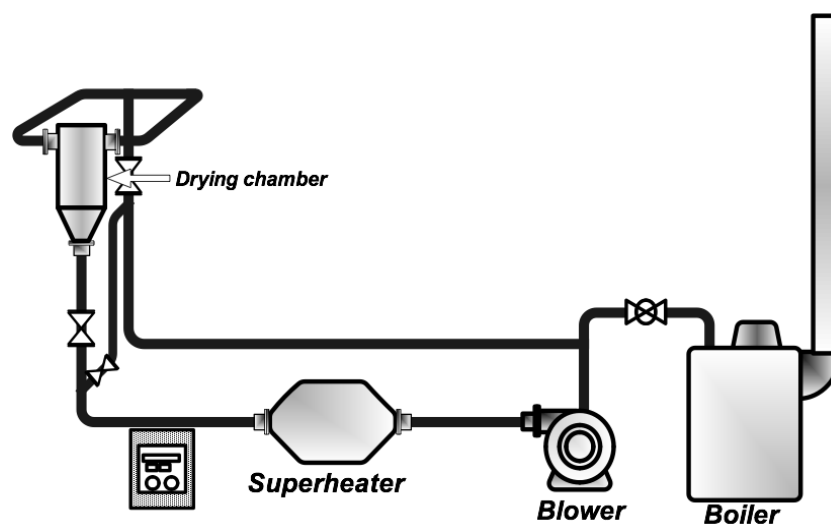


Figure 1. A schematic of the experimental dryer

During the superheated steam drying, saturated steam was produced by the boiler. The steam generator generated the saturated-steam at about 200 kPa (absolute pressure) with the corresponding temperature of 120 °C. Its pressure was reduced nearly to atmospheric pressure when the steam passed through the pressure regulator, a backward curve fan was conveying the drying media through the system. It was driven by a 2 kW, 3 phase electric motor with the media flow rate controlled by a frequency inverter. The media flow rate was measured using pitot static tube together with

multifunction meter (Testo 454). The media was adjusted to the preselected temperature by the auxiliary heaters with a maximum heating capacity of 15 kW that was automatically controlled by proportional-integral detector controller with an accuracy of ± 1 °C before passing through the drying chamber.

3.3. Drying conditions

Samples were dried by a superheated steam fluidized bed dryer with temperatures of 110, 130 and 150 °C at a superficial air velocity of 2.3 m/s until its moisture content reached to around 21-23% (d.b.) after that, the sample was shade-dried until the final moisture content of the sample was around 16% (d.b.). It was kept in a sealed plastic bag at 4-6 °C for 2 weeks before quality analysis.

3.4. Qualities test

3.4.1. Head brown parboiled rice yield

The Paddy was dehusked to obtain brown rice by a bench-top dehusker (Otake, model no. FC2K, Tokyo, Japan). The sample was separated into broken and whole grains by an indent cylinder (Satake, model no. TRG-05A, Hiroshima, Japan). Head brown rice yield was calculated by dividing the mass of whole by an initial paddy mass.

3.4.2. Degree of gelatinization

The thermal properties of glutinous rice flour were investigated by using Differential Scanning Calorimeter (Perkin Elmer, model DSC-7, Norwalk, CT). Flour samples (3 mg) were weighed in balance of resolution 10^{-4} g and placed into an aluminium DSC pan; 10 μ L of distilled water was added, and the pan was hermetically sealed. The samples were left to stand for 1 h at room temperature (25 °C) before DSC scanning. The instrument was calibrated using indium and an empty aluminium pan was used as a reference. All samples were heated from 40 to 100 °C at a scanning rate of 10 °C/min. The major parameters of each DSC profile were described as onset temperature, peak temperature and conclusion temperature. From the DSC profile, the transition enthalpy was determined and the degree of gelatinization (DG) of glutinous rice flour was then calculated by the following equation as studied by Elbert et al., (2001):

$$DG(\%) = \left(1 - \left[\frac{\Delta H}{\Delta H_c} \right] \right) \times 100 \quad (2)$$

Where DG is the degree of gelatinization, ΔH is the transition enthalpy of treated glutinous rice (J/g (dry matter)) and ΔH_c is the transition enthalpy of reference before soaking glutinous rice (J/g dry matter). All experiments were performed in duplicate and the average values were reported.

3.4.3. Microstructure

The microstructure of the reference and dried by superheated steam grains were observed by a scanning electron microscope (SEM; JSM-5600, model no. JSM-5600LV, Tokyo, Japan). The

glutinous rice kernel was broken cross-sectionally in half by hand then, attached to an SEM stub, and coated with gold by a sputter coater. The coated sample was then photographed at an accelerated voltage of 15 kV. The inspected location of the kernel was between the kernel surface and the endosperm center.

3.4.4. Color

The color of sample was measured by a Hunter Lab ColorFlex (Reston, VA), using a D65 light source and a 10° standard observer. The results are expressed as L^* , a^* and b^* values. The L^* value measures lightness and varies from 100 for a perfect white to 0 for black; a^* and b^* when positive measure redness and yellowness, respectively, but negative a measure mean greenness and blueness, respectively. The measurement was performed in triplicate. The total color difference (ΔE^*) from a reference color (L_0^* , a_0^* , and b_0^*) to a target color (L_1^* , a_1^* , and b_1^*) in the CIELAB space is given by:

$$\Delta E^* = \left[(\Delta L^*)^2 + (\Delta a^*)^2 + (\Delta b^*)^2 \right]^{1/2} \quad (3)$$

Where $\Delta L^* = L_1^* - L_0^*$, $\Delta a^* = a_1^* - a_0^*$, $\Delta b^* = b_1^* - b_0^*$

3.4.5. Statistical analysis

The data reported are the average of triplicate observations. The data were subjected to one-way analysis of variance (ANOVA) with a significance level of 5% was done and Duncan's test was applied to determine the differences between the means using SPSS® software.

4. Results and discussion

4.1. Head brown parboiled rice yield

Head brown parboiled rice yield of reference glutinous rice and dried samples at different superheated steam temperatures are shown in table 1. It was found that, the head brown parboiled rice yield of dried samples was significantly higher than that of shade-dried sample. Drying at temperature of 150 °C showed highest yield of 63.4 and significant different from another dried samples. This result indicated that starch gelatinization during high-temperature drying resulted in stronger kernels, which could resist the shear force during the de-husking process (Thuwapanichayanan, 2015).

Table 1. Head brown parboiled rice yield of glutinous rice at different drying conditions.

Drying conditions	Head brown parboiled rice yield (%)
Reference, RD6	46.8 ± 1.4 ^a
SHS 110 °C, RD6	57.3 ± 0.8 ^b
SHS 130 °C, RD6	58.8 ± 0.4 ^b
SHS 150 °C, RD6	63.4 ± 0.8 ^c

RD6, rice department 6; SHS, superheated steam

Different superscripts in the same column mean that the mean values are significantly different at $p \leq 0.05$.

4.2. Color

The reference and dried samples decreased darkness while increase redness and yellowness of RD6 rice kernels are listed in table 2. Color represented in terms of L^* , a^* and b^* values and calculated to ΔE^* . Dried samples showed L^* , a^* and b^* values significantly different from reference sample whereas ΔE^* did not different among dried samples group.

Table 2. Color of brown parboiled glutinous rice at different drying conditions.

Drying conditions	L^*	a^*	b^*	ΔE^*
Reference, RD6	60.0 ± 0.2^a	4.60 ± 0.3^a	22.5 ± 0.4^a	0
SHS 110 °C, RD6	55.1 ± 01^b	5.1 ± 0.1^b	25.2 ± 0.1^b	5.67
SHS 130 °C, RD6	55.0 ± 0.3^b	5.2 ± 0.1^b	24.9 ± 0.4^b	5.62
SHS 150 °C, RD6	55.2 ± 0.9^b	5.3 ± 0.2^b	25.4 ± 0.5^b	5.63

RD6, rice department 6; SHS, superheated steam

Different superscripts in the same column mean that the mean values are significantly different at $p \leq 0.05$.

Color changes during parboiling are caused by diffusion of husk and bran pigments and non-enzymatic Millard browning reaction products. Moreover, rice bran or rice hull pigments can affect parboiled rice color as they leach out during soaking in excess water and diffuse into the endosperm during steaming (Hapsari et al., 2016). In this study, the drying with superheated steam in a fluidized bed dryer can include the steaming and drying step in a parboiling process that can be save time and prevent the yellowing of rice grains, which easily occurs at high temperature (Taechapairoj et al., 2003; Jaiboon et al., 2016).

4.3. Thermal properties

The thermal properties of reference and dried samples are presented in Table 3. The onset temperature (T_o), peak temperature (T_p) and conclusion temperature (T_c) corresponding to gelatinization of flour slightly decreased at drying temperature of 110 °C whereas, higher drying temperature of rice samples cannot detect the transition temperatures. This is due to high drying temperature could destroyed the starch granule in glutinous rice kernels and fully gelatinization occurred when drying at over 130 °C that can be seen in Figure 2.

Table 3. Thermal property of brown parboiled glutinous rice flour at different drying conditions.

Drying conditions	Transition temperature			ΔH (J/g)	DG (%)
	(°C)				
	T_o	T_p	T_c		
Reference, RD6	67.4	74.3	81.1	9.5	0
SHS 110 °C, RD6	67.0	74.2	81.4	2.2	76.8
SHS 130 °C, RD6	-	-	-	-	100
SHS 150 °C, RD6	-	-	-	-	100

4.4. Microstructure

Figure 2 showed microstructures of reference and dried RD6-brown parboiled glutinous rice kernels. The reference sample displayed the starch granule characteristically irregular polygons with diameter in 2-9 micron. After drying at 110 °C, the starch granules of glutinous rice samples were fused to some parts of the kernel that the degree of gelatinization was 76.8% (Table 3.). While drying at temperature of 130 °C and 150 °C displayed fully starch gelatinization, therefore the transition temperature and enthalpy disappeared as well as DG was 100% as can depicted in Table 3 and Figure 2. The fully gelatinization resulted in a smaller fraction of broken glutinous rice kernels that showed in Table 1.

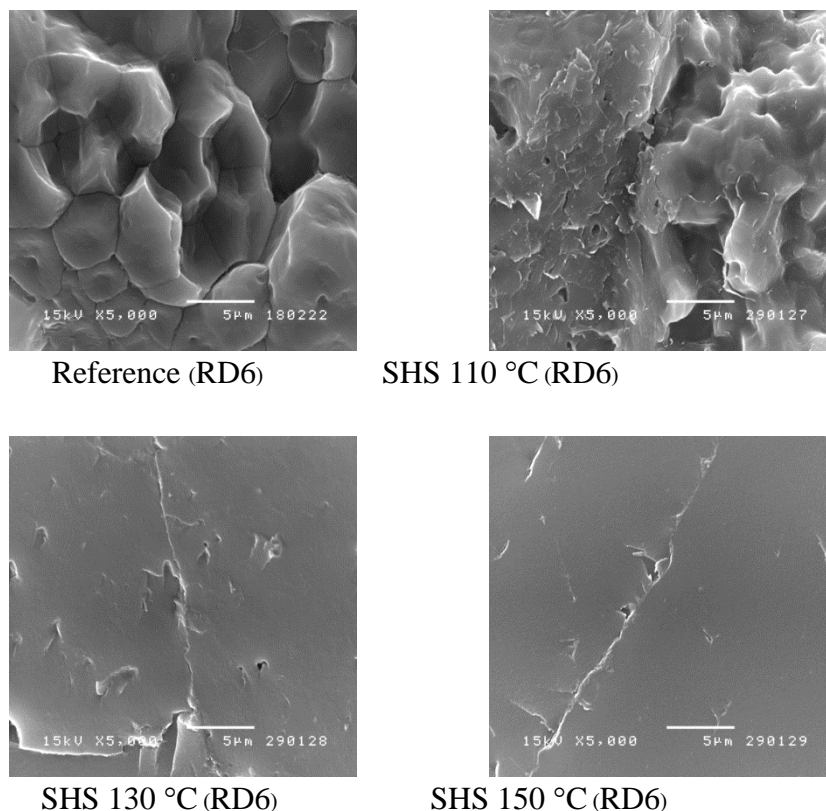


Figure 2. Microstructure of brown parboiled glutinous rice at various drying conditions

5. Conclusions

High temperature of superheated steam in a fluidized bed dryer could be improved head brown parboiled rice yield of RD6 and drying at temperature of 150 °C showed highest yields of 63.4. The L^* -, a^* - and b^* values of dried samples decreased significantly different from reference sample. The T_o -, T_p and T_c decreased at drying temperature of 110 °C whereas drying at temperature over 130 °C of glutinous rice samples displayed fully starch gelatinization as can be seen by SEM. The suitable of superheated steam fluidized bed temperature drying for good qualities of brown parboiled glutinous rice was 150 °C.

Acknowledgements

The authors express their sincere appreciation to the Commission on Higher Education, the Thailand Research Fund, Sakon Nakhon Rajabhat University (No.MRG5680088) for supporting this work financially. Authors also would like to thanks for the Faculty of Engineering, Mahasarakham University that allowed to use a fluidized bed dryer and color equipment, the Faculty of Agriculture Technology, Sakon Nakhon Rajabhat University for using flour grinder; and the Rice Research Institute, Sakon Nakhon province, for test the quality of milling.

References

- Elbert, G., Tolaba, M. P., & Suarez, C. (2001). Effects of drying conditions on head rice yield and browning index of parboiled rice. *Journal of Food Engineering*, 47, 37-41.
- Hapsari, A.H., Kim, S.-J., & Eun, J.-B. (2016). Physical characteristics of parboiled Korean glutinous rice (Olbyeossal) using a modified method. *LWT-Food Science and Technology*, 68, 499-505.
- Jaiboon, P., Poomsa-ad, N., Tungtrakul, P., & Soponronnarit, S. (2016). Improving head rice yield of glutinous rice by novel parboiling process. *Drying Technology*, 34, 1991-1999.
- Soponronnarit, S., & Prachayawarakorn, S. (1994). Optimum strategy for fluidized bed paddy drying. *Drying Technology*, 12(7), 1667-1686.
- Soponronnarit, S., Nathakaranakule, A., Jirajindalert, A., & Taechapiroj, C. (2006). Parboiling brown rice using superheated steam fluidization technique. *Journal of Food Engineering*, 75, 423-432.
- Subba Rao, P. V., & Bhattacharya, K. R. (1966). Effect of parboiling on thiamine content of rice. *Journal of Agriculture and Food Chemistry*, 14(5), 479-482.
- Taechapiroj, C., Dhuchakallaya, I., Soponronnarit, S., Wetchacama, S., & Prachayawarakorn, S. (2003). Superheated steam fluidized bed paddy drying. *Journal of Food Engineering*, 58, 67-73.
- Thuwapanichayanan, R., Yoosabai, U., Jaisut, D., Soponronnarit, S., & Prachayawarakorn, S. (2015). Enhancement of γ -aminobutyric acid in germinated paddy by soaking in combination with anaerobic and fluidized bed heat treatment. *Food and Bioproducts Processing*, 95, 55-62.

The preparation of hybrid material of cobalt complex into mesoporous silica from the rice husk

Pornpan Tana, Netchanok Jansawang, and Patcharaporn Pimchan*

Department of chemistry, faculty of Science and Technology, Rajabhat Maha Sarakham University,
Maha Sarakham, Thailand
E-mail; patcharaporn145@gmail.com

Abstract

A luminescence hybrid material, bis(8-hydroxyquinoline)cobalt(II) (Co(8hq)₂), was incorporated into the mesoporous silica. To study the preparation of mesoporous silica from rice husk and the development of fluorescence efficiency. The mesoporous silica was prepared by swelling-shrinking mechanism which used the sodium silicate from rice husk as the precursor. The hybrid materials were prepared by solid-state reaction at room temperature with two different ways; the first one was the hybrid material processes via the in situ formation of cobalt(II)chloride hexahydrate (CoCl₂·6H₂O) as well as 8hq into the mesoporous silica (MCM) mixed ground (MCM_Co(8hq)₂) and the another one was step by step ground of the mesoporous silica, cobalt(II)chloride hexahydrate and 8hq (MCMCo(II)_8hq). The hybrid materials were characterized by SEM, FT-IR, AAS, as well as PL. The FT-IR spectra showed the 8hq characteristic at 820, 786, 784, and 747 cm⁻¹ that all of the FT-IR spectra shifted to higher frequencies of free 8hq (815, 778, and 739 cm⁻¹), confirming the coordination between cobalt(II) cation and 8-hydroxyquinoline. The excellent photoluminescence of MCM_Co(8hq)₂ revealed at 492 nm and MCMCo(II)_8hq demonstrated blue-shifted peak at 474 nm in this comparison, indicating that the formation of different nanostructures and/or packing of bis (8-hydroxyquinoline)cobalt(II) were formed into the mesoporous silica.

Keywords: Hybrid material; Mesoporous silica; Bis(8-hydroxyquinoline)cobalt(II); Rice husk

1. Introduction

In recent years, the luminescence of metal complexes has attracted significant attention due to the coordination chemistry of inorganic and organic components, electron-transfer substitution of metal or ligand provides an effective means can serve as an efficient approach for the development of electroluminescent materials [Singh et al., 2018, pp. 215-228; Li & Li, 2009, pp. 128-132]. As a common ligand in metal complexes are widely used aromatic rings such as 8-hydroxyquinoline, pyridine, and benzoic acid that have conjugate double-bonds as well as stronger absorption than metal ions in the ultraviolet (UV) region [Li & Li, 2009, pp. 128-132; Świdorski et al., 2018, pp. 97-109; He et al., 2018, pp. 15-21]. Among these ligands, 8-hydroxyquinoline (8hq) has attracted much attention because of a variety of one-dimensional (1D) nanostructures of the metal-8-hydroxyquinoline complexes have been obtained such as nanorods, nanowire, and nanoribbon that nanostructures of the complexes are also tunable electronic and optical properties [Li et al., 2012, pp. 293-302; Tsuboi et al., 2012, pp. 524-528; Behzad et al., 2014, pp. 219-228; Pimchan et al., 2014, pp. 310-316].

The metal complexes illustrate potential applications in organic light-emitting devices (OLED) and efficient light-conversion molecular devices. However, their practical application in many fields

limited by the low light and thermal stability and poor mechanical strength of metal complexes [He et al., 2018, pp.15-21; Pimchan et al., 2014, pp. 310-316]. A wide variety of metal chelates were prepared base-on the nanospace of mesoporous silica, boron nitrite porous, and inter layer as an appropriate host solid that an effective way to solve and protect the metal complexes [He et al., 2018, pp.15-21; Pimchan et al., 2014, pp. 310-316; Sábio et al., 2016, pp. 1-5]. These hybrid materials also have been reported to have many possible applications as photocatalyst and so on [Patriarca et al., 2019, pp. 133-141; Maučec et al., 2018, pp. 32-41].

As an emerging host, mesoporous silica has attracted much research because of the possibility of tailoring the pore structure, framework composition, and morphologies over a wide range [Lui et al., 2015, pp. 280-282; Sohmiya et al., 2015, pp. 1-17; Kazuyuki et al., 2011, pp. 24-26]. The porous surface of mesoporous silica could be modified by a swelling-shrinking mechanism with proper organic functional groups and provide accessibility for anchoring other substances. This technique offers the advantages of high control of the hybrid chemical composition at low temperature and large-area processing [Sohmiya et al., 2015, pp. 1-17; Kazuyuki et al., 2011, pp. 24-26]. Accordingly, host-guest complexes have been synthesized from mesoporous silica for such purposes as sensors, adsorption, and optical applications [Zhao et al., 2017, pp. 803-811; Kudo et al., 2017, pp. 189-194; Li et al., 2017, pp. 459-465]. Moreover, the immobilization of luminary on rigid support is a very important way to prepare new solid luminescent materials [Li et al., 2017, pp. 459-465; Zhang et al., 2018, pp. 220-225]. Recently, the preparation of metal complexes base-on mesoporous silica to improve their performances have attracted increased attention. For example, the aluminum quinolate complex was attached covalently to this functionalized SBA-15 by using coordinating ability of bifunctional precursor (Si-SQ) on the surface of mesoporous material and the observed blue-shift in the emission spectra of the prepared Al(8hq)₃ functionalized material is attributed to the improved molecular interactions of grafted Al(8hq)₃ complexes on the surface and electron withdrawing effect of sulfonamide group that covalently linked to the 8hq in grafted precursor (Si-SQ) [Badiei et al. 2011, pp. 63-69]. The adsorption of tris(2,2'-bipyridine)ruthenium(II) ([Ru(bpy)₃]²⁺) onto aluminum containing mesoporous silicas was conducted and the photoluminescence of the products was examined as a function of the loaded [Ru(bpy)₃]²⁺ amounts. The result suggests that the pore size and the interactions between [Ru(bpy)₃]²⁺ and the pore surface affects the efficiency; the larger pore size and the weaker interactions between and the pore surface results in the higher self-quenching efficiency [Sohmiya and Ogawa, 2011, pp. 363-370]. Thus, the luminescence properties and stabilities of mesoporous silica-based hybrids can be meticulously designed and tuned.

Solid-state reaction is a facile and feasible method for preparing nanomaterial and has achieved some success in fabricating complex materials [Rahman, 2016, pp. 1-13]. It showed that the promising luminescent properties can be obtained by linking the metal complexes to the mesoporous materials [Ma et al., 2019, pp. 7905-7914; Vibulyaseak et al., 2019, pp. 162-172]. Therefore, the synthesis of metal complexes in mesoporous silica via solid-state may be predominant features such as high color quality, wide-viewing angle, wide operating temperature range, and fast response.

In this paper, we reported the preparation of the cobalt(II) complex of 8-hydroxyquinoline (8hq) into mesoporous silica with different methods. The mesoporous silica was prepared from rice husk which was calcined in air. The cobalt(II) complexes in mesoporous silica were prepared by solid-state between mesoporous silica and Co(II):8hq. The different methods may enhance the photoluminescence efficiency of Co(8hq)₂ complex by reducing the concentration quenching and self-

absorption. The role of preparation processes may affect the molecular structure and/or packing, as well as optical properties of Co(8hq)₂ complex into the porous space.

2. Objectives

To synthesize the mesoporous silica from rice husk and preparation of the hybrid materials of cobalt(II) complex into mesoporous silica to improve the luminescence efficiency for optical applications.

3. Methodology (Materials and Methods)

3.1 Materials

Rice husk (RH) used in this research were obtained from the rice milling process in Thailand. Cetyltrimethylammonium (CTA) bromide (C₁₉H₄₂NBr, CTAB) was supplied from Sigma-Aldrich Co., Ltd. Cobalt(II)chloride hexahydrate (CoCl₂·6H₂O) was obtained from Carlo Erba Reagenti SpA. 8-Hydroxyquinoline (C₉H₇NO, 8hq) was supplied from Junsei Chemical Co., Ltd., and the reagents were analytical grade and were used without further purification.

3.2 Synthesis

3.2.1 Synthesis mesoporous silica (MCM)

In the beginning, the sodium silicate preparation was synthesized by silicon dioxide (SiO₂) from RH. The raw RH was boiled in 1 M HCl solution for 4 h, washed with distilled water, and then dried at 100 °C for 24 h. The dried RH was calcined in a muffle furnace, which was preheated to 900 °C, for 8 h [Bakar et al., 2016, pp. 189-195]. Then, 100 mL of 2 M NaOH and 5 g of SiO₂ were stirring at 80-100 °C for 3 h. After the reaction period and cooling to room temperature the sodium silicate solution (Na₂Si₃O₇) formed was filtered and stored in a sealed polypropylene flask at room temperature [Pimprom et al., 2015, pp. 156-166]. Finally, the mesoporous silica was synthesized by the amount 0.8448 g of cetyltrimethylammonium bromide (C₁₉H₄₂NBr, CTAB), 70.8 mL of deionized water, 800 mL of 99% methanol, and 29.2 mL of 28% aqueous ammonia were mixed and the mixture was stirred for 3 h at 20 °C. The 1.48 mL Na₂Si₃O₇ was added to the solution and then the suspension was aged at 4 °C for another 24 h. The solid particles were collected by evaporation. The product was calcined in air at 660 °C for 10 h to form a porous silica shell. [Kazuyuki et al., 2011, pp. 24-26].

3.2.2 Preparation of hybrid material

The ligand cobalt complex-mesoporous silica hybrids were obtained by solid-state reaction at room temperature [Pimchan et al., 2014, pp. 310-316]. The amount of Co(II) cation determined by atomic absorption spectrometry (AAS) was 221.33 mg/L. The hybrids were obtained by two different processes as follows; the first method 0.1 g of mesoporous silica (MCM), 0.0305 g of CoCl₂·6H₂O, and 0.0648 g of 8hq at the molar ratio of 1:2 for Co(II) to 8hq ligand were mixed ground in a agate mortar at room temperature for 10-15 min (MCM_Co(8hq)₂) and the another method was ground step by step, 0.1 g of mesoporous silica with 0.0305 g of CoCl₂·6H₂O were mixed ground in a agate mortar at room temperature for 10-15 min then add 0.0648 g of 8hq (the molar ratio 1:2 for Co(II):8hq

ligand) mixed ground in a agate mortar at room temperature for 10-15 min respectively (MCMCo(II)_8hq).

3.3 Characterization

Material characterizations: A HITACHI TM3000 scanning electron microscope (SEM) was used for the identification of morphology and size of nanoparticles. Fourier-transform infrared spectroscopy (FTIR) was measured on a Spectrum One spectrometer over the spectral region of 600-4000 cm^{-1} by Bruker TENSOR27 confirmed the structural properties. The metal components were confirmed by atomic absorption spectrometry (AAS) was taken on PinAAcle 900F Atomic Absorption Spectrometer. The optical properties were studied by the photoluminescence spectroscopy (PL) was carried out using Spectrofluorometer FluoroMax 4 at the condition of a working voltage of 400 V and a slit width of 0.5 nm by the excitation of Xenon lamp at 320 nm.

4. Results and discussion

4.1 Mesoporous silica

The mesoporous silica was confirming the phase purity and identification through the SEM (Fig.1) and FT-IR (Fig.2). From the image (Fig.1) illustrated that the prominent morphology of particles is a mostly short rod-like cylinder and homogeneous aggregation of the particles is also observed. The diameters of particles approximately 1 μm and length up approximately 4 μm which is typically the morphology for mesoporous materials [Puratane & Amnuaypanich, 2018, pp. 496-505; Barczak, 2018, pp. 291-300; Cong, V. T. et al., 2018, pp. 881-892] and Figure 1b and 1c showed the morphology after loading cobalt(II) complex into mesoporous silica from different route.

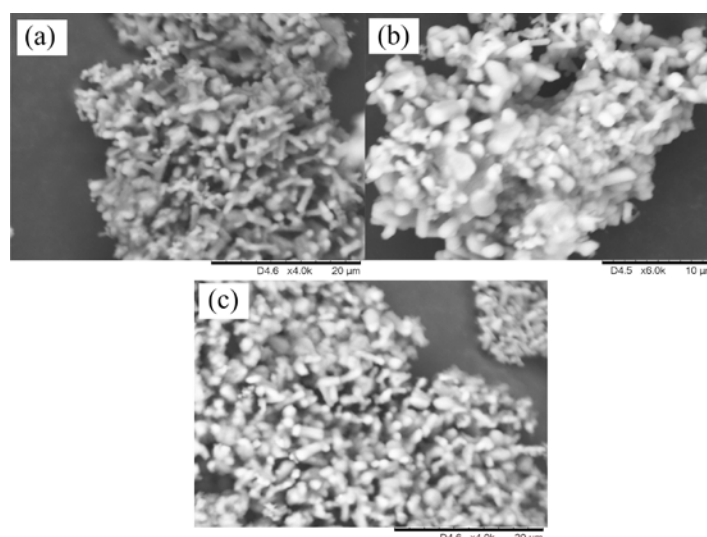


Figure 1. The SEM images of MCM (a) MCM_Co(8hq)₂ (b) and MCMCo(II)_8hq (c)

The FT-IR spectrums demonstrate organic functional incorporation in silica framework (Fig.2) that the broad absorption band around 1024 cm^{-1} corresponding absorption with a shoulder of Si-O-Si asymmetric stretching [Ogata, 2014, pp. 705-712], 966 cm^{-1} shown stretching vibrations Si-OH [Yang et al., 2009, pp. 178-184; Yang et al., 2007, pp. 1-10; La-Salvia et al., 2017, pp. 1461-1469; Ogata, 2014, pp. 705-712]. In addition, the absorption bands at 710 and 876 cm^{-1} also corresponding O_nSiH_x

deformation [Ogata, 2014, pp. 705-712], may due to a little CTAB still in mesoporous silica, which shows all the absorption band substantiate formation of mesoporous silica. The absorption band 2975 and 1428 cm^{-1} which are assigned to C-H vibrations of $-\text{CH}_3$ and $-\text{CH}_2-$ carbon chain, which is due to alkylammonium vibrations of the surfactant [Jiang et al., 2014, pp. 2454-2462; Jabariyan & Zanjanchi, 2012, pp. 1087-1093]. This shows that still the template molecules have been unremoved out of the MCM.

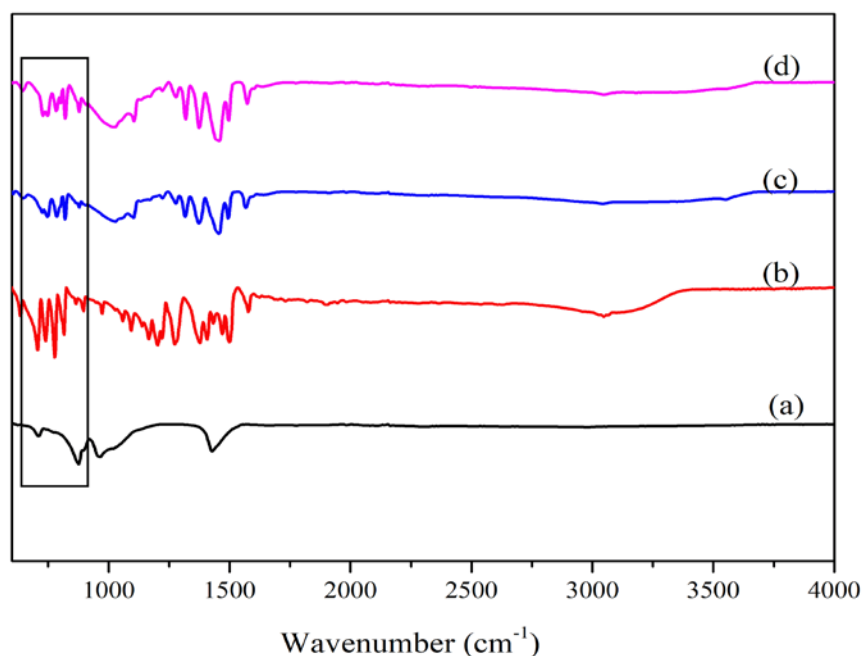


Figure 2. The FT-IR spectra of MCM (a), 8hq (b), MCM_Co(8hq)₂ (c) and MCMCo(II)_8hq (d)

4.2 Bis(8-hydroxyquinoline)cobalt(II) into mesoporous silica

The preparation of the hybrid material of the cobalt(II) complex into mesoporous silica from the rice husk was confirmed by FT-IR and PL spectroscopies. The vibrations of CH_2 stretching as well as C-H vibration modes due to the characteristics of 8-hydroxyquinoline in $\text{Co}(8\text{hq})_2$ of the products are summarized in Figure 2. The absorption bands due to the C-H out of plane bending modes of the neat 8-hydroxyquinoline were observed at 815, 778, and 739 cm^{-1} , that all of the FT-IR spectra of the hybrids were shifted to higher frequencies were 820, 784 and 747 cm^{-1} for MCM_Co(8hq)₂ as well as the frequencies of MCMCo(II)_8hq at 820, 786 and 747 cm^{-1} , confirming the coordination between cobalt (II) cation and 8-hydroxyquinoline [Pimchan et al., 2014, pp. 310-316]. The stretching vibrations of metal oxide for tetrahedrally coordinated Co(II) ions of both products were observed at 645 and 647 cm^{-1} respectively, indicating the formation of Co-O bonding in hybrid material [Li & Li, 2009, pp. 128-132; Saurav et al., 2015, pp. 21471-21479], supporting the interaction between hydroxyl group and cobalt(II) cation. A broad infrared absorption band in the region from 3000 to 3400 cm^{-1} identified the water of hydration in the samples [Li & Li, 2009, pp. 128-132], which was consistent with the photoluminescence spectra.

Table 1. Color and Photoluminescence band of hybrid materials

Substances	color	λ_{em}
------------	-------	-----------------------

		(nm)
Co(8hq) ₂	Dark green	468
MCM_Co(8hq) ₂	Orange green	492
MCMCo(II)_8hq	Light green	474

Photoluminescence was a very important characteristic for the hybrid materials. All summaries were shown in Table 1. The luminescence spectrum of Co(8hq)₂ complex showed the emission band due to a π to π^* charge transfer from the electron-rich phenoxide ring to the electron-deficient pyridyl ring of the ligand at 468 nm [Li & Li, 2009, pp. 128-132]. When the product from a mixed ground method, the luminescence maxima was observed at 492 nm for MCM_Co(8hq)₂, as well as the color appearance was a dark green-orange (Fig.4b). In another route, the intense emission band of MCMCo(II)_8hq hybrids revealed at 474 nm and the feature observe as light-green (Fig.4c). The PL spectra was red-shifted in comparison with its precursor of the luminescence maxima observed for MCM_Co(8hq)₂ (492 nm), and MCMCo(II)_8hq (474 nm) reflected the change in HOMO/LUMO level and/or bandgap energy of the interaction complexes contributes to the broad blue PL [Pimchan et al., 2014, pp. 310-316], implying that the cobalt complex with different nanostructures and packing formed and /or changes the coordination number of cobalt(II) complexes in the mesoporous silica spaces. For example, cobalt(II)-bis(8-hydroxyquinoline) nanosheets demonstrated the red-shift and the fluorescence quenching when the complex formation between p-nitroaniline molecules [Li & Li, 2009, pp. 128-132]. The emission peak of CA_[n]@SiO₂@CdTe nanoparticles (NPs) was red-shifted in comparison with its precursor SiO₂@CdTe NPs, which may be attributed to the increased size of NPs [Li & Qu, 2007, pp. 3536-3544], while zinc(II)-8-hydroxyquinoline complex in channels of mesoporous silica nanoparticles (MSN) which functionalized with or without mercapto groups, the PL emission peaks of these samples are red-shifted from 500 nm for MSN-Zn(8hq) to 511 nm for MSN-SH₂-Zn(8hq), the optical properties of these samples are dependent on the interior circumstances and the concentration of mercapto groups in channels of MSNs [Li et al., 2012, pp. 293-302]. In addition, the reported that the emission peak maxima of nanoporous silica-Al(8hq)₃, nanoporous silica-Al(8hq)₂ and Al(8hq)₃ are 505, 497, and 510 nm respectively. The greater blue-shift observed in the emission spectra of nanoporous silica-Al(8hq)₂ can be attributed to changing the coordination sphere of Al ions in nanoporous silica-Al(8hq)₂ in comparison with nanoporous silica-Al(8hq)₃ [Badiei & Goldooz, 2012,

pp. 151-159]. From these observations, the formation of cobalt complex into mesoporous silica were proved.

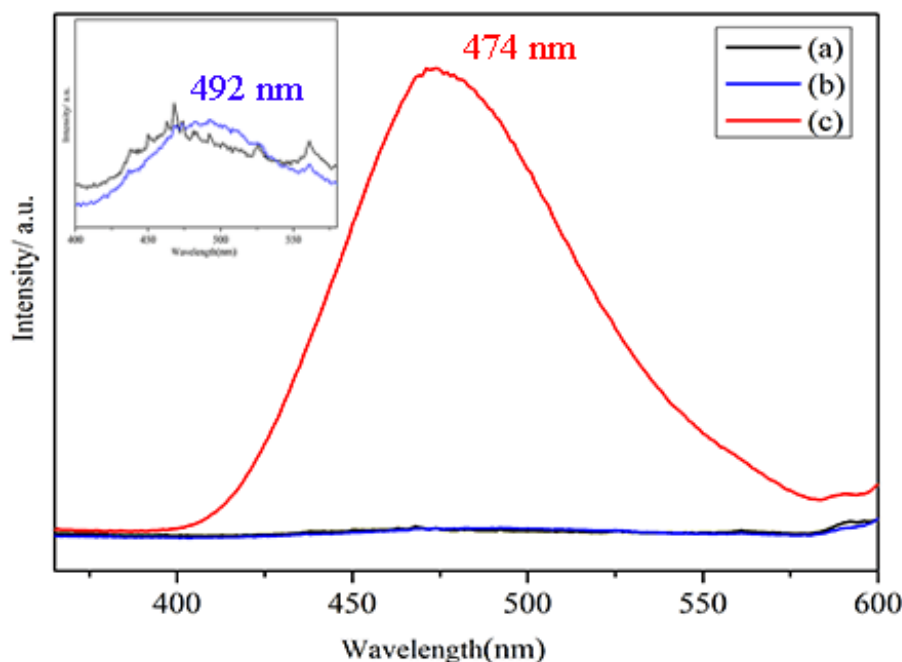


Figure 3. Photoluminescence spectra of Co(8hq)₂ (a), MCM_Co(8hq)₂ (b) and MCMCo(II)_8hq (c)

In comparison of the PL efficiencies between MCM_Co(8hq)₂ and MCMCo(II)_8hq in Figure 3 demonstrate excellence luminescence intensity of MCMCo(II)_8hq, while MCM_Co(8hq)₂ no significant change from Co(8hq)₂ complex, indicating the sequenced ground direction can efficiency improved the luminescence intensity of metal complex [Pimchan et al., 2014, pp. 310-316]. It was illustrated that the cobalt complex of 8-hydroxyquinoline was successfully prepared in mesoporous silica by solid-state reaction at room temperature and the immobilized complexes exhibited excellent photoluminescence properties. Moreover, the method via step by step ground affected the molecular structure and/or packing of the complexes, which are thought to be correlated with the increased luminescence efficiencies. From these observations, the present hybrids showed the outstanding photoluminescence efficiencies as well as the shift of luminescence maxima due to the energy level changes [Pimchan et al., 2014, pp. 310-316].

Finally, the present systems are the preparation of mesoporous silica, which conventional method as well as advantage rice husk. Applications such as the host material, absorbent, and insulator as well as the cobalt complexes composition controlled by the mesoporous silica host. Suggestions for the incorporation of the other ligand metal complexes with different metal ions, ligands and/or other host structures are foreshadowing because of the ease of operation, the enhancement of luminescence efficiencies and the stability of the incorporated complexes.

5. Conclusions

The mesoporous silica which synthesized by swelling-shrinking mechanism from rice husk was successfully prepared. The hybrids material of bis(8-hydroxyquinoline)cobalt(II) complex were prepared by solid-state reaction between mesoporous silica, cobalt ion, and 8-hydroxyquinoline at room temperature. The emission maxima was 492 nm for MCM_Co(8hq)₂ hybrid and 474 nm for

MCMCo(II)_8hq hybrid. The photoluminescence efficiency of MCMCo(II)_8hq hybrid was higher than MCM_Co(8hq)₂, indicating that the MCMCo(II)_8hq hybrid can be an excellent optical properties material. The difference in the microstructure and/or packing of the cobalt(II) complex into mesoporous silica could be adjusted by changing the loading/packing method. The solid-state reaction is applicable to prepare various complexes in the porous hosts.



Figure 4. Colors of Co(8hq)₂ (a), MCM_Co(8hq)₂ (b) and MCMCo(II)_8hq (c)

References

- Singh, D., Nishal, V., Bhagwan, S., Saini, R. K., & Singh, I. (2018). Electroluminescent materials: Metal complexes of 8-hydroxyquinoline-A review. *Materials & Design*, 156, 215-228.
- Li, H., & Li, Y. (2009). Synthesis of highly luminescent cobalt(ii)-bis(8-hydroxyquinoline) nanosheets as isomeric aromatic amine probes. *Nanoscale*, 1(1), 128-132.
- Świdorski, G., Kalinowska, M., Wilczewska, A. Z., Malejko, J., & Lewandowski, W. (2018). Lanthanide complexes with pyridinecarboxylic acids-Spectroscopic and thermal studies. *Polyhedron*, 150, 97-109.
- He, X., Yu, C., Lin, J., Zhang, X., Li, Q., Fang, Y., Liu, Z., Li, L., H, Yang., & Tang, C. (2018). Porous boron nitride/rare earth complex hybrids with multicolor tunable photoluminescence. *Journal of Alloys and Compounds*, 768, 15-21.
- Li, H., Fu, Y., Zhang, L., Liu, X., Qu, Y., Xu, S., & Lü, C. (2012). In situ route to novel fluorescent mesoporous silica nanoparticles with 8-hydroxyquinolate zinc complexes and their biomedical applications. *Microporous and Mesoporous Materials*, 151, 293-302.
- Tsuboi, T., Nakai, Y., & Torii, Y. (2012). Photoluminescence of bis(8-hydroxyquinoline) zinc (Znq₂) and magnesium (Mgq₂). *Open Physics*, 10(2), 524-528.
- Behzad, S. K., Najafi, E., Amini, M. M., Janghour, M., Mohajerani, E., & Ng, S. W. (2014). Yellow-green electroluminescence of samarium complexes of 8-hydroxyquinoline. *Journal of Luminescence*, 156, 219-228.
- Pimchan, P., Khaorapong, N., Sohmiya, M., & Ogawa, M. (2014). In situ complexation of 8-hydroxyquinoline and 4,4'-bipyridine with zinc(II) in the interlayer space of montmorillonite. *Applied Clay Science*, 95, 310-316.
- Sábio, R. M., Gressier, M., Caiut, J. M. A., Menu, M.-J., & Ribeiro, S. J. L. (2016). Luminescent multifunctional hybrids obtained by grafting of ruthenium complexes on mesoporous silica. *Materials Letters*, 174, 1-5.
- Patriarca, M., Daier, V., Camí, G., Pellegrini, N., Rivière, E., Hureau, C., & Signorella, S. (2019). Biomimetic Cu, Zn and Cu₂ complexes inserted in mesoporous silica as catalysts for superoxide dismutation. *Microporous and Mesoporous Materials*, 279, 133-141.

- Maučec, D., Šuligoj, A., Ristić, A., Dražić, G., Pintar, A., & Tušar, N. N. (2018). Titania versus zinc oxide nanoparticles on mesoporous silica supports as photocatalysts for removal of dyes from wastewater at neutral pH. *Catalysis Today*, 310, 32-41.
- Liu, Y., Wang, Z., Zeng, H., Chen, C., Liu, J., Sun, L., & Wang, W. (2015). Photoluminescent mesoporous carbon-doped silica from rice husks. *Materials Letters*, 142, 280-282.
- Sohmiya, M., Saito, K., & Ogawa, M. (2015). Host-guest chemistry of mesoporous silicas: precise design of location, density and orientation of molecular guests in mesopores. *Science and Technology of Advanced Materials*, 16(5), 1-17.
- Nakamura, K. J., Ide, Y., & Ogawa, M. (2011). Molecular recognitive photocatalytic decomposition on mesoporous silica coated TiO₂ particle. *Materials Letters*, 65(1), 24-26.
- Zhao, H., Zhang, T., Qi, R., Dai, J., Liu, S., Fei, T., & Lu, G. (2017). Organic-inorganic hybrid materials based on mesoporous silica derivatives for humidity sensing. *Sensors and Actuators B: Chemical*, 248, 803-811.
- Kudo, T., Ito, T., & Kim, S.-Y. (2017). Adsorption Behavior of Sr(II) from High-level Liquid Waste using Crown Ether with Ionic Liquid Impregnated Silica Adsorbent. *Energy Procedia*, 131, 189-194.
- Li, F., Li, H., & Cui, T. (2017). One-step synthesis of solid state luminescent carbon-based silica nanohybrids for imaging of latent fingerprints. *Optical Materials*, 73, 459-465.
- Zhang, X., Tang, J., Li, H., Wang, Y., Wang, X., Wang, Y., Huang, L., & Belfiore, L. A. (2018). Red light emitting nano-PVP fibers that hybrid with Ag@SiO₂@Eu(tta)₃phen-NPs by electrostatic spinning method. *Optical Materials*, 78, 220-225.
- Badie, A., Goldooz, H., Ziarani, G. M., & Abbasi, A. (2011). One pot synthesis of functionalized SBA-15 by using an 8-hydroxyquinoline-5-sulfonamide-modified organosilane as precursor. *Journal of Colloid and Interface Science*, 357(1), 63-69.
- Sohmiya, M., & Ogawa, M. (2011). Controlled spatial distribution of tris(2,2'-bipyridine)ruthenium cation ([Ru(bpy)₃]²⁺) in aluminum containing mesoporous silicas. *Microporous and Mesoporous Materials*, 142(1), 363-370.
- Rahman, A. Z. M. S. (2016). Solid State Luminescent Materials: Applications. *Reference Module in Materials Science and Materials Engineering*.
- Ma, J. S., Lin, L. Y., & Chen Y. S. (2019). Facile solid-state synthesis for producing molybdenum and tungsten co-doped monoclinic BiVO₄ as the photocatalyst for photoelectrochemical water oxidation. *International Journal of Hydrogen Energy*, 44(16), 7905-7914.
- Vibulyaseak, K. (Guy), Depracha, S. (Benz), & Ogawa, M. (2018). Immobilization of titanium dioxide in mesoporous silicas; structural design and characterization. *Solid State Chemistry*, 270, 162-172.
- Bakar, R. A., Yahya R., & Dan, S. N. (2016). Production of high purity amorphous silica from rice husk. *Procedia Chemistry*, 19, 189-195.
- Pimprom, S., Sriboonkham, K., Dittanet, P., Föttinger, K., Rupprechter, G., & Kongkachuichay, P. (2015). Synthesis of copper-nickel/SBA-15 from rice husk ash catalyst for dimethyl carbonate production from methanol and carbon dioxide. *Journal of Industrial and Engineering Chemistry*, 31, 156-166.
- Puratane, C. & Amnuaypanich, S. (2018). Mesoporous silica particles (MSPs) prepared by diol-functionalized natural rubber (ENR50-diol) and cationic surfactant (CTAB) dual templates, *KKU Sci. J.* 46(3), 496-505.

- Barczak, M. (2018). Functionalization of mesoporous silica surface with carboxylic groups by Meldrum's acid and its application for sorption of proteins. *Journal of Porous Materials*, 26(1), 291-300.
- Cong, V. T., Gaus, K., Tilley, R. D., & Gooding, J. J. (2018). Rod-shaped mesoporous silica nanoparticles for nanomedicine: recent progress and perspectives. *Expert Opinion on Drug Delivery*, 15(9), 881-892.
- Ogata, Y. H. (2014). Characterization of Porous Silicon by Infrared Spectroscopy. *Handbook of Porous Silicon*, 705-712.
- Yang, J., Chen, J., & Song, J. (2009). Studies of the surface wettability and hydrothermal stability of methyl-modified silica films by FT-IR and Raman spectra. *Vibrational Spectroscopy*, 50(2), 178-184.
- Yang, P., Quan, Z., Lu, L., Huang, S., Lin, J., & Fu, H. (2007). MCM-41 functionalized with YVO₄:Eu³⁺: a novel drug delivery system. *Nanotechnology*, 18(23), 1-10.
- La-Salvia, N., Lovón-Quintana, J. J., Lovón, A. S. P., & Valença, G. P. (2017). Influence of Aluminum Addition in the Framework of MCM-41 Mesoporous Molecular Sieve Synthesized by Non-Hydrothermal Method in an Alkali-Free System. *Materials Research*, 20(6), 1461-1469.
- Li, K.-M., Jiang, J.-G., Tian, S.-C., Chen, X.-J., & Yan, F. (2014). Influence of Silica Types on Synthesis and Performance of Amine-Silica Hybrid Materials Used for CO₂ Capture. *Physical Chemistry C*, 118(5), 2454-2462.
- Jabariyan, S., & Zanjanchi, M. A. (2012). A simple and fast sonication procedure to remove surfactant templates from mesoporous MCM-41. *Ultrasonics Sonochemistry*, 19(5), 1087-1093.
- Patel, V. K., Saurav, J. R., Gangopadhyay, K., Gangopadhyay, S., & Bhattacharya, S. (2015). Combustion characterization and modeling of novel nanoenergetic composites of Co₃O₄/nAl. *RSC Advances*, 5(28), 21471-21479.
- Li, H., & Qu, F. (2007). Selective inclusion of polycyclic aromatic hydrocarbons (PAHs) on calixarene coated silica nanospheres englobed with CdTe nanocrystals. *Journal of Materials Chemistry*, 17(33), 3536-3544.
- Badie, A., & Goldoos, H. (2012). A Simple Method for Preparation of Fluorescent Nanostructure Silica with Hexagonal Array. *International Journal of Modern Physics: Conference Series*, 05, 151-159.

Effect of PEG-based triazolyl substituents of copper-catalyzed aerobic alcohol oxidation

Chomtisa Borsap^{1,a,*} Vasut Nakarajouyphon^{1,b} Preeyanuch Sangtrirutnugul^{1,c}

¹Department of Chemistry and Center of Excellence for Innovation in Chemistry (PERCH-CIC), Faculty of Science, Mahidol University, RamaVI Rd, Bangkok, Thailand

E-mail; ^achomtisa.bor@gmail.com, ^bvasut.nak@gmail.com, ^cpreeyanuch.san@mahidol.ac.th

Abstract

Oxidation of alcohols to aldehydes is one of the most fundamental and important organic reactions with wide industrial applications. However, alcohol oxidation reactions usually require toxic oxidizing agents such as NaOCl, HClO₄, and H₂O₂ under harsh conditions. Recently, Cu-catalyzed aerobic alcohol oxidation has attracted a considerable interest due to its high catalytic efficiency under mild reaction conditions. To further reduce environmental impacts, we wish to develop copper catalyst systems that are water soluble and recyclable. In this work, a series of bis(amine-triazole) ligands featuring *n*-hexyl and water-soluble poly(ethylene glycol) (PEG) substituents with different chain lengths (PEG200 and mPEG550) were prepared and used as Cu catalyst supports. Catalytic studies toward aerobic oxidation of benzyl alcohol and its derivatives in H₂O as well as CH₃CN were carried out using the catalyst system [Cu]/ligand/TEMPO/base (TEMPO = 2,2,6,6-tetramethylpiperidiny-1-oxyl). In particular, the effects of triazolyl substituent's chain length on catalytic oxidation activities were examined.

Keywords: PEG; amine-triazole ligand; alcohol oxidation; copper catalyst; water

1. Introduction

The selective alcohol oxidation to the corresponding aldehyde is among the most valuable organic reactions with a wide range of applications in various fields such as agricultural, perfume and pharmaceutical.¹ Traditional alcohol oxidation methods are usually achieved *via* the use of a stoichiometric amount of toxic oxidizing agents, performed under harsh conditions.^{2,3} To develop more benign and environmentally friendly oxidation processes, the use of ligand-stabilized copper catalysts has emerged as a promising alternative because only low catalyst loadings and readily available O₂ in air were required.⁴ In particular, we are interested in employing 1,4-disubstituted-1,2,3-triazole compounds as stabilizing ligands due to their ease of synthesis and substituent modification through Cu-catalyzed azide-alkyne cycloaddition (CuAAC or “click” reaction).^{5,6} Recently, our research group has shown that copper(II) catalysts supported by pyridine-triazole ligands exhibited high activity toward aerobic alcohol oxidation of benzyl alcohol and its derivatives.⁷ Along the same line, copper(II) complexes of benzimidazole-triazole ligands showed high catalytic performances for aerobic oxidation of activated 1° alcohols including benzyl alcohol, cinnamyl alcohol, 2-thiophenemethanol and 1-hexanol.⁸ In another example, Ding *et al.* demonstrated that the pyridine-triazole ligand-functionalized SBA-15 was an efficient stabilizer for palladium nanoparticles, leading to highly active catalysts for alcohol oxidation.⁹

Most of the metal-promoted aerobic alcohol oxidation reactions require organic solvents as reaction medium to achieve high product yields. However, organic solvents are generally flammable, toxic, and harmful to human and environment. Based on these disadvantages, water which is non-flammable, benign, and safer to the environment is the ideal solvent for chemical reactions.¹⁰ To improve the solubility of catalysts in water, water-soluble linear hydrophilic polymer such as poly(ethylene glycol) or PEG has gained considerable attentions as ligands for catalysis due to its cheap, non-toxic, biocompatible, and facile modifications of PEG end-group. In addition, metal catalysts supported by PEG-functionalized ligands are easily recovered from catalytic reactions *via* separation or precipitation.¹¹⁻¹³ Previously, Sun *et al.* used pyridine-triazole ligand-functionalized by PEG as a catalyst support for copper-mediated alcohol oxidation in water. It was found that the copper-PEG catalyst system was highly active with excellent reusability.¹⁴

To further develop water-soluble ligands for copper-catalyzed aerobic alcohol oxidation, we prepared a series of bis(amine-triazole) ligands functionalized with *n*-hexyl and water-soluble PEG substituents with different chain lengths: PEG200 (average M_w ~ 200) and mPEG550 (average M_w ~ 550). Catalytic activities of the resulting copper catalysts supported by these bis(amine-triazole) ligands toward aerobic alcohol oxidation were evaluated and compared. In particular, the effect of PEG chain lengths on the catalytic efficiency was also determined.

2. Objectives

In this work, *n*-hexyl- and two water-soluble, PEG-functionalized bis(amine-triazole) ligands: PEG200 (average M_w ~ 200) and mPEG550 (average M_w ~ 550) were synthesized via Cu-catalyzed azide-alkyne cycloaddition (CuAAC) or “click” reaction and used to stabilize copper complexes. The corresponding copper complexes were characterized and investigated as catalysts for aerobic alcohol oxidation. Accordingly, the objectives of this research are as follows:

1. To synthesize and characterize *n*-hexyl-, PEG200- and mPEG550-functionalized bis(amine-triazole) ligands.
2. To prepare and characterize copper complexes supported by hexyl-, PEG200 and mPEG550-functionalized bis(amine-triazole) ligands.
3. To evaluate the effect of PEG chain lengths on catalytic activity and reusability of the corresponding copper complexes catalysts toward aerobic alcohol oxidation under mild conditions.

3. Methodology (Materials and Methods)

3.1 Materials

All chemicals including *p*-phenylenediamine (Aldrich), Boc anhydride (Boc₂O; TCI), propargyl bromide (80 wt% in toluene) (TCI), NaH (TCI), 1-bromohexane (TCI), tetraethylene glycol (TCI), poly(ethylene glycol) methyl ether average M_n ~ 550 (TCI), NaN₃ (TCI), *p*-toluenesulfonyl chloride (TCI), cyanuric chloride (TCI), NaOH (Carlo Erbo), CuSO₄·5H₂O (TCI), sodium ascorbate (Aldrich),

Ethylenediaminetetraacetic acid (EDTA; TCI), Na₂CO₃ (TCI), 30% NH₄OH (Panreac), CF₃COOH (TCI) and 33% HCl (RCI Labscan) were of reagent grade and used as received without further purification. *n*-C₆H₁₃N₃¹⁵, PEG200N₃¹⁶, mPEG550N₃^{17,18}, and tris(benzyltriaazolylmethyl)amine (TBTA)¹⁹ were prepared according to the literature methods. All organic solvents used were purchased from RCI Labscan and purified according to standard procedures. Deionized water ($R \square 18.2 \text{ M}\square\text{-cm}$) was obtained from Nanopure® Analytical Deionization Water.

3.2 Instruments

For physical measurements and instrumentation, Fourier transform nuclear magnetic resonance (NMR) spectra were acquired using Bruker's Ascend 400 high-resolution magnetic resonance spectrometer for ¹H (400MHz) and ¹³C{¹H} (100 MHz) nuclei. Chemical shifts were reported in δ unit (parts per million) using residual solvent peaks as references (CDCl₃: ¹H δ 7.26 and, ¹³C δ 77.16). Electrospray ionization (ESI) mass spectrometry was carried out using a microTOF in the positive mode ion. Fourier transform infrared (FT-IR) spectra were recorded in the range of 400-4000 cm⁻¹ using Bruker model Alpha spectrometer (Bruker Optics GmbH, Ettlingen, Germany).

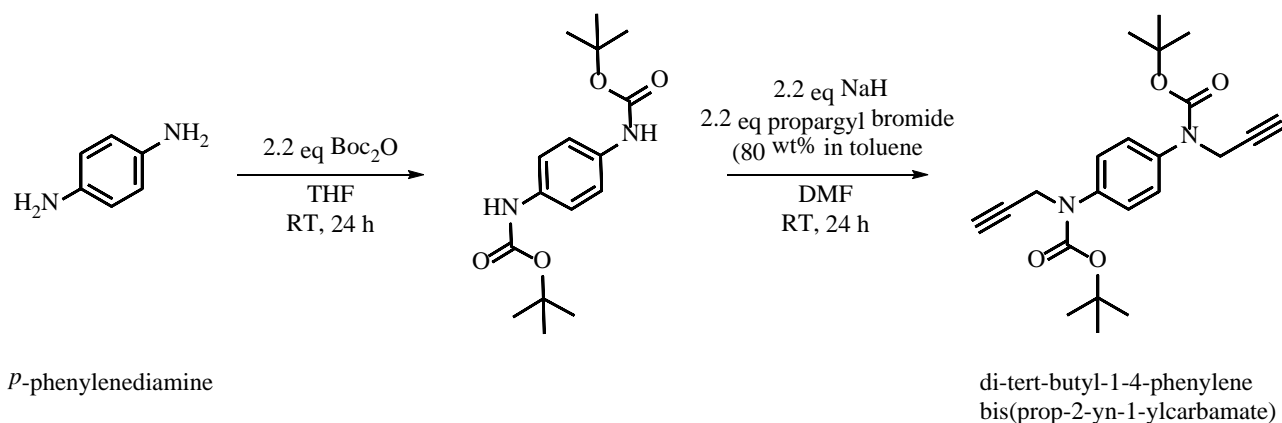
3.3 General procedure

Air-sensitive experiments were carried out under N₂ using standard Schlenk techniques. Propargyl bromide was stored under N₂ in a PTFE valve flask at 5 °C and used as received. 1 M HCl and 10% NH₄OH were freshly prepared before use.

3.4 Methods

3.4.1 Synthesis of di-tert-butyl-1,4-phenylenebis(prop-2-yn-1-ylcarbamate)

To a 10 mL THF solution of *p*-phenylenediamine (0.500 g, 4.62 mmol) was added Boc₂O (2.40 mL, 10.2 mmol) upon which the reaction solution was stirred at room temperature. After 24 h, the white precipitates (1.40 g) were collected using vacuum filtration, air dried, and added to a 15.0 mL DMF suspension of NaH (0.450 g, 11.4 mmol) at 0 °C. The reaction mixture was stirred at this temperature for 15 min, after which propargyl bromide (80 wt% in toluene; 1.10 mL, 10.0 mmol) was added dropwise. Then, the reaction was allowed to warm up to room temperature and stirred for 24 h. Extraction with CH₂Cl₂ (3 x 30 mL) afforded a dark brown solid, which was identified as the desired product based on ¹H NMR spectroscopy, in 91% yield (1.63 g, 4.24 mmol) (Scheme 1).

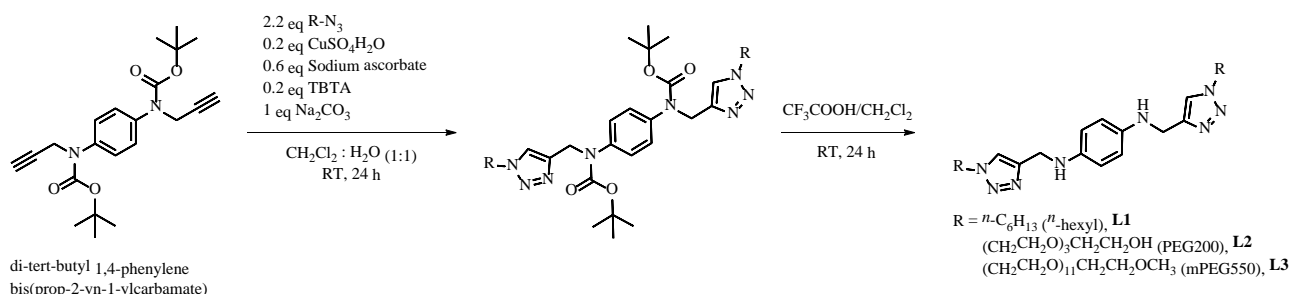


Scheme 1. Synthesis of di-tert-butyl-1,4-phenylenebis(prop-2-yn-1-ylcarbamate)

3.4.2 Synthesis of *n*-hexyl-, PEG200- and mPEG550-functionalized bis(amine-triazole) ligands

Di-tert-butyl-1,4-phenylenebis(prop-2-yn-1-ylcarbamate) (0.10 g, 0.26 mmol) was dissolved in 3 mL of CH₂Cl₂, followed by an addition of Na₂CO₃ (0.028 g, 0.26 mmol), RN₃ (*n*-C₆H₁₃N₃, PEG200N₃ or mPEG550N₃) (0.57 mmol), tris(benzyltriaazolylmethyl)amine (TBTA; 0.028 g, 0.052 mmol), CuSO₄·5H₂O (0.013 g, 0.052 mmol), and a 3 mL aqueous solution of sodium ascorbate (0.031 g, 0.16 mmol), respectively. The reaction mixture was stirred at room temperature for 24 h, after which EDTA (0.076 g, 0.26 mmol) in 3 mL of 10% NH₄OH was added and the solution was stirred at room

temperature for 4 h. The reaction solution was quenched with saturated brine solution, and extracted with CH₂Cl₂ (3 x 15 mL). The Boc-protected triazole ligands were purified by column chromatography, resulting in an off-white solid in 94%, 90%, and 83% yields. Boc deprotection was carried out by adding excess amount of CF₃COOH (0.5 mL) to a 2 mL CH₂Cl₂ solution of the Boc-protected ligand. The reaction mixture was stirred for 24 h at room temperature, after which the solution was quenched with saturated aqueous solution of NaHCO₃ and the product was extracted with CH₂Cl₂ (3 x 10 mL). Solvent evaporation produced the corresponding amine-triazole ligands **L1-L3** in 80%, 74%, and 68% overall yields, respectively (Scheme 2).



Scheme 2. Synthesis of *n*-hexyl-, PEG200- and mPEG550-functionalized bis(amine-triazole) ligands

3.5 General procedure of alcohol oxidation

To a 2 mL CH₃CN or aqueous solution of alcohol (1.0 mmol), base (NMI or Na₂CO₃) (0.014 g, 0.10 mmol), and TEMPO (0.050 mmol) was added a 3 mL of CH₃CN or aqueous solution of CuCl/L (0.050 mmol Cu, **L** = **L1-L3**). The reaction mixture was allowed to stir in air at various reaction temperatures for a given time. Then, the reaction mixture was filtered through a silica in short column with 10 mL EtOAc. The percent conversion was determined by GC-MS method using anisole (0.1 mmol) as an internal standard.

4. Results and discussion

4.1 Synthesis and characterization of *n*-hexyl-, PEG200- and mPEG550-functionalized bis(amine-triazole) ligands

A reaction between di-tert-butyl-1,4-phenylenebis(prop-2-yn-1-ylcarbamate) and different organic azide including *n*-C₆H₁₃N₃, PEG200N₃, and mPEG550N₃ in CH₂Cl₂ in the presence of CuSO₄·5H₂O, TBTA, sodium ascorbate and Na₂CO₃ afforded the corresponding Boc-protected bis(amine-triazole) compounds. Subsequent Boc deprotection produced the bis(amine-triazole) ligands **L1-L3** in 80%, 74%, and 68% yields, respectively.

L1: ¹H NMR (400 MHz, CDCl₃) δ 7.47 (s, 2H), 6.62 (s, 4H), 4.39 (s, 4H), 4.30 (t, 4H), 1.86 (s, 4H), 1.29 (s, 12H), 0.87 (s, 6H). ¹³C{¹H} (100 MHz, CDCl₃) δ 121.54, 115.40, 50.56, 41.33, 31.34, 30.47, 26.34, 22.62, 14.15. ESI-MS (microTOF, m/z) [*M* + H⁺]: Calcd. For C₂₄H₃₈N₈, 439.3293; found 439.3292. FT-IR (ATR, cm⁻¹): 3281, 2955, 2930, 2856, 2362, 1625, 1517, 1458, 1239, 1053, 810, 727, 658, 523, 408.

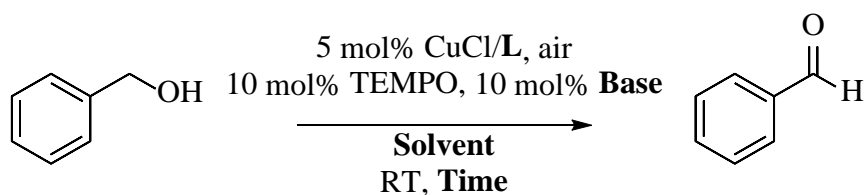
L2: ¹H NMR (400 MHz, CDCl₃) δ 7.68 (s, 2H), 6.59 (s, 4H), 4.42 (t, 4H), 4.35 (s, 4H), 3.81 (t, 4H), 3.67 (t, 4H), 3.60 (d, 4H), 3.53 (m, 16H), 1.23 (s, 3H). ¹³C{¹H} (100 MHz, CDCl₃) δ 122.34, 114.65, 72.62, 70.66, 70.57, 70.47, 70.37, 61.59, 50.60. ESI-MS (microTOF, m/z) [*M* + H⁺]: Calcd. For C₂₈H₄₆N₈O₈, 622.3439; found 622.5734. and FT-IR (ATR, cm⁻¹): 3397, 2882, 2362, 2344, 1675, 1619, 1521, 1456, 1425, 1350, 1200, 1180, 1123, 1059, 935, 887, 831, 799, 721, 517.

L3: ¹H NMR (400 MHz, CDCl₃) δ 7.68 (s, 2H), 6.62 (s, 4H), 4.50 (t, 4H), 4.36 (s, 4H), 3.83 (t, 4H), 3.63 (m, 98H), 3.46 (m, 4H), 3.36 (s, 6H). ¹³C{¹H} (100 MHz, CDCl₃) δ 122.36, 115.76, 72.96, 72.04, 71.49, 70.67, 59.16, 42.88. ESI-MS (microTOF, m/z) [*M* + H⁺]: Calcd. For C₆₂H₁₁₂N₈O₂₄, 1359.2473; found 1359.3275. and FT-IR (ATR, cm⁻¹): 3470, 2922, 2868, 2362, 2339, 1657, 1591, 1520, 1462, 1346, 1303, 1248, 1198, 1090, 1034, 946, 826, 670, 528.

4.2 Catalytic aerobic alcohol oxidation

To compare the catalytic activity toward aerobic alcohol oxidation of the copper stabilized by hexyl- (**L1**) and PEG-functionalized bis(amine-triazole) ligands with different PEG chain lengths [PEG200 (**L2**) and mPEG550 (**L3**)], benzyl alcohol was used as a model substrate in the presence of 5 mol% CuCl/Ln, TEMPO (5 mol%) and base (NMI or Na₂CO₃) (10 mol%) in CH₃CN or water at room temperature for 24 h with air as an oxidant. The GC-MS techniques were used to identify and analyze percent conversion of alcohols to the aldehyde products. The results showed that CuCl/**L1** possessed the highest catalytic activity up in to 98% conversion in CH₃CN at room temperature for 2 h in the presence of NMI base (entry 1, Table 1). For water-soluble, PEG-functionalized bis(amine-triazole) ligands, only 14% and 35% conversions were observed for the CuCl/**L2** and CuCl/**L3** catalysts when Na₂CO₃ was used as a base in water at room temperature after 24 h (entries 2 and 4, Table 1). However, in the presence of NMI base, percent conversions of benzyl alcohol to benzaldehyde increased to 89% and 43% for CuCl/**L2** and CuCl/**L3**, respectively (entries 3 and 5, Table 1).

Table 1. Catalyst comparison for selective alcohol oxidation ^a



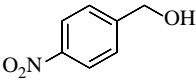
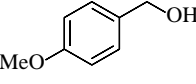
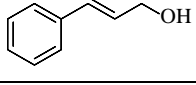
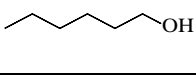
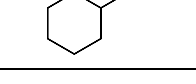
Entry	L	Base	Solvent	Time	% Conversion ^b
1	L1	NMI	CH ₃ CN	2 h	98
2	L2	Na ₂ CO ₃	H ₂ O	24 h	14
3	L2	NMI	H ₂ O	24 h	89
4	L3	Na ₂ CO ₃	H ₂ O	24 h	35
5	L3	NMI	H ₂ O	24 h	43

^a Reaction condition: benzyl alcohol (1.0 mmol), CuCl (0.050 mmol), L (**L1-L3**; 0.050 mmol), TEMPO (0.050 mmol), Base (0.10 mmol), in solvent (5.0 mL) under aerobic conditions at room temperature for given time with anisole (0.10 mmol) as an internal standard. ^b Based on GC analysis.

4.3 Substrate scope

From the optimized condition, a mixture of CuCl/**L1**/TEMPO/NMI was further investigated as the catalyst system for aerobic oxidation of various alcoholic substrates in CH₃CN at room temperature. Catalytic results have shown that benzyl alcohol derivatives such as 4-nitrobenzyl alcohol, 4-methoxybenzyl alcohol as well as cinnamyl alcohol were converted to the corresponding aldehydes in high yields at 2 h (entries 1-3, Table 2). For aliphatic alcohols such as hexanol and cyclohexanol, only 15% and 24% conversions were obtained, respectively, at room temperature after 3 h (entries 4-5, Table 2)

Table 2. Substrate scope for aerobic alcohol oxidation catalyzed by CuCl/L1^a

Entry	Alcohol	% Conversion ^b
1		90
2		95
3		88
4		15 ^c
5		24 ^c

^a Reaction condition: Alcohol Substrate (1.0 mmol), CuCl (0.050 mmol), L1 (0.050 mmol), TEMPO (0.050 mmol), NMI (0.10 mmol) in CH₃CN (5 mL) under aerobic conditions at room temperature for 2 h with 0.010 mmol of anisole as an internal standard. ^b Based on GC analysis. ^c Reaction time = 3 h.

5. Conclusions

A series of *n*-hexyl- (L1) and water-soluble PEG-functionalized bis(amine-triazole) ligands with different PEG chain length, PEG200 (average M_w ~ 200; L2) and mPEG550 (average M_w ~ 550; L3) have been successfully synthesized and characterized. The catalyst systems CuCl/L/TEMPO/NMI promoted excellent conversions of benzyl alcohol to benzaldehyde in CH₃CN (for L1) and H₂O (for L2) at room temperature after 2 h. Catalytic studies toward aerobic oxidation of benzyl alcohol have also shown that the shorter PEG chain length (PEG200) resulted in the copper catalyst system with higher activity in water than that of mPEG550 (89% *cf.* 43% conversions at 2 h). Furthermore, the catalyst system CuCl/L1/TEMPO/NMI exhibited high oxidation activities in CH₃CN toward benzyl alcohol derivatives and cinnamyl alcohol but lower activities for the more challenging 1° alcohols such as 1-hexanol and cyclohexanol.

References

- [1] Feng, B., Hua, L., Hou, Z., Yang, H., Hu, Y., Li, H., & Zhao, X. (2008). The functionalized poly(ethylene glycol) supported palladium nanoparticles as a high efficient catalyst for aerobic oxidation of alcohols. *Catalysis Communications*, 10, 1542 – 1546.
- [2] March, J. (1992). *Advanced Organic Chemistry: Reactions Mechanisms, and Structure* (4th ed.). New York.
- [3] Parmeggiani, C. & Cardona, F. (2012). Transition metal based catalysts in the aerobic oxidation of alcohols. *Green Chemistry*, 14, 547 – 564.
- [4] Mendoza-Espinosa, D., Negrón-Silva, G. E., Ángeles-Beltrán, D., Álvarez-Hernández, A., Suárez-Castillo, O. R. & Santillán, R. (2014). Copper(II) complexes supported by click generated mixed NN, NO, and NS 1,2,3-triazole based ligands and their catalytic activity in azide-alkyne cycloaddition. *Dalton Transactions*, 43, 7069 -7077.
- [5] Jin, T., Kamijo, S. & Yamamoto, Y. (2004). Copper-Catalyzed Synthesis of N-Unsubstituted 1,2,3-Triazoles from Nonactivated Terminal Alkynes. *European Journal of Organic Chemistry*, 3789 – 3791.
- [6] Meldal, M. & Tornøe, C. W. (2008). Cu-Catalyzed Azide-Alkyne Cycloaddition. *Chemical Reviews*, 108, 2952 – 3015.

- [7] Thongkam, P., Jindabot, S., Prabpai, S., Kongsaree, P., Wititsuwannakul, T., Surawatanawong, P. & Sangtrirutnugul, P. (2015). Pyridine-triazole ligands for copper-catalyzed aerobic alcohol oxidation. *RSC Advances*, 5, 55847 – 55855.
- [8] Kongkaew, M., Sitthisuwannakul, K., Nakarajouyphon, V., Pornsuwan, S., Kongsaree, P. & Sangtrirutnugul, P. (2016). Benzimidazole-triazole ligands with pendent triazole functionality: unexpected formation and effects on copper-catalyzed aerobic alcohol oxidation. *Dalton Transactions*, 45, 16810 – 16819.
- [9] Zhang, G., Wang, Y., Wen, X., Ding, C. & Li, Y. (2012). Dual-functional click-triazole: a metal chelator and immobilization linker for the construction of a heterogeneous palladium catalyst and its application for the aerobic oxidation of alcohols. *Chemical Communications*, 48, 2979 – 2981.
- [10] Feng, B., Hua, L., Hou, Z., Yang, H., Hu, Y., Li, H. & Zhao, X. (2009). The functionalized poly(ethylene glycol) supported palladium nanoparticles as a highly efficient catalyst for aerobic oxidation of alcohols. *Catalysis Communications*, 10, 1542 – 1546.
- [11] Kadajji, V. G. & Betageri, G. V. (2011). Water Soluble Polymers for Pharmaceutical Applications. *Polymers*, 3, 1972 – 2009
- [12] Bergbreiter, B. E. (2002). Using soluble polymers to recover catalysts and ligands. *Chemical Reviews*, 102, 3345 – 3383.
- [13] Chen, J., Spear, S. K., Huddleston, J. G. & Rogers, R. D. (2005). Polyethylene glycol and solutions of polyethylene glycol as green reaction media. *Green Chemistry*, 7, 64 – 82.
- [14] Sun, N., Zhang, X. Jin, L., Hu, B., Shen, Z. & Hu, X. (2017). Recyclable copper-catalyzed ambient aerobic oxidation of primary alcohols to aldehydes in water using water-soluble PEG-functionalized pyridine triazole as ligand. *Catalysis Communications*, 101, 5 – 9.
- [15] Alvarez, S. G. & Alvarez M. T. (1997). A Practical Procedure for the Synthesis of Alkyl Azides at Ambient Temperature in Dimethyl Sulfoxide in High Purity and Yield. *Synthesis*, 4, 413 – 414.
- [16] DeForest, C. A. & Tirrell, D. A. (2015). A photoreversible protein-patterning approach for guiding stem cell fate in three-dimensional gels. *NATURE MATERIALS*, 14, 523 – 531.
- [17] Luca, L. D., Giacomelli, G. & Porcheddu, A. (2002). An Efficient Route to Alkyl Chlorides from Alcohols Using the Complex TCT/DMF. *ORGANIC LETTERS*, 4(4), 553 – 555.
- [18] Semple, J. E., Sullivan, B., Vojkovsky, T. & Sill, K. N. (2016). Synthesis and Facile End-Group Quantification of Functionalized PEG Azides. *JOURNAL OF POLYMER SCIENCE, PART A: POLYMER CHEMISTRY*, 54, 2888 – 2895.
- [19] Chan, T. R., Hilgraf, R., Sharpless, K. B. & Fokin, V. V. (2004). Polytriazoles as Copper(I)-Stabilizing Ligands in Catalysis. *ORGANIC LETTERS*, 6(17), 2853 – 2855.

DFT investigation of toluene adsorption on silicon carbide nanosheet doping with transition metal for storage and sensor application

Pasakorn Sangnikul^{1,a}, Chanukorn Tabtimsai^{1,b}, Wandee Rakrai^{1,c}, Banchob Wann^{2,d}

¹Computational Chemistry Center for Nanotechnology and Department of Chemistry, Faculty of Science and Technology, Rajabhat Maha Sarakham University, Maha Sarakham, Thailand

²Center of Excellence for Innovation in Chemistry and Supramolecular Chemistry Research Unit, Department of Chemistry, Faculty of Science, Mahasarakham University, Maha Sarakham, Thailand

E-mail; ^achamp9yod@gmail.com, ^btabtimsai.c@gmail.com, ^cwandee.rakrai@gmail.com, ^dbanchobw@gmail.com

Abstract

Nowadays, the emission of volatile organic compounds (VOC) is giving rise to several health hazards and damage to the environment. Consequently, the nanomaterial development is considerably important for VOC adsorption and sensing. In this work, the adsorptions of toluene on silicon carbide nanosheets doping with transition metal atoms (TM-doped SiCNS) were investigated using the density functional theory method (DFT). The B3LYP/LanL2DZ was employed in all calculations for the geometric, energetic, and electronic properties. In addition, the doping of TM atom at different sites will have different effects on the adsorption behavior of the systems. Calculation results reveal that the adsorption distances and adsorption energies of TM doping on SiCNSs are suitable for toluene adsorption greater than pristine SiCNS. According to the changes of electronic properties of TM-doped SiCNS show highly sensitive to toluene molecule. The results indicate that the introducing of TM doping on SiCNS significantly improve the sensitivity toward toluene molecule. Therefore, the results of our work may be useful in developing and designing new types of storage and sensor materials.

Keywords: DFT; Silicon carbide nanosheet; Toluene; Transition metals; VOC

1. Introduction

Volatile organic compounds (VOC) are common air pollutants emitted by the chemical industries such as production of adhesives, paints, printing materials, building materials, and chemicals for synthesis [1]. For this reason, it is an important issue to develop sensors for detect and manage VOC. In the recent year, the experimental and theoretical studies about VOC adsorption on different nanostructures have been reported widely [2,3]. Manaschai Kunaseth *et al.* have investigated the adsorption of VOC on transition metal deposited graphene which adsorption energy of benzene was -1.93 eV calculated by using Perdew-Wang functional (PW91) [4]. The para-nitrophenol molecule adsorption on vacancy and Pt-doped graphene sheets showed that the adsorption capacity of graphene can be significantly increased [5]. Toluene is volatile organic compound that evaporate at room temperature. Toluene is harmful to human health, and may cause various diseases such as headache, nausea, coryza, pharyngitis, emphysema, lung cancer, and even death [6]. Also study of the adsorptions of VOCs on activated carbon/metal oxide composites have been performed by Ke Zhou *et al.*, that calculation shows that the highest adsorption energy of toluene on activated carbon was -20.87 kJ/mol calculated by using JW-BK132Z functional [7]. Lian Yu *et al.* have reported the adsorption of VOC on reduced graphene oxide, and the results suggested that graphene oxide is excellent adsorption performance for toluene molecule [8]. As previously mentioned, Experimental and theoretical studies on the adsorption of VOC are showed extremely interesting and it is necessary to understand more.

The silicon carbide nanosheet (SiCNS) has recently attracted considerable attention due to it has the notable properties such as thermal stability, chemical inertness, high thermal conductivity, and

others [9,10]. They also have wide range of applications in different fields such as energy conversion, enhance materials strength, gas storage and sensing applications [11]. However, pristine SiCNS has been explored as low efficient for adsorption or storage and low sensitive to small molecule [12]. Therefore, many studies are devoted to improving the surface sensibility of silicon carbide nanostructures by introducing doping metal atoms. Doping of transition metal (TM=Fe, Co, Al, Cu, and Zn) atoms on SiCNS can improve the adsorption abilities of TM-doped SiCNS to small molecule and change electronic properties of TM-doped SiCNS [13]. Ga- and B-doped SiCNSs show better capability of small molecule adsorption capability than undoped SiCNS [14]. The silicon carbide nanotube (SiCNT) doping with group 8B transition metal are appropriate for hydrogen storage and show better hydrogen adsorption capability than undoped SiCNT [15].

To the best of our knowledge, there are no reports the adsorption abilities of toluene molecule on TM-doped SiCNS. Therefore, aim of this work, we investigate the geometric, energetic, and electronic properties of pristine and TM-doped SiCNSs by density functional theory (DFT) and subsequently we evaluate their ability in adsorption of toluene molecules.

2. Computational details

The structure optimization of SiCNS ($C_{39}Si_{39}H_{24}$) was modeled and used. The edges of the sheet were saturated by hydrogen atoms to avoid the boundary effects. The doping of TM atom on the center of SiCNS was modeled. The transition metal atoms, i.e., V, Nb, Ta, Cr, Mo, W, Mn, Tc, and Re were doping on carbon (TM_C) or silicon (TM_{Si}) atom at the center of SiCNS. Geometrical optimizations of their systems were taken under the DFT calculation. The calculation was performed under hybrid density functional B3LYP, Becke's three parameter exchange functional with the Lee-Yang-Parr correlation functional (B3LYP) [16-18] and the Los Alamos LanL2DZ split-valence basis set [19-21]. All calculations were performed by using GAUSSIAN 09 program [22]. The geometrical parameters as equilibrium structural and natural bond orbitals (NBO) charges of studied compounds were specified at $T=0$ K. The molecular graphics of all related species were generated with the MOLEKEL 4.3 program [23]. The electronic density of states (DOSs) of all systems were plotted by the GaussSum 2.2 program [24]. Adsorption energy (E_{ads}) of toluene molecule adsorbed on the pristine and TM-doped SiCNS were obtained from equations $E_{ads} = E_{toluene, SiCNS \text{ or } TM, SiCNS} - (E_{SiCNS \text{ or } TM, SiCNS} + E_{toluene})$, where $E_{toluene, SiCNS \text{ or } TM, SiCNS}$ are the total energy of the adsorption of toluene molecule on pristine or TM-doped SiCNS. The $E_{SiCNS \text{ or } TM, SiCNS}$ and $E_{toluene}$ are the total energies of pristine or TM-doped SiCNS and toluene molecule, respectively. Considering the electronic properties in term of the highest occupied molecular orbital energies (E_{HOMO}), the lowest unoccupied molecular orbital energies (E_{LUMO}), the energy gaps (E_{gap}) referred to the energy difference between HOMO and LUMO orbitals and changes of energy gaps (ΔE_{gap}) referred to the gap difference between before and after gas adsorption were investigated at the same theoretical level.

3. Results and discussion

3.1 Geometrical structures

The B3LYP/LanL2DZ-optimized structures of the pristine and their adsorption with toluene molecule are displayed in Fig. 1. In addition, the doping sites are showed in Fig. 1a. The calculated average Si-C bond lengths and bond angles of pristine SiCNS are found to be 1.780 Å and 120.0°, respectively, which are in accordance with the previous reports [9]. The bond lengths, bond angles, and adsorption distances of toluene adsorbed on pristine, V-, Nb-, Ta-, Cr-, Mo-, W-, Mn-, Tc-, and

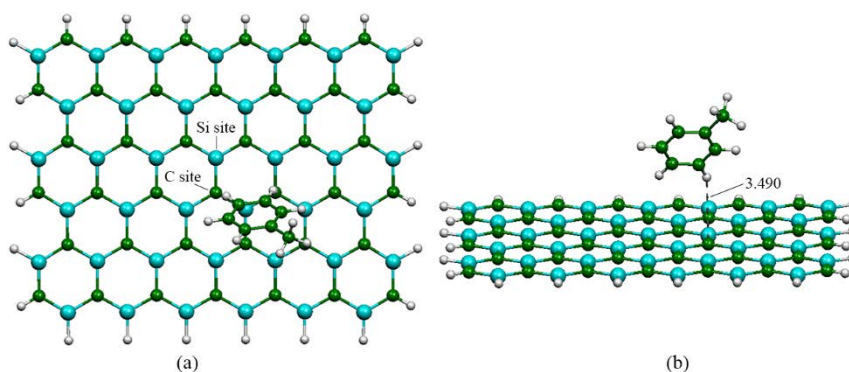


Figure 1. The B3LYP/LanL2DZ optimized structures of top views of (a) pristine SiCNS and (b) toluene adsorbed on pristine SiCNS.

Re-doped SiCNSs are listed in Table 1. In comparison of pristine SiCNS with the toluene adsorbed on pristine SiCNS (toluene/SiCNS), the bond lengths and bond angles of pristine SiCNS system are slightly changed. Therefore, toluene/SiCNS reflected that toluene molecule occur the weak interaction.

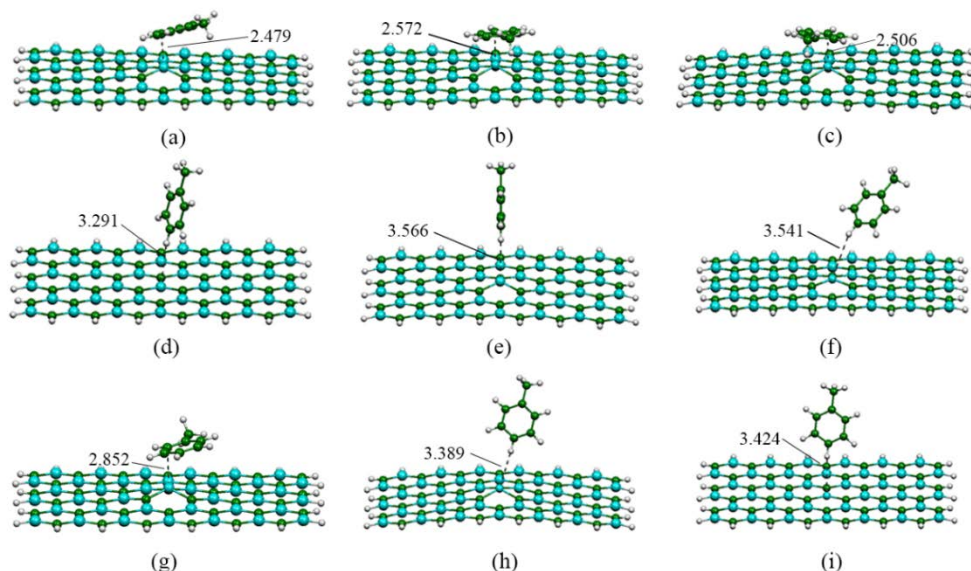
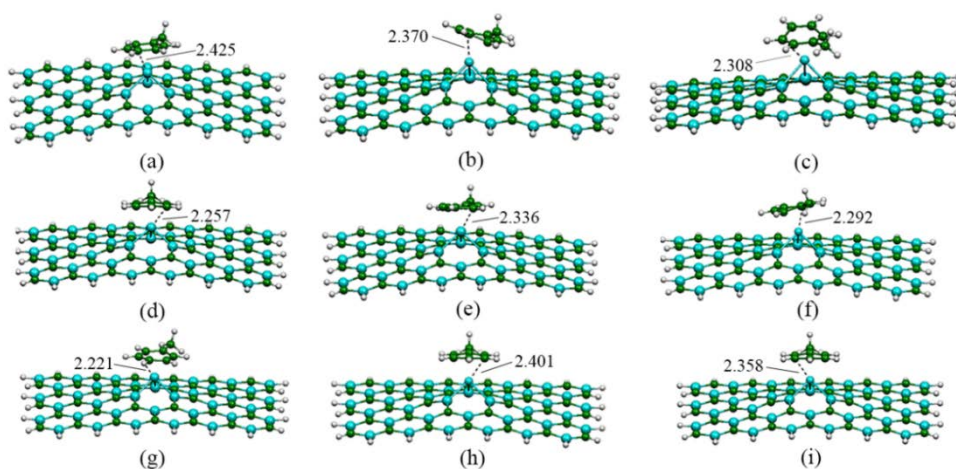


Figure 2. The B3LYP/LanL2DZ optimized structures of toluene adsorbed on TM-SiCNSs, (a) toluene/ V_C -, (b) toluene/ Nb_C -, (c) toluene/ Ta_C -, (d) toluene/ Cr_C -, (e) toluene/ Mo_C -, (f) toluene/ W_C -, (g) toluene/ Mn_C -, (h) toluene/ Tc_C -, and (i) toluene/ Re_C -doped SiCNSs.

The toluene adsorptions on TM_C -SiCNS (toluene/ TM_C -SiCNS) are showed in Fig 2., the Si-TM bond lengths are in the ranges of 2.294-2.563 Å, while the Si-TM-Si bond angles are in the ranges of 78.6-97.3°. Obviously, after toluene adsorption, the surface of TM_C -SiCNS still reveal the protruded geometrical structures which were similar trends can be found in other works [25]. In another hand, the B3LYP/LanL2DZ-optimized structures of toluene/ TM_{Si} -SiCNS are displayed in Fig 3. The C-TM bond lengths of toluene/ TM_{Si} -SiCNS obtained in this study are in the ranges of 1.825 - 2.035 Å, which are significantly shorter than C-TM of TM_C -SiCNS, while the bond angles of C-TM-C at the doping



site of toluene/SiCNS_{Si}-TM are in the range of 107.5 - 121.0°, which were wider than that of the Si-TM-Si bond angles of toluene/TM_C-SiCNS.

Figure 3. The B3LYP/LanL2DZ optimized structures of toluene adsorbed on (a) toluene/V_{Si}-, (b) toluene/Nb_{Si}-, (c) toluene/Ta_{Si}-, (d) toluene/Cr_{Si}-, (e) toluene/Mo_{Si}-, (f) toluene/W_{Si}-, (g) toluene/Mn_{Si}-, (h) toluene/Tc_{Si}-, and (i) toluene/Re_{Si}-doped SiCNSs.

The adsorption distances (AD) between toluene molecule and pristine SiCNS or TM-doped SiCNS are listed in Table 1. The AD between toluene molecule and the pristine SiCNS is calculated to be 3.490 Å. The AD between the toluene molecule and TM-SiCNSs are found in the range 2.234-2.476 and 2.479-3.566 Å for TM_C-SiCNS and TM_{Si}-SiCNS, respectively. This indicates that interactions between toluene molecule and TM_C-SiCNS are stronger than TM_{Si}-SiCNS.

Table 1. The selected geometrical parameters and adsorption distances (AD) of toluene molecule adsorbed on pristine and TM-doped SiCNS.

Species							AD (Å)
	Si1-TM	Si2-TM	Si3-TM	Si1-TM-	Si1-TM-	Si2-TM-	
	or	or	or	Si2 or	Si3 or	Si3 or	
C1-TM	C2-TM	C3-TM	C1-TM-C2	C1-TM-C3	C2-TM-C3		
	(Å)	(Å)	(Å)	(°)	(°)	(°)	
toluene/SiCNS	1.798 ^a	1.824 ^a	1.798 ^a	119.3 ^a	121.2 ^a	119.3 ^a	3.490
toluene/V _C -SiCNS	2.464	2.481	2.465	83.3	86.1	83.4	2.476
toluene/Nb _C -SiCNS	2.513	2.546	2.510	84.3	85.0	78.5	2.370
toluene/Ta _C -SiCNS	2.554	2.534	2.546	82.4	81.4	83.1	2.309
toluene/Cr _C -SiCNS	2.415	2.315	2.311	80.9	85.0	96.4	2.234
toluene/Mo _C -SiCNS	2.398	2.563	2.393	80.6	94.5	79.9	2.336
toluene/W _C -SiCNS	2.437	2.479	2.426	81.5	88.6	86.4	2.292
toluene/Mn _C -SiCNS	2.294	2.310	2.320	91.0	87.9	86.7	2.267
toluene/Tc _C -SiCNS	2.355	2.427	2.353	85.2	92.0	85.2	2.473
toluene/Re _C -SiCNS	2.368	2.427	2.368	85.5	91.4	85.5	2.358
toluene/V _{Si} -SiCNS	1.891	1.983	1.884	109.2	115.2	109.6	2.479
toluene/Nb _{Si} -SiCNS	1.986	2.035	1.982	107.6	108.3	107.5	2.572
toluene/Ta _{Si} -SiCNS	1.978	2.023	1.982	107.5	108.5	107.6	2.506
toluene/Cr _{Si} -SiCNS	1.825	1.883	1.825	119.4	121.0	119.4	3.291
toluene/Mo _{Si} -SiCNS	1.932	1.982	1.930	113.2	114.5	113.1	3.566
toluene/W _{Si} -SiCNS	1.933	1.964	1.933	116.9	116.9	116.9	3.541
toluene/Mn _{Si} -SiCNS	1.938	1.972	1.938	109.2	112.5	109.4	2.852
toluene/Tc _{Si} -SiCNS	1.938	1.972	1.938	110.2	111.2	110.3	3.389
toluene/Re _{Si} -SiCNS	1.880	1.914	1.880	120.3	119.3	120.3	3.424

^aBond lengths and bond angles of toluene adsorbed on pristine SiCNS

3.2 Adsorption abilities of pristine and TM-doped SiCNSs onto toluene adsorbed

The adsorption energies (E_{ads}) of toluene adsorbed on the pristine, V-, Nb-, Ta-, Cr-, Mo-, W-, Mn-, Tc-, and Re-doped SiCNSs are listed in Table 2. The adsorption energy of toluene adsorbed on pristine SiCNS is -0.416 kcal/mol. This confirms that pristine SiCNS is slightly sensitive to toluene molecule. The adsorption energies of toluene adsorbed on TMC-doped SiCNS are in a range of - 51.604 and -30.922 kcal/mol. Their E_{ads} are in the following order: toluene/WC-SiCNS (-51.604 kcal/mol) > toluene/CrC-SiCNS (-46.172 kcal/mol) > toluene/MoC-SiCNS (-41.204 kcal/mol) > toluene/TaC-SiCNS (-40.483 kcal/mol) > toluene/MnC-SiCNS (-38.511 kcal/mol) > toluene/ReC-SiCNS (- 35.833 kcal/mol) □ toluene/V_C-SiCNS (-35.583 kcal/mol) □ toluene/Nb_C-SiCNS (-35.469 kcal/mol) > toluene/TcC-SiCNS (-30.922 kcal/mol). The parameters of adsorption energies indicate that the TMC-SiCNS are exothermic reactions. Surprisingly, the TM doping on C site significantly improved adsorption ability of SiCNS. The large adsorption energies and short AD reflected that toluene

molecule underwent the strong interaction with TM_C-doped SiCNS. These adsorption energies were in according to concordance with the previous studies [3].

The adsorption energies of toluene adsorbed on TM_{Si}-doped SiCNS are also exothermic reactions which are in the range of -34.004 to -0.027. Their E_{ads} order is found as follow: toluene/Mn_{Si}-SiCNS (-34.004 kcal/mol) > toluene/Ta_{Si}-SiCNS (-14.721 kcal/mol) > toluene/Nb_{Si}-SiCNS (-13.747 kcal/mol) > toluene/V_{Si}-SiCNS (-5.815 kcal/mol) > toluene/Re_{Si}-SiCNS (-1.060 kcal/mol) > toluene/Cr_{Si}-SiCNS (-1.021 kcal/mol) > toluene/W_{Si}-SiCNS (-0.997 kcal/mol) > toluene/Mo_{Si}-SiCNS (-0.027 kcal/mol). The TM doping on Si site also improved adsorption ability of SiCNS. Therefore, the Mn_{Si}-SiCNS, Ta_{Si}-SiCNS, Nb_{Si}-SiCNS and V_{Si}-SiCNS are suitable adsorption energies and short AD that toluene molecule underwent the strong interaction with TM_{Si}-doped SiCNS. Except for the Re_{Si}-SiCNS, Cr_{Si}-SiCNS, W_{Si}-SiCNS, Mo_{Si}-SiCNS, and Tc_{Si}-SiCNS display the small adsorption energies, and large AD reflected that toluene molecule underwent the weak interaction. Whereas, the toluene adsorbed on Tc_{Si}-SiCNS (7.531 kcal/mol) is the endothermic reaction.

Apparently, the adsorption ability of SiCNS onto toluene molecule is improved by TM doping which is similar with that of adsorption of volatile organic compounds onto Al-doped C₂N monolayer [19], and volatile organic compounds adsorption on transition metal deposited graphene [2]. Additionally, TM doping on C site of SiCNS displays higher interaction with toluene molecule than Si site. The results that are similar to previous work in which we found that Ni-doped silicon carbide nanocage displayed the higher adsorption energies of hydrogen than Si site [26]. Its could be concluded here that the TM doping SiCNS are much more suitable for toluene adsorption than pristine SiCNS.

Table 2 Adsorption energies (E_{ads}), E_{HOMO} , E_{LUMO} , E_{gap} , $\square E_{gap}$, and partial charge transfers (PCT) of toluene molecule adsorbed on pristine and TM-doped SiCNSs, computed at the B3LYP/LanL2DZ level of theory.

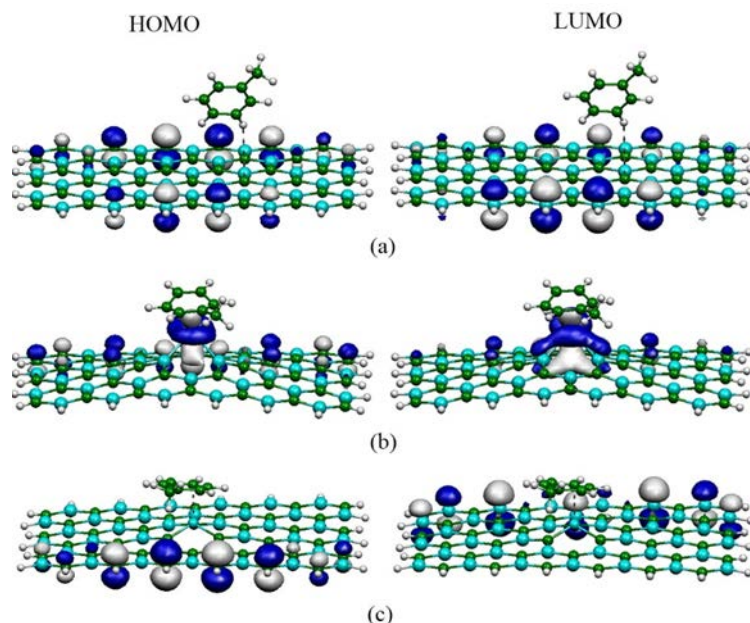
Species	E_{ads} (kcal/mol)	E_{HOMO} (eV)	E_{LUMO} (eV)	E_{gap} (eV)	$\square E_{gap}$ (eV)	PCT (e)
toluene/SiCNS	-0.416	-3.919	-3.728	0.190	0.027	0.007
toluene/V _C -SiCNS	-35.583	-4.027	-3.293	0.735	-0.408	0.341
toluene/Nb _C -SiCNS	-35.469	-3.973	-3.728	0.245	0.218	0.162
toluene/Ta _C -SiCNS	-40.483	-4.055	-3.565	0.490	-0.245	0.052
toluene/Cr _C -SiCNS	-46.172	-3.837	-3.646	0.190	0.000	0.448
toluene/Mo _C -SiCNS	-41.204	-3.837	-3.619	0.218	-0.082	0.437
toluene/W _C -SiCNS	-51.604	-3.864	-3.646	0.218	0.109	0.303
toluene/Mn _C -SiCNS	-38.511	-4.082	-3.265	0.816	-0.082	0.414
toluene/Tc _C -SiCNS	-30.922	-4.055	-3.456	0.599	-0.109	0.283
toluene/Re _C -SiCNS	-35.833	-3.837	-3.646	0.190	0.000	0.204
toluene/V _{Si} -SiCNS	-5.815	-4.055	-3.374	0.680	0.163	0.204
toluene/Nb _{Si} -SiCNS	-13.747	-3.782	-3.402	0.381	0.463	0.212
toluene/Ta _{Si} -SiCNS	-14.721	-3.755	-3.402	0.354	0.490	0.236
toluene/Cr _{Si} -SiCNS	-1.021	-3.973	-3.755	0.218	0.000	-0.092
toluene/Mo _{Si} -SiCNS	-0.708	-3.973	-3.755	0.218	-0.027	-0.002
toluene/W _{Si} -SiCNS	-0.997	-3.973	-3.755	0.218	0.000	-0.002
toluene/Mn _{Si} -SiCNS	-34.004	-4.163	-3.347	0.816	-0.027	0.155
toluene/Tc _{Si} -SiCNS	7.531	-4.163	-3.402	0.762	0.163	0.003
toluene/Re _{Si} -SiCNS	-1.060	-3.919	-3.538	0.381	0.136	0.001

3.3 Electronic properties for the systems

To further investigate the adsorption phenomenon of the toluene molecule on the pristine and TM-doped SiCNSs is investigated, then we consider the E_{HOMO} , E_{LUMO} , E_{gap} , and $\square E_{gap}$ of the stable configuration of toluene molecule adsorbed on pristine and TM-doped SiCNSs. In Table 2, theoretical calculation reveals that the E_{gap} of toluene/SiCNS is 0.190 eV. The E_{gap} of toluene/TM_C- and TM_{Si}-SiCNSs are in the range of 0.816 to 0.190 and 0.762 to 0.218 eV, respectively, which are smaller than the E_{gap} of pristine SiCNS (E_{gap} = 2.49 eV). For the pristine SiCNS, V_C-SiCNS, Nb_C-SiCNS, Ta_C-SiCNS,

Mo_C-SiCNS, W_C-SiCNS, Mn_C-SiCNS, Tc_C-SiCNS, V_{Si}-SiCNS, Nb_{Si}-SiCNS, Ta_{Si}-SiCNS, Mo_{Si}-SiCNS, Mn_{Si}-SiCNS, Tc_{Si}-SiCNS, and Re_{Si}-SiCNS systems, the E_{gap} are changed by toluene adsorption, meaning the electronic properties of the systems are also exponentially changed. The reducing of E_{gap} of TM-doped SiCNS due to toluene adsorption is in excellent agreement with the previous calculated results of TM-doped SiCNS [25]. Except for toluene adsorption on Cr_C-SiCNS, Re_C-SiCNS, Cr_{Si}-SiCNS, and W_{Si}-SiCNS, the E_{gap} are not change.

Moreover, the HOMO and LUMO orbital distributions of the toluene adsorptions on pristine and TM-doped SiCNSs are also reported. The results show that, for toluene/SiCNS and toluene/TM_{Si}-



SiCNS systems, the HOMO and LUMO orbitals are localized around the sheet (Figs. 4a and 4c). Whereas, the HOMO and LUMO orbitals of TM_C-SiCNS are localized on the adsorption sites. The localization of the HOMO and LUMO orbitals of the toluene/Ta_C-SiCNS is clearly clustered (Fig. 4b). These results indicating the electron conduction through these systems.

Figure 4. Plots of HOMO and LUMO distributions of (a) toluene/SiCNS, (b) toluene/Ta_C-SiCNS, and (c) toluene/Ta_{Si}-SiCNS.

The partial charge transfers (PCT) between toluene molecule and SiCNS were calculated. The loss and gain of electrons could also be determined by natural bond orbital (NBO) charge calculations before and after toluene adsorptions (Table 3). The PCT was defined as $Q_{\text{toluene,SiCNS}} - Q_{\text{toluene}}$, where $Q_{\text{toluene,SiCNS}}$ is the total charge of toluene adsorbed on pristine and TM-doped SiCNS, and Q_{toluene} is the charge of toluene in free case. We found that the PCTs between toluene molecule and pristine SiCNS is about -0.007 e. The PCTs between toluene molecule and TM_C-SiCNS are in the ranges of 0.052 - 0.448 e. While the PCTs between toluene molecule and Mn_{Si}-SiCNS, Ta_{Si}-SiCNS, Nb_{Si}-SiCNS and V_{Si}-SiCNS are in the ranges of 0.236 - 0.155 e corresponding with strong adsorption abilities. The PCTs indicate that the large charge transfers between toluene molecule and TM_C-SiCNS and Mn_{Si}-SiCNS, Ta_{Si}-SiCNS, Nb_{Si}-SiCNS and V_{Si}-SiCNS are strongly bond due to covalent interaction. The covalent interaction between toluene molecule and TM-doped SiCNS is strong hybridization between the C's *p* orbital or H's *s* orbital of toluene and TM *d* orbital of TM-doped SiCNS. For the PCTs of toluene/TM_{Si}-SiCNS system, the PCTs between toluene molecule and Re_{Si}-SiCNS, Cr_{Si}-SiCNS, W_{Si}-SiCNS, Mo_{Si}-SiCNS, and Tc_{Si}-SiCNS are in the ranges of 0.001 to -0.092 e corresponding with weak adsorption abilities. Therefore, computations demonstrate that weak adsorption abilities of pristine SiCNS, Re_{Si}-SiCNS, Cr_{Si}-SiCNS, W_{Si}-SiCNS, Mo_{Si}-SiCNS, and Tc_{Si}-SiCNS slightly sensitive to toluene molecule.

The density of states were (DOSs) also calculated and plotted. The DOSs of pristine and TM-doped SiCNSs before and after toluene adsorption are displayed in Fig. 5. The DOSs of pristine SiCNS are slightly changed by toluene adsorption. This confirms that toluene molecule has slightly sensible effect on the electronic properties of the pristine SiCNS (Fig. 5a.). However, the DOSs of TM-doped SiCNS such as Ta_C- and Ta_{Si}-doped SiCNSs are significantly changed by toluene adsorption. These

results are similar with Fe-doped SiCNS, reported by D. Farmanzadeh *et al* [25]. The changes of the DOSs are expected to bring about obvious changes in the corresponding electronic properties.

In summary, the adsorptions abilities of TM-doped SiCNS to toluene molecule are larger than that of the pristine SiCNS. This supported the notion that the TM doping has an influence on the electronic properties of the SiCNS substantially, which was consistent with the previous results of Pd-doped SiCNS[27]. The results indicated that the changes of electronic properties are beneficial for sensing applications.

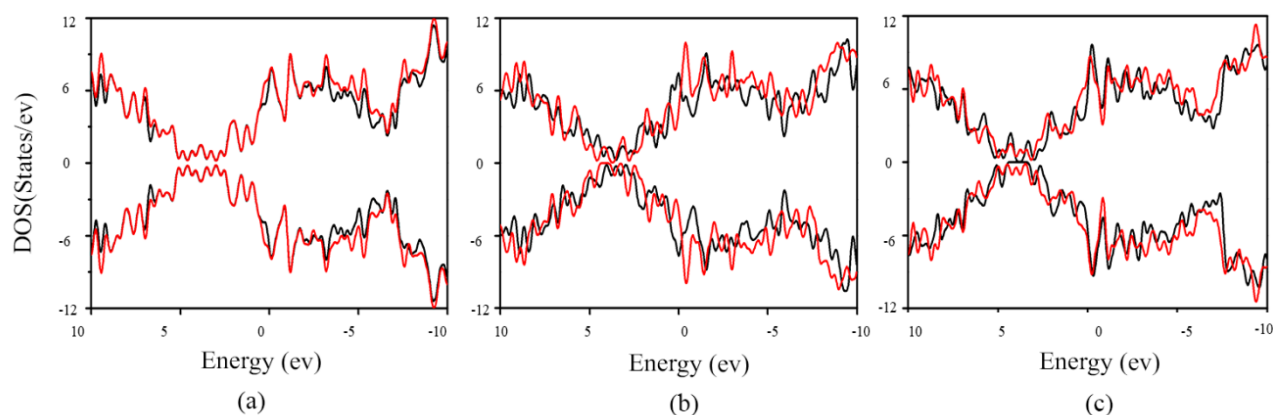


Figure 5. DOSs of (a) pristine SiCNS and toluene/SiCNS, (b) TaC-SiCNS and toluene/TaC-SiCNS, and (c) TaSi-SiCNS and toluene/TaSi-SiCNS. Before and after toluene adsorption are black and red lines, respectively.

4. Conclusions

In order to search for novel nanomaterials for toluene storage and sensing applications, the transition metals (TM = V, Nb, Ta, Cr, Mo, W, Mn, Tc, and Re) doping on SiCNS are selected. The geometric, energetic, and electronic properties of toluene adsorption on TM-doped SiCNS are calculated using the density functional theory method at B3LYP/LanL2DZ level of theory. It is found toluene molecule displays weak adsorption on the surface of pristine SiCNS ($E_{\text{ads}} = -0.416$ kcal/mol), whereas toluene molecule shows strong adsorption on the surface of TM-doped SiCNSs. The WC-doped SiCNS displays the strongest interaction with toluene molecule ($E_{\text{ads}} = -51.604$ kcal/mol). The E_{gap} and DOSs of the TM-SiCNSs present dramatic changes after adsorption with toluene molecules. A better understanding of these interactions is achieved by NBO analysis which confirms considerable charge transfers during the adsorption of toluene molecule onto the TM-doped SiCNS. The observations show that TM-doped SiCNSs are highly sensitive toluene molecules. Thus, TM-doped SiCNSs are suitable to be storage and sensing materials for toluene molecule.

5. Acknowledgement

The authors gratefully acknowledge the Computational Chemistry Center for Nanotechnology (CCCN) and Department of Chemistry, Faculty of Science and Technology, and Research and Development Institute, Rajabhat Maha Sarakham University for the facilities provided. Our also extends to gratitude Promotion of Science and Mathematics Talented Teachers (PSMT) for partial financial support.

References

1. Kim, K.-H., Szulejko, J. E., Raza, N., Kumar, V., Vikrant, K., Tsang, D. C. W., ... Khan, A. (2019). Identifying the best materials for the removal of airborne toluene based on performance metrics - A critical review. *Journal of Cleaner Production*, 241, 118408.
2. Chiang, Y.-C., Chiang, P.-C., & Huang, C.-P. (2001). Effects of pore structure and temperature on VOC adsorption on activated carbon. *Carbon*, 39(4), 523-534.
3. Su, Y., Ao, Z., Ji, Y., Li, G., & An, T. (2018). Adsorption mechanisms of different volatile organic compounds onto pristine C₂N and Al-doped C₂N monolayer: A DFT investigation. *Applied Surface Science*, 450, 484-491.

4. Kunaseth, M., Poldorn, P., Junkeaw, A., Meeprasert, J., Rungnim, C., Namuangruk, S., ... Jungsuttiwong, S. (2017). A DFT study of volatile organic compounds adsorption on transition metal deposited graphene. *Applied Surface Science*, 396, 1712-1718.
5. Mandeep, Sharma, L., & Kakkar, R. (2018). DFT study on the adsorption of p-nitrophenol over vacancy and Pt-doped graphene sheets. *Computational and Theoretical Chemistry*, 1142, 88-96.
6. Yi, F.-Y., Lin, X.-D., Chen, S.-X., & Wei, X.-Q. (2008). Adsorption of VOC on modified activated carbon fiber. *Journal of Porous Materials*, 16(5), 521-526.
7. Zhou, K., Ma, W., Zeng, Z., Ma, X., Xu, X., Guo, Y. Guo, H. Li, L. Li, (2019). Experimental and DFT study on the adsorption of VOCs on activated carbon/metal oxides composites. *Chemical Engineering Journal*, 372, 1122-1133.
8. Yu, L., Wang, L., Xu, W., Chen, L., Fu, M., Wu, J., & Ye, D. (2018). Adsorption of VOCs on reduced graphene oxide. *Journal of Environmental Sciences*, 67, 171-178.
9. Delavari, N., & Jafari, M. (2018). Electronic and optical properties of hydrogenated silicon carbide nanosheets: A DFT study. *Solid State Communications*, 275, 1-7.
10. Ansari, R., Rouhi, S., Mirnezhad, M., & Aryayi, M. (2013). Stability characteristics of single-layered silicon carbide nanosheets under uniaxial compression. *Physica E: Low-Dimensional Systems and Nanostructures*, 53, 22-28.
11. Chabi, S., Chang, H., Xia, Y., & Zhu, Y. (2016). From graphene to silicon carbide: ultrathin silicon carbide flakes. *Nanotechnology*, 27(7), 075602.
12. Wang, N., Tian, Y., Zhao, J., & Jin, P. (2016). CO oxidation catalyzed by silicon carbide (SiC) monolayer: A theoretical study. *Journal of Molecular Graphics and Modelling*, 66, 196-200.
13. Sun, L., & Hu, J. (2018). Adsorption of O₂ on the M doped (M=Fe, Co, Al, Cu, and Zn) SiC sheets: DFT study. *Computational Condensed Matter*, 16, e00323.
14. Tabtimsai, C., Kansawai P., Phoson P., Pooboontong P., Wannoo B., Adsorption of CO₂ on Ga- and B-doped silicon carbide nanosheets: A theoretical study. *The 5th International Conference on Sciences and Social Sciences 2015 (ICSSS 2015): Research and Innovation for Community and Regional Development*, Rajabhat Maha Sarakham University, Thailand, September 17-18, 2015.
15. Tabtimsai, C., Ruangpornvisuti, V., Tontapha, S., & Wannoo, B. (2018). A DFT investigation on group 8B transition metal-doped silicon carbide nanotubes for hydrogen storage application. *Applied Surface Science*, 439, 494-505.
16. A.D. Becke, Density-functional exchange-energy approximation with correct asymptotic behavior, *Phys. Rev. A* 38 (1988) 3098-3100.
17. A.D. Becke, Density-functional thermochemistry. III. The role of exact exchange, *J. Chem. Phys.* 98 (1993) 5648-5652.
18. C. Lee, W. Yang, R.G. Parr, Development of the Colle-Salvetti correlation-energy formula into a functional of the electron density, *Phys. Rev. B* 37 (1988) 785-789.
19. P.J. Hay, W.R. Wadt, Ab initio effective core potentials for molecular calculations. Potentials for the transition metal atoms Sc to Hg, *J. Chem. Phys.* 82 (1985) 270-283.
20. W.R. Wadt, P.J. Hay, Ab initio effective core potentials for molecular calculations. Potentials for main group elements Na to Bi, *J. Chem. Phys.* 82 (1985) 284-298.
21. P.J. Hay, W.R. Wadt, Ab initio effective core potentials for molecular calculations. Potentials for K to Au including the outermost core orbitals, *J. Chem. Phys.* 82(1985) 299-310.
22. M.J. Frisch, G.W. Trucks, H.B. Schlegel, G.E. Scuseria, M.A. Robb, J.R. Cheeseman, J.A. Jr. Montgomery, T. Vreven, K.N. Kudin, J.C. Burant, J.M. Millam, S.S. Iyengar, J. Tomasi, V.

- Barone, B. Mennucci, M. Cossi, G. Scalmani, N. Rega, G.A. Petersson, H. Nakatsuji, M. Hada, M. Ehara, K. Toyota, R. Fukuda, J. Hasegawa, M. Ishida, T. Nakajima, Y. Honda, O. Kitao, H. Nakai, M. Klene, X. Li, J.E. Knox, H.P. Hratchian, J.B. Cross, V. Bakken, C. Adamo, J. Jaramillo, R. Gomperts, R.E. Stratmann, O. Yazyev, A.J. Austin, R. Cammi, C. Pomelli, J.W. Ochterski, P.Y. Ayala, K. Morokuma, G.A. Voth, P. Salvador, J.J. Dannenberg, V.G. Zakrzewski, S. Dapprich, A.D. Daniels, M.C. Strain, O. Farkas, D.K. Malick, A.D. Rabuck, K. Raghavachari, J.B. Foresman, J.V. Ortiz, Q. Cui, A.G. Baboul, S. Clifford, J. Cioslowski, B.B. Stefanov, G. Liu, A. Liashenko, P. Piskorz, I. Komaromi, R.L. Martin, D.J. Fox, T. Keith, M.A. Al-Laham, C.Y. Peng, A. Nanayakkara, M. Challacombe, P.M.W. Gill, B. Johnson, W. Chen, M.W. Wong, C. Gonzalez, J.A. Pople GAUSSIAN 09, Revision A.02, Gaussian Inc, Wallingford CT, 2009.
23. P. Flükiger, H.P. Lüthi, S. Portmann, MOLEKEL 4.3, Swiss center for scientific computing. Manno, Switzerland, 2000.
24. O'boyle, N. M., Tenderholt, A. L., & Langner, K. M. (2008). cclib: A library for package-independent computational chemistry algorithms. *Journal of Computational Chemistry*, 29(5), 839-845.
25. Farmanzadeh, D., & Ardehjani, N. A. (2018). Adsorption of O₃, SO₂ and NO₂ molecules on the surface of pure and Fe-doped silicon carbide nanosheets: A computational study. *Applied Surface Science*, 462, 685-692.
26. Goudarziafshar, H., Abdolmaleki, M., Moosavi-zare, A. R., & Soleymanabadi, H. (2018). Hydrogen storage by Ni-doped silicon carbide nanocage: A theoretical study. *Physica E: Low-Dimensional Systems and Nanostructures*, 101, 78-84.
27. Bezi Javan, M., Houshang Shirdel-Havar, A., Soltani, A., & Pourarian, F. (2016). Adsorption and dissociation of H₂ on Pd doped graphene-like SiC sheet. *International Journal of Hydrogen Energy*, 41(48), 22886-22898.

Rapid Analysis of Alpha-Mangostin Content in Anti-Acne Gel by Near-Infrared Spectroscopy

Sumaporn Kasemsumran^{1,a}, Udomlak Sukatta^{2,b}, Krairuek Ngowsuwan^{1,c}, Sirimada Monkolwit^{1,d},
Nattaporn Sinunta^{1,e}, Prapassorn Rugthaworn^{2,f}

¹Nondestructive Quality Evaluation of Commodities Technology Unit, Kasetsart Agricultural and Agro-Industrial Product Improvement Institute (KAPI), Kasetsart University, Bangkok, 10900 Thailand

²Herb and Bioactive Compound Technology Unit, KAPI, Kasetsart University, Bangkok, 10900 Thailand

E-mail; ^aaapspk@ku.ac.th, ^baapuls@ku.ac.th, ^caapkkn@ku.ac.th, ^dtoon_body_0036@hotmail.com, ^eaapntp@ku.ac.th, ^faappspr@ku.ac.th

Abstract

Mangosteen is considered as the queen of fruit in Thailand. In addition, it gives the delicious taste liked by both Thailand and overseas countries. Moreover, there are essential substances of xanthenes in mangosteen pericarp that have great bioactivities. Currently, the cosmetic and other industries employ the use of crude extracts from the mangosteen a lot. However, the crude extract may contain a small amount of xanthenes, in which it affects the quality of the product. Especially, the alpha-mangostin is the highest substance in xanthone that actives for the anti-oxidant, anti-inflammatory, and anti-microbial activities. Therefore, it is essential to determine the content of alpha-mangostin in the product, in order to evaluate the effect and to control the quality. The conventional method for qualitative analysis of alpha-mangostin in the cosmetic product is consisting of several processes as extraction and then separation by of high-performance liquid chromatography (HPLC). This conventional method is very hard work, in which it consumes time, labors, costs, chemicals, materials, and samples. The objective of this study is to apply the near-infrared spectroscopic (NIRS) technique to analyze the amount of alpha-mangostin in the cosmetic product of anti-acne gel. NIRS technique is well-known as the non-destructive method and can be solved the weaknesses of that conventional method. A total of fifty-seven samples of anti-acne gel adding the purified xanthone from 0.00-0.05%w/w were prepared. NIR spectral data of these anti-acne gels samples were obtained by two NIR spectrophotometers in the wavelength region of 680-1278 nm and 10000-4000 cm⁻¹, respectively. Next, all anti-acne gel samples were chemically extracted and determined alpha-mangostin content with the conventional method of HPLC. The actual content of alpha-mangostin found in the samples, were 0.00-36.11 ug/mL. The calibration models were developed by using partial least squares regression (PLSR) method. Current results demonstrated that the NIR analysis can be used to determine alpha-mangostin content in anti-acne gels, in which the best obtained model using the region of 10000-4000 cm⁻¹ with a principal component of 11, yielded high value for the coefficient of determination (R²) of 0.958 and low values for the standard error of calibration of 2.131 ug/mL and the standard error of cross-validation of 4.389 ug/mL.

Keywords: Near-Infrared spectroscopy (NIRS); xanthone; alpha-mangostin; mangosteen; cosmetic

Introduction

The fruit queen of Thailand is mangosteen. Mangosteen is popularly grown in the eastern and southern regions of Thailand, which can produce much mangosteen every year to meet the needs of the domestic market and for export. It has both potentials as fruit and herb with high nutritional and health benefits for consumers. There are many health benefits, such as mangosteen fiber helps to excrete and give high vitamins and minerals, including calcium, phosphorus and iron. The benefits of mangosteen are not just the flesh of the mangosteen that we use as food only. But also, there are many medicinal and bioactive properties found in the mangosteen pericarps (Sukatta et al., 2013, pp.984-987).

Currently, the mangosteen crude extract and purified xanthone are utilized very much in the cosmetic and health supplement industries. Especially, the purified xanthenes have played a significant role when considering the bioactivity and physical characteristics in comparison to the crude extract. When it is used in combination with cosmetic formulas of product, the acceptable

quality of the product has to be assured. Once the product is in place, the xanthenes by mean of alpha-mangostin detection in the product enable manufacturers to control product quality efficiently. However, the general inspection method at the laboratory level takes a long time with complicated procedures. It also requires analytical techniques consisting of advanced tools such as High Performance Liquid Chromatography (HPLC) and many chemicals. These conventional analyses produce chemical waste. Besides, the product samples that have passed quality inspection are destroyed.

Near-Infrared (NIR) spectroscopy has proved to be a powerful method for the quantitative analysis of the constituents in various products. Our previous researches, we reported the study of the analytical method of bioactive substances in herbs and products using NIR spectroscopic technique, such as curcuminoids in turmeric rhizomes (Kasemsumran et al., 2010, pp.263-269) and curcumin in turmeric herbal medicine filled in capsules (Kasemsumran et al., 2014, pp. 113-120). NIR is an alternative method for rapid and non-destructive analysis by using the absorption band in the NIR wavelength region rising from those NIR active molecules in the sample. It can increase the opportunity for 100% quality inspection of the sample.

The aim of the present study was non-destructive determination for alpha-mangostin content in anti-acne gel by using NIR spectroscopy. In this study, two different of the short wavelength-NIR region (680-1278 nm) with the grating system and long wavelength-NIR region (10000-4000 cm^{-1}) with the Fourier-Transform (FT) system were investigated in order to prove the best informative NIR spectral ranges for alpha-mangostin modeling development and recommend for further application.

Methodology

1.1. Xanthone purification and Anti-acne gel sample

The waste from consumption of mangosteen is the fresh pericarps, in which they were collected and cleaned prior slicing, drying at 50°C for 48 hours by using a hot air oven (Memmert, Germany), and grinding into powder passed through the 20 mesh of sieve size by Cyclotec1093 (FOSS, Hillerod, Denmark). The different lots of mangosteen pericarp powder were prepared from different waste origins. After that, each dried powder of mangosteen pericarp was extracted and purified. The xanthone purification was done to prepare the high purity of xanthone (100%) as the active ingredient for anti-acne gel samples as the following steps. HPLC was used to find the purity of xanthone, which obtained alpha-mangostin higher than 70%. All process of extraction and purification of xanthone from mangosteen pericarp powder were reported in our previous study (Sukatta et al., 2013, pp.984-987).

The production of anti-acne gel containing xanthone from mangosteen pericarp using the basic formula of anti-acne gel reported in our previous research (Sukatta et al., 2008, pp. 163-168), which passed the stability test of the basic formula with high stability. A total of 57 anti-acne samples were prepared by mixing the purify xanthone with fixing the concentration level of 0.00, 0.01, 0.02, 0.03, 0.04 and 0.05%w/w, respectively.

1.2. Spectral acquisition

Two NIR spectrophotometers, a grating NIR spectrophotometer model SpectraStar™ 2500 (Unity Scientific, USA) (Figure 1A) and a FT-NIR spectrophotometer model NIRFlex N-500 (Buchi Labortechnik AG, Switzerland) (Figure 1B) were used with the same sensor type of InGaAs by reflectance mode for the NIR spectral acquisition of anti-acne gel samples with the different wavelength region between 680-1285 nm and 10000-4000 cm^{-1} , respectively. A sample container with 0.2 mm of pathlength called “Dutch cup” was employed in the NIR spectral acquisition of an anti-acne gel sample for both instruments throughout the experiment. Each sample was scanned twice by random sampling in the same sample. The average spectrum of each sample was employed for data analysis.

1.3. Reference analysis

After the anti-acne gel sample was collected NIR spectral data from two NIR instruments. Then, the same anti-acne gel samples were extracted by ethanol and were detected of alpha-mangostin content by HPLC model LC-10Avp (Shimadzu, JAPAN) with column Ascentis®C18, 4.6mm ID x 250mm 5 μm (Supelco, USA) as a reference method. The alpha-mangostin standard was purchased

from Sigma-Aldrich (Missouri, USA) and employed without further purification. The purity of alpha-mangostin standard was determined by the HPLC method to be higher than 98%. The HPLC equipped with LC solution software, quaternary pump, online degasser and auto-injector were used. The detector used was a UV detector at 254 nm. The HPLC conditions were maintained as follows; mobile phase; 0.4% formic acid in water: methanol (10:90), flow rate; 1.0 mL/min, column temperature; 35 oC, and injection volume; 10 µL. Statistical characteristics of alpha-mangostin content in the anti-acne gel samples determined by the HPLC method as reference analysis are shown in Table 1.

1.4. Data analysis

All spectral preprocessing and partial least squares (PLS) regression were performed using The Unscrambler 9.8 (CAMO AS, Trondheim, Norway). PLS method is a linear regression technique. It is a bilinear modeling method using the information of X-data that are obtained absorbance at each NIR wavelength region, projected to compressed variables so-called principal component (PC). Y-data are the content of analysts obtained from the reference analyses, which are used in estimating PC for their relevance (Næs, Isaksson, Fearn, and Davies, 2002). The NIR spectral data were subjected to the preprocessing methods of multiplicative scatter correction (MSC), second-derivative (2D; 7-point Savitsky-Golay filter) and standard normal variate (SNV) algorithms before developing PLS models using the data of the calibration samples. The optimum number of PC can be obtained from the lowest standard error of cross-validation SECV). Validation was performed by using the same sample set by mean of the full-cross validation method. The statistical results of the PLS models built using the raw and pretreated spectra were compared.



Figure 1. The same anti-acne gel sample was carried on to collect the NIR spectra using a grating NIR spectrophotometer model SpectraStar™ 2500 (A) and a FT-NIR spectrophotometer model NIRFlex N-500 (B).

Table 1. Statistical characteristics of the anti-acne gel sample used to develop PLS calibration model of alpha-mangostin content for NIR analysis.

Analyst (ug/mL)	Samples	Minimum	Mean	Maximum	Standard deviation
Alpha-mangostin	57	0.000	14.695	36.109	10.391

Results and discussion

1.1. NIR spectra of anti-acne gel containing xanthone

Figure 2 shows raw NIR spectra in the region of 680-1278 nm (Figure 1A) and 10000-4000 cm^{-1} (Figure 1B) of anti-acne gel samples. A major component of anti-acne gel is water. Therefore, a strong absorption band near 960 nm (Figure 1A) is assigned to the third overtone of OH, and 6900 cm^{-1} and 5150 cm^{-1} (Figure 1B) are assigned to the combination of OH symmetric and antisymmetric stretching modes, and the combination of OH stretching and bending vibrations, respectively (Maeda et al., 1995, pp.191-201). The chemical structure of xanthone groups consists of aromatic group and hydrogen bond in the form of CH and OH, which can affect highly response in the NIR region. It can be seen from Figure 2 that the xanthenes yield a relatively weak absorption band near 1250 nm and in the 4800-4200 cm^{-1} region. Bands due to the combinations of stretching and deformation modes of CH and OH groups fall in this region (Workman & Weyer, 2007).

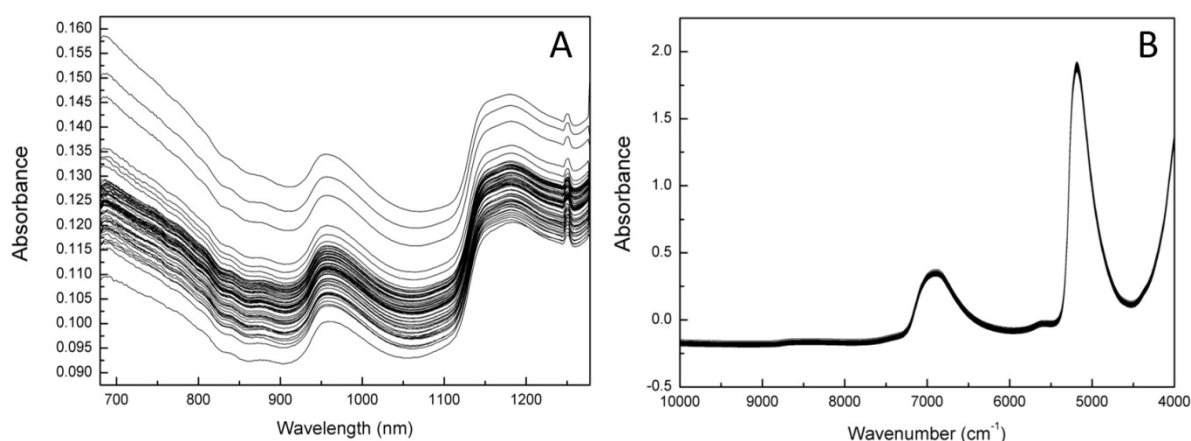


Figure 2. Raw NIR spectra of all anti-acne gel samples obtained using a grating NIR spectrophotometer model SpectraStar™ 2500 in the wavelength region of 680-1278 nm (A) and a FT-NIR spectrophotometer model NIRFlex N-500 in the wavenumber region of 10000-4000 cm^{-1} (B).

1.2. Calibration and validation results

PLS regression method was applied to the whole regions for the quantitative determination of alpha-mangostin in the anti-acne gel samples. Table 2 summarizes the results for the calibration and validation. We compare the calibration and validation results between the 680-1278 nm (SW-NIR) and 10000-4000 cm^{-1} (LW-NIR) regions obtained by the PLS method. It can be seen from Table 2 that the PLS model built using the second derivative (2D) SW-NIR spectra of 10000-4000 cm^{-1} region is the best model with the lowest SECV for cross-validation of 4.389 $\mu\text{g/mL}$, the high R^2 values of 0.958 and the optimum PC number of 11. The most important criteria to select the best model is the validation result with giving the lowest error by using an optimum PC number (the number should not too small or too big that cause high error due to effect of the underfitting and overfitting results, respectively) and the high R^2 values (William, 2007). The 2D pretreatment method was required to enhance the signal for this PLS model development in the LW-NIR region of 10000-4000 cm^{-1} , especially the informative absorption band in the 4800-4200 cm^{-1} region (Figure 3A). This model using the 2D spectra yielded better statistical results among those models developed from the same region. As mentioned above, the peaks attributable to water observed in the SW-NIR spectral region. The PLS regression models indicate that the SW-NIR spectral region is the less informative band of xanthone, so the use of SW-NIR regions (680-1278 nm) did not improve the predictive performance of PLS model for prediction of alpha-mangostin contents in the anti-acne gel. The presence of the relative significant peaks in the SW-NIR spectral may relate to water more than xanthone. The scatter plot for the best calibration model for the quantitative determination of alpha-mangostin in the anti-acne gel samples built using the 2D pretreated LW-NIR spectra of 10000-4000 cm^{-1} are shown in Figure 3B.

Table 2. PLS calibration results for predicting alpha-mangostin content in anti-acne gel.

Region	Spectra pretreatment	PC	Calibration		Full-Cross Validation	
			R ²	SEC (ug/mL)	R ²	SECV (ug/mL)
680-1278 nm	none	14	0.982	1.385	0.584	6.825
	2D	6	0.852	3.994	0.311	8.782
	MSC	7	0.803	4.609	0.424	8.027
	SNV	17	0.994	0.826	0.543	7.150
10000-4000 cm ⁻¹	none	20	0.992	0.939	0.773	5.036
	2D*	11	0.958	2.131	0.828	4.389
	MSC	14	0.958	2.124	0.759	5.196
	SNV	14	0.958	2.123	0.759	5.195

PC = principal component; R² = coefficient of determination; SEC = standard error of calibration; SECV = standard error of cross validation; 2D = second derivative; MSC = multiplicative scattering correction; SNV = standard normal variate

*The selected NIR calibration model.

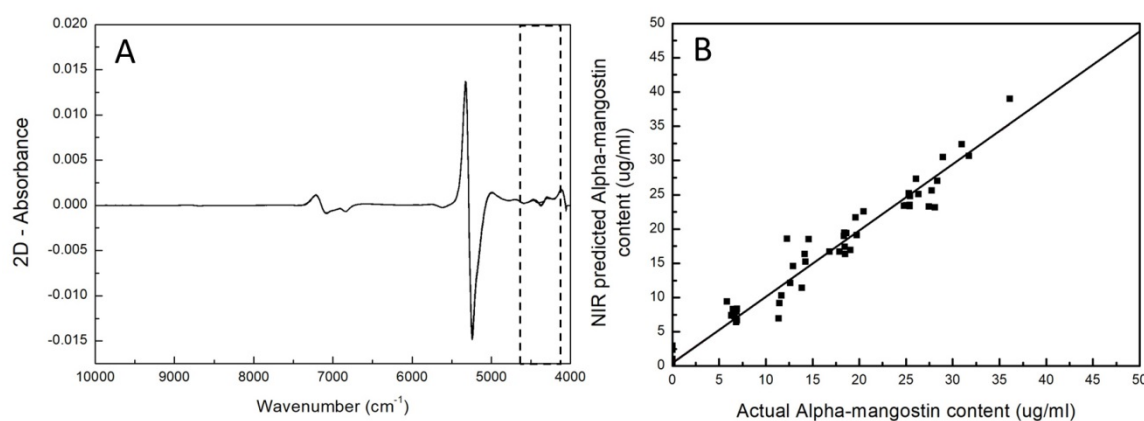


Figure 3. Second derivative (2D) pretreated NIR spectra of all anti-acne gel samples in the LW-NIR region of 10000-4000 cm⁻¹(A) and scatter plot for actual alpha-mangostin content and LW-NIR predicted alpha-mangostin content in anti-acne gels for the best calibration model built by using 2D pretreated spectral data (B).

Conclusion

The NIR spectra of anti-acne gels containing xanthone were collected in the region of 680-1278 nm and 10000-4000 cm⁻¹ using the same reflectance mode and sample container. The PLS calibration models for the alpha-mangostin content were developed and compared. The results obtained in the present study have demonstrated that the 10000-4000 cm⁻¹ region (LW-NIR range) and the second derivative pretreatment spectra achieved superior PLS model performance compared with the models developed using spectral data obtained from the 680-1278 nm region. The results showed the success of NIR spectroscopy in the quantitative analysis of alpha-mangostin in the anti-acne gel containing xanthone. This study revealed that NIR is a promising and possible technique for quality control in the cosmetic industry.

Acknowledgements

The authors gratefully thank to Kasetsart University for the financial support.

References

- Kasemsumran, S., Keeratinijakal, V., Thanapase, W. & Ozaki, Y. (2010) Near infrared quantitative analysis of total curcuminoids in rhizomes of *Curcuma longa* by moving window partial least squares regression. *Journal of Near Infrared Spectroscopy*, 18, 263-269.
- Kasemsumran, S., Apiwatanapiwat, W., Suthiwijitpukdee, N., Vaithanomsat, V., & Thanapase, W. (2014). Evaluation of fourier transform - near infrared spectroscopic measurements for the quantification of curcumin in turmeric herbal medicines. *Journal of Near Infrared Spectroscopy*, 22, 113-120.
- Maeda, H., Ozaki, Y., Tanaka, M., Hayashi, N., & Kojima, T. (1995). Near infrared ipectroscopy and chemometrics studies of temperature-dependent spectral variations of water: Relationship between spectral changes and hydrogen bonds. *Journal of Near Infrared Spectroscopy*, 3, 191-201.
- Næs, T., Isaksson, T., Fearn, T., & Davies, T. (2002). *A user-friendly guide to multivariate calibration and classification*. West Sussex, UK. NIR Publications.
- Sukatta, U., Takenaka, M., Ono, H., Okadome, H., Sotome, I, Nanayama, K., Tanapase, W., & Isobe, S. (2013). Distribution of major xanthones in the pericarp, aril, and yellow gum of mangosteen (*garcinia mangostana* Linn.) fruit and their contribution to antioxidative activity. *Bioscience, Biotechnology, and Biochemistry*, 77, 984-987.
- Sukatta, U., Rugthaworn, P., Pitpiangchan, P., & Dilokkunanant, U. (2008). Development of mangosteen anti-acne gel. *Kasetsart Journal (Natural Science)*, 42,163-168.
- Williams, P. (2007). *Near-infrared technology-Getting the best out of light*. (5th ed.) PDK Grain, Nanaimo, British Columbia, and Winipeg, Manitoba, Canada.
- Workman, J., & Weyer, Jr. L. (2007). *Practice guide to interpretive near infrared spectroscopy*. New York. CRC press.

Screening and identification of the phytase producing bacteria isolated from natural environments and swine manure

Songkran Chuakrut^{1, a}, Apiwat Limsawad^{2, b}, Lakkhana Pom Khet^{3, c}, Aunchalee Thanwisai^{1, d}

¹Department of Microbiology and Parasitology, Faculty of Medical Science,
Naresuan University, Phitsanulok, Thailand

²Central Laboratory (Thailand) Co.,Ltd, Chiangmai, Thailand

³Asia Medical and Agricultural Laboratory and Research Center Co.,Ltd, Bangkok, Thailand

E-mail; ^asongkranc@nu.ac.th, ^bapiwat.juy@gmail.com, ^ctewter16@gmail.com, ^daunchaleet@nu.ac.th

Abstract

Swine waste odor caused by the degradation of the residue organic phosphorus, phytate, in animal diet by heterotrophic bacteria is a major community problem of the local swine farms. This research aimed to isolate, screen and identify the photosynthetic bacteria and lactic acid bacteria that produced an intracellular or extracellular phytase to hydrolyze phytate. A total of 124 isolates of photosynthetic bacteria were purified on Glutamate-malate medium under anaerobic-light conditions and 115 isolates of lactic acid bacteria were isolated on deMan, Rogosa and Sharpe medium. The phytase producing strains were screened on the same agar media containing phytate as a sole phosphorus source and detected by flooding the cultures with cobalt chloride and ammonium molybdate-vanadate solutions. Both bacterial groups could grow on the modified media and had a clear zone around the cultures or under the cultures, indicating a localization of phytase. Although the 63 isolates of photosynthetic bacteria had a clear zone under the cultures, an intracellular phytase activity was not detectable from the bacterial cells. In contrast, extracellular phytase activities were detected in the culture broth of 61 lactic acid bacteria isolates. P6C3 and TPS9, lactic acid bacteria isolates, showed the maximum phytase specific activity as 6.42 ± 0.16 and 6.08 ± 0.28 U mg⁻¹, respectively. These isolates were selected to study the physiological and biochemical characteristics. The selected strains were identified by the 16S rDNA sequencing using 27F and 1492R as forward and reverse primers, respectively. The phytase producing lactic acid bacteria isolated from fresh swine manure were identified as 5 different species: *Lactobacillus plantarum*, *L. agilis*, *L. farciminis*, *L. fermentum* and *Enterococcus faecium*.

Keywords: Photosynthetic bacteria; Lactic acid bacteria; Phytase; Swine wastewater; Identification

1. Introduction

A major problem of the local swine farming is an odor from swine wastewater in the lagoons. The swine waste odor is caused by the heterotrophic bacterial degradation of the residue organic phosphorus. GC-MS analysis indicates that swine waste odor was composed of 167 volatile organic carbon (VOCs) (Schiffman, *et al.* 2001) including phytate, an inositol ester found in plant foods such as cereal grains, nuts and legumes. The monogastric animals such as swine lack an endogenous phytase to hydrolyze phytate. Therefore, this VOC is released to the farming areas and nearby community, causing severe environmental pollution. Many researchers try to solve this problem by employing bioremediation to clean up swine wastewater. Hirotani, *et al.* (1990) used photosynthetic bacteria, *Rhodobacter capsulatus*, to purify swine wastewater. They found that this bacterium could produce anti-viral compound to inactivate coliphage in wastewater over 80%. Kim, *et al.* (2004) used a photosynthetic bacterium, *Rhodospseudomonas palustris*, to treat odorous swine wastewater. The results showed that this bacterium removed odorous organic acids, COD and phosphate. While phytase enzymes have been extensively studied in other microbes such as lactic acid bacteria, no previous work reported the presence of these enzymes in photosynthetic bacteria. The purified phytase can be applied to the animal feeds to improve their nutrition nutritional quality for young animals whereas the phytase producing bacteria can reduce environmental impact of phytate from farm animals.

This research aimed to isolate, screen and identify the photosynthetic bacteria and lactic acid bacteria that produced the phytase enzyme to hydrolyze phytate *in vitro*.

2. Objectives

2.1 To isolate the photosynthetic bacteria and lactic acid bacteria from natural environments and swine manure

2.2 To screen the phytase producing bacteria and assay the enzyme

2.3 To identify the species of the selected bacterial strains

3. Methodology (Materials and Methods)

3.1 Isolation of the bacteria

3.1.1. Photosynthetic bacteria

Samples of waters, paddy soils in rice fields and swine wastewaters in Phitsanulok, Sukhothai, Phetchanum, Phichit and Kamphaeng Phet provinces were collected in the sterile plastic tubes. All the samples were mixed with 0.85% NaCl solutions by the ten-fold serial dilution method. The 10^{-1} - 10^{-4} dilutions were spread on Glutamate-Malate (GM) agar medium. Then, the agar plates were incubated under anaerobic-light conditions by replacement of the air with nitrogen gas and using tungsten bulb as the light source. The cultures were grown at 35-38 °C and light intensity of approximately 3,000 Lux for 3-5 days. After an incubation period, the colonies of photosynthetic bacteria appeared to be greenish brown, rust and red colors on the GM agar plates. For each color, a single colony was picked and stabbed into a GM agar deep tube. The agar deep cultures were covered with sterilized liquid paraffin for anaerobic-light incubation. Pure cultures were stored at 4 °C and subcultured every 3 months.

3.1.2. Lactic acid bacteria

Samples of fresh swine manure in Phitsanulok and Sukhothai provinces were collected in the sterile plastic tubes and transferred to laboratory within 2 hours. All the samples were serially diluted to 10^{-5} with 0.85% NaCl solutions. The 10^{-3} - 10^{-5} dilutions were spread on De Man, Rogosa and Sharpe (MRS) agar medium plus 1.0% CaCO_3 . The agar plates were incubated under anaerobic condition by using Anaero Pack (Mitsubishi, Japan) at 30-32 °C for 48 hours. After incubation, the grey-white colonies of lactic acid bacteria appeared on the agar plates with clear zone. A single colony from the different characteristics was transferred into MRS broth and incubated for 24 hours. Each liquid culture was mixed in equal volume with 80% sterilized glycerol solution for preparation of the glycerol stock. The glycerol stock was stored at -80 °C until use.

3.2 Screening of the phytase producing bacteria

3.2.1 Photosynthetic bacteria

Pure cultures were streaked on the modified GM medium that did not have any phosphate ingredient, had ammonium sulphate as an inorganic nitrogen source and 0.5% sodium phytate (Sigma-Aldrich, USA) as a sole phosphorus source. Cultures were incubated at 35-38 °C under anaerobic-light conditions for 5 days. To screen for an extracellular phytase produced from the photosynthetic bacteria, 2.0% cobalt chloride solution was flooded on the agar plates for 5 minutes. During incubation, cultures on the surface medium were removed by scrapping with a cotton bud. Then, the solution was poured out and replaced by the fresh mixture in equal volume of 6.25% ammonium molybdate solution and 0.42% ammonium metavanadate solution for 5 minutes. The occurrence of a clear zone around a colony on an opaque background indicates the presence of phytate hydrolysis by phytase enzyme (Yanke *et al.*, 1998).

3.2.2 Lactic acid bacteria

Pure cultures were streaked on the modified MRS medium that did not have K_2HPO_4 and had sodium phytate as a sole phosphorus source. Cultures were incubated at 30-32 °C under anaerobic condition for 72 hours. The cultures were flooded with cobalt chloride solution and the mixture of molybdate-vanadate solution, respectively. A clear zone around a colony indicates the presence of an extracellular phytase.

3.3 Phytase assay

3.3.1 Intracellular phytase

The bacteria with clear zone on the modified medium were streaked on the same medium supplemented with 0.25% sodium phytate. Cultures were incubated under an optimum growth condition for each bacterial group. Crude enzyme was prepared by scrapping the cultures on surface medium. Bacterial cells were washed and resuspended in 0.1 M acetate buffer pH 6.0. To obtain an intracellular phytase, cells were disintegrated by ultra-sonication (Sonics & Materials Vibra Cell, USA) for 3 minutes. Crude enzyme within the disrupted cells was separated by centrifugation at 7,280 ×g, 4 °C for 10 minutes (Beckman Avanti 30 Refrigerated Centrifuge, USA). The supernatant was collected and designated as a crude phytase. An assay procedure was based on the ammonium molybdate method (Heinonen and Lahti, 1981). The reaction mixture for the phytase assay consisted of 0.1 M sodium acetate 250 µL and 3.6 mM sodium phytate 100 µL. An enzymatic reaction was started by adding crude enzyme 50 µL and incubated at 37 °C for 30 minutes. The reaction was stopped by adding 5% trichloroacetic acid. To determine an enzymatic activity of phytate hydrolysis to inositol and inorganic phosphate, 10 mL color reagent (1.5% molybdate, 5.5% sulfuric acid and 2.7% ferrous sulfate) was added and mixed well by a vortex mixer. A color of the solution developed to be blue. An absorbance at 700 nm of the solution was measured using a spectrophotometer. Amount of the liberated inorganic phosphate from the phytase hydrolysis was compared to the standard curve of K_2PO_4 that reacted with the color reagent. One unit (U) of phytase was defined as amount of the enzyme that hydrolysed phytate and liberated inorganic phosphate 1.0 µmol per minute at pH 6.0.

3.3.2 Extracellular phytase

The bacterial colonies with clear zone on the modified medium were inoculated in the modified liquid medium. Cultures were grown under an optimum growth condition for each bacterial group. Crude enzyme was prepared by centrifugation of the culture broth at 7,280 ×g, 4 °C for 10 minutes. The supernatant was collected and designated as a crude phytase. An assay procedure was based on the method of Sigma-Aldrich. Preincubation of 44.1 mM sodium phytate 500 µL was performed at 37 °C in a waterbath for 5 minutes. Then, 200 mM glycine buffer pH 2.5, 500 µL was added and mixed well. The reaction was started by adding crude enzyme 500 µL and incubated at 37 °C for 30 minutes. The reaction was stopped by adding the color reagent 4 mL (5% ammonium molybdate solution, 5 N sulfuric acid and acetone in the ratio of 1:1:2, respectively). This reaction produced green color which can be quantified by measuring light absorption at 435 nm. The amount of liberated inorganic phosphate was estimated by comparing 435 nm light absorption of the sample to that of KH_2PO_4 standard curve as described above.

One unit of phytase was defined as the amount of the enzyme that hydrolysed phytate and liberated inorganic phosphate 1.0 µmol per minute at pH 2.5.

3.4 Identification of the selected bacteria

3.4.1 Biochemical and physiological characteristics

Photosynthetic bacteria were characterized by the following properties: Gram reaction; cell shape and arrangement; motility; growth under anaerobic-light conditions and maximum absorption spectra of the extracted pigments (acetone:methanol). For lactic acid bacteria, the following characteristics were confirmed: Gram reaction; cell shape and arrangement; catalase test; acid production on MRS supplemented with 1% CaCO₃; gas production from glucose fermentation.

3.4.2 Analysis of 16S rDNA sequence

3.4.2.1 Amplification of the 16S rDNA gene

The selected strains of the bacteria were cultured on the agar plates. A single colony of each bacterial strain was picked by a sterile pipette tip and resuspended in 50 µL sterilized distilled water. Cell suspension was heated in boiling water for 5 minutes. Then, the suspension was centrifuged at 12,303 ×g, 4 °C for 2 minutes. The supernatant 2.0 µL was pipetted into a sterile RCR tube as a DNA template. The reaction mixture for the polymerase chain reaction was prepared as following compositions: sterilized distilled water 9.0 µL; 2× PCR buffer KOD Fx Neo 25 µL; 2.0 mM dNTPs (each) 10 µL; 10 pmol µL⁻¹ forward primer (27F) 1.5 µL; 10 pmol µL⁻¹ reward primer (1492R) 1.5 µL and 1.0 U µL⁻¹ DNA polymerase of KOD Fx Neo (Toyobo, Japan) 1.0 µL. The mixture 48 µL was added to the DNA template. The 16S rDNA genes were amplified by polymerase chain reaction (PCR). The PCR conditions were as follow: initial denaturation at 94 °C for 2 min; 30 cycles of denaturation at 98 °C for 10 sec, annealing at 50 °C for 30 sec, extension at 50 °C for 30 sec and final extension at 68 °C for 5 min.

3.4.2.2 Analysis of PCR products

Amplification of the 16S rDNA gene was checked by an agarose gel electrophoresis. The PCR products 5.0 µL were mixed with the Novel juice DNA staining reagent 1.0 µL (GeneDireX, Taiwan). M23 (2.5 µL or 0.5 µg DNA) consisted of 100 bp + 1.5 Kb DNA ladder was used as DNA marker (SibEnzyme, Russia). The different DNA fragment lengths were separated on 1.0% agarose gel with a constant voltage (50 V cm⁻¹). The separated DNA bands compared to the DNA marker were visualized in the agarose gel under UV light.

3.4.2.3 Nucleotide sequencing and analysis

The PCR products which had a positive DNA band approximate 1.5 kb on the agarose gel were sent for DNA sequencing at the company (BioBasic, Canada). The 16S rDNA gene was sequenced by using both forward (27F) and reverse (1492R) primer. DNA sequencing results from forward and reverse primer were aligned using ClustalW program. Those two DNA sequences were connected into a full 16S rDNA gene sequence. These new sequences were compared to similar sequences in the database by nucleotide blast (blastn) search (NCBI, U.S. National Library of Medicine). The highest 16S rDNA sequence identity score implies the most closely related species.

3.5 Statistical analysis

Experiments were performed in triplicate and the data was shown in the range and mean ± standard deviation with 95% confidence level.

4. Results and discussion

4.1 Isolation of the bacteria

4.1.1. Photosynthetic bacteria

Photosynthetic bacteria in this study are purple nonsulfur bacteria (PNSB) due to ability to grow well under photoheterotrophic conditions. PNSB used glutamate and malate as an organic carbon source whereas they absorbed light as an energy source (Madigan and Jung, 2009). When these bacteria grew on the medium under anaerobic-light conditions, a numerous pigmented colonies shading from brown to red were easily observed by eyes. In this study, PNSB were predominantly found in swine wastewaters, paddy soils and water in rice fields, respectively. The populations of PNSB in swine wastewaters were range from 2.5×10² to 7.5×10⁵ CFU mL⁻¹ (average 2.0±1.6×10⁴)

whereas the populations in paddy soils were range from 7.0×10^2 to 3.6×10^3 CFU g^{-1} (average $2.6 \pm 1.1 \times 10^3$). PNSB were found in the lowest number (average $2.0 \pm 1.7 \times 10^2$ CFU mL^{-1}) in the waters collected from rice paddy fields. These results are in consistent with that of Okubo *et al.* (2005) that reported populations of PNSB in treating wastewater ranged from 10^4 to 10^7 CFU mL^{-1} . One of the most favourable nutrients for PNSB is the short chain volatile fatty acids which accumulated in high organic loading wastewaters. In addition, two species of PNSB were isolated from swine waste lagoon and swine sewage wastewater. *Rhodobacter* sp. strain PS9 was isolated for odor remediation by Do, *et al.* (2003) and *Rhodopseudomonas faecalis* strain A was isolated and characterized by Wei, *et al.* (2016). In this study, PNSB 124 isolates were isolated in pure cultures. The culture characteristics of PNSB on GM medium were shown in Figure 1a.

4.1.2. Lactic acid bacteria

Lactic acid bacteria were isolated from fresh swine manure samples in Phitsanulok and Sukhothai provinces. The bacterial colonies with clear zone were observed and counted on MRS agar medium with 1.0% $CaCO_3$. The clear zone around the colonies result from the solubilisation of $CaCO_3$ by the acid(s) that produced from lactic acid bacteria. A number of lactic acid bacteria in the samples of fresh swine manure were range from 1.9×10^7 to 3.5×10^7 CFU g^{-1} (average $2.74 \pm 0.58 \times 10^7$). This result is similar to the report of Petsuriyawong and Khunajakr (2011) that screened probiotic lactic acid bacteria in piglet feces. They isolated and enumerated lactic acid bacteria that ranged from 8.03 to 8.97 log CFU g^{-1} . In this study, a number of lactic acid bacteria were lower than that report approximate 1 log CFU. It might be due to farm management, diet and animal health. One hundred fifteen isolates of lactic acid bacteria were isolated for further enzyme screening. The culture characteristics of lactic acid bacteria on MRS plus 1.0% $CaCO_3$ medium were shown in Figure 1b.

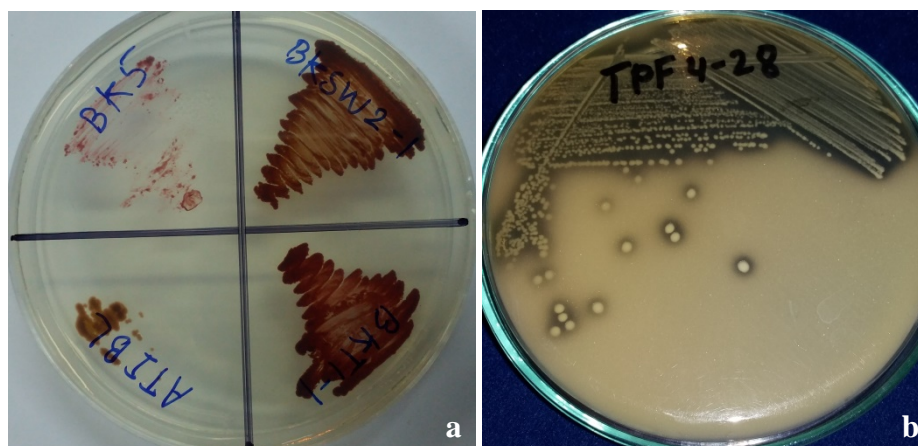


Figure 1. Culture characteristics of PNSB on GM agar plate (a) and lactic acid bacteria on MRS plus 1.0% $CaCO_3$ agar plate (b)

4.2 Screening of the phytase producing bacteria

4.2.1 Photosynthetic bacteria

A total of 124 PNSB isolates were screened for the production of phytase to hydrolyzed phytate. All the isolates were streaked on the modified GM medium with phytate as a sole phosphorus source. It was found that yeast extract in the medium affected bacterial growth. PNSB grew faster when amount of yeast extract was increased. To avoid an effect of yeast extract on the production of phytase, the modified GM medium was supplemented with 0.01 and 0.05% yeast extract. PNSB grew poorly when lower concentration of yeast extract was used. Therefore, yeast extract at the same original concentration (0.2%) was added into the modified GM medium.

It was interesting to note that most red to brown PNSB isolates were able to grow on the medium whereas the greenish brown isolates could not grow. It might be possible that those red to brown isolates were capable of hydrolyzing phytate and used the products as a phosphorus source for their growth. In this study, we could not find any clear zone around the PNSB cultures when the phytase was detected by flooding the color reagent. It means that they were not able to produce an

extracellular phytase. However, when the cultures were scrapped off, the clear zone under the cultures was seen with an opaque background. This clear zone possibly resulted from intracellular phytase. A total of 63 PNSB isolates had clear zone under the culture (Figure 2a). To test this hypothesis, an intracellular phytase from PNSB cells should be assayed. Up to date, there is no report about phytase enzyme produced from PNSB.

4.2.2 Lactic acid bacteria

All of lactic acid bacteria, 115 isolates, were streaked on the modified MRS medium supplemented with 0.5% phytate as a sole phosphorus source. To detect the bacterial strains that produced phytase, the molybdate-vanadate solution was used as a specific color reagent. This method can reduce an interference of clearing zone caused by acid production from lactic acid bacteria (Yanke, *et al.* 1998). The results showed that 61 isolates of lactic acid bacteria had clear zone either around culture or under culture (Figure 2b-c). It indicated the presence of extracellular phytase and/or intracellular phytase was produced by lactic acid bacteria.

Many previous studies have reported phytase activity in lactic acid bacteria (Raghavendra, *et al.* 2009; Didar, *et al.* 2010; Andrabi, *et al.* 2016). An example includes the isolation of phytase producing probiotic lactic acid bacteria from piglet feces (Dowarah *et al.* 2018). 16S rRNA sequence identified this isolated bacteria as *Pediococcus acidilactici*.

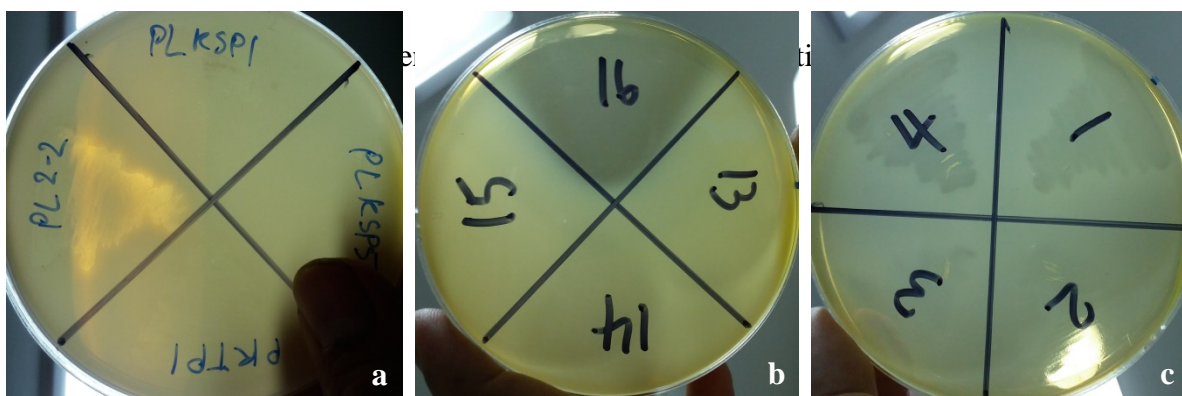


Figure 2. Phytase screening plate of PNSB (a) and lactic acid bacteria (b, c)

4.3 Phytase assay

All 63 PNSB isolates were streaked on the modified GM plate supplemented with 0.5% phytate as a sole phosphorus source. Then, the cultures were scrapped and disrupted to extract crude enzymes. All crude enzymes were assayed by the method of Heinonen and Lahti (1981). The results revealed that there were no difference between an absorbance of control (blank) and the samples. Absorbance at 700 nm cannot be measured due to strong background color of the tested samples. Thus, other alternative assays should be used for testing phytase activity. However, it is possible that some PNSB (red and brown isolates) may contain an intracellular phytase or cell-bound phytase as described in the previous report (Lan, *et al.* 2011).

For lactic acid bacteria, an extracellular phytase produced in the modified MRS broth was assayed by the colorimetric determination method (Sigma-Aldrich). The activity of phytase to hydrolyze a substrate, phytate, in the reaction mixture was observed. This assay method can differentiate an enzyme activity in the sample tubes and a control tube by the color change to be green (Figure 3). The phytase activities were range from 1.91 ± 0.52 to 12.39 ± 0.34 U mL⁻¹ whereas the specific activities were range from 0.98 ± 0.25 to 6.42 ± 0.16 U mg⁻¹. The strains with the highest activity and specific activity were selected to report in the Table 1.

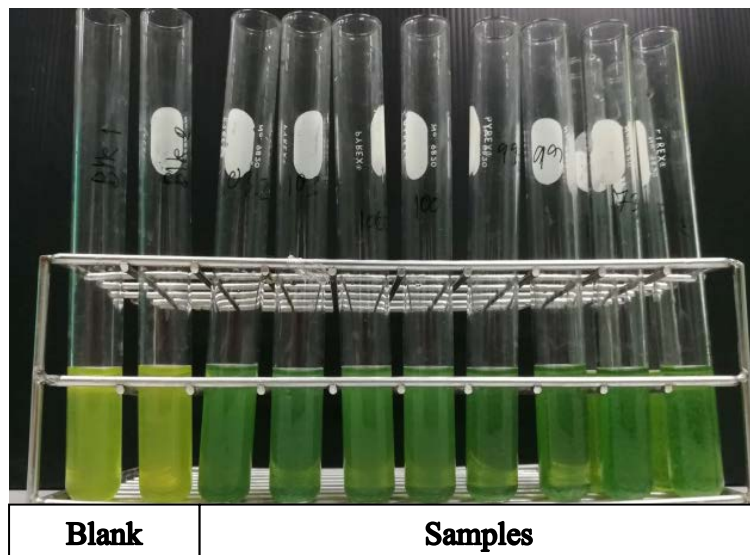


Figure 3. Assay of phytase activity by the colorimetric determination method.

Table 1. Top five highest phytase activities and specific activities from the selected strains of lactic acid bacteria

Lactic acid bacteria	Growth (OD600)	Activity (U mL ⁻¹)	Specific activity (U mg ⁻¹)
1. P6C3	0.123±0.01	12.39±0.34	6.42±0.16
2. TPS9	0.146±0.01	12.58±0.42	6.08±0.28
3. CW4C1	0.163±0.02	11.28±0.45	5.67±0.25
4. SW19M9	0.454±0.03	10.2±0.28	5.31±0.36
5. P23C3	0.369±0.02	10.42±0.51	4.48±0.18

4.4 Identification of the selected bacteria

All the isolates of photosynthetic bacteria in this study were identified as PNSB by the following properties: Gram negative; cell shape: rod to ovoid; cell arrangement: rosette-like cluster in some species; motile by flagella; able to grow under anaerobic-light conditions; photosynthetic pigments: bacteriochlorophyll and carotenoids; maximum absorption peak of the extracted pigments (bacteriochlorophyll): 770 nm.

The characteristics of lactic acid bacteria were confirmed: Gram positive; cell shape: short rod-long rod and cocci; cell arrangement: irregular; catalase negative; all isolates produce acid from glucose; a few isolates produced gas from glucose fermentation. Eleven strains of lactic acid bacteria that had different colony characteristics were identified by 16S rDNA sequencing. The results showed that there are 5 groups of phytase producing lactic acid bacteria used in this study (Table 2). Four groups are belonging to the genus *Lactobacillus* and another group is identified as the genus *Enterococcus*.

Table 2. Identification of the selected strains of lactic acid bacteria by 16S rDNA sequencing

Group	Representative strain (A number of isolates)	Amplicon length (bp)	Identification as	Percent identity
1	TPF1-4 (5)	1,472	<i>Lactobacillus plantarum</i> JCM 1149	99.45
2	TPF3-19 (1)	1,468	<i>L. farciminis</i> BCRC 14043	99.32
3	TPF5-39 (3)	1,463	<i>L. agilis</i> JCM 1187	99.18
4	TPF8-53 (1)	1,481	<i>L. fermentum</i> CIP 102980	99.66
5	TPF8-59 (1)	1,466	<i>Enterococcus faecium</i> DSM 20477	99.59

The species *L. plantarum* was usually isolated from pig feces. Angelis, *et al.* (2006) could isolate 35 lactic acid bacteria in the genus *Lactobacillus*. They were identified by 16S r RNA into 8 species. Only one species, *L. plantarum*, is similar to this study. *L. plantarum* and *L. reuteri* were selected based on the abilities to resist bile salt, pH, antimicrobial activity and heat resistance. In addition, four lactobacilli species namely *L. fermentum*, *L. salivarius*, *L. plantarum* and *L. reuteri* were isolated from pig feces. They could inhibit growth of two bacterial pathogens, *E. coli* K88 and *Salmonella typhimurium* (Yun, *et al.* 2009). Recently, Sirichokchatchawan, *et al.* (2018) reported that two strains of *L. plantarum*, *Pediococcus pentosaceus* and *P. acidilactici* had the strongest antibacterial activity against enteric pathogenic bacteria in pig. These four strains were also isolated from pig feces.

5. Conclusions

A total of 124 PNSB isolates were isolated on GM agar plate under anaerobic-light conditions whereas 115 isolates of lactic acid bacteria were isolated on MRS agar under anaerobic condition. Pure cultures of both bacterial groups were screened on the modified media to produce an intracellular or extracellular phytase by using the vanadate-molybdate method. The 63 isolates of PNSB and 61 isolates of lactic acid bacteria had phytase activity.

An intracellular phytase from PNSB were not detectable by the method of Heinonen and Lahti (1981). However the activities of an extracellular phytase from lactic acid bacteria were detected by the colorimetric determination method (Sigma-Aldrich). The selected strains of lactic acid bacteria were identified by using 16S rDNA sequencing. Five groups of phytase producing lactic acid bacteria isolated from fresh swine manure were identified as: *L. plantarum*, *L. agilis*, *L. farciminis*, *L. fermentum* and *E. faecium*.

6. Acknowledgements

We are grateful to Dr. Pakpoom Subsoontorn for critical reading of this manuscript. This work (P2558B167) was financially supported by the Naresuan University research fund.

7. References

- De Angelis, M., Siragusa, S., Berloco, M., Caputo, L., Settanni, L., Alfonsi, G., Amerio, M., Grandi, A., Ragni, A., & Gobbetti, M. (2006). Selection of potential probiotic lactobacilli from pig feces to be used as additives in pelleted feeding. *Research in Microbiology*, 157(8), 792-810.
- Do, Y. S., Schmidt, T. M., Zahn, J. A., Boyd, E. S., de la Mora, A., & DiSpirito, A. A. (2003). Role of *Rhodobacter* sp. strain PS9, a purple non-sulfur photosynthetic bacterium isolated from an anaerobic swine waste lagoon, in odor remediation. *Applied and Environmental Microbiology*, 69(3), 1710-1720.
- Dowarah, R., Verma, A. K., Agarwal, N., Singh, P., & Singh, B. R. (2011). Selection and characterization of probiotic lactic acid bacteria and its impact on growth, nutrient digestibility, health and antioxidant status in weaned piglets. *PloS One*, 13(3), e0192978.

- Heinonen, J. K., & Lahti, R. J. (1981). A new and convenient colorimetric determination of inorganic ortho-phosphate and its application to the assay of inorganic pyrophosphatase. *Analytical Biochemistry*, 113, 313-317.
- Hirotsu, H., Agui, Y., Kobayashi, M., & Takahashi, E. (1990). Removal of coliphages from wastewater effluent by phototrophic bacteria. *Water Science. Technology*, 22(9), 59-63.
- Kim, M. K., Choi, K.-M., Yin, C.-R., Lee, K.-Y., Im, W.-T., Lim, J. H., & Lee, S.-T. (2004). Odorous swine wastewater treatment by purple non-sulfur bacteria, *Rhodospseudomonas palustris*, isolated from eutrophicated ponds. *Biotechnology Letters*, 26, 819-822.
- Kim, T. W., & Lei, X. G. (2005). An improved method for a rapid determination of phytase activity in animal feed. *Journal of Animal Science*, 83, 1062-1067.
- Lan, G. Q., Abdullah, N., Jalaludin, S., & Ho, Y. W. (2011). Purification and characterization of a phytase from *Mitsuokella jalaludinii*, a bovine rumen bacterium. *African Journal of Biotechnology*, 10(59), 12766-12776.
- Madigan, M. T., & Jung, D. O. (2009). An overview of purple bacteria: systematics, physiology, and habitats. In C. N. Hunter, F. Daldal, M. C. Thurnauer, & J. T. Beatty (Eds.), *The purple phototrophic bacteria* (pp. 1-15). Dordrecht: Springer
- Okubo, Y., Futamata, H., & Hiraishi, A. (2005). Distribution and capacity for utilization of lower fatty acids of phototrophic purple nonsulfur bacteria in wastewater environments. *Microbes and Environments*, 20(3), 135-143.
- Petsuriyawong, B., & Khunajakr, N. (2011). Screening of probiotic lactic acid bacteria from piglet feces. *Kasetsart Journal (Nat. Sci.)*, 45, 245-253.
- Schiffman, S. S., Bennett, J. L., & Raymer, J. H. (2001). Quantification of odors and odorants from swine operations in North Carolina. *Agricultural and Forest Meteorology*, 108, 213-240.
- Sirichokchatchawan, W., Pupa, P., Praechansri, P., Am-in, N., Tanasupawat, S., Sonthayanon, P., & Prapasarakul, N. (2018). Autochthonous lactic acid bacteria isolated from pig faeces in Thailand show probiotic properties and antibacterial activity against enteric pathogenic bacteria. *Microbial pathogenesis*, 119, 208-215.
- Wei, H., Okunishi, S., Yoshikawa, T., Kamei, Y., & Maeda, H. (2016). Isolation and characterization of a purple non-sulfur photosynthetic bacterium *Rhodospseudomonas faecalis* strain A from swine sewage wastewater. *Biocontrol Science*, 21(1), 29-36.
- Yanke, L. J., Bae, H. D., Selinger, L. B., & Cheng K. J. (1998). Phytase activity of anaerobic ruminal bacteria. *Microbiology*, 144, 1565-1573.
- Yun, J. H., Lee, K. B., Sung, Y. K., Kim, E. B., Lee, H. G., & Choi, Y. J. (2009). Isolation and characterization of potential probiotic lactobacilli from pig feces. *Journal of Basic Microbiology*, 49(2), 220-226.

<https://www.sigmaaldrich.com/technical-documents/protocols/biology/enzymatic-assay-of-phytase.html>

Development of high anthocyanin crispy rice bar

Nuttawut Lainumngen^{1,a}, Janpen Saengprakai^{1,b}, Siriporn Tanjor^{1,c}, Wasan Phanpho², Aran Phodsoongnoen²

¹ Department of Nutrition and Health, Institute of Food Research and Product Development, Kasetsart University, Bangkok 10903, Thailand

² Faculty of Agro-industrial Technology, Rajamangala University of Technology Tawan-ok, Chanthaburi 22210, Thailand

E-mail; ^aifrnwl@ku.ac.th, ^bifrijps@ku.ac.th, ^cifrspta@ku.ac.th

Abstract

Nowadays, consumers are increasingly interested in healthy food and have more behavioural changes in meal eating patterns as snacks. This study aimed to increase the nutritional value of crispy rice as the healthier snack by using Thai rice which presented important natural ingredients. Five formulations were developed including Thai colored indica rice (*Oryza sativa* cv. Riceberry), black sticky rice (*Oryza sativa* cv. Leum Phua), white glutinous rice (*Oryza sativa* cv. RD6), RD6 soaking in water obtained from Leum Phua sticky rice, and a combination of RD6 and Leum Phua glutinous rice. Water activity, moisture content, crispness, color, total anthocyanin content, and sensory evaluation were analysed. The results showed that there was no significant difference in crispness and moisture content of products. The lowest free water was observed in both Riceberry and soaked RD6 formulations with water activity below 0.42. Leum Phua and Riceberry recipes had the lowest brightness. Obviously, crispy rice bar from Leum Phua sticky rice had the highest total anthocyanin content, followed by Riceberry rice. According to sensory test, there was no significant difference in odor, flavour and texture, as well as overall liking scores. The color score was high in the RD6 and soaked RD6 formulations. During the storage for 2 months, the increase of water activity and lipid peroxidation were observed. Additionally, there was no growth of pathogenic microorganisms. The crispy rice by soaked RD6 formula was acceptable up to 2 months of storage. Therefore, it can be concluded that the RD6 sticky rice soaking with water from black glutinous rice is suitable for commercial production because it can increase the nutritional value for consumers by providing high total anthocyanin content.

Keywords: Riceberry rice; Oryza sativa cv. Leum Phua; Oryza sativa cv. RD6; Black glutinous rice; Anthocyanin

1. Introduction

Many studies have been pointing out to the critical issue of food eating awareness related to physical illness throughout the past few decades. Eating behavior is an important factor that impacts on human health. Thus, healthier food choice is recommended for healthy consumers. In the present, human lifestyle has been completely changed to hurry in living which directly influences trend of food decision as well as their dietary pattern consumption. Food characteristics, suitable for people who living in a hurry each day, should be ready-to-eat and easy-to-carry such as sandwiches, bread and snacks. Importantly, making decision of eating food must include both healthy and safe as the priority. In present, people are facing a challenge to develop nutritious food product which fit in daily lifestyle. Therefore, this ongoing issue causes of global food industry focusing on functional ingredients from natural plants for developing healthier products. Hence, utilization of anthocyanin-based food is needed to add the value in food products and also enriched nutrition in food with natural source.

Thailand is well known as the land of agriculture, especially rice cultivation in different strains with high quality. Thai colored indica rice (*Oryza sativa* cv. Riceberry), black glutinous rice (*Oryza sativa* cv. Leum Phua) and white glutinous rice (*Oryza sativa* cv. RD6) have been cultivated widely in Thailand. Interestingly, pigmented rice contains phytonutrient which is higher antioxidant activity and phenolic compounds than non-pigmented rice. Several varieties of pigmented rice, particularly Riceberry rice and Leum Phua sticky rice have been exhibited as source of anthocyanin. It is water-soluble, phenolic of plant which contributes to red, purple or blue colors in rice. Anthocyanin-based food products have been developing for healthier choice. It has becoming popular in food and beverage research, such as substitution of Riceberry flour in noodle and fortification of anthocyanin from Riceberry rice in milk chocolate (Sirichokworrahit, Phetkhut, Khommoon, 2015; Ngamdee, Bunnasart, Sonda, 2019). Moreover, effect of anthocyanin has been reported as a potent nutraceutical by its antioxidant capacity. Health benefits were reported in previous literature that mainly involved in anti-oxidative stress and anti-inflammation throughout the body. Furthermore, pharmacological effect of anthocyanin in Thai rice as anti-hyperlipidemic and anti-cancer property have been reported. (Khoo, Azlan, Tang, Lim, 2017; Sivamaruthi, Kesika, Chaiyasut, 2018). Glutinous rice can be modified in many kinds of food such as snack or dessert. Leum Phua and RD6 are Thai glutinous rice with pigmented and non-pigmented carrier, respectively. Leum Phua, black glutinous rice, has been reported that it exhibited high anthocyanin profile, phenolic compounds and radical scavenging activity than Black Rose, Hawm Nil, and Klam rice (Suwannalert & Rattanachittawat, 2011). White glutinous rice RD6 is one of the popular rice grown in Thailand. It is commonly modified and developed to snack or cake due to puffable property even though lower antioxidant activity is exhibited when compared to other colored Thai rice.

Recently, Thai rice containing anthocyanin has been widely studied due to rise of concern in healthier eating habits. The application of natural material on Thai traditional snack is still needed. In addition, to our knowledge, the comparison of pigmented rice utilization in snack bar is rarely observed. Therefore, the objective of this study was to increase the nutritional value of crispy snack bar using colored rice, as the main ingredient. In this study, physicochemical properties of three rice varieties including Riceberry rice, Leum Phua glutinous rice, and RD6 sticky rice were compared. This study provided the development of crispy rice bar as healthier snack recipe and suggested for further utilization in prospective commercial grade.

2. Objectives

The aims of this study was to increase the nutritional value of crispy rice as the snack bar using Thai rice from 5 experimental groups with different rice materials, including crispy rice from the Riceberry rice, black glutinous rice (*Oryza sativa* ver. Leum Phua), the RD6 glutinous rice, the combination of RD6 with black glutinous rice and the RD6 soaking in water from black glutinous rice. In addition, this study compared physicochemical property, sensory scores and total anthocyanin content as well as product quality during storage for 2 months.

3. Methodology

3.1 Materials

Raw materials include black glutinous rice (Leum Phua), white glutinous rice (RD6 rice), Riceberry rice, sunflower seeds, pumpkin seeds, cashew nuts, black sesame, white sesame, raisins, ripe banana (cv. Kluai Kai), glucose syrup, gum arabic, honey, brown sugar, salt, vegetable oil. Chemical reagents including ethanol, acetic acid, sodium acetate, potassium chloride, sulfuric acid, sodium hydroxide and 3,5-dinitrosalicylic acid were used in this study.

3.2 Experimental design

To develop nutritious snack bar with Thai rice mixed cereals, the sample of each type of rice varieties were conducted in Thailand. There were five experimental groups in this study, consisted of crispy rice product by Riceberry rice, black glutinous rice (Leum Phua), white glutinous rice (RD6), soaked white glutinous rice in water from black glutinous rice (soaked RD6 rice), and a combination of white and black sticky rice (combined RD6 with Leum Phua). Physicochemical and sensory test were evaluated.

3.3 Crispy rice formulation development

3.3.1 Crispy rice preparation with/without oil

RD6 glutinous rice was dried at 65° C. 10 g of dried RD6 was roasted without oil on pan fried at 270° C. Crispy rice characteristics in terms of rice seed inflation, color, odor and texture were observed after roasting the rice. Another dried RD6 (10 g) was fried at 230° C for 7 to 9 sec. Characteristic descriptions of crispy rice were noted. The effect of rice preparation with/without oil on product characters were reported.

3.3.2 Cereals preparation

Pumpkin seeds were roasted at 270° C for 10 min. Cashew nuts were roasted at 150° C for 15 min. Black and white sesame were roasted at 270° C for 7 min. All roasted cereals were packed in polyethylene bag.

3.3.3 Banana syrup preparation

Ripe bananas were cleaned and peeled. Banana pulps were sliced and mixed with water. The ratio of bananas and water was 1:1. Sliced banana was heated at 100° C for 5 min. Banana pulp was filter. The clear banana juice was heated at 80° C and further concentrated to 60 to 70° Brix. Banana syrup was contained in sterile bottles and stored at 4 to 5° C.

3.4 Formulation

Standard formulation for crispy rice mixed cereals bar includes crispy rice 200 g, glucose syrup 160 g, Kluai Kai syrup 50 g, honey 60 g, brown sugar 50 g, salt 3 g, pumpkin seeds 30 g, sunflower seeds 30 g, white sesame 10 g, black sesame 10 g and raisin 50 g. Crispy rice and cereals were mixed and rested in the bowl for a while. Subsequently, glucose syrup mixed with Kluai Kai syrup were heated for 5 min. Honey, brown sugar and salt were added to mixed syrup and stewed for 2 min until the mixture was homogeneous. The mixture was poured into the bowl and immediately mixed with crispy rice and cereals. Then, look it cool down for 5 min and cut into small pieces with

equal size (2.5×5×1 cm). Crispy rice mixed cereal bar were packed in polyethylene bag and stored at room temperature for further analysis.

3.5 Product quality analyses

3.5.1 Physical property of crispy rice bar

Color and water activity (a_w) were analyzed by a spectro-photo-colorimeter and LabMaster- A_w , respectively. Color value was expressed as L^* , a^* and b^* . Degree of whiteness or darkness were indicated by L^* (0 = black, 100 = white). Degree of redness (+) or greenness (-) were expressed as a^* . Yellowness (+) and blueness (-) scales were indicated as b^* . Water activity was expressed as the ratio of the vapor pressure in food to the vapor pressure of pure water. A texture analyzer (TA.XT.Plus) was used to measure the crispness.

3.5.2 Chemical property of crispy rice bar

Moisture content was determined by A.O.A.C method (1995). Reducing sugar was analyzed using dinitrosalicylic acid (DNS) method as previously described by James, C. S. (1995).

3.5.3 Quantification of total anthocyanin content

Total anthocyanin content was determined by pH differential method (modified from Lee *et al.*, 2005). Ethanol solvent at 70% was used to extract the anthocyanin. Absorbance was read at 510 nm in a spectrophotometer.

3.5.4 Organoleptic evaluation

Crispy rice sensory evaluation was obtained from 24 untrained panels by 9-point hedonic scale test. Color, odor, flavor, and texture as well as the overall liking were evaluated from extremely dislike as '1 point' to extremely like as '9 point'.

3.5.5 Product quality during storage

The final formula of crispy rice was selected by the highest sensory point for product quality analysis during storage for 2 months. The selected product was evaluated for color, lipid oxidation, and water activity as well as bacterial growth. Product was observed and reported at day 0, 15, 30 and 60.

3.6 Data analysis

All analyses were carried out in triplicate. The results were expressed as mean values and standard deviation (SD). The mean of three or more groups were analyzed for the statistically significant differences using one-way analysis of variance (ANOVA) and Duncan's Multiple Range Test (DMRT). Two-sided p -value < 0.05 were regarded as statistically significant. All statistical analyses were performed using Statistical Package for the Social Science (SPSS) 17.0 software.

4. Results and discussion

This study explored the effect of cooking process on quality characteristics of crispy rice by the comparison of frying with /without vegetable oil. The result showed that cooking oil influenced on crispy rice quality in terms of seed swelling, color, odor and texture. Crispy rice with cooking oil represented more pleasant product quality than crispy rice without cooking oil (Table 1). Fat and oil play important roles to food product. One of oil capacity is the heat absorption which is more effective than air or water. It transfers heat to rice seed surface as well as enhances color and texture of the crispy rice. It plays important role in food product which is responsible for developing texture and enhancing flavor of fried foods. In addition, oil penetrates and replaces water in food during frying, resulting in more tenderizing. Oil also releases ingredient flavor and produces moistness feeling in the mouth. (Oke *et al.*, 2017, pp. 1-21) Hence, heating process with vegetable oil resulted in better characteristics in terms of crispness, desirable color and pleasing smell of the fried crispy rice while

another cooking process was slightly burnt and hard. The crispy rice by optimum oil usage was considerably more acceptable.

Table 1. Qualitative characteristics of crispy rice by heated with/ without vegetable oil

Rice characters	Without oil	With oil
Rice seed inflation	Little inflated	More inflated
Color	Yellow-brown	Yellow-white
Odor	Burnt smell	Pleasing scent
Texture	Crisp with hard cracked	Crisp with easily cracked

Total anthocyanin contents in Leum Phua sticky rice and Riceberry rice were compared before the heating process and after food processes by drying and frying (Table 2). The result indicated that food processing affected on anthocyanins. Total anthocyanin content was high at raw and subsequently decreased during food process. Significantly, Leum Phua glutinous rice had higher anthocyanins than Riceberry rice at stage of raw material and after drying. However, total anthocyanin contents were no different between Riceberry rice and Leum Phua sticky rice after frying process. In fact, anthocyanin are easily oxidized during process and storage by several factors such as pH, light, and oxygen, as well as enzymes. One of the important factors to be considered is processing temperature. Anthocyanin stability was affected and degraded into various intermediate compounds by heat. (Patras *et al.*, 2010, pp. 3-11). The finding was consistent with Surh and Koh's study (2014, pp. 1-9) that presented higher anthocyanins at raw in two cultivars of black rice (*Oryza sativa* cv. Sintoheugmi and Sinnongheuchal). The large amount of anthocyanins were decreased after heat process, for example, roasting, pan-frying, steaming and boiling. As same as the study of Hiemori, Koh and Mitchell (2009, pp. 1908-1914) that revealed the degradation of total anthocyanins into the protocatechuic acid in cooking black rice (*Oryza sativa* L. *Japonica* var. SBR). Leum Phua and Riceberry rice showed total anthocyanins content in approximately 317.28 and 235.64 mg/100 g of rice, respectively (Table 2). The result was in range from previous study of Riceberry in different areas of Thailand which was 24.69-272.76 mg/100 g of rice (Settapramote *et al.*, 2018, pp. 84-94).

Table 2. Comparison of total anthocyanins in Leum Phua and Riceberry rice after heat process

	Total anthocyanins content (mg/100 g of rice)		
	Raw	After drying	After frying
Leum Phua sticky rice	5712.87±1273.34 ^a	1384.15±141.00 ^a	450.87±28.92 ^a
Riceberry rice	669.81±125.25 ^b	317.28±130.43 ^b	235.64±57.93 ^a

Values are shown as mean±standard deviation. Means within each column bearing different superscripts are significantly different (p<0.05).

Crispy rice product were fried using vegetable oil. All formulas were developed as shown in Figure 1. The brightness was observed in RD6 crispy rice, followed by soaked RD6, combined RD6 with Leum Phua, Riceberry rice, and Leum Phua sticky rice, respectively (Table 3). The highest redness and yellowness were also detected in RD6 formula. Obviously, pigmented rice as Riceberry and Leum Phua were expressed lower scale of brightness and increased blue and green colors. According to the finding by previous reports in Thailand, Leum Phua and Riceberry rice significantly presented the darkness color whereas RD6 sticky rice showed more brightness (Poomipak *et al.*, 2018,

pp. 134-143). It can be explained that anthocyanin accumulation in Leum Phua and Riceberry resulted in lower of brightness scale.

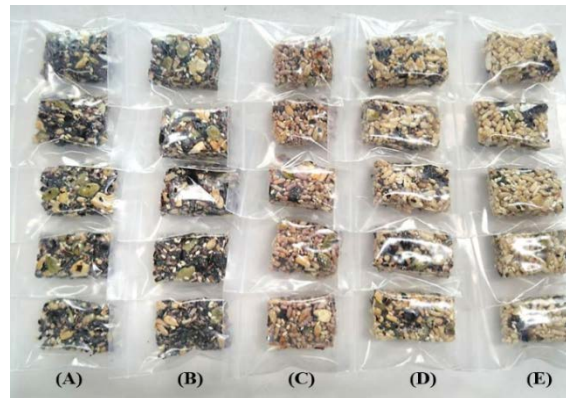


Figure 1. Crispy rice bar products (A) Leum Phua sticky rice, (B) Riceberry rice, (C) soaked RD6 in water from Leum Phua sticky rice, (D) combined RD6 with Leum Phua sticky rice, and (E) RD6 sticky rice

Table 3. Color scale of crispy rice products by different formulations

	Color scale		
	L*	a*	b*
Leum Phua glutinous rice	46.74±0.19 ^c	2.20±0.15 ^d	0.43±0.00 ^e
Riceberry rice	47.08±0.33 ^c	2.80±0.04 ^c	6.18±0.18 ^d
RD6 glutinous rice	54.69±0.80 ^a	5.12±0.18 ^a	16.64±0.31 ^a
Combined RD6 with Leum Phua glutinous rice	51.92±0.70 ^b	3.86±0.07 ^b	12.30±0.01 ^b
Soaked RD6 in water from Leum Phua glutinous rice	54.26±0.57 ^a	4.11±0.20 ^b	11.00±0.04 ^c

Values are shown as mean±standard deviation. Means within each column bearing different superscripts are significantly different (p<0.05).

Reducing sugar, moisture, and free water as well as texture were reported in Table 4. There was no significant difference of moisture and texture among groups. Factors affecting the textural quality of crispy rice snack include amylose content and moisture content. Amylose molecules are aligned by hydrogen bonds and release water molecules. However, the RD6, riceberry and Leum Phua are the rice with very low amylose content (5-12%) (Boonmeejoy *et al.*, 2019, pp. 42-62). Thus, the moisture content and crispness were not difference in this study. The higher amount of reducing sugar was found in combined RD6 with Leum Phua, followed by soaked RD6, RD6, Riceberry, and Leum Phua glutinous rice, respectively. The reducing sugar of formulations with RD6 sticky rice were likely to be high because white glutinous rice had higher starch digestibility than colored rice varieties. Therefore, increasing amount of reducing sugar can be imply to degradation of the starch during the process (Pasakawee *et al.*, 2018, 1-12). The lowest free water in product was observed in both Riceberry and soaked RD6 formulas with water activity 0.41. All formulations were within the range 0.41-0.44 which reaction rate was low for undesirable microorganism growth, browning, and enzyme activity (Sandulachi, 2003, pp. 40-48).

Table 4. Reducing sugar, moisture content, water activity and texture of crispy rice product by different formulations

	Reducing sugar (g/ml)	Moisture (%)	Free water	Crispness (N)
Leum Phua glutinous rice	12.91	7.08±0.30 ^a	0.43±0.00 ^a	51.54±26.02 ^a
Riceberry rice	13.02	7.05±0.42 ^a	0.41±0.00 ^b	63.73±33.23 ^a
RD6 glutinous rice	13.11	7.22±0.57 ^a	0.42±0.00 ^a	75.34±60.71 ^a
Combined RD6 with Leum Phua glutinous rice	13.56	7.07±0.25 ^a	0.42±0.00 ^a	38.05±17.39 ^a
Soaked RD6 in water from Leum Phua glutinous rice	13.22	6.77±0.21 ^a	0.41±0.00 ^b	61.55±21.13 ^a

Values are shown as mean±standard deviation. Means within each column bearing different superscripts are significantly different (p<0.05).

Mean of total anthocyanin contents were compared by various formulations as shown in Figure 2. Total anthocyanins significantly differed between pigmented rice and pure RD6 sticky rice. There was no significance difference among Riceberry rice, combined RD6 and soaked RD6 formulations. Additionally, Leum Phua crispy rice had the highest total anthocyanin content (371.09±11.58 mg/100g), followed by Riceberry (144.72±16.70 mg/100g), combined RD6 with Leum Phua (128.02±25.51 mg/100g), soaked RD6 (122.46±22.27 mg/100g), and RD6 sticky rice (87.21±47.99), respectively. Notably, colored rice, particularly Leum Phua was represented as the rich source of anthocyanins. In this sense, the previous study additionally supported that Leum Phua and Riceberry rice had higher phenolic compounds and scavenging ability than white glutinous rice, RD6 (Poomipak *et al.*, 2018, pp. 134-143).

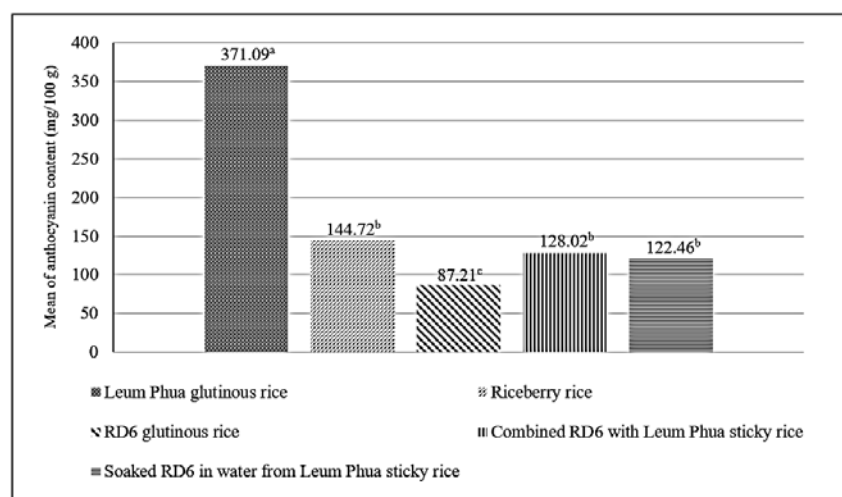


Figure 2. Mean of total anthocyanins content in crispy rice products by different formulas

All formulas were ranked score from 1-9 in terms of color, odor, flavor, texture, and overall liking. There was no significant difference in odor, flavor, texture, and overall liking among groups. RD6 and soaked RD6 rice were obtained higher score in color and the highest score was found in soaked RD6 formula (Table 5). The lower score was observed in product with dark color by pigmented rice as based-material. The sensory test was inconsistent with previous study by Poomipak *et al.* (2018, pp. 134-143). They showed that unpolished Leum Phua sticky rice had higher scores in color. However, in this present, color score of developed sticky rice was high in RD6 and soaked RD6 formula. This may be explained by difference of age duration of panelists between the studies. Thus, the desirable formula of crispy rice product for consumers was made from soaked RD6 rice in Leum Phua's water sticky rice. Subsequently, the selected product was analyzed for proximate composition and quality during storage life. Moisture, protein, fat, ash and carbohydrate were 6.77, 681, 16.05, 0.73, and 69.64%, respectively (data not shown).

Table 5. Means sensory scores of crispy rice products by different formulas

	Black glutinous rice	Riceberry rice	RD6 glutinous rice	Combined RD6 with Leum Phua glutinous rice	Soaked RD6 in water from Leum Phua glutinous rice
Color	6.25±1.73 ^b	6.83±1.63 ^b	7.21±1.02 ^a	6.46±1.59 ^b	7.42±0.93 ^a
Odor ^{ns}	6.38±1.38	6.08±1.38	6.13±1.26	6.42±1.53	6.46±1.18
Flavor ^{ns}	6.30±1.55	6.46±1.35	6.33±1.34	6.42±1.25	6.58±1.21
Texture ^{ns}	5.38±1.93	6.13±1.62	6.08±1.79	5.88±1.78	6.08±1.50
Overall liking ^{ns}	6.17±1.46	6.42±1.50	6.33±1.27	6.58±1.21	6.46±1.30

Values are shown as mean±standard deviation. Means within each column bearing different superscripts are significantly different (p<0.05). ns means no significant difference.

Product quality was measured after storage for 2 months at day 0, 15, 30, and 60. The scale of product color had been changing during storage at room temperature. Yellowness was increase while brightness and redness were decrease (Table 6). This phenomenon can be explained by browning reaction due to the increase of available water and lipid oxidation during storage. Non-enzymatic browning is occurred by the interaction of reducing sugars and amino acids. This reaction further to amadori compounds and form dark pigments. It causes of the quality change in food product due to darkening of light colored product (Singh & Anderson, 2004, pp. 3-23).

Table 6. Color analysis of crispy rice (soaked RD6 rice formula) during storage for 2 months

	Color scale		
	L*	a*	b*
Day 0	51.92±1.73 ^a	3.86±0.08 ^a	12.30±0.32 ^a
Day 15	51.80±2.82 ^a	3.82±0.03 ^a	12.70±0.12 ^a
Day 30	49.67±2.08 ^a	3.43±0.11 ^b	17.04±0.23 ^b
Day 60	48.25±2.76 ^a	3.04±0.06 ^c	17.19±0.37 ^b

Values are shown as mean±standard deviation. Means within each column bearing different superscripts are significantly different (p<0.05).

Malondialdehyde and thiobituristic acid (TBA) reactivity was used as an index of lipid peroxidation. Lipid peroxidation and water activity were observed during the storage for 2 months (Figure 3). The increase of water activity and lipid peroxidation were detected. Water activity was not significant difference among periods. Noticeably, at day 60, the TBA value was significantly higher than day 0 and 15. Lipid oxidation is affected by light, oxygen, water activity and temperature as well as material composition. The snack formula included cereals as the main ingredient and using cooking oil for food process. Lipid reactions are catalyzed by both of non-enzymatic and enzymatic involvement which presenting in cereal components such as its membrane structure. Additionally, water content in mature grain and food processing also affected the lipid mobility and promoted reactions between lipids and other ingredients. Moreover, free fatty acids in rice and subsequently lipid oxidation products is partially attributed to storage under warm and humid conditions even the lipid content of rice is slightly low. Thus, crispy rice stored in laminated bags containing CO₂ or under refrigerated conditions were likely to be more stable than stored at ambient temperature (Lehtinen, 2003, pp. 1-47; Angelo et al., 2009, pp. 175-224). Similar results were reported by previous study (Thaweeseang *et al.*, 2017, pp. 212-223) that showed ongoing increase of TBA value and water activity in nutritious cereal bar during the 30 days storage. However, in this study, the TBA value was in range 0.34-0.53 within 2 months that was lower than acceptance limit for rancidity (1.0 mg/kg).

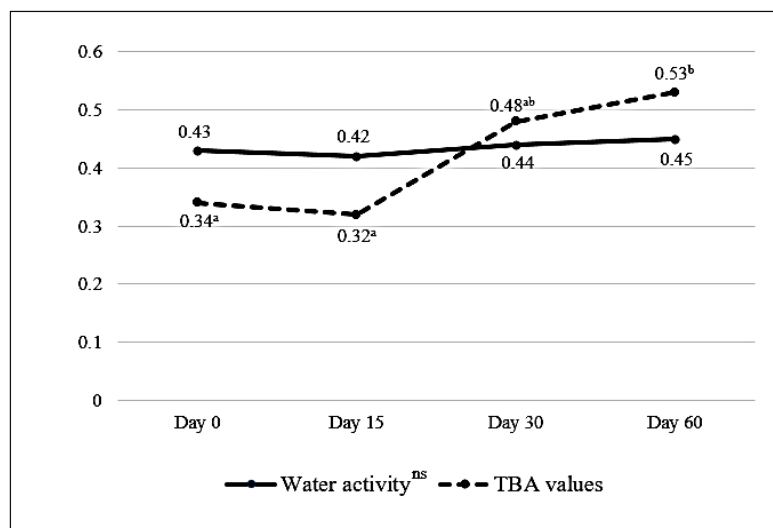


Figure 3. Means of water activity and TBA values (mg MDA/kg) in crispy rice product (the soaked RD6 formula) during storage for 2 months. The values with different superscript letters mean significantly different ($p < 0.05$). ns means no significant difference.

The crispy rice products of the RD6 soaking with water from black glutinous rice were examined for microbiology count on days 0, 15, 30, and 60. Total bacterial count was below 10 at day 0 and 15. The spoilage were observed at the 30th and 60th storage day but not beyond the standard range. This result was supported by the increase of water activity during the storage period. Yeast and mould were lower than 10 CFU/g through the study. In addition, there was no growth of Coliform bacteria, *Staphylococcus aureus*, and *E. coli* during 2 months of storage (Table 7). Hence, the product was microbiologically safe within 2 months of storage period at room temperature.

Table 7. Bacterial count of crispy rice product (soaked RD6 formula) stored at 25° C for 2 months

	Day 0	Day 15	Day 30	Day 60
Total bacterial count (CFU/g)	<10	<10	2.5×10	1.26×10 ²
Yeast and moulds (CFU/g)	<10	<10	<10	<10
Coliform bacteria (MPN/g)	ND	ND	ND	ND
Staphylococcus aureus (MPN/g)	ND	ND	ND	ND
Escherichai coli (MPN/g)	ND	ND	ND	ND

ND-Not detected

5. Conclusion

In this study, cooking process with vegetable oil resulted in the desirable quality of the crispy rice product. According to this result, five formulations, including black glutinous rice (Leum Phua), Riceberry rice, white glutinous rice (RD6), RD6 soaking in water from Leum Phua sticky rice, and combined RD6 with Leum phua sticky rice were developed to high anthocyanin snack bar by frying method. The anthocyanin from black rice was high at raw and subsequently decreased during the heating process. Obviously, Leum Phua crispy rice had the highest anthocyanin, followed by Riceberry rice. However, the color of pigmented rice affected the sensory scores. Low brightness of product was associated with lower score. The RD6 soaking in water from Leum Phua represented as the final product formula of crispy rice bar due to high anthocyanin and acceptable sensory score. Therefore, it can be concluded that crispy rice bar from glutinous rice and glutinous rice RD6 soaking with black glutinous rice are suitable for commercial production because it can increase the nutrition value for consumers by providing high anthocyanin content. Moreover, the RD6 crispy rice soaking in water from black glutinous rice was be able to store up to 2 months of storage.

References

- Angelo, A. J. St., Vercellotti, J., Jacks, T., & Legendre, M. (2009). Lipid oxidation in foods. *Critical Review in Food Science and Nutrition*, 36(3), 175-224.
- AOAC. (1995). Official methods of analysis of AOAC international. In T. R. Mulvaney (Ed.), *AOAC International* (p. 42-1-42-2). Arlington, VA.
- Boonmeejoy, J., Wichaphon, J., & Jiamyangyuen, S. (2019). Classification of rice cultivars by using chemical, physicochemical, thermal, hydration properties, and cooking quality. *Food and Applied Bioscience Journal*, 7(2), 42-62.
- James, C.S. (1995). *Analytical chemistry of food*. Seale-Hayne faculty of agriculture, university of Plymouth, UK.
- Khoo, H. E., Azlan, A., Tang, S. T., & Lim, S. M. (2017). Anthocyanidins and anthocyanins: colored pigments as food, pharmaceutical ingredients, and the potential health benefits. *Food and Nutrition Research*, 61(1), 1-22.
- Lee, J., Durst, R. W., & Wrolstad, R. E. (2005). Determination of total monomeric anthocyanin pigment content of fruit juices, beverages, natural colorants, and wine by the pH differential method: Collaborative study. *Journal of AOAC International*, 88(5), 1269-1278.
- Lehtinen, P. (2003). *Reactivity of lipids during cereal processing* (Doctoral thesis). Helsinki University of Technology. Finland.
- Hiemori, M., Koh, E., & Mitchell, A. E. (2009). Influence of cooking on anthocyanins (*Oryza sativa* L. japonica var. SBR). *Journal of Agriculture and Food Chemistry*, 57(5), 1908-1914.

- Ngamdee, P., Bunnasart, A., & Sonda, A. (2019). Development of a functional food: milk chocolate fortified with anthocyanin from broken Riceberry. *Rajabhat Journal of Sciences, Humanities & Social Sciences*, 20(1), 81-89.
- Oke, E. K., Idowu, M. A., Sobukola, O. P., Adeyeye, S. A. O., & Akinsola, A. O. (2017). Frying of food: a critical review. *Journal of Culinary Science & Technology*, 1-21.
- Pasakawee, K., Laokuldilok, T., Srichairatanakool, S., & Utama-ang, N. (2018). Relationship among starch digestibility, antioxidant, and physicochemical properties of several rice varieties using principal component analysis. *Current Applied Science and Technology*, 18(3), 1-12.
- Patras, A., Brunton, N. P., Donnell, C. O., & Tiwari, B. K. (2010). Effect of thermal processing on anthocyanin stability in foods; mechanisms and kinetics of degradation. *Trends in Food Science & Technology*, 21(1), 3-11.
- Poomipak, N., Samakradhamrongthai, R. S., Utama-ang, N. (2018). Consumer survey of selected Thai rice for elderly using focus group and acceptance test. *Food and Applied Bioscience Journal*, 6(special issue on food and applied bioscience), 134-143.
- Sandulachi, E. (2003). Water activity concept and its role in food preservation. In, Mrema, G. C. (Eds.), *Handling and preservation of fruits and vegetables by combined methods for rural areas* (pp. 40-48). Rome: Food and Agriculture Organization of the United Nations.
- Settaramote, N., Laokuldilok, T., Boonyawan, D., & Utama-ang, N. (2018). Physicochemical, antioxidant activities and anthocyanin of Riceberry rice from different locations in Thailand. *Food and Applied Bioscience Journal*, 6(special issue on food and applied bioscience), 84-94.
- Singh, R. P., & Anderson, B. A. (2004). The major type of food spoilage: An overview. In Steele, R. (Ed.), *Understanding and measuring the shelf-life of food* (p. 3-23). Aspen Publications, Gaithersburg, MD.
- Sirichokworrakit, S., Phetkhut, J., & Khommoon, A. (2015). Effect of partial substitution of wheat flour with Riceberry flour on quality of noodles. *Procedia-Social and Behavioral Sciences*, 197, 1006-1012.
- Sivamaruthi, B. S., Kesika, P., & Chaiyasut, C. Anthocyanins in Thai rice varieties: distribution and pharmacological significance. *International Food Research Journal*, 25(5), 2042-2032.
- Surh, J., & Koh, E. (2014). Effects of four different cooking methods on anthocyanins, total phenolics and antioxidant activity of black rice. *Journal of the Science of Food and Agriculture*, 94(15), 1-9.
- Suwannalert, P., & Rattanachitthawat, S. (2011). High levels of phytochemicals and antioxidant activities in *Oryza sativa*-unpolished Thai rice strain of Leum Phua. *Tropical Journal of Pharmaceutical Research*, 10(4), 431-436.
- Thaweeseang, N., Katakul, S., Sreela-or, C. (2017). Product development of nutritious cereal bar. *Rajamangala University of Technology Srivijaya Research Journal*, 9(2), 212-223.

The effect of extraction methods on phenolic, anthocyanin, and antioxidant activities of Riceberry bran

Supatchalee Sirichokworakit^{1, a}, Hathairat Rimkeeree^{1, b}, Withida Chantrapornchai^{1, c} Udomluk Sukatta^{2, d}, Prapasson Rukyhaworn^{2, e}

¹Department of Product Development, Faculty of Agro-Industry, Kasetsart University, Bangkok, Thailand

²Kasetsart Agricultural and Agro-Industrial Product Improvement Institute, Kasetsart University, Bangkok, Thailand

E-mail; ^asupatchalee.si@ssru.ac.th, ^bfagihru@ku.ac.th, ^cwithida.c@ku.ac.th, ^daapuls@ku.ac.th, ^eaappsr@ku.ac.th

Abstract

Riceberry bran, byproduct from the rice milling process, is one of bioactive compounds sources. In order to increase Riceberry bran value, the purpose of this study was to compare the effect of different Riceberry bran extraction methods, including accelerated solvent extraction (ASE), ultrasonic-assisted extraction (UAE), soxhlet extraction (SE), and maceration method (MC) on bioactive compounds and antioxidant activities. It was found that the Riceberry bran extract from ASE presented the highest total phenolic, total anthocyanin content (55.45 mg GAE/g and 3.06 mg/g) and antioxidant properties including IC₅₀ of DPPH assay (0.109 mg/mL), FRAP value (688.04 mmole Fe(II)/kg) and IC₅₀ of ABTS assay (3.42 mg/mL) among the four methods. These results imply the potential to use the ASE method for extraction of phenolic and anthocyanin compounds from Riceberry bran.

Keywords: Accelerated solvent extraction; Maceration; Riceberry bran; Soxhlet; Ultrasonic-assisted extraction

1. Introduction

Riceberry, deep purple grain; (*Oryza Sativa* L.), a cross-bred strain from the Khao Hom Nin Rice variety which is well known as containing high antioxidant properties and Khao Hom Mali 105 well known as fragrant rice (Leardkamolkarn et al., 2011). Consumption of Riceberry is becoming popular in Thailand because of high nutrition and so as to meet the increasing market demand, the Thai government is supporting farmers to grow Riceberry (Peanparkdee, Yanauchi, & Iwamoto, 2018). Riceberry bran is a by-product of the rice milling process. It is always extracted oil and defatted Riceberry bran is used as an ingredient in animal feed. A number of studies have reported the presence of bioactive compounds in Riceberry bran. For instance, Riceberry bran is a rich source of phenolic compounds, anthocyanins, vitamin E and oryzanol which have shown great antioxidant activities (Peanparkdee, Yanauchi, & Iwamoto, 2018). In addition, several studies reported that Riceberry possessed chemopreventive properties including decreasing inflammation, managing diabetes and improving the regenerative changes of the pancreas, kidneys, heart and liver (Leardkamolkarn et al., 2011; Posuwan et al., 2013; Prangthip et al., 2013).

Extraction, the first step of bioactive compounds study, plays a significant and important role in the final quality of the extract. There are many extraction techniques that have been developed for the extraction of bioactive components from rice bran such as UAE, ASE microwave and ohmic heating-assisted extraction, etc. Peanparkdee, Yanauchi, and Iwamoto (2018) extracted phenolic and anthocyanins from Riceberry bran using UAE. Suttiarporn, Sookwong, and Mahatheeranont (2016) studied fractionation and identification of antioxidant compounds from Riceberry bran using solvent extraction (hexane, dichloromethane and methanol). However, there is little published information to compare extraction methods of bioactive compound from Riceberry bran. Conventional solvent extraction is used in extracting bioactive compounds from plants, based on many parameters, including the amount of solvents, extraction time, polarity of the antioxidant, and temperature (Peanparkdee, Yanauchi, & Iwamoto, 2018). The conventional methods such as SE, and MC are still considered to be compared with new extraction methods. Recently, new extraction methods have obtained increasing attentiveness to produce more environmentally sustainable, more effective, decreasing cost and faster extraction (Barros, Dykes, Awika, & Rooney, 2013). New extraction methods were used in various bioactive compounds, such as phenolic from rice bran (Tabaraki & Nateghi, 2011) using UAE since it can increase the efficiency of solvent extraction. ASE was also used to extract phenolic compounds from sorghum brans (Barros, Dykes, Awika, & Rooney, 2013), and anthocyanin composition from blue wheat, purple corn, and black rice (Abdel-Aal, Akhtar, Rabalski, & Bryan, 2014). This method uses a combination of elevated temperature and pressure with common solvents to increase the efficiency of the extraction process. The result is faster run times and a significant reduction in solvent use. Therefore, the main objective of the present study was to extract Riceberry bran using ASE, UAE, SE, and MC followed by the evaluation of the total phenolic content, total anthocyanin content and antioxidant activities in order to increase the utilization of Riceberry bran.

2. Methodology

2.1. Raw Material

Defatted Riceberry bran (*Oryza sativa*) obtained from Sunfood Corp Limited (Samutprakan, Thailand). It was sieved through 20 –100 mesh screen. It was kept in a sealed container at -18°C. All measurements were performed in triplicate.

2.2. Chemicals

Folin-Ciocalteu reagent gallic acid, 2,2'-diphenyl-1-picrylhydrazyl (DPPH), 2,2'-azaino-bis (3-ethylbenzothiazoline-6-sulfonic acid) diammonium salt (ABTS), ascorbic acid (vitamin C), α -tocopherol and 2,6-di-tert-butyl-4-methyl-phenol were purchased from Sigma-Aldrich (St. Louis, MO). Potassium chloride and sodium carbonate were purchased from Ajax Finechem (NSW, Australia). Sodium acetate hydrate and ferrous sulphate were purchased from Carlo Erba (Chaussee du Vexin, France). Hydrochloric acid was purchased from Merck (Darmstadt, Germany).

2.3. Determination of extract yield

The yield of extracts on a dry weight basis was calculated from equation (1) as shown below:

$$\text{Extract yield (\%)} = (W_1 \times 100) / W_2 \quad (1)$$

W_1 was the weight of extract after evaporation of ethanol

W_2 was the dry weight of the fresh plant sample

2.4. Determination of moisture content

The moisture content of the Riceberry bran was analysed according to AOAC methods (AOAC, 2019).

2.5. Determination of water activity (a_w)

The water activity was determined at 25 °C using aw meter, Aqua Lab (Series 3 TE (Decagon Devices Inc., U.S.A.)). Approximately 2 g of the ground sample was used for the analysis.

2.6. Determination of color value

The color of rice bran was measured with spectrophotometer (Hunter Lab, Color Quest XE, USA) equipped with a D65 illuminant using the CIE $L^* a^* b^*$ system.

2.7. Sample extraction

Four extraction methods, ASE, UAE, SE, and MC were investigated. Riceberry bran was extracted with ethanol using UAE method according to Tabaraki and Nateghi (2011) method with some modifications. The bran (10 g) was dissolved in 200 ml of 67% (v/v) aqueous ethanol. The sample was sonicated (37 kHz) in an ultrasonic cleaner (Ultrasonic bath, Elama series Elmasonic P, Germany) at 55 °C for 40 min. The resulting extract was filtered through a Whatman No. 1 filter paper and vacuum-dried in a rotary evaporator (Rotavapor R-100, Buchi, Switzerland) at 40°C. The crude extract was stored at -18 °C until use.

ASE was performed on a Dionex ASE 350 system (Thermo Scientific, USA). The bran sample of 10 g was mixed with diatomaceous earth (DE) in a proportion of 1:1 and placed in a 66 mL stainless steel extraction cell. A cellulose D28 filter (Dionex Corporation) was placed at the bottom of the extraction cell to avoid the collection of suspended particles in the collection vial. The extraction cells were arranged in the sample carousel and prefilled with the solvent (67% ethanol), static time 10

minutes, and heated at 55 °C. The extraction was done using 5 cycles and the cell was rinsed with 100% flush. The extract was collected in 250 mL collection vials. The resulting extract was filtered through a Whatman No. 1 filter paper and vacuum-dried in a rotary evaporator at 40 °C. The crude extract was stored at -18 °C until use.

The SE was based on the UAE method. The bran (10 g) was placed in a thimble and put it in the extractor that dissolved in 50 ml of 67% ethanol. The distillation flask was filled with 250 ml of 67% ethanol, and heat source. The sample was placed in a thimble-holder that was gradually filled with condensed fresh extractant from a distillation flask. When the solvent reached the overflow level, a siphon aspirates the solute from the thimble-holder and unloaded it back into the distillation flask, thus carrying the extracted analyses into the bulk liquid. This operation was repeated until the solvent in the extractor was clear. The resulting extract was filtered through a Whatman No.1 filter paper and vacuum-dried in a rotary evaporator at 40 °C. The crude extract was stored at -18 °C until use.

MC was investigated at room temperature. The bran (10 g) was dissolved in 200 ml of 67% ethanol in closed bottles. After 48 h of extraction, the extract was filtered through a Whatman No. 1 filter paper and repeat 3 times until the extract was clear. The collection of the extract was vacuum-dried in a rotary evaporator at 40°C. The crude extract was stored at -18 °C until use.

2.8. Determination of total phenolic content

The total phenolic content of Riceberry bran extracts was determined by the Folin-Ciocalteu reagent using different concentration (0-200 µg/mL) of Gallic acid as standard (Wolfe, Wu, & Liu, 2003) with some modifications. 125 µL of samples were mixed with 500 µL distilled water in a test tube followed by the addition of 125 µL of Folin-Ciocalteu reagent and allowed to stand at room temperature for 6 minutes. Then it was mixed with 1,250 µL of 7% Na₂CO₃ and followed by the addition of 1,000 µL of distilled water and allowed to stand at room temperature for 90 minutes. The absorbance of the mixtures was determined at 760 nm in spectrophotometer (UV mini-1240, Shimadzu, USA). Total phenolic content in the extract was expressed in mg Gallic acid equivalent/g.

2.9. Determination of anthocyanin content

The analysis method for anthocyanin content was modified from the method used by Giusti & Worsltad (2005). The Riceberry bran extracts (1 mL) in 25 mL of volume metric flasks were adjusted with potassium chloride buffer (0.03 mol/L, pH 1.0) and the other was adjusted with sodium acetate buffer (0.4 mol/L, pH 4.5). Each of them was left for 15 minutes in the dark at room temperature. The absorbance of the mixtures was determined at 510 nm and 700 nm in spectrophotometer. The anthocyanin concentration (mg/L) of sample was calculated according to the following formula (2) and expressed as Cyanidin-3-glucoside equivalents:

$$\text{Total anthocyanin content (mg/g)} = \frac{(A_{\lambda 700} - A_{\lambda 510})_{\text{pH 1.0}} - (A_{\lambda 700} - A_{\lambda 510})_{\text{pH 4.5}}}{(\epsilon \times l \times G)} \quad (2)$$

A was $(A_{\lambda 700} - \lambda_{510})_{\text{pH 1.0}} - (A_{\lambda 700} - \lambda_{510})_{\text{pH 4.5}}$

MW was the molecular weight of Cyanindin-3glucoside (449.2 g/mol)

DF was the dilution factor (20 µL sample is diluted to 2 mL, DF = 1000)

ϵ was the extinction coefficient ($L \times cm^{-1} \times mol^{-1}$) = 26,900 for Cyanindin-3-glucoside where L (path length in cm) = 1

l was the volume of solvent

G was the weight of sample

2.10. Determination of antioxidant activities

2.10.1. IC_{50} of DPPH scavenging activity

The free radical scavenging activity of Riceberry bran extracts will be evaluated using the stable radical DPPH according to the method of Re et al. (1999). Various concentration of each extract was pipetted into 1 mL DPPH working solution. The mixture was shaken and incubated for 30 minutes in the dark at room temperature. Ascorbic acid, α -tocopherol, and BHT were used as standard. The analysis was done in triplicate for standard and each extract. The absorbance of the mixtures was determined at 517 nm relative to the control (as 100%) using a spectrophotometer. The percentage of radical scavenging ability was calculated by using the formula (3):

$$\text{Scavenging ability (\%)} = \frac{(\text{Absorbance 517 nm of control} - \text{Absorbance 517 nm of sample}) \times 100}{\text{Absorbance 517 nm of control}} \quad (3)$$

IC_{50} of DPPH scavenging activity of each extract could be calculated using its calibration curve.

2.10.2. Ferric reducing antioxidant power (FRAP)

The FRAP assay was modified from Benzie and Strain (1999). 60 μ L of samples were mixed with 1.8 ml of the FRAP reagent and 180 μ L of distilled water. The absorbance of the mixtures was determined at 593 nm using a spectrophotometer after 4 minutes incubation at 37 °C. FRAP reagent was prepared daily and consisted of 0.3 M acetate buffer (pH 3.6), 10 mM TPTZ in 40 mM HCl, 20 mM $FeCl_3$ and distilled water in a ratio of 10:1:1:1.2 (v/v/v/v). FRAP value was obtained by comparing the absorbance change in the test mixture with doses obtained from increasing concentrations of Fe(III) and expressed as mmol of Fe(II) equivalents per g extract. Ascorbic acid, α -tocopherol, and BHT were used as standard.

2.10.3. IC_{50} of ABTS radical scavenging assay

ABTS radical scavenging activity was determined according to Re et al. (1999) with some modification. A stable stock solution of ABTS radical cation was produced by reacting a 7 mM aqueous solution of ABTS with potassium persulfate in the dark at room temperature for 12-16 h before use. The working solution was diluted with 95% ethanol to reach an absorbance of 0.7 ± 0.02 at 734 nm. 20 μ L of samples were mixed with 2 mL of working solution, and the absorbance was measured immediately at 734 nm after 6 minutes at room temperature in the dark. Ascorbic acid, α -tocopherol, and BHT were used as standard. The analysis was done in triplicate for standard and each sample. Antioxidant capacity of each sample was determined based on the reduction of ABTS absorbance by calculating the percentage of antioxidant activity. IC_{50} of ABTS scavenging activity of each extract could be calculated using its calibration curve.

3. Results and discussion

3.1. Quality of raw material

Chemical and physical properties of defatted Riceberry bran are presented in Table 1. Defatted Riceberry bran had low moisture content and a_w and dark purple in color. The particle size of Riceberry bran was mostly 60-80 mesh.

Table 1. Chemical and physical properties of Riceberry bran.

Chemical and physical properties	Measurement values
Moisture (%)	5.65±0.12
a_w	0.33±0.01
L*	35.33±0.17
a*	5.69±0.11
b*	4.28±0.12
Particle size 20-40 Mesh (%)	4.55±0.78
40-60	19.24±0.95
60-80	65.16±0.86
80-100	7.80±0.84
≥ 100	3.25±0.75

3.2. Effect of extraction methods on total phenolic and total anthocyanin content

The extracts obtained from ASE, UAE, SE and MC were investigated. Percentage of extraction yield, total phenolic and total anthocyanin contents are shown in Table 2. There were no significant differences in the percentage of extraction yield ($p>0.05$). The percentages of extraction yield from each method were in the range of 18.07 – 21.73%. Total phenolic content was determined in comparison with gallic acid and the results were shown in terms of mg GAE/g extract. The results showed that the Riceberry bran extract from ASE had significantly higher total phenolic and total anthocyanin content than the other methods. This method uses high pressures during the extraction process so they allow the solvent to be heated at higher temperatures than their boiling point which increases diffusion rates, disturbs the strong solute–matrix interactions and reduces liquid solvent viscosity, allowing better penetration into the matrix and then improving extraction (Barros, Dykes, Awika, & Rooney 2013). Total phenolic content of the Riceberry bran extract from SE was 54.18 mg GAE/g extract while total anthocyanin content was 0.91 mg/g extract. The increase of total phenolic content in the Riceberry bran extract from SE due to high temperature and long extraction time. During extraction, heating of the sample might soften the plant tissue and weaken the phenol–protein and phenol–polysaccharide interactions, leading to more polyphenols diffusion into the solvent (Das Das, Goud, & Das, 2017; Tao, Wu, Zhang, & Sun, 2014). The Riceberry bran extract from UAE had lower total phenolic content than other methods because it took a shorter extraction time than MC and lower temperature than SE.

There were significant differences in total anthocyanin content ($p\leq 0.05$). The results obtained from four methods showed that the Riceberry bran extract from ASE had higher total anthocyanin content than the other methods because this method took a short time to heat. This result was in agreement with previous reports that ASE was more appropriate in extracting anthocyanin from

colored grains as being comparable with the commonly used solvent extraction method based on changes in anthocyanin composition (Abdel-Aal, Akhtar, & Rabalski, 2014). The Riceberry bran extract from UAE had higher anthocyanin than the Riceberry bran extract from SE and MC since ultrasound induced swelling of plant cells or breakdown of cell walls during sonication.

Table 2. Effect of extraction methods on a percentage of extract yield, total phenolic content and total anthocyanin content.

Method	Extract yield ^{ns} (%)	Total phenolic (mgGAE/g extract)	Total anthocyanin (mg/g extract)
ASE	20.97±0.07	55.45±0.11 ^a	3.06±0.13 ^a
UAE	19.57±0.11	48.52±0.50 ^d	2.28±0.13 ^b
SE	18.07±0.45	54.18±0.60 ^b	0.91±0.07 ^d
MC	21.73±0.25	50.03±0.17 ^c	1.44±0.21 ^c

^{a-c} Means in same columns followed by different letter are significantly different ($p \leq 0.05$).

^{ns} Means not significant ($p > 0.05$).

Therefore, antioxidants can be released from plant cells into the solvent. A decrease in anthocyanin of the Riceberry bran extract from SE because the extract was obtained high temperature and long extraction time as a result that anthocyanin was decomposed. An increase in temperature up to 74°C could increase phenolic content but it decreased anthocyanin content (Sripum, Kukreja, Chareonkiatkul, Kriengsinyos, & Suttisansanee, 2017; Cacace & Mazza, 2003). The degradation rate of anthocyanin depends on time and temperature. Therefore, high temperature and short extraction time were used successfully to retard anthocyanin degradation in plants (Ju & Howard, 2003).

3.3. Effect of extraction methods on radical scavenging activities

The radical scavenging activities of Riceberry bran were evaluated for DPPH, ABTS and FRAP assay as shown in Table 3. DPPH, ABTS radical scavenging activity of different extraction methods which express in terms of IC₅₀ value. Lower IC₅₀ value means more antioxidant potential. The chelating ability on ferrous ion in Riceberry bran extract was determined by FRAP assay. The radical scavenging activities were compared with ascorbic acid, α-tocopherol and BHT as standard. There were significantly different in IC₅₀ of DPPH and ABTS assay and FRAP assay amongst the extraction methods ($p \leq 0.05$).

Table 3. Effect of extraction methods on radical scavenging activities (DPPH, ABTS and FRAP assay)

Method	DPPH assay IC ₅₀ (mg/mL)	ABTS assay IC ₅₀ (mg/mL)	FRAP assay mmole Fe(II)/kg
ASE	0.109±0.000 ^a	3.42±0.05 ^a	688.04±1.12 ^a
UAE	0.144±0.004 ^d	4.16±0.04 ^c	543.51±0.67 ^c
SE	0.127±0.000 ^b	3.45±0.06 ^a	649.76±0.99 ^b
MC	0.137±0.002 ^c	3.75±0.06 ^b	668.65±1.22 ^{ab}
BHT	0.135±0.002	0.499±0.002	3,937.00±10.00

Ascorbic acid	0.004±0.001	0.207±0.002	5,943.00±10.07
α-tocopherol	0.117±0.000	0.779±0.014	15,471.00±23.01

^{a,d} Means in same columns followed by different letter are significantly different ($p \leq 0.05$).

^{ns} Means not significant ($p > 0.05$).

The results showed that the Riceberry bran extract from ASE had lower IC_{50} of DPPH and ABTS assay than the other methods. The IC_{50} of DPPH assay in the Riceberry bran extract from ASE was 0.109 mg/mL which was comparatively lower than the IC_{50} of DPPH assay in BHT and α-tocopherol, the IC_{50} showed that the Riceberry bran extract from ASE had more effective antioxidant activities than antioxidant compared to BHT and α-tocopherol. Previously, Soradech et al. (2016) compared IC_{50} of six species of colored rice and it was found that the extract of Gum-Doy-Moo-Ser and Riceberry had an effective antioxidant activities than other species of colored rice in that study.

The IC_{50} of ABTS in the Riceberry extract from ASE was not significantly different from SE but significantly lower than UAE and MC ($p \leq 0.05$). The Riceberry bran extract from ASE and SE has more effective antioxidant activities than UAE and MC. The FRAP values from each method were in the range of 543.51–688.04 mmole Fe(II)/kg. The highest FRAP value was the Riceberry bran extract from ASE. There were no significant differences in FRAP value of the Riceberry bran extract from ASE and MC method ($p > 0.05$). The Riceberry bran extraction from UAE showed weak radical scavenging activities despite of high total anthocyanin content. The results indicated that phenolic gave antioxidant activity greater than anthocyanin. This result is in agreement with the previous report by Chen, Nagao, Itani, & Irifune (2012) that anthocyanin pigments of colored rice gave a low antioxidant activities.

Table 4. The Pearson's correlation coefficient (r) between total phenolic content and antioxidant activities measured by DPPH, ABTS and FRAP assays.

	TPC	DPPH	ABTS	FRAP
TPC	1			
DPPH	-0.933*	1		
ABTS	-0.936*	0.841*	1	
FRAP	0.853*	-0.822*	-0.959*	1

* Means correlation is significant ($p \leq 0.01$).

Pearson's correlation coefficients between total phenolic content and antioxidant activities measured by DPPH, ABTS and FRAP assays were computed and the results are shown in table 4. Significant correlations were found between total phenolic content and antioxidant activity ($p \leq 0.01$) but the results of antioxidant activities were not significantly correlate to total anthocyanin content. Total phenolic content had negative correlation with IC_{50} of DPPH assay and IC_{50} of ABTS assay ($r = -0.933$ and $r = -0.936$). Significant positive correlation was obtained for total phenolic content with FRAP value ($r = 0.853$). The highest correlation was found between FRAP value and IC_{50} of ABTS assay ($r = -0.959$). The lowest correlation was found between the IC_{50} of DPPH assay and FRAP value ($r = -0.822$). These results corresponded to the previous research (Dudonne et al., 2009), which

reported that significant correlations were found between DPPH, ABTS, and FRAP assays and total phenolic content determined by the Folin-Ciocalteu method. Therefore, phenolic compounds in plant extracts contribute significantly to their antioxidant potential.

4. Conclusion

Analysis of the total phenolic and anthocyanin content and radical scavenging activities of Riceberry extracts showed differences depending on extraction method. Amongst the extraction methods, The Riceberry bran extraction from ASE was the most effective method in antioxidative reactions and high total phenolic and total anthocyanin content. It can be concluded that the Riceberry bran extraction SE had high total phenolic content and strong antioxidative reactions but it had a long extraction time and high costing. The Riceberry bran extract from UAE had high total anthocyanin content and it used the lower energy input. The Riceberry bran extract from MC had low bioactive compounds and antioxidant activities but it took a long extraction time.

References

- Abdel-Aal, E. Akhtar, H. Rabalski, I., & Bryan, M. (2014). Accelerated, microwave-assisted, and conventional solvent extraction methods affect anthocyanin composition from colored grains. *Journal of Food Science*. 79(2): C138-C145.
- AOAC. (2019). *Official methods of analysis* (21th ed.). Washington DC: Association of Official Analytical Chemists.
- Barros, F., Dykes, L., Awika, J.M., & Rooney, L.W. (2013). Accelerated solvent extraction of phenolic compounds from sorghum. *Journal of Cereal Science*. 58: 305-312.
- Benzie, I.F.F., & Strain, J.J. (1999). *Ferric reducing/antioxidant power assay: Direct measure of total antioxidant activity of biological fluids and modified version for simultaneous measurement of total antioxidant power and ascorbic acid concentration. Methods in Enzymology*. 299: 15-27.
- Cacace, J.E., & Mazza, G. (2003). Optimization of extraction of anthocyanins from black currents aqueous ethanol. *Journal of Food Science*. 68(1): 240-248.
- Chen, X.Q., Nagao, N., Itani, T., & Irifune, K. (2012). Anti-oxidative analysis, and identification and quantification of anthocyanin pigments in different colored rice. *Food Chemistry*. 135: 2783-2788.
- Das, A. B., Goud, V. V., & Das, C. (2017). Extraction of phenolic compounds and anthocyanin from black and purple rice bran (*Oryza sativa* L.) using ultrasound: A comparative analysis and phytochemical profiling. *Industrial Crops and Products*. 95: 332-341.
- Dudonne, S., Vitrac, X., Coutiere, P., Woillez, M., & Merillon, J. (2009). Comparative study of antioxidant properties and total phenolic content of 30 plant extracts of industrial interest using DPPH, ABTS, FRAP, SOD, and ORAC assay. *Journal of Agricultural and Food Chemistry*. 57: 1768-1774.
- Giusti, M. M., & Worsltad, R. E. (2005). Characterization and measurement of anthocyanins by UV-visible spectroscopy. *Current protocols in food analytical chemistry*. 1: F1. 2.1-F1. 2.13.
- Ju, Z. Y., & Howard, L. R. (2003). Effects of Solvent and Temperature on Pressurized Liquid Extraction of Anthocyanins and Total Phenolics from Dried Red Grape Skin. *Journal of Agricultural and Food Chemistry*. 57: 5207-5213.
- Leardkamolkarn, V., Thongthep, W., Suttarporn, P., Kongkachuichai, R., Wongpornchai, S., & Wanavijitr, A. (2011). Chemopreventive properties of the bran extracted from a newly-

- developed Thai rice: The Riceberry. *Food Chemistry*, 125(3), 978-985. doi:https://doi.org/10.1016/j.foodchem.2010.09.093
- Peanparkdee, M., Yanauchi, R., & Iwamoto, S. (2018). Characterization of antioxidants extracted from Thai Riceberry bran using ultrasonic-assisted and conventional solvent extraction methods. *Food and Bioprocess Technology*, 11: 713-722.
- Posuwan, J., P. Prangthip, V., Leardkamolkarn, U., Yamborisut, R., Surasiang, R., Charoensiri R., & Kongkachuichai, R. (2013) Long-term supplementation of high pigmented rice bran oil (*Oryza sativa* L.) on amelioration of oxidative stress and histological changes in streptozotocin-induced diabetic rats fed a high fat diet; Riceberry bran oil. *Food Chemistry*. 138: 501-508.
- Prangthip, P., Surasiang, R., Charoensiri, R., Leardkamolkarn, V., Komindr, S., Yamborisut, U., Vanavichit, A., & Kongkachuichai, R. (2013). Amelioration of hyperglycemia, hyperlipidemia, oxidative stress and inflammation in streptozotocin-induced diabetic rats fed a high fat diet by Riceberry supplement. *Journal of Functional Foods*. 5: 195-203.
- Re, R., Pellegrini, N., Proteggente, A., Pannala, A., Yang, M., & Rice-Evans, C. (1999). Antioxidant activity applying an improved ABTS radical cation decolorization assay. *Free Radical Biology and Medicine*, 26(9-10): 1231-1237.
- Tabaraki, R., & Nateghi, A. (2011). Optimization of ultrasonic-assisted extraction of natural antioxidants from rice bran using response surface methodology. *Ultrasonics Sonochemistry*. 18: 1279-1286.
- Tao, Y., Wu, D., Zhang, Q., & Sun, D. (2014). Ultrasound-assisted extraction of phenolics from wine: Modeling, optimization and stability of extracts during storage. *Ultrasonics Sonochemistry*. 21(2): 706-715.
- Soradech, S., Reungpatthanaphong, P., Tangsatirapakdee, S., Panaphong, K., Thammachat, T., Manchun, S. & Thubthimthed, S. (2016). Radical scavenging, antioxidant and melanogenesis stimulating activities of different species of rice (*Oryza sativa* L.) extracts for hair treatment formulation. *Thai Journal of Pharmaceutical Sciences*. 40:92-92.
- Sripum, C., Kukreja, R. K., Chareonkiatkul, S., Kriengsinyos, W. & Suttisansanee, U. (2017). The effect of extraction conditions and antioxidant activities and total phenolic content of different processed Thai Jasmine rice. *International Food Research Journal*. 24(4): 1644-1650.
- Suttiarporn, P., Sookwong, P., & Mahatheeranont, S. (2016). Fractionation and Identification of Antioxidant Compounds from Bran of Thai Black Rice cv. Riceberry. *International Journal of Chemical Engineering and Applications*. 7(2): 109-114.
- Wolfe, K., Wu, X., & Liu, R. H. (2003). Antioxidant activity of apple peels. *Journal of Agricultural and Food Chemistry*. 51: 609-614.

A Research of Model of Professional Basketball Management for Professional Basketball Players

Jatuporn Banroengsanoh

Major Field: Sports Science, Faculty of Sports Science, Kasetsart University

E-mail; jatupornarm@gmail.com

Abstract

An objective of a research in a Management of Professional Basketball Players in the Thailand Basketball League is to study the model of Professional Basketball Players Management in the Thailand Basketball League. The researcher used a Survey Research Method to interview involved people in managing Professional Basketball Players in the Thailand Basketball League. The Simple Random Sampling Method was used in 250 samples, and statistics which were used to analyze data were Percentage, Mean and Standard Deviation. The researcher found that the model of Professional Basketball Players Management in the Thailand Basketball League contained 4 steps as below.

- 1) Sourcing of Professional Basketball Players; the evaluation was in the highest level at 4.56 of Mean and 0.4062 of SD.
- 2) Selection of Professional Basketball Players; the evaluation was in the highest level at 4.75 of Mean and 0.4333 of SD
- 3) Development of Professional Basketball Players; the evaluation was in the highest level at 4.60 of Mean and 0.518 of SD
- 4) Retention of Professional Basketball Players; the evaluation was in the highest level at 4.61 of Mean and 0.519 of SD

Keywords: A Study of Management Model, Professional Basketball Club, Professional Basketball Players

1. Introduction

The Basketball Association in Thailand finds that to re-light up the popularity of basketball among Thai teens and people needs to run professional tournaments all around Thailand. Not only attract basketball players themselves to determine to play in the professional level, but also attract governmental organizations and private companies to support teams in the league. Moreover, Professional tournaments are set to target to develop players to have a real career by playing basketball. The First Professional League in Thailand was held in 2555 B.C. which was supported by the Sports Authority of Thailand,

and this league was back to be popular again, and in 2556 B.C., it was held for the second time with more interests from press to broadcast all over the country; furthermore, in 2557 B.C. there was clear to set up the real basketball league (Professional Basketball League Project, 2018).

In present, there is a professional basketball league which is under the name of TBL (Thailand Basketball League) to provide the real career to players. Mr.Nipondh Chawalitmontien, Basketball Association of Thailand President, said that there was a very good performance from team Thailand so that he had some initiative to set up the professional league to provide the real career to players to earn money for their livings. (<https://www.tnews.co.th/sat>, 18 August 2019)

2.Objective

To study the model of Professional Basketball Players Management in the Thailand Basketball League

3. Research Methods

In this research, the research creates the Management of Professional Basketball Players survey instrument which is checked by experts. Also the interview of team managers, coaches and players are collected from 10 teams, 250 people in Thailand Basketball League

4. Results

1. Sourcing of Professional Basketball Players; the evaluation was in the highest level. That means the source of professional basketball players are from inside and outside the country.
2. Selection of Professional Basketball Players; the evaluation was in the highest level. That means clubs need to analyze team weakness to have data to select positions of players.
3. Development of Professional Basketball Players; the evaluation was in the highest level. That mean clubs need to plan and develop each professional player based on an analysis in each individual player.
4. Retention of Professional Basketball Players; the evaluation was in the highest level. That mean clubs have to have a clear direction of target also give faith to players.

5. Table 1 Indicate Mean and SD of comments in questionnaires of the Management of Professional Players in Thailand Basketball League

Comments of the Management of Professional Players	Mean	SD	Result
1. Sourcing of Professional Basketball Players	4.56	0.406	Highest
2. Selection of Professional Basketball Players	4.75	0.433	Highest
3. Development of Professional Basketball Players	4.60	0.518	Highest
4. Retention of Professional Basketball Players	4.61	0.519	Highest
Average	4.63	0.470	Highest

6. Conclusion and Discussion

From the study, it was found that 1) Sourcing of Professional Basketball Players was related to the quote of Sawanee Kaewmanee and Rattanawadee Bunnasit (2006). that said, the step of sourcing efficient people has to start from pointing which is the most important position to lead to the target of the organization by finding manpower from inside and outside officially and unofficially. 2) Selection of Professional Basketball Players was related to Wichian Wittayaudom (2008: 130). that said, the selection of people inside the organization is a good way because it is an opportunity to open for insiders to encourage them to stay, and does not to hire from outside. 3) Development of Professional Basketball Players was related to Berger & Berger's concept (Berger & Berger, 2004). that said, there needs to have a plan for individual development in good and efficient people for them to maintain their strengths and solve their weaknesses. Development methods can be to teach, to provide urgent special projects, to self-study, to attend management and development seminars inside and outside and to apply self-online learning. 4) Retention of Professional Basketball Players was related to the research of Pornrat Sadaengharn (2013). The data from

a review of literature and survey of Eastern Seaboard Industrial Estate showed that factors to retain top talented people were work culture and environment which were work relationship, flexibility and good communication as well as a role model from superiors. Moreover, good work which can attract manpower to stay is one of main factors.

7. Recommendation

A Professional Basketball Players Management in an international League such as ABL (Asean Basketball League) should be studied to lift up and promote the management system of the professional basketball league in the country.

References

- Pornrat Sadaengharn. (2013). Retaining Talented People in Organization, .38-33 ,(3)33
- Wichian Wittayaudom. (2008). Organization & Management. Published 2nd Edition Bangkok: Thanathud Printing Co.,Ltd
- Sawanee Kaewmanee and Rattanawadee Bunnasit. (2006). Talent Management. Self Management Journal. 27 (4): 10-18.
- Berger, D.R. and L.A. Berger. (2004). The Talent Management Handbook: Creating Organizational Excellence by Identifying, Developing, and Promoting Your Best People. New York: McGraw-Hill.
- Sports Authority of Thailand. (2018). Dissecting basketball plans Direction towards professional sports. Retrived August 18, 2019 from <https://www.tnew.co.th/sat/Contents/480451>.

Biomonitoring of metals exposure in Aranyik handicraft workers

Churairat Srimanee^{1,2 a}, Suwalee Worakhunpiset^{1,b}, Yanin Limpanont¹, Kraichat Tantrakanapa¹

¹Department of Social and Environmental Medicine, Faculty of Tropical Medicine, Mahidol University, Thailand

²Department of Diseases Control, Ministry of Public Health, Thailand

E-mail; ^as.churairat@gmail.com, ^bsuwalee.wor@mahidol.ac.th

Abstract

Purpose: Aranyik handicraft workers are exposed to hazardous materials including metal dust and fumes while working. Here, chromium, manganese, and nickel concentrations in samples from Aranyik handicraft workers were determined, and associations between risk factors and the metal concentrations in the samples were address all of the following elements: Purpose of the article, methods, results, conclusions assessed.

Methods: A cross-sectional study was performed with 60 Aranyik handicraft workers. Manganese concentrations in blood and nickel and chromium concentrations in urine were determined, and each participant completed a questionnaire (administered in an interview).

Results: The manganese concentrations in blood were acceptable for 57 (89%) of the participants but exceeded the reference value for three (17%) of the participants. The nickel and chromium concentrations in urine did not exceed the reference values for any participant. Some participants exhibited unsafe behaviors, 85.0% drinking and eating while working, 68.30% not wearing goggles, 73.30% not wearing face shields, and 26.70% not using ventilation in the work area. Pearson correlation analyses were performed, and no significant correlations were found between manganese concentrations in blood and either health risk behavior scores ($r=-0.61$, $p=0.64$) or working environment factors ($p<0.05$).

Conclusions: Aranyik handicraft workers are occupationally exposed to manganese, and some workers have manganese concentrations in blood exceeding the reference value. The workers are exposed to acceptable amounts of chromium and nickel. Unsafe behaviors may affect exposure to metals, but statistical analyses did not strongly support this. Good personal hygiene and safe working practices should be recommended to decrease the risks posed by occupational exposure to metals.

Keywords: Biomarker : Metals : Aranyik : Handicraft workers

1. INTRODUCTION

Thailand is famous for handicrafts, and handicrafts are made in almost every Thai province. Handicraft products such as knives and related equipment are made by families and communities that have inherited the production methods involved. Most of the handicraft products are made from iron and steel sheets selected to suit the intended design and function of the product and to perform appropriately.

Knife production involves cutting, heating, and grinding metal sheet and making handles. Steel sheet contains metals such as chromium, manganese, selenium, and zinc that prevent corrosion and improve the strength of the sheet, so people working with steel sheet may be exposed to various metals during the production process, particularly during grinding. Most handicraft processes are performed using both hand-held tools and machines that can generate dust and welding fumes. Metal dust and fumes that can be emitted to the air during certain processing conditions and contaminate the working area can pose hazards to handicraft workers.

Interactions between susceptible cellular targets and free metals and/or metal ions can lead to toxic effects. [1] Inhalation and ingestion of metal dust in the workplace are important routes through

which workers are exposed to metals. Metal dust containing beryllium, cadmium, lead, manganese, and nickel produced during handicraft production may lead to systemic intoxication and may affect the blood, kidneys, and/or central nervous system.[2] Exposure to chromium VI, nickel, or manganese can cause allergic dermatitis, bronchial asthma, neurotoxicity, and nephrotoxicity. Exposure to hazardous substances can be estimated by measuring the concentrations of the substances and/or metabolites in blood or urine. Metabolites and other species can be used as biomarkers for various hazardous species.

The aims of this study were (1) to determine blood manganese, urinary chromium, and urinary nickel concentrations of Aranyik handicraft workers who may be exposed to potentially toxic metals while working and (2) to compare the concentrations with reference values to assess the risks posed by heavy metals to the workers. Personal factors such as the time each worker is exposed to metal dust, the use of personal protective equipment, and ventilation were taken into account.

2. MATERIALS AND METHODS

2.1 Participants and sampling methods

A cross-sectional study involving Aranyik handicraft workers in Ban Ton Poa and Ban Pai Nong (in Tha Chang District, Ayutthaya Province, Thailand) was performed between October and December 2016. The protocol used was approved by the Ethical Committee of the Faculty of Tropical Medicine, Mahidol University (approval no. TMEC 16-056) and was in accordance with the 1964 Helsinki declaration (and later A cross-sectional study involving Aranyik handicraft workers in Ban Ton Poa and Ban Pai Nong (in Tha Chang District, Ayutthaya Province, Thailand) was performed between October and amendments) or comparable ethical standards. Written informed consent was obtained from each participant. A walk-through survey was performed to observe the communities and identify the locations of relevant households in the communities, and participants were randomly selected from each relevant household. Male and female handicraft workers who were 20–70 y old and exposed to heavy metals while working were selected. Only willing participants permanently resident in the study areas and having manufactured handicrafts for at least 1 y were selected. Handicraft workers known to have chronic kidney disease or cancer were excluded. A total of 60 Aranyik handicraft workers were involved in the study.

2.1.1 Blood sample collection

Blood samples were collected at the end of the last working shift of the week, and the manganese concentrations in the blood samples were determined. A 5 mL blood sample was collected from each participant by venipuncture into a polypropylene tube containing heparin or EDTA (to act as an anticoagulant). The blood samples were transferred to the laboratory in a container containing ice packs and then kept at 4 °C until they were analyzed.

2.1.2 Urine sample collection

A 20 mL mid-stream urine sample was collected from each participant at the end of the last working shift of the week, and the chromium and nickel concentrations in the samples were determined. The containers the urine sample were collected in were rinsed with HNO₃ and deionized water and dried before being used. The urine samples were transferred to the laboratory in a container containing ice packs and then kept at 4 °C until they were analyzed.

2.1.3 Questionnaire

A questionnaire was used to collect personal data (age and sex), information on behaviors posing health risks (smoking, drinking water and eating in the working area, and the use of personal protective equipment), and information on work environment factors (work duration and ventilation in the workplace) from the participants. The questionnaire was administered by trained interviewers.

2.2 Heavy metal analysis

2.2.1 Determination of manganese concentrations in the blood samples

The protocol used to determine the manganese concentrations in the blood samples is described here. A solution containing chemical modifiers was prepared by adding 100 g Triton-x and 5 g diammonium hydrogen phosphate to a 1000 mL volumetric flask and adding deionized water to give a final volume of 1000 mL. A 1% nitric acid solution was prepared by adding 15.4 mL of 65% nitric acid to a 1000 mL volumetric flask and making the solution up to 1000 mL with deionized water. Working manganese standard solutions at manganese concentrations of 5, 10, 20, 30, 50, 70, and 90 $\mu\text{g/L}$ were prepared by adding appropriate amounts of a manganese standard to 1% nitric acid. A 900 μL aliquot of the modifier solution and 100 μL of a blood sample were added to a microcentrifuge tube, which was then placed on a roller mixer for 10 s. The mixture was then transferred into a sample cup. The manganese concentration was determined by graphite furnace atomic absorption spectrophotometry with Zeeman background correction (using a Varian Model SpectrAA 880 instrument; Agilent technologies, Santa Clara, California, United States). Light emitted from a hollow cathode lamp at a wavelength of 279.50 nm was used. The correlation coefficient (r) was 0.9996, and was acceptable. The limit of quantification for manganese in blood was 3.0 $\mu\text{g/L}$. Seronorm Trace Elements Whole Blood Level 2 (Sero AS; Billingstad, Norway) and ClinChek Whole Blood Control Lyophilized for Trace Elements Level 1 (RECIPE Chemicals + Instruments; Munich, Germany) were used as quality control samples.

2.2.2 Determination of chromium and nickel concentrations in the urine samples

The protocol used to determine the chromium and nickel concentrations in the urine samples is described here. A solution containing chemical modifiers was prepared by adding 15.4 mL of 65% nitric acid and 20 mL of palladium nitrate to a 1000 mL volumetric flask and making the solution up to 1000 mL with deionized water. Working chromium and nickel standard solutions at concentrations of 5, 10, 20, 30, 50, 70, and 90 $\mu\text{g/L}$ were prepared by adding appropriate amounts of chromium and nickel standards to 1% nitric acid. A 900 μL aliquot of the modifier solution and 100 μL of a urine sample were added to a microcentrifuge tube, which was then placed on a roller mixer for 10 s. The mixture was then transferred into sample cups. The chromium and nickel concentrations were determined by graphite furnace atomic absorption spectrophotometry with Zeeman background correction (using a Varian Model SpectrAA 880 instrument) using a wavelength of 357.90 nm for chromium and a wavelength of 232.00 nm for nickel. The correlation coefficients (r) were both 0.9996, and were acceptable. The limits of quantification for chromium and nickel in urine were 3.0 and 5.0 $\mu\text{g/L}$, respectively. Lyphochek Urine Metals Control Level 2 (Bio Rad Laboratories, Hercules, CA, United States) and ClinChek Urine Controls Lyophilized for Trace Elements Level 1 (RECIPE Chemicals + Instruments; Munich, Germany) were used as quality control samples.

2.3 Data analysis and statistics

Descriptive statistics were used to describe the distributions of the variables. A rating scale was used to classify the score of health risk behaviors. The answers to the 15 questions each had three possible answers, 1 for never, 2 for sometimes, and 3 for always, but the values were positive for some questions and negative for others. The level of health risk behavior 1 was defined as the sum of the values. Values of 1.00–1.99 were taken to indicate unsafe behavior, and values of 2.00–3.00 were taken to indicate safe behavior. Pearson correlation coefficients were used to assess the relationships between the heavy metal concentrations and risk factors. The level used to identify a statistically significant relationship was $p < 0.05$.

3. RESULTS

3.1 General characteristics of the participants

There were 47 female participants (78.30%) and 13 male participants (21.70%). The mean age was 53.22 y (standard deviation 6.48 y). The maximum age was 66 y and the minimum was 39 y. Nine (15%) of the participants never ate or drank at work, 23 (38.30%) of the participants sometime ate and drank at work, and 28 (46.70%) of the participants always ate and drank at work. A total of 49 (81.7%) of the participants always washed their hands before eating, 10 (16.7%) sometimes washed their hands before eating, and one (1.60%) never washed their hands before eating. Two (3.3%) participants were smokers with a maximum of 20 cigarettes per day. One participant (1.60%) always smoked at work, one sometimes smoked at work, and both never washed their hands before smoking. All the participants used personal protective equipment while working, but not all the types of personal protective equipment available were used by all the participants. Cotton masks were always worn by 91.70% of the participants, goggles by 31.70%, face shields by 26.70%, and gloves by 88.3%. A total of 23 (38.3%) of the participants had hypertension, 10 (16.7%) had diabetes, and two (3.3%) had cardiovascular disease. The participants had been Aranyik handicraft workers for between 11 and 40 y, and the mean was 24.05 y (standard deviation 7.22 y). Most (51.70%) of the participants had been Aranyik handicraft workers for between 21 and 30 y. The longest and shortest daily working hours were 12 and 3 h, respectively. A total of 26 (43.30%) of the participants worked less than 8 h per day. The most common number of days worked per week was five, and the most was six. All of the workers used ventilation systems in their working areas. Most (96%) of the ventilation systems were electric fans, and most (73.30%) were used each day.

The knife production process has four steps. A total of 16 (26.67%) of the participants performed cutting work, 17 (28.33%) heating work, 16 (26.67%) grinding work, and 11 handle making

3.2 Metal concentrations in the blood and urine samples

A total of 57 (89%) of the participants had acceptable manganese concentrations in their blood. The mean manganese concentration in blood and the mean nickel concentration in urine were 12.12 and 5.55 $\mu\text{g/L}$, respectively. Three participants had manganese concentrations in blood exceeding the reference value. All three of these participants were female. One, a 51 y old who had worked for 27 y, had a manganese concentration in blood of 23 $\mu\text{g/L}$. She was a non-smoker with no history of hypertension, diabetes, or cardiovascular diseases, and performed grinding work. Another, a 50 y old who had worked for 23 y, had a manganese concentration in blood of 20 $\mu\text{g/L}$. She was a non-smoker

with a history of hypertension and cardiovascular diseases, and performed grinding work. The third, a 60 y old who had worked for 27 y, had a manganese concentration in blood of 20.40 µg/L. She was a non-smoker with hypertension, and performed heating work.

None of the participants had nickel or chromium concentrations in urine exceeding the reference values.[3][4] The highest and lowest nickel concentrations in the urine samples were 12.90 and 5.00 µg/L, respectively. Chromium was not detected in any urine sample (Table 1).

Table 1. Numbers and percentages of participants with metal concentrations in specified ranges (N=60)

Metal	Concentration (µg/L)	N (total 60)	% of participants	Number (%) of participants with a metal concentration exceeding the reference value
Manganese (in blood)	0-9.90	22	36.67	-
	10.00-19.90	35	58.33	-
	20.00-29.90	3	5.00	3 (5)
Mean 12.12, standard deviation 3.71, minimum 7.00, maximum 23.00				
Nickel (in urine)	0-9.90	56	93.33	-
	10.00-19.90	4	6.67	-
Mean 5.55, standard deviation 1.57, minimum 5.00, maximum 12.90				
Chromium (in urine)	not detected	60	-	-

3.3 Health risk behaviors

The questionnaire contained nine questions about workplace behaviors affecting health risks. These behaviors were drinking and eating while working, washing hands before eating, smoking at work, washing hands before smoking, wearing a cotton mask, wearing goggles, wearing a face shield, wearing glove gloves, and using ventilation in the work area. A scale was used to classify the health risk scores, and the results are shown in Table 2

Table 2. Number (percentage) of participants with behaviors affecting health risks, and the health risk scores

Variable	Health risk behavior		Mean	SD
	Safe behavior	Unsafe behavior		
1. Drinking and eating while working	9 (15.0%)	51 (85.0%)	1.68	0.93
2. Washing hands before eating	59 (98.30%)	1 (1.70%)	2.80	0.57
3. Smoking at work	59 (98.30%)	1 (1.70%)	2.95	0.37
4. Washing hands before smoking	58 (96.70%)	2 (3.30%)	2.93	0.47
5. Wearing a cotton mask	55 (91.70%)	5 (8.30%)	2.50	0.84
6. Wearing goggles	19 (31.70%)	41 (68.30%)	1.39	0.75
7. Wearing a face shield	16 (26.70%)	44 (73.30%)	1.33	0.78
8. Wearing gloves	53 (88.33%)	7 (11.67%)	2.68	0.84
9. Using ventilation in the work area	44 (73.30%)	16 (26.70%)	2.73	0.58

SD = standard deviation

The highest and lowest scores of health risk behaviors were 25.00 and 18.00, respectively, and the mean was 22.25 (standard deviation 1.57). The health risk scores for 31.70% of the participants were ≥ 23. Pearson correlation coefficients were calculated to allow correlations between the health risk scores, working environment parameters, and manganese concentrations in blood to be identified. No significant correlation was found between the health risk score and manganese concentration in blood

($r = -0.61$, $p = 0.64$) or between the working environment parameters and manganese concentration in blood ($p > 0.05$). The results are shown in Table 3.

Table 3. Correlations between the working environment parameters and manganese concentration in blood (N=60)

Variable	r	p
Number of years working	0.06	0.66
Working hours per day	-0.15	0.24
Working hours per week	0.03	0.98

4. DISCUSSION

Occupational exposure to metals depending on type of work and working activities. In regards to working characteristic, Aranyik handicraft workers may expose to toxic metals via inhalation, ingestion and dermal absorption of metal dust or fume created by working processes such as heating and grinding. In this study, blood manganese, urinary chromium and urinary nickel were determined as biomarkers of exposure according to the recommendation of previous studies.[5-8] Our study revealed the variation of blood manganese and urinary nickel among workers, whereas chromium were not detected. This might be due to types of work and working hours were varied. However, the level of blood manganese and urinary nickel were not significant difference among job tasks which might be affected by similar exposure level since their working area located in the same general location.

Most of participants had blood manganese and urinary nickel in acceptable levels, except three workers had blood manganese exceeded the reference value. One of them had performed heating work meanwhile two workers had performed grinding work for more than 20 y. This accord to the study of Santos [9] that found urinary nickel and manganese levels of nonferrous metal foundries was lower than the reference values, however, significant differences between exposed and non-exposed groups was found. Nevertheless, no statistical significance was found when comparing blood manganese concentrations by type of work, working hour, and duration of work. This accord to the study of Roels et al [10] but inconsistent with previous studies that revealed the effect of blood manganese level with life-estimated exposure and possible threshold of exposure duration.[11-13] It might be explained that although individuals exposed to the same chemical, but the route of exposure and the ability (or inability) to metabolize the agent of individuals were difference leading to the variation of metal level remain in the body.[14]

It has been reported that working environment factors such as the working duration, working hours per day, and working days per week affect metals exposure. In this study, the longest working duration was 40 y, the longest working day was 12 h, and the longest working week was 6 d. Long working hours and working weeks could increase exposure to metals, give poorer health and safety outcomes, and increase the risks of acute myocardial infarction, diabetes mellitus, and hypertension occurring.[15] Inappropriate working conditions, unsafe environments, and long working hours may also negatively affect health, as found previously by Kivimaki and Kawachi [16] who found a significant association between long working hours and risk of cardiovascular diseases.

In terms of working experience, our study results were similar to that found in metal workers of urban Kano which revealed no significant difference of blood manganese level among workers with different working experience. Contrary to the study of Cowan et al [17] which found the mean blood manganese level in ferrous foundry workers who had working experience for less than three months was lower than those 3-12 months working experience. In addition, our study found the average concentration of blood manganese was higher than that found in ferrous foundry workers who had working experience for less than three months but lower than workers with 3-12 months working experience. This might be due to the influence of working activities of Aranyik workers which were varied leading to the temporal variation of heavy metals exposure comparing to the worker in industrial sector which usually working in a specific job.[17-19]

There was a study showed the workers who did not regularly wear their protective device had higher heavy metals level than those who applied.[20] Our results opposed to that study since heavy metals level in blood and urine of workers who always applied and those who did not applied protective device was not significant difference. This might be due to most of the participants in this study always wore cotton mask (91.70%), used gloves (88.3%) whereas only 31.7% wore goggles during work. Cotton mask might seem to be an inappropriate tool for protecting metal exposure, however cotton masks are basic safety equipment to protect workers from dust generated during knife-making processes. This conformed to previous studies that found cotton mask is a common personal protection equipment applied in various job tasks. The reason behind this event related to uncomfortable to work with metal fume mask.[21]

Effects of unsafe behaviors such as smoking, eating and drinking at work on heavy metals level in biological specimens has been reported.[22][23] Our study results indicated that some Aranyik handicraft workers had unsafe behaviors such as drinking and eating while working (85.0%), not wearing goggles (68.30%), not wearing a face shield (73.30%), and not using ventilation in the working area (26.70%). However, the levels of blood manganese and urinary chromium between workers with safe and unsafe behavior were not significant difference. The unsafe behaviors found in this study were similar to that found in knife workers at Naton (Nakhon Phanom, Thailand) including working without goggles and face shields while cutting and welding metal sheet, did not wear gloves while heating, and did not cover external surfaces while grinding.[24]

Our study also found two participants were smokers and smoked a maximum of 20 cigarettes per day. These participants smoked during working hours and never washed their hands before smoking. Metal particles being transferred from the hand to the mouth during smoking could be an important source of exposure to metals for these participants. In addition, cigarette contain several metals such as cadmium, chromium, manganese and nickel leading to higher possibility of exposure in smoker. However, the level of blood manganese, urinary chromium and nickel in smoker and non-smoker did not significant difference. The result was dissimilar to the study of Afridi et al [25] and Mulyana et al [23] that found the correlation of chromium, manganese and nickel with smoking status.

Ventilation system has been suggested to be the most effective method to reduce exposure to air pollutants. [26] Moghaddasi et al. [27] suggested that occupational asthma in bakery workers could decrease as the ventilation rate increases. Since most of workers in our study used electric fans in the working areas and used every day. They have less exposure to metals dust. This might be a reason that contribute heavy metals level in biological samples of almost workers were in acceptable levels.

A biomarker is a marker of exposure to a chemical or agent or a marker of the effects of exposure to a chemical or agent in the body. It is useful indicators that respond to exposure to species of interest. Biomarkers in biological fluids can be used to evaluate exposure to chemicals, to indicate the health risks posed. In this study, 89% of the participants had acceptable manganese concentrations in blood but three (17%) of the participants had manganese concentrations in blood exceeding the reference value. The chromium and nickel concentrations in urine did not exceed the reference values for any of the participants. Santos et al.[9] found lower manganese and nickel concentrations in urine from workers at nonferrous metal foundries than the reference values and significant differences between the concentrations in samples from exposed and non-exposed groups. Alkhatib et al.[28] found that nickel concentrations in urine from jewelry technicians were not statistically significant higher than the concentrations in urine from the control group ($p>0.05$). Individuals may be exposed to the same chemical but through different exposure routes and may have different abilities to metabolize the chemical, and these differences can cause variations in metal concentrations in tissues from different individuals.[14]

Age, sex, diet, and metabolic factors may play roles in metal uptake, metabolism, and excretion and act as confounders when assessing relationships between biomarkers and the outcomes of interest. [29] The sample collection, preparation, preservation, and analysis methods may affect the measurement errors, and the concentration of a metal in a sample must be sufficiently high for the concentration to be reliably concluded to be higher than the background. [30]

It was found that 46.70% of the participants drank and ate while working, 68.30% did not wear goggles, 73.30% did not wear a face shield, and 26.70% did not use ventilation in the work area. The highest and lowest health risk scores were 25.00 and 18.00, and the mean was 22.25 (standard deviation 1.57). In total, 19 (31.70%) of the participants had the most common score of 23. These results agreed with the results of a study by Harasan and Pusapakdeepob [31] of the relationships between

various factors and safety behaviors in workers at automobile parts industry in Chonburi Province. In that study, 50.4% of the workers had high workplace safety behavior scores.

Pearson correlation coefficients showed no significant negative relationship between the health risk score and blood manganese concentration ($r = -0.61$, $p = 0.64$). The workers with more safe behaviors had lower manganese concentrations in blood. These results agreed with the results of a study by Junhom [32] in which cadmium, chromium, and lead concentrations in blood and urine from painting workers in Hat Yai Municipality were determined. No significant correlations were found in that study between the cadmium, chromium, and lead concentrations and the use of personal protective equipment at work ($p > 0.05$). However, our results disagreed with the results of a study by Awodele et al [33] in which the risks of paint workers in Lagos, Nigeria, being exposed to arsenic, cadmium, chromium, and lead were determined. In that study, the metal concentrations in urine from the paint workers were significantly higher than the concentrations in urine from the control group ($p < 0.05$).

Pearson correlation coefficients were also used to assess the relationships between working environment factors and the manganese concentrations in blood. No significant correlations were found between the working environment factors and the manganese concentration in blood. This did not support the hypothesis that workers with long working periods will be exposed to larger amounts of metals. The results disagreed with the results of studies by Decharat [22][34] in which higher body burdens of toxic metals were found in sanitary landfill workers than in the control group and occupational exposure to metals was associated with the number of working hours per day, number of working days per week, working duration (years), type of work, and personal hygiene practices.

Our results also disagreed with the results of a study by Sani and Abdullahi³⁵ in which heavy metal concentrations in body fluids from metal workers in the Kano metropolis in Nigeria were determined. In that study, no correlations were found between the chromium, nickel, and manganese concentrations in blood and the number of years of exposure ($p > 0.05$), but the manganese concentration in urine and number of years of exposure did correlate ($p < 0.05$).

5. CONCLUSIONS

Most participants had manganese concentrations in blood that were acceptable, but three participants, all of whom had been working for >20 y, had manganese concentrations in blood that exceeded the reference value. None of the participants had chromium or nickel concentrations in urine exceeding the reference values. No significant relationships were found between behaviors related to health risks or environmental factors and the manganese concentrations in blood. The lowest, highest, and mean lengths of time the Aranyik handicraft workers had been working were 11, 40, and 24.05 y, respectively. Nineteen participants worked >8 h d^{-1} . No significant relationships between working times and manganese concentrations in blood were found. The results indicated that the ventilation systems were not adequate for controlling exposure to metal dust. Aranyik handicraft workers should be encouraged to improve their personal hygiene and safety practices to decrease their exposure to metals that may pose health risks.

ACKNOWLEDGMENTS

The authors would like to thank Faculty of Tropical Medicine, Mahidol University for partial support of this study by Research Fund for Thesis. We also thank the Aranyik handicraft workers in Ayutthaya Province, Thailand, for allowing the samples analyzed in the study to be collected and thank staff in the Department of Social and Environmental Medicine, the Faculty of Tropical Medicine, and the Bureau of Occupational and Environmental Disease (Department of Disease Control, Ministry of Public Health) for support and encouragement.

DISCLOSURE

Approval of the research protocol: Approved by the Ethical Committee of the Faculty of Tropical Medicine, Mahidol University (approval no. TMEC 16-056). Informed consent: All individuals gave informed consent. Registry and the registration no. of the study/trial: N/A. Animal studies: N/A. Conflict of interest: no conflict of interest for this article.

REFERENCES

1. Lee RV. (2015). Introduction. In: Harbison RD, Bourgeois MM, Johnson GT, eds. *Hamilton and Hardy's Industrial Toxicology*. (6th ed., pp. 21-23). New Jersey, John Wiley & Sons.
2. Behrman AJ. Welders and joiners. (2003). In: Greenberg ML, Hamilton RJ, Phillips SD, McCluskey GJ, (eds.) *Occupational, Industrial, and Environmental Toxicology*. (2nd ed., pp. 398-404). London, L Mosby.
3. Lauwerys RR, Hoet P. (2001). *Industrial chemical exposure guidelines for biological monitoring*. (3rd ed., pp. 1-19). Florida, CRC Press.
4. ACGIH. (2015). Documentation of the threshold limit value and biological exposure indices. American Conference of Governmental and Industrial Hygienists, Cincinnati, USA.
5. Bader M, Dietz MC, Ihrig A, et al. (1999). Biomonitoring of manganese in blood, urine and axillary hair following low-dose exposure during the manufacture of dry cell batteries. *Int Arch Occup Environ Health*. 72, 521-527.
6. Bermacki EJ, Parsons GE, Roy BR, et al. (1978). Urine nickel concentrations in nickel-exposed workers. *Ann Clin Lab Sci*. 8(3), 184-189.
7. Canterbury Health Laboratories. (2009). Hand book of biological monitoring for health. (3rd ed.). New Zealand.
8. Wongwit W, Kaewkungwal J, Chantachum Y, et al. (2004). Comparison of biological specimens for manganese determination among highly exposed welders. *SEAMEO*. 35, 764-9.
9. Santos C R D, Saliva C S D, Nascimento E S. (2016). Assessment of exposure to cadmium, lead, manganese, and nickel in workers from foundries. *Toxicol Ind Health*. 32(10), 1784-90.
10. Roels HA, Ghyselen P, Buchet JP, et al. (1992). Assessment of the permissible exposure level to manganese in workers exposed to manganese dioxide dust. *Br J Ind Med*. 49, 25-34.
11. Lucchini R, Apostoli P, Perrone C, et al. (1999). Long-term exposure to "low levels" of manganese oxides and neurofunctional changes in ferroalloy workers. *Neurotoxicology*. 20(2-3), 287-97.
12. Baker MG, Stover B, Simpson CD, et al. (2015). Using exposure windows to explore an elusive biomarker: blood manganese. *Int Arch Occup Environ Health*. 89(4), E679-687. doi: <http://dx.doi.org/10.1007/s0042015-1105-3>.
13. Razavian SMH. (2017). Effects of manganese exposure on blood iron indices in miners of Iran manganese mines co. (Qom). *Zehedan J Res Med Sci*. 19(4), E9358.
14. Sillins I, Hogberg J. (2011). Combined toxic exposure and human health: Biomarkers of exposure and effect. *Int J Environ Res Public Health*. 8, 629-47.
15. Caruso C.C., Hitchcock E.M, Dick R.B, et al. (2004). Overtime and extended work shifts: recent finding on illness, injuries, and health behaviors. <http://www.cdc.gov/niosh>. Accessed January 20, 2019.
16. Kivimaki M, Kawachi I. (2015). Work stress as a risk factor for cardiovascular disease. *Curr Cardiol Rep*. 17, 74.

17. Cowan DM, Fan Q, Zou Y, et al. (2009). Manganese exposure among smelting workers: blood manganese-iron ratio as a novel tool for manganese exposure asses. *Biomarker*. 14(1), 3-16.
18. Hobson A, Seixas N, Sterling D, et al. (2011). Estimation of particulate mass and manganese exposure levels among welders. *Ann Occup Hyg*.55(1),113-125.
19. Ellingsen DG, Dubeikovskaya L, Dahl K, et al. (2006). Air exposure assessment and biological monitoring of manganese and other major welding fume components in welders. *J Environ Monit*. 8(10),1078-1086.
20. Malkin R, Brandt-Rauf P, Graziano J, et al. (1992). Blood lead levels in incinerator workers. *Environ. Res*. 59(1), 265-270.
21. Roy AK, Medhi JK, Baruah B, et al. (2010). Environment, occupational health & safety in the craft sector in India: Baseline study of selected craft clusters. https://www.switch-asia.eu/fileadmin/user_upload/research-baseline-study-environment-occupational-health-safety-issues-the-crafts-sector.pdf. Accessed July 7, 2019.
22. Decharat S. (2016). Heavy metals exposure and hygienic behaviors of workers in sanitary landfill areas in Southern Thailand. *Scientifica*. 1-9.
23. Mulyana M, Reismala M, Nikopama C, et al. (2015). Biomonitoring for iron, manganese, chromium, aluminum, nickel and cadmium in workers exposed to welding fume: A preliminary study. *RusOMJ*, 4(2),CID e0202. doi: 10.15275/rusomj.2015.0202.
24. Sriprasan T, Tanuanrum V, Hmoohmeausri N. (2005). Technical support for quality control and production management practice of products from steel of Ban Na Thon Community Enterprise. Ministry of Science and Technology. <http://www.most.go.th>. Accessed February 20, 2018.
25. Afridi H, Kazi T, Kazi N, et al. (2010). Evaluation of cadmium, lead, nickel and zinc status in biological samples of smokers and nonsmokers hypertensive patients. *J Hum Hyperten*. 24,34-43.
26. Unnikrishnan S, Iqbal R, Nimkar IM. (2015). Safety management practices in small and medium enterprises in India. *Saf Health Work*. 1,46-55.
27. Moghaddasi Y, Mirmohammadi S, Ahmad A, et al. (2014). Health-risk assessment of workers exposed to flour dust: a cross-sectional study of random samples of bakeries workers. *Atmos Pollut Res*. 5,113-118.
28. Alkhatib HJ, Boran AM, Hourani ZA, et al. (2014). Occupational exposure to nickel, cadmium and copper among workers in jewelry manufacturing. *Eur Sc*. 10, 1857-1881.
29. Mayeux R. (2004). Biomarkers: potential uses and limitations. *Neurotherapeutics*. 1,182-188.
30. Strimbu K, Tavel AJ. (2010). What are biomarkers? *Curr Opin HIV AIDS*. 5,463-466.
31. Harasan K, Pusapakdeepob J. (2015). Factors related to the safety behavior among workers in an automobile parts, Chonburi Province. *J Ind Technol Ubon Ratchathani University*. 1,84-102.
32. Junhom S. (1999). A study of blood lead levels, urinary cadmium and chromium [dissertation]. Songkla, Prince of Songkla University.
33. Awodele O, Popoola DT, Ogbudu BS, et al. (2014). Occupational hazards and safety measures amongst the paint factory workers in Lagos, Nigeria. *Saf Health Work*. 5,106-111.
34. Decharat S. (2012). Mercury exposure among garbage workers in southern Thailand. *Saf Health Work*. 4,268-277.
35. Sani A, Abdullahi IL. (2017). Evaluation of some heavy metals concentration in body fluids of metal workers in Kano metropolis, Nigeria. *Toxicol Rep*. 4,72-76.

The Effect of Viscosity-imparting Agent on Textural Properties of Toddy Palm Syrup

Jitlada Chumee¹, Saowanee Kumpun¹, Ploysai Ohama¹ and Daungporn Pupaka²

1 Department of chemistry, Faculty of Science and Technology, SuanSunandha Rajabhat University, Bangkok, Thailand

Email: jitlada.ch@ssru.ac.th, saowanee.kum@ssru.ac.th, ploysai.oh@ssru.ac.th

2 Department of chemistry, Faculty of Science and Technology, Rajabhat Rajanagarindra University, Chachoengsao, 24000

Email: daungpornpupaka@gmail.com

Abstract

The objective of this research was to develop a table syrup product from toddy palm sugar. To be acceptable to consumers, table syrup should have an appropriate and stable viscosity. In this study, the effects of xanthan gum (0.1 – 0.5%), guar gum (0.1 – 0.9%) and carboxymethyl cellulose gum (CMC) (0.2 - 0.8%) on viscosity and textural properties of syrup samples were investigated. The results showed that addition of 0.1% xanthan gum made significant increase in viscosity and decrease in water activity of toddy palm syrup. Toddy palm syrup with 0.1% xanthan gum in combination with 0.8% guar gum and 0.4% CMC had highest viscosity whereas syrup with 0.1% xanthan gum in combination with 0.7% guar gum and 0.2% CMC showed lower viscosity but higher hardness and adhesiveness value. However, syrup with only 0.5% xanthan gum added was rated the highest scores from the sensory evaluation.

Keywords: viscosity, syrup, xanthan gum, guar gum, cmc

1. Introduction

In recent years, food industries have looked to develop new syrup from local plants to support consumer demand by addressing health and adding nutritional ingredients into syrup (Arancibia et al., 2011; Keshtkaranet al., 2013). Toddy palm sugar, a sweetener traditionally used in South and Southeast Asia, is one of alternative sweeteners material that can be converted to syrup for added value and convenient use. Toddy palm sugar is produced from Toddy palm juice by heating and constantly stirred until thickens and crystallizes to solid form. The color of the Toddy palm sugar varies from light to dark brown (J. Wrage et al., 2019). The syrup viscosity and texture are essential properties characterizing the quality product. However, concerns have been raised about the concurrent temporal trend between simple sugar intakes, especially of fructose or high-fructose corn syrup (HFCS), and rates of health problems (Chung et.al., 2014). In the last decades, therefore, many different thickeners, stabilizers, and texture enhancers were offered for enhancing the sweetness and viscosity instead of sugar. These were hydrocolloids such as plant gums, alginates, seaweed extracts, starch and its derivatives, pectin, cellulose and its derivatives, etc.

The polysaccharides such as xanthan gum, starch, guar gum and carboxymethyl cellulose gum (CMC) are commonly added to adjust viscosity, modify texture, or to enhance stability. Adding of xanthan gum 0.1-0.5% of syrup could modify the quality and thermal stability and network structure being strengthened caused decreasing moisture content (Simseke, 2009, Altay and Gunasekaran, 2013, Tunnarut and Pongsawatmanit, 2018). The concentration of CMC (0.1 - 1.5%) was studied, the 0.6% of CMC of sucrose

solution is optimum sensory texture and the sweet taste perception, the 1.5% of CMC of sucrose solution the caused reduction in sweet taste of product (Wagoner et al., 2019).

The objective of this research was to develop a table syrup product from toddy palm sugar and investigated the effect of polysaccharides additive, xanthan gum, guar gum and CMC on viscosity and textural properties of syrup samples.

2. Materials

Toddy palm sugar was purchased from Tambon Paknam Amphur Bangkra in Chachoengsao province, Thailand and used as composition of Toddy Palm Syrup. Food grade of xanthan gum, guar gum and carboxymethyl cellulose gum (CMC) were purchased from UNION CHEMICAL 1986 CO, LTD for study effect of viscosity-imparting agent on textural properties of toddy palm syrup.

3 Methods

3.1 Preparation of toddy palm syrup

Toddy palm syrups were prepared by dissolving toddy palm sugar in boiling water until giving a solution of 70 °Brix (use a refractometer) as the starter. The viscosity-imparting agents, including xanthan gum (0.1 – 0.5%), guar gum (0.1 – 0.9%) and carboxymethyl cellulose gum (CMC) (0.2 -0.8%) were added in 300 mL of starter are specified in Table 1.

Table 1. The percent of viscosity-imparting agent components for toddy palm syrup

Toddy palm syrup	Xanthan gum (%)	Guar gum (%)	CMC (%)
starter	0.0	0.0	0.0
TPS1	0.1	0.1	0.8
TPS2	0.1	0.3	0.6
TPS3	0.1	0.5	0.4
TPS4	0.1	0.7	0.2
TPS5	0.1	0.9	0.0
TPS6	0.1	0.0	0.0
TPS7	0.5	0.0	0.0

3.2 Characterization of toddy palm syrup

The pH values and total soluble solids content (TSS, °Brix) were analyzed by using pH meter and a refractometer. The water activity (aw) of toddy palm sugar was measured for the availability of water of the metabolic activity and growth of micro-organisms. Most bacteria are unable to grow in foods having a water activity below 0.90 (Brooker, 2015). The color with CIELab coordinates (L*, a*, b*) of toddy palm syrup was determined by using a Hunter Lab spectrophotometer Color Quest XE given: L* corresponding to the brightness (100 = white, 0 = black), a* to the red – green coordinate (+a= red, -a= green) and b* to the yellow – blue coordinate (+b= yellow, -b= green). Total color difference (ΔE^*) is expressed using the following equation:

$$\Delta E^* = \sqrt{(L^* - L_0^*)^2 + (a^* - a_0^*)^2 + (b^* - b_0^*)^2}$$

(Mercalietal.2014; MinoltaCo.2007)

In addition, the viscosity and textural Properties of syrup were determined by using Brookfield viscometer and texture analyzer (reporting with values of hardness and adhesiveness).

3.3 Sensory Analyses

Sensory evaluation was based on color, viscosity, flavor, aroma and overall quality. Every attribute was assigned a suitable quantity on the 9-point hedonic scale from one (dislike extremely) to nine (like extremely) by thirty (17 female and 13 male, 17-24 years old) trained panel.

4 Results and Discussion

As shown in Table 2., the CIE L*, a*, b* color values of the toddy palm syrup treated with the viscosity-imparting agents showed lighter colors (increasing in L* values) than the starter. The highest L* was found when 0.5% xanthan gum was added and the lowest L* was found with TPS4 sample (0.1%XG+0.7%GG+0.2%CMC). A single numerical value for describing color change expressed as total color difference (ΔE^*) has become one of the best parameter since it combines all color parameters L*a*b* (Chutintrasri and Noomhorm 2007; Rattanathanalerk et al. 2005). In this research, the ΔE^* showed good agreement with L* values.

Table 2. Color parameters, pH and TSS for Toddy palm syrup samples with different viscosity-imparting agent components.

Toddy palm syrup	Color Coordinates				pH	TSS (°Brix)
	L*	a*	b*	ΔE^*		
starter	3.51	8.83	5.66		4.7	72.6
TPS1 (0.1%XG+0.1%GG+0.8%CMC)	32.57	22.72	53.08	57.32	5.3	61.3
TPS2 (0.1%XG+0.3%GG+0.6%CMC)	26.88	23.48	44.75	47.84	5.2	75.0
TPS3 (0.1%XG+0.5%GG+0.4%CMC)	26.25	22.58	43.81	46.49	5.1	72.5
TPS4 (0.1%XG+0.7%GG+0.2%CMC)	20.25	19.62	33.87	34.53	5.0	70.0
TPS5 (0.1%XG+0.9%GG)	20.97	13.73	33.22	32.99	4.9	45.0
TPS6 (0.1%XG)	32.55	24.66	54.00	58.57	4.7	64.2
TPS7 (0.5%XG)	50.33	37.32	83.13	94.90	5.0	62.2

* XG: xanthan gum, GG: guar gum, CMC: carboxymethyl cellulose gum

The effect of the viscosity-imparting agent on the viscosity of Toddy palm syrup is shown in Figure 1. Figure 1a shows that the viscosity of syrup significantly increased with thickener addition. The viscosity increased with increasing ratio of guar gum and shows the highest value in TPS3 sample (0.1%XG+0.5%GG+0.4%CMC). The viscosity of commercial glucose syrups was 1800 Cp, whereas the viscosity of laboratory obtained syrups was in the range of 200 – 2600 Cp.

The results of the texture profile analysis are presented in Figure 2. Hardness is the strength of the gel structure under compression. The highest value of hardness was the TPS4, syrup with 0.1%XG, 0.7%GG and 0.2%CMC, and the lowest was TPS1, syrup with 0.1%XG, 0.1%GG and 0.8%CMC (Fig.2a). The values of adhesiveness show similar results. It was indicated that the addition of guar gum will result in greater gel strength. It was reported that the unique chemical structure of guar gum makes the ability of strong water absorption, a wide range of viscosity stability and good water solubility and crosslinking (Ruihuan, 2017).

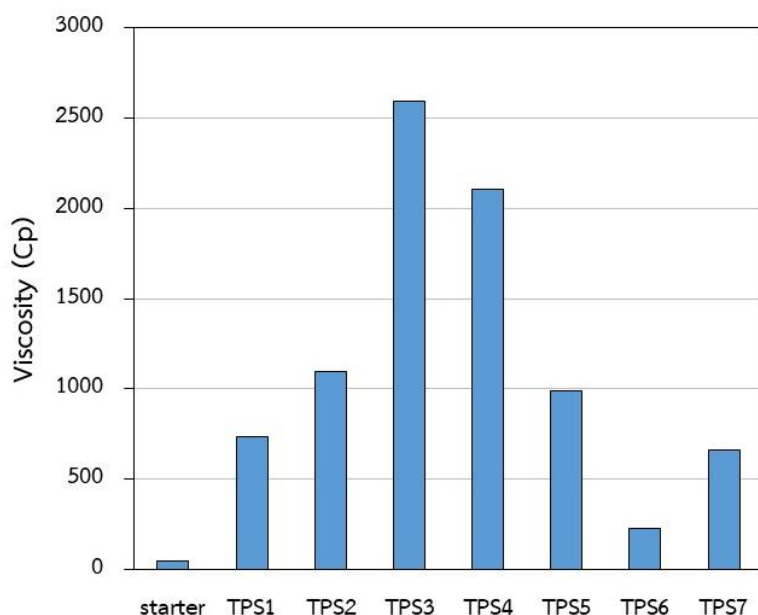


Figure 1 The viscosity of Toddy palm syrup with different viscosity-imparting agent components.

There are many researchers study mixture compatibilities between both polysaccharides in product. The caramel sauces with 0.3% potato starch and 0.02% xanthan gum were received the highest score for rheological, textural and sensory properties (Keshtkaran et al., 2012). The guar gum can be used to partially replaced CMC, the combined between 0.1% guar gum and 0.03% CMC gave an optimal formulation in orange juice (Ruihuan et al., 2017). Moreover, the sweet and sour properties of sauces with three-component oat starch–oat hydrolysate–xanthan gum thickener were most stable on storage (Marek et al, 2006). In this study, although the addition of guar gum resulted in higher viscosity and textural properties, however, the combination between those of three viscosity-imparting agents showed the optimum condition with the highest viscosity, hardness and adhesiveness values.

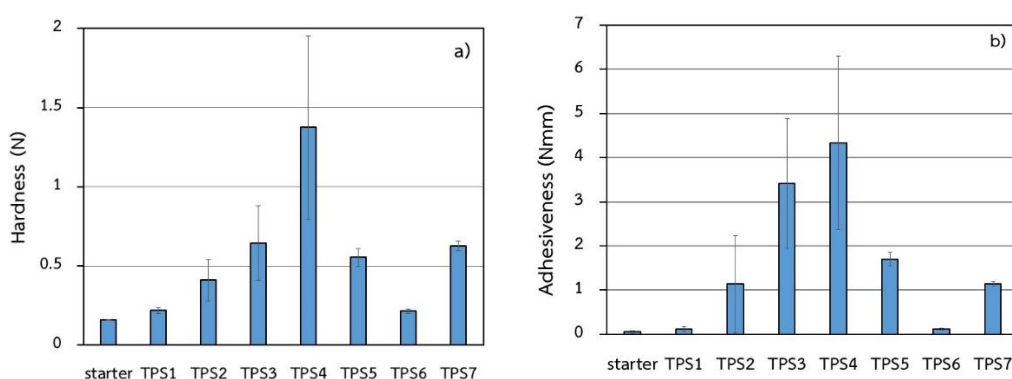


Figure 2 Textural properties of Toddy palm syrup with different viscosity-imparting agent components. a) Hardness, b) Adhesiveness. All determinations were performed in triplicate.

Water activity (a_w) brings a supplement of information as it accounts for the availability of water for degradation reactions and should hold an important place in the identification of the food product, especially as regards its shelf life (Mathlouthi, 2001). The a_w values of Toddy palm syrup with different

viscosity-imparting agent components were presented in fig.3. It was shown that TPS5, which has the highest guar gum ratio, has the highest a_w value and TPS6 with lowest viscosity-imparting agent showed the lowest a_w value, which considered to have a longer shelf life.

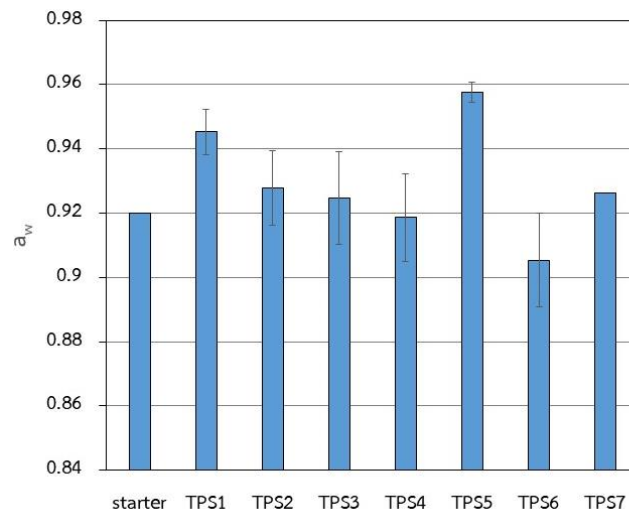


Figure 3 Water activity of Toddy palm syrup with different viscosity-imparting agent components.

Sensory evaluation of three Toddy palm syrup samples, TPS1, TPS5 and TPS7 were shown in Fig. 4. The TPS7 was rated the highest scores in all of the attributes. TPS1 and TPS5 had significantly lower ratings for viscosity (6.5 – 6.7) compared to TPS7 (7.9). In summary, participants found the sensory attributes of Toddy Palm syrup to be very acceptable.

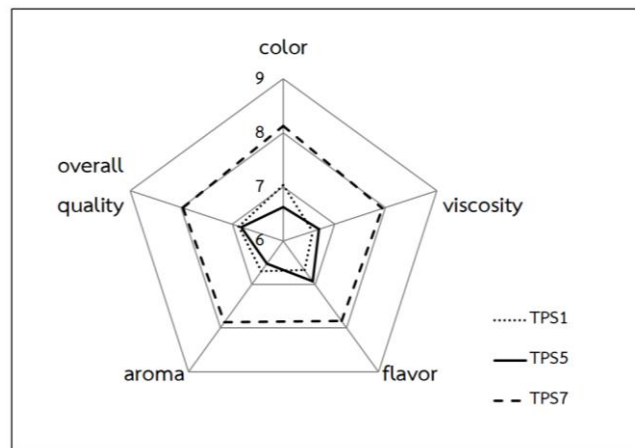


Figure 4 Sensory evaluation of three Toddy palm syrup samples

Conclusions

The effects of xanthan gum, guar gum and carboxymethyl cellulose gum (CMC) on viscosity and textural properties of Toddy Palm syrup samples have been studied. The addition of 0.1% xanthan gum made a significant increase in viscosity and decrease in water activity of toddy palm syrup. Toddy palm syrup with 0.1% xanthan gum in combination with 0.8% guar gum and 0.4% CMC had highest viscosity

whereas syrup with 0.1% xanthan gum in combination with 0.7% guar gum and 0.2% CMC showed lower viscosity but highest hardness and adhesiveness value. Syrup with 0.1% xanthan gum and 0.9% guar gum has the highest water activity value. However, syrup with only 0.5% xanthan gum added was rated the highest scores from the sensory evaluation.

Acknowledgements

This research was granted by Thailand Science Research and Innovation (TSRI). The authors would like to thank Suan Sunandha Rajabhat University for laboratory support and the residents of Tambon Paknam community for cooperation.

References

- Altay, F., &Gunasekaran, S. (2013). Gelling properties of gelatin–xanthan gum systems with high levels of co-solutes. *Journal of Food Engineering*, 118(3), 289–295. doi:10.1016/j.jfoodeng.2013.04.018
- Arancibia, C., Costell, E., &Bayarri, S. (2011). Fat replacers in low-fat carboxymethyl cellulose dairy beverages: Color, rheology, and consumer perception. *Journal of Dairy Science*, 94(5), 2245–2258. doi:10.3168/jds.2010-3989
- Brooker, D. J. (2015). Quality Assurance for Corn and Wheat Flour Tortilla Manufacturing. *Tortillas*, 97–123. doi:10.1016/b978-1-891127-88-5.50004-9
- Gibiński, M., Kowalski, S., Sady, M., Krawontka, J., Tomasik, P., &Sikora, M. (2006). Thickening of sweet and sour sauces with various polysaccharide combinations. *Journal of Food Engineering*, 75(3), 407–414. doi:10.1016/j.jfoodeng.2005.04.054
- Keshtkaran, M., Mohammadifar, M. A., Asadi, G. H., Nejad, R. A., &Balaghi, S. (2013). Effect of gum tragacanth on rheological and physical properties of a flavored milk drink made with date syrup. *Journal of Dairy Science*, 96(8), 4794–4803. doi:10.3168/jds.2012-5942
- Krystyan, M., Sikora, M., Adamczyk, G., &Tomasik, P. (2012). Caramel sauces thickened with combinations of potato starch and xanthan gum. *Journal of Food Engineering*, 112(1-2), 22–28. doi:10.1016/j.jfoodeng.2012.03.035
- Lv, R., Kong, Q., Mou, H., & Fu, X. (2017). Effect of guar gum on stability and physical properties of orange juice. *International Journal of Biological Macromolecules*, 98, 565–574. doi:10.1016/j.ijbiomac.2017.02.031
- Mohamed Mathlouthi. (2001). Water content, water activity, water structure and the stability of foodstuffs. *Food Control*, 12(7), 409-417.
- Simsek, S. (2009). Application of xanthan gum for reducing syruping in refrigerated doughs. *Food Hydrocolloids*, 23(8), 2354–2358. doi:10.1016/j.foodhyd.2009.06.017

Tunnarut, D., &Pongsawatmanit, R. (2018). Modified quality of seasoning syrup for coating and enhancing properties of a food model using xanthan gum. *Agriculture and Natural Resources*, 52(3), 298–304. doi:10.1016/j.anres.2018.06.012

Wagoner, T. B., Çakır-Fuller, E., Drake, M., &Foegeding, E. A. (2019). Sweetness perception in protein-polysaccharide beverages is not explained by viscosity or critical overlap concentration. *Food Hydrocolloids*, 94, 229–237. doi:10.1016/j.foodhyd.2019.03.010

Wrage, J., Burmester, S., Kuballa, J., &Rohn, S. (2019). Coconut sugar (*Cocos nucifera* L.): Production process, chemical characterization, and sensory properties. *LWT*, 112, 108227. doi:10.1016/j.lwt.2019.05.125